Characterization of progenitor cells during the development of the ventral telencephalon of the mouse

Dissertation

Zur Erlangung des Doktorgrades der Naturwissenschaften
(Dr. rer. nat.) an der Fakultät für Medizin
der Ludwig-Maximilians Universität München

Aus dem Institut für Stammzellforschung des Helmholtz Zentrums München
Arbeitsgruppe von Prof. Dr. Magdalena Götz

Vorstand: Prof. Dr. Magdalena Götz

Vorgelegt von
Gregor-Alexander Pilz
aus München
2014

Gedruckt mit Genehmigung der Medizinischen Fakultät der Ludwig-Maximilians-Universität München

Betreuerin: Prof. Dr. Magdalena Götz

Zweitgutachter: Prof. Dr. Michael Kiebler

Dekan: Prof. Dr. Dr. h.c. Maximilian Reiser, FACR, FRCR

Tag der mündliche Prüfung: 15. Oktober 2014

Eidesstattliche Erklärung

Ich versichere hiermit an Eides statt, dass ich die vorgelegte Dissertation selbstständig verfasst, mich außer der angegebenen keiner weiteren Hilfsmittel bedient und alle Erkenntnisse, die aus der Literatur ganz oder annähernd übernommen sind, als solche kenntlich gemacht und nach ihrer Herkunft einzeln nachgewiesen habe.

Zürich, den _____

(Unterschrift)

Summary

During development of the mammalian telencephalon stem cells and more lineage restricted progenitor cells give rise to all cell types which later are contributing to this fascinatingly orchestrated organ. Initially, at the stage of neuroepithelial cells, these stem cells increase their pool by symmetric proliferative divisions and later, when matured to radial glia (RG) cells they give rise to neurons either directly, or indirectly via intermediate progenitors. At later stages of development, radial glia generate glial progenitor cells or differentiate to glial cells directly. How stem cells orchestrate this sequel of tissue genesis has been unraveled by pioneer studies focusing on stem cells of the murine cerebral neocortex. However, the ways how one of the biggest brain regions of the murine brain, the ventral telencephalon which later forms the basal ganglia, facilitates this process, have been largely unknown. Over the past years, increasing interest has been put forward in understanding how the human cortex and its dramatically expanded surface with gyri and sulci is build up on a cellular level during embryonic development. Studies both on embryonic human and primate brains revealed that an expanded germinal zone, the outer subventricular zone (OSVZ), seeded with a heterogeneous population of progenitor cells which are rare in lissencepahlic brains, is responsible to form this enormously elevated brain region. However, both human and primate material is rare and genetically modified models are not available. To investigate the cellular mechanisms taking place in an expanded mammalian brain region in the mouse would be of great interest technically and from an evolutionary perspective. Therefore, live-imaging studies of individual progenitor cells in embryonic brainslices which have been labeled in the lateral ganglionic eminence (LGE) by in-utero electroporation were carried out to reveal lineages emanating from single RG cells. The development of the ventral telencephalon precedes that of the dorsal telencephalon, the cerebral neocortex, and already at early stages prominent bulges begin to form into the ventricular lumen. One characteristic of ventral forebrain development is the early appearance of a non-apically dividing cell population away from the ventricle, which outnumbers from stages of midneurogenesis on apically dividing cells. Amongst these non-apically dividing cells a proportion divides in the ventricular zone, a region that in the neocortex is largely devoid of mitotic cells. These subapically dividing cells were termed according to their location subapical progenitors (SAP). The characterization of these SAPs both by immunohistochemistry and live imaging revealed a morphologically heterogeneous population, with cells bearing processes towards apical, basal or both directions in addition to cells without processes resembling the morphology of basal progenitors, during mitosis. Indeed, bipolar cells amongst these SAPs were characterized as a new type of radial glia, which does not reach the ventricular surface for mitosis but divides in the VZ and generates a basally migrating bRG. By this SAPs contribute to the seeding of the LGE SVZ with a cell type that is characteristic for enlarged SVZ, like the OSVZ in gyrified brains and fundamental for the formation of gyri and sulci. The long-term observation of RG lineages in the LGE uncovered the potential to generate large progeny at midneurogenesis. RG give rise to daughter cells which divide once more in the ventricular zone and generate cells with further proliferative potential, thereby amplifying the cellular output. This amplification of progenitor cells goes along with a shortening in cell cycle length, a feature observed also in the expanded germinal zones of gyrified cortices. In conclusion the developing murine LGE turns out to be a suitable model to study the cellular mechanisms of an expanded brain region.

Zusammenfassung

Im Verlauf der Entwicklung des Vorderhirnes von Säugetieren werden alle Zelltypen, die dieses faszinierende Organ ausmachen von Stammzellen oder in ihrem Differenzierungspotential mehr eingeschränkten Vorläuferzellen gebildet. Zu Beginn der Entwicklung, im Stadium von Neuroepithelzellen, teilen sich diese Zellen in symmetrisch proliferativen Teilungen, um das Reservoir an Zellen zu vergrößern. Danach reifen sie zu radialen Gliazellen heran, die dann direkt, oder über eine Zwischenstufe von Vorläuferzellen, Nervenzellen bilden. Zu einem späteren Zeitpunkt der Gehirnentwicklung bilden radiale Gliazellen dann Vorläuferzellen für Gliazellen, oder differenzieren sich direkt zu diesen aus. Wie Stammzellen diese sequenzielle Zellbildung und schlussendlich den Aufbau eines komplexen Organs orchestrieren wurde durch grundlegende Forschung an Stammzellen des zerebralen Neocortex der Maus aufgeklärt. Wie jedoch das ventrale Vorderhirn, einer der größten Bereiche des Mausgehirns, welcher sich dann im adulten Gehirn zu den Basal Ganglien sich entwickelt, gebildet wird, ist zu einem großen Teil nicht bekannt. In den letzten Jahren wurde der Fragestellung, wie der humane Neocortex mit seiner immens vergrößerten Oberfläche mit ihren charakteristischen Gyri und Sulci während der Embryonalentwicklung entsteht, großes Interesse zuteil. Studien, sowohl am embryonalen humanen, als auch am Neocortex von Primaten, konnten feststellen, dass eine deutlich erweiterte proliferative Zone (die äußere Subventrikulärzone, OSVZ) mit einer größeren Zahl heterogener Vorläuferzellen, welche im lissencephalen Cortex der Maus nur in geringer Zahl vorkommen, für die Bildung dieser hochentwickelten Gehrinregion verantwortlich ist. Jedoch ist embryonales Studienmaterial sowohl vom Menschen, als auch von Primaten rar und genetisch modifizierte Tiermodelle existieren nicht. Um die zellulären Abläufe in einer expandierten Gehirnregion eines Säugetiers zu untersuchen wäre das Mausmodell sowohl aus technischer und praktikabler Sicht, als auch aus evolutionsbiologischer Sicht äußerst interessant. Aus diesem Grund wurden live-imaging Experimente von einzelnen radialen Gliazellen die in embryonalen Gehirnschnitten der lateral ganglionic eminence durch in-utero Elektroporation markiert wurden durchgeführt um die Bildung aller Tochterzellen einer solchen Stammzelle aufzuklären. Die Entwicklung des ventralen Vorderhirns geht derjenigen des dorsalen Vorderhirnes, des Neocortex voran und schon früh sind die charakteristischen Wölbungen welche in den Ventrikel reichen zu erkennen. Eine weitere Eigenart des ventralen Vorderhirns ist die frühe Existenz von Vorläuferzellen, die sich nicht apikal am Ventrikel, sondern weiter basal im Gewebe teilen. Vom mittleren Stadium der Neurogenese an (ab Embryonaltag 14 bei der Maus) übertreffen sie zahlenmäßig die sich apikal teilenden Vorläuferzellen. Unter diesen sich nicht apikal teilenden Vorläuferzellen befinden sich Zellen die sich in der Ventrikulärzone teilen, einem Bereich in dem im Neocortex kaum Zellteilungen stattfinden. Diese Zellen wurden entsprechend dem Ort ihrer Mitose subapikale Vorläuferzellen genannt (SAPs). Die Charakterisierung dieser SAPs mit immunhistochemischen und live-imaging Methoden zeigte, dass sie eine heterogene Population darstellen, welche während der Mitose Fortsätze in apikale, basale oder in beide Richtungen beibehält, oder aber keine Fortsätze zeigt, was morphologisch basalen Vorläuferzellen (BPs) entsprechen würde. In der Tat sind die bipolaren Zellen unter den SAPs ein neuer Typus von radialen Gliazellen, welcher sich nicht am Ventrikel sondern in der Ventrikulärzone teilt und eine weiter nach basal migrierende basale RG (bRG)

generiert. Durch dies tragen SAPs dazu bei, die SVZ des LGE mit einem Zelltyp zu besiedeln, welcher der charakteristisch für die vergrößerten OSVZ von gyrifizierten Gehirnen und maßgeblich verantwortlich ist für die Ausbildung von Gyri and Sulci ist. Des weiteren brachte längeres live-imaging zum Höhepunkt der Neurogenese die Erkenntnis, dass RG im LGE viele Tochterzellen bilden können. RG im LGE bilden häufig Tochterzellen, die sich ein weiteres mal entweder am Ventrikel oder in der VZ teilen um wiederum Tochterzellen mit proliferativen Potential zu bilden, was die Zahl der generierten Zellen pro RG deutlich erhöht. Diese Amplifikation von Vorläuferzellen geht einher mit einer Verkürzung der Zellzyklusdauer dieser Zellen, ein Phänomen, welches auch in den vergrößerten proliferativen Subventrikulärzonen von gyrifizierten Cortices festzustellen ist. Es lässt sich zusammengefasst sagen, dass sich der LGE der Maus als Modell eignet um das Zellverhalten in erweiterten Gehirnregionen verstehen zu lernen.

Meinen Eltern Marlis und Claus-Peter

herzlich gewidmet

Table of Contents

1 Introduction

1.1 Expansion of the cerebral cortex during evolution

1.1.1 The cerebral cortex increases in size during phylogeny

In the course of the evolution of species, various brain regions increased in size and complexity and undertook more and more elaborate tasks in cognition and behaviour. The telencephalon which evolves during embryonic development from the most anterior part of the neural tube can be divided into the dorsal telencephalon (pallium) that generates the neocortex and ventral telencephalon (subpallium) which forms the striatum in the adult brain (see Figure 1).

During embryonic development the ventral telencephalon forms three prominent structures bulging into the ventricular lumen, the lateral ganglionic eminence (LGE) and the medial ganglionic eminence (MGE) and most caudal the caudal ganglionic eminence (CGE). The ganglionic eminences appear in a temporal order with the MGE first at embryonic day 9 (E9), followed by LGE (E10) and CGE (E11; Smart 1976). The LGE which is located more dorsally gives rise to the caudate and the putamen, whereas the more ventrally situated MGE forms amygdala and globus pallidus (reviewed in Reiner 1998). The evolution of the two major telencephalic brain regions, the cerebral neocortex and the basal ganglia, are the topic of this and the following section (see also 1.1.2 The subpallium during evolution).

The cerebral neocortex is the region of the brain with most marked changes in mammals which culminated in the human cerebral cortex, the region that accounts for about 80% of the human brain and enables highly elaborate behavioural and cognitive functions.

Early amniote ancestors, which appeared about 340 million years ago diverged into a branch of synapsids that gave rise to mammals and a branch of sauropsids which contains both reptiles and birds (reviewed in Kaas 2013). Whereas reptiles possess 3 neuronal layers with projection neurons and birds a non-layered structure in the dorsal cortex (Molnar 2011, Wang et al 2010), the mammalian neocortex is a structure of 6 neuronal layers which are generated in an inside out manner during embryonic development (Molyneaux et al 2007). One hypothesis for the emergence of the six-layered cortex is that it is derived from

the dorsal ventricular ridge (DVR), a ball-like structure protruding into the ventricle in reptiles and birds, by relocation and migration of cells present in the DVR (Karten 1997). The "dorsal cortical germinal zone elaboration hypothesis" rather suggests a homologous relationship of reptilian and mammalian dorsal cortex with more extensive neurogenesis from the mammalian progenitor zones (Molnar et al 2006). More complex dorsal cortical layers enabled more extensive computations and therefore behaviour, e.g. guiding input from thalamic neurons first to layer 4 neurons which then target more superficial neurons (reviewed in Kaas 2013). With the appearance of placental mammals in evolution more specified cortical regions like motor and premotor cortex developed (Beck et al 1996) and the corpus callosum connects both cerebral hemispheres (Ringo et al 1994). Amongst mammals, the increase in brain size is achieved in different ways: in rodents, neuronal size increases and neuronal density decreases, in primates the number of neurons increases while density remains the same, leading possibly to the higher cognitive functions of brains with similar size compared to rodents (Herculano-Houzel et al 2006, Herculano-Houzel et al 2007). An increase in body size during evolution is not always accompanied by an isometric scaling in brain size due to biomechanical constraints. Instead the increase in brain size results in an enlargement of brain surface rather than total brain size (Kelava et al 2013, Striedter 2005).

The first primates emerged about 82 million years ago and they represent a family of more than 350 species ranging from mouse lemurs of 2g brain size to humans with 16,000g brain size (reviewed in Kaas 2013). Several cerebral cortical regions in primates developed further with new functional emphasis: for example the primary visual cortex (Tong 2003) and the representation of the hand, which is used in an elaborate way in primates, in the primary somatosensory cortical field (Wang et al 1995). The human brain can be distinguished from the brains of its monkey and ape ancestors by three main features: (1) the brain, in particular the neocortex increased enormously in size yielding 80% of the human brain, (2) regions like the lateral temporal, parietal and frontal cortex expand in evolution compared to their ancestors; interestingly these areas also develop further in postnatal brain development, (3) the human brain is divided into many functional areas (about 200), which is a 10-fold increase to early mammals (Azevedo et al 2009, Hill et al 2010, reviewed in Kaas 2013). The granular prefrontal cortex, which is implicated in

cortical functions like comprehension, planning and perception is expanded disproportionally in size in humans and shows an increased density in neurons and spines (Miller & Cohen 2001, Elston et al 2006).

The increase in functional areas in the human brain is accompanied by a tremendous enlargement in cortical surface area that results in a folding of the cortical plate and the appearance of gyri and sulci. This expansion of surface area comes along with only a modest increase in thickness of the 6 neuronal layers, for example the human cortex is only about 2x the thickness of rodents, with the surface being 1000x larger (Rakic 2009). Which developmental processes led to this expansion in neuronal number, cortical surface and in consequence intellectual ability still are a fascinating topic in research. Various hypotheses have been postulated to explain the cellular groundwork underlying cortical expansion and the resulting gyrification of the cortical surface. However the brain region which is expanded most rapidly during murine embryonic development is the subpallium or ventral telencephalon. Its evolvement during evolution is introduced in the next paragraph.

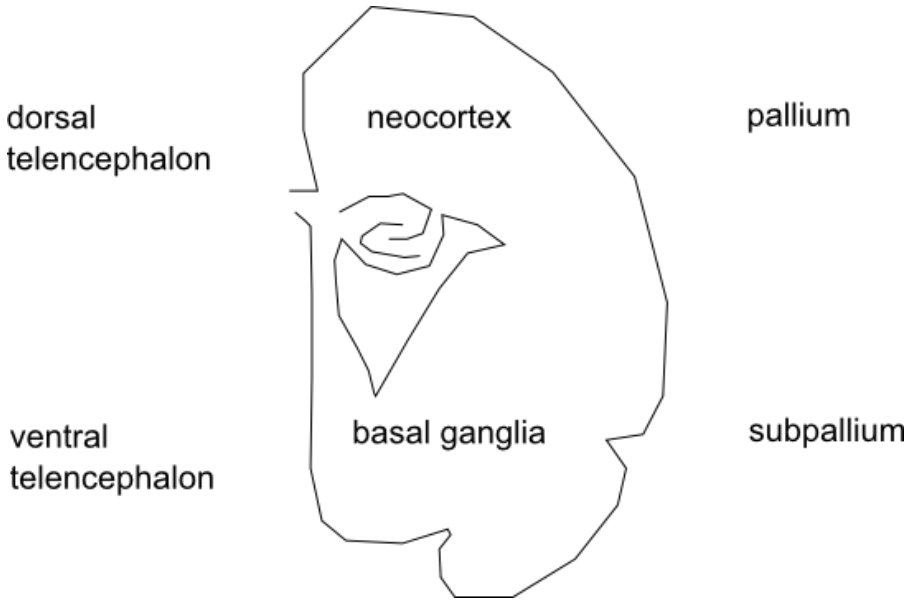

Figure 1 Simplified scheme of an adult mammalian forebrain viewed as a crosssection of one hemisphere. The neocortex is structure of the pallium and the basal ganglia are subpallial. Scheme modified after Karten 1997

1.1.2 The subpallium during evolution

The basal ganglia (BG) are the key region of the brain that processes information about body position delivered by the cerebral cortex into directed movements. It is believed that this part of the brain became crucial during evolution at the transition from amphibians to reptiles & mammals when these acquired a fully terrestrial circle of life (reviewed in Moreno et al 2009 and Reiner et al 1998). Basal ganglia neuronal connections and neurotransmitters usage have been well conserved during evolution (Wang et al 2010, Molyneaux et al 2007, Karten 1997, Molnar et al 2006). The common characteristics of the BG in all amniotes are: (1) a common developmental subpallial origin, (2) existence of dorsal and ventral striatum and pallidum, (3) presence of two types of striatal projection neurons that differ in neurotransmitters and targeted area, (4) a diverse system of interneurons, inputs coming from cortex and thalamus, (5) projections towards the mesencephalic tegmentum and to mesencephalic and isthmic pre-motor centres and (6) dopaminergic innervation from mesencephalic system (reviewed in Moreno et al 2009). A common feature of basal ganglia in mammals, birds and reptiles is its subdivision in a dorsal part (striatum) with sensorimotor function and a ventral part (pallidum) that connects to the limbic system. In addition in all amniotes the basal ganglia lie underneath the pallial areas, which are the cortex in mammals and the DVR in birds and reptiles (reviewed by Reiner et al 1998). Whereas the majority of striatal neurons are medium sized spiny neurons which share also common neurotransmitters, the organization into patch and matrix compartments is unique to the mammalian striatum (Reiner et al 1998). In contrast to projection neurons in the cerebral cortex that build up a cortical plate of 6 layers, the striatum is organized in a mosaic pattern of patches and surrounding matrix (Molyneaux et al 2007, Gerfen 1992). Patch neurons are born in two waves (1. wave E10.5-E11.5) before matrix neurons, depending on Notch1 and retinoic acid signaling (2. wave of patch neurons E12.5-E13.5) whereas matrix neurons are born later and depend on Notch3 (Fishell & van der Kooy 1987, Mason et al 2005, Liao et al 2008). The correct migration of patch and matrix neurons into the different compartments is facilitated by ephrin signaling (Passante et al 2008).

As the subpallium is the major source of inhibitory interneurons migrating tangentially into the mammalian neocortex (about 20% of cortical neurons are inhibitory interneurons), this region also had to adapt to the needs resulting from an increased cortical size and new neuronal layers. Whereas the tangential migration of interneurons from the subpallium into the cortex is well conserved in amniotes (Metin et al 2007), the ability of interneurons to enter layers 2-4 in the cortical plate developed later and is not yet present in turtle and chicken (Tanaka & Nakajima 2012). It has been suggested that the majority of GABAergic interneurons in the primate human neocortex arise within the pallium, e.g. in the human 65% and only a smaller portion originates from the subpallium (35%; Letinic et al 2002). Recent studies on the developing primate and human brain challenge this view and attribute the origin of the majority of interneurons in these species to ventral regions of the telencephalon (Ma et al 2013, Hansen et al 2013). How the formation of pallial and subpallial structures is instructed on molecular levels in the brain of the mouse will be addressed in the following section.

1.2 Molecular governing of telencephalic development

Several gradients of morphogens pattern the telencephalon from early stages on and give progenitor cells that line the neural tube a region specific identity. The transcriptional program initiated by morphogens determines the proliferative action and the cell type specific output during different stages of neurogenesis. Morphogens that determine identity of the ventral telencephalon will be discussed in this paragraph. See also Figure 2.

Shh signaling

Sonic Hedgehog is first secreted from the notochord and in the following from the neural plate where it can be detected by E9.5 (Shimamura et al 1995, reviewed in Rallu et al 2002a). The core function of Shh is to counteract the dorsalizing function of the transcription factor (TF) Gli3, which is initially broadly expressed, in the ventral part of the telencephalon. This repressive function was evident from work on Shh -/- mutant embryos, where ventral cell types are lost (Chiang et al 1996) and the comparison to Shh -/- Gli3 -/- double mutants where the Shh -/- phenotype is largely rescued (Aoto et al 2002, Rallu et al

2002b). Gli3 repression by Shh enables fibroblast growth factor (FGF) signaling to take effect on the generation of ventral structures and the expression of ventral genes (Dlx2, Nkx2.1, Gsx2), which is lost for example in FGF receptor mutant mice (Gutin et al 2006, reviewed in Hebert & Fishell 2008).

Shh action does not only vary due to the ventral to dorsal concentration gradient, but most likely also due to changes in the responsiveness of progenitor cells. It induces medial ganglionic eminence (MGE) fate earlier in development and lateral ganglionic eminence (LGE) fate at later stages (Kohtz et al 1998). The Fishell lab proposes three temporal windows of competence in which Shh acts for specification of the ventral telencephalon: at early stages from closure of the neural tube to E9.5 Shh antagonizes Pax6 expression and colocalizes with Nkx2.1 at E9.5 establishing an early dorsal-ventral boundary and the identity of the MGE (competence window 1, C1). At E10 Shh determines LGE identity by inducing Gsx2 expression in a region between the Pax6+ dorsal and the Nkx2.1 ventral portion of the neural tube (competence window 2, C2). Shh signaling is necessary for a wide variety of ventrally generated cell types, including oligodendrocytes (Nery et al 2001) and cortical interneurons (Fuccillo et al 2004).

Foxg1 /Fgf8

The expression of the forkhead TF Foxg1 (also called brain factor-1, BF1) starts at E8.5 in the anterior neural ridge (ANR; Shimamura et al 1995, Hebert & McConnell 2000). Foxg1 mutants lack the development of ventral telencephalic cell types and of subpallial regions due to premature neurogenic divisions which are accompanied by a longer cell cycle length (Xuan et al 1995, Dou et al 1999 and Martynoga et al 2005). This effect on cell cycle length is caused by a reduction in Pax6 which also acts as a cell cycle organizer (Manuel et al 2011). One has to note, that loss of Foxg1 also severely affects the development of the dorsal telencephalon (Hanashima et al 2002). Foxg1 induces the expression of Fgf8 and itself is regulated by Fgf8 (Shimamura & Rubenstein 1997, Storm et al 2006). Fgf8 plays an essential role in the development of the ventral telencephalon as mice with conditional null mutations lack both a MGE and a LGE (Storm et al 2006).

Retinoic acid

Retinoic acid (RA) is oxidized from vitamin A (retinol) to retinaldehyde by cytosolic alcohol dehydrogenases (ADHs) and retinol dehydrogenases (RDHs) which is then further oxygenized to RA by three retinaldehyde dehydroxygenases (RALDHs 1-3). RA then binds to RA receptors (RARα,β and γ) which are nuclear receptors and form heterodimers with retinoid X receptors (RXRα,β and γ). When translocated to the nucleus these receptor dimers then bind to specific DNA motifs (RAREs) and open with co-activators chromatin to initiate transcription of target genes like genes of the retinoid pathway (for review see Rhinn & Dolle 2012). The enzyme RALDH3 and the receptor RARα is expressed in the SVZ of the LGE from E12.5 on and dependent on the TF Gsx2 (Li et al 2000, Toresson et al 1999, Waclaw et al 2004). Only by E14.5 also RA can be detected in the LGE and acts in GABAergic neuronal differentiation by inducing Gad67 and thereby promoting GABA synthesis (Chatzi et al 2011). Radial glia cells of the LGE being positive for cellular retinol binding protein 1 (CRBP1) might as well be a source for RA, and thereby directly guide radially migrating neurons towards a striatal, DARP-32+ fate (Toresson et al 1999). It is important, that in chick RA expression from the neuroepithelium of the frontonasal process (FNP) ensures sufficient Shh and Fgf8 generation and subsequent correct forebrain and FNP development (Schneider et al 2001). In addition RA responsive slow dividing presumptive stem cells remain persisting in the subependymal zone (SEZ) into adulthood and are present as radial glia (RG) cells in dLGE (Pax6+, Gsx2+, Er81+ region of dLGE) during development (Haskell & LaMantia 2005). One target gene of RA signaling is the TF Nolz1 which is expressed in the subventricular zone (SVZ) and mantle zone (MZ) of the vLGE and promotes cell cycle exit of progenitor cells as well as striatal neurogenesis through up-regulation of RARβ (Urban et al 2010).

1.2.1 Transcription factors in the development of the ventral telencephalon

The subpallial anlage of the neural tube is characterized by the expression of Vax1 (Hallonet et al 1998). At around E9 Nkx2.1 and Gsx1/2 start to be expressed in the ventricular zone of the ventral telencephalon (Shimamura et al 1995, Yun et al 2003) with Gsx2 being expressed stronger in the LGE getting weaker in the MGE and Gsx1 showing

the opposing distribution (Yun et al 2001, Toresson et al 2000, Yun et al 2003). In contrast Nkx2.1 is strongly expressed in the MGE and the preoptic area but absent in the LGE (Sussel et al 1999). See also Figures 2 and 3.

In the following section the main TFs (Gsx1/2, Ascl1 and Dlx1/2) governing development of the ventral telencephalon and neurogenesis therein will be described (reviewed in Wang et al 2013).

Gsx2

Gsx2 is expressed from E9 – E10 on in the ventricular zone (VZ) of the developing LGE (Toresson et al 2000, Corbin et al 2003) and shows a more scattered and weaker expression in the more ventral MGE (Waclaw et al 2009). At midneurogenesis Gsx2 expression is strongest in the dLGE, adjacent to the Sp8 positive olfactory bulb (OB) interneurons, whereas it is weaker expressed in the vLGE close to the Islet1+ striatal projection neurons. Gsx2 follows a temporal role in specification: early in development it promotes striatal projection neuron fate, at mid-neurogenesis and later timepoints it instructs OB interneuron identity. Further it directly leads to a fate conversion to ventral cell types positive for Ascl1 and Dlx2 when ectopically expressed in the dorsal telencephalon (Waclaw et al 2009). In addition Gsx2 is necessary for the temporal switch from neurogenesis to oligodendrogenesis in the dLGE, where it suppresses the generation of oligodendrocyte progenitor cells (OPCs) destined to the cortex at early stages and enables the formation of OPCs when downregulated at later stages (Chapman et al 2013). Gsx2 initiates the expression of three downstream TFs that exert different effects on GE development:

Ascl1

Acheate scute like 1 (Ascl1; also called Mash1) is a pro-neural TF of the basic helix-loop-helix family of TFs that binds to other proneural TFs and targets the regulation of early and later steps of neurogenesis (Castro et al 2011). By forced expression Ascl1 can promote cell cycle exit and direct neurogenesis even in non-neuronal cell types (Farah et al 2000, Berninger et al 2007, Karow et al 2012). Ascl1 plays a bivalent role as it also binds to pro-proliferative genes that mediate G1-S and G2-M transition. Further, Ascl1 promotes a sustaining function on neighboring progenitor cells by upregulation of Dll1 and Dll3

ligands which lead to Notch signaling and Hes5 expression in target cells (Casarosa et al 1999, Yun et al 2002).

Dlx1,2

Dlx TFs are homologous to drosophila distal less homeobox TFs and consist of 6 members in mouse with Dlx1, 2, 5 and 6 being expressed during forebrain development. Dlx1 and 2 are expressed in the VZ and SVZ of LGE and MGE whereas Dlx5 and 6 are restricted to more differentiated cells in the SVZ and MZ. Double mutants of Dlx1 and 2 revealed their role in generation of later born neurons from the LGE SVZ and their necessity for the differentiation and migration of GABAergic interneurons (Anderson et al 1997b, Anderson et al 1997a). Further Dlx2 promotes expression of key enzyme Gad67 and is able to instruct GABAergic neuronal phenotype directly (Long et al 2007, Long et al 2009, Anderson et al 1999, Heinrich et al 2010). Further it is important to suppress both dorsal and MGE neuronal fate (Long et al 2009). Dlx1 and 2 function in later steps of neurogenesis than Ascl1.

Olig2

Olig1 and Olig2 are basic helix-loop-helix (bHLH TFs) that are induced upon Shh signals and accordingly are expressed in a ventral (MGE, strong) to dorsal (LGE, weaker; CTX absent) gradient (Takebayashi et al 2000, Lu et al 2000). Three different classes of cells arise from Olig2 progenitor cells: Olig2 positive progenitors in the MGE give rise to cholinergic as well as GABAergic neurons in a temporal sequence (Furusho et al 2006, Miyoshi et al 2007). At later stages of development both astrocytes and oligodendrocytes are generated from Olig2 positive progenitor cells (Ono et al 2008). Oligodendrocytes are generated by three waves during development. Early oligodendrocyte precursors (OPCs) arise from the MGE and the preoptic area around E12.5 from Nkx2.1+ progenitors and a second wave is born from Gsx2+ progenitors in the LGE and CGE. A third wave of OPCs then emanates from postnatal cortex. Interestingly the OPCs generated in the first wave are eliminated at postnatal stages (Kessaris et al 2006, Richardson et al 2006). The early specification and generation of OPCs (E11.5-E13.5) depends on an interplay of Olig2 and Ascl1 (Parras et al 2007). Ascl1 prevents Dlx1/2 to exert its repressive function on Olig2

expression and therefore supports oligodendogenesis instead of neurogenesis (Petryniak et al 2007). However, depending on the developmental stage, the cell to cell environment, and the progression of the progenitor cells (from VZ to SVZ) Ascl1 can also exert a pro neuronal function of its dual role, when lateral inhibition is not taking place (in VZ) but direct activation of Dlx1/2 genes is the case and GABAergic neurons are generated (Petryniak et al 2007, Poitras et al 2007).

In summary Gsx2 is instructing progenitor identity in the dLGE by 1) driving neurogenesis through induction of Dlx1 and 2 expression 2) by progenitor cell maintenance via Ascl1 mediated delta expression and therefore Notch signaling and 3) by enabling oligodendrogenesis through Olig2 (Wang et al 2013). See Figure 3. How the dorsal telencephalon, the cerebral neocortex is instructed by TFs during development will be the topic of the following paragraph.

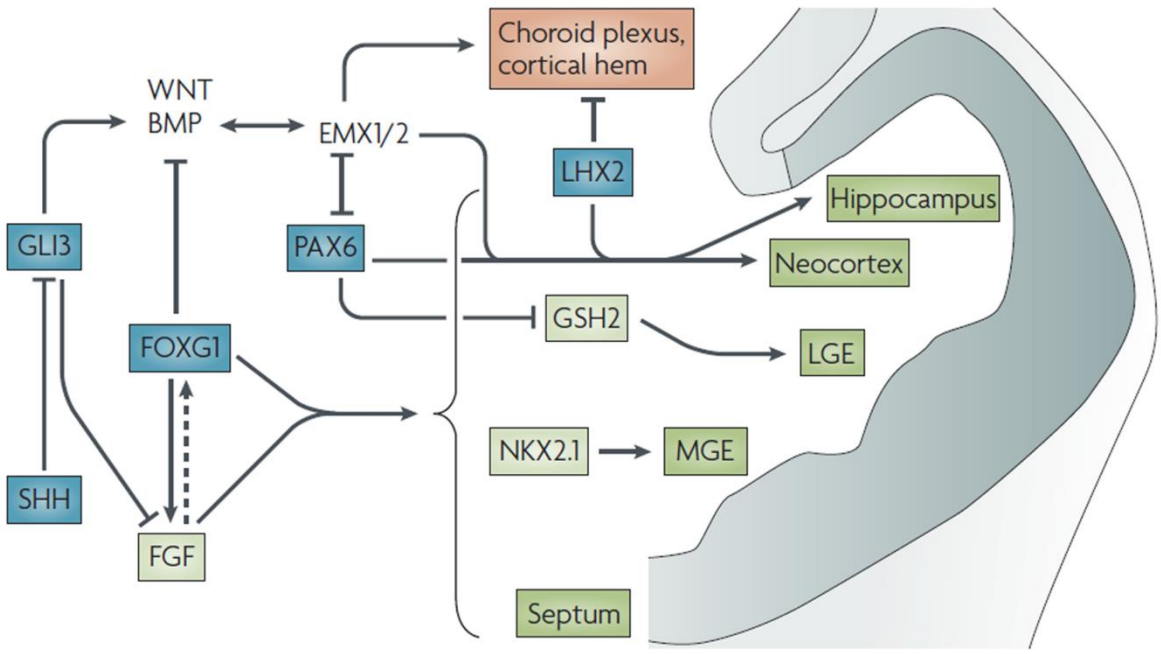

Figure 2 Factors that act early to establish broad telencephalic regions are shown in blue. Sonic hedgehog (SHH) ventralizes the telencephalon by antagonizing the dorsalizing effect of GLI3. By repressing *Gli3*, SHH, together with forkhead box G1 (FOXG1), activates fibroblast growth factor (FGF) expression. FGF might feedback and promote *Foxg1* expression (dotted arrow). FOXG1 and FGF signalling are necessary for forming all regions of the telencephalon (shown in green), except for the dorsomedial region (shown in

orange). Downstream transcription factors, such as GSH2 and NKX2.1, then form specific subdivisions. In the dorsal telencephalon, GLI3's promotion of the expression of bone morphogenetic proteins (BMPs) and Wingless/Int proteins (WNTs) is required for EMX-gene expression. The products of the EMX genes, along with PAX6 and LHX2, further subdivide the dorsal telencephalon. LGE, lateral ganglionic eminence; MGE, medial ganglionic eminence. Taken from Hebert & Fishell 2008

1.2.2 Specification of the dorsal cortex

Progenitor cells lining the ventricle of the dorsal telencephalon are specified in their identity by different morphogens than in the ventral telencephalon and discrete dorsal TFs define cerebral cortical development. The roof plate secrets proteins of the bone morphogenetic protein (BMP) family, BMP2 and BMP4, which induce expression of homeodomain TF Lhx2 (Monuki et al 2001). Lhx2 is an essential selector gene for cortical identity acting on early progenitor cells and thereby inhibiting alternative fates (e.g. hem and antihem; Mangale et al 2008). Further Wingless/INT proteins (Wnt) and BMP proteins activate the expression of the TF empty spiracles homologue 2 (Emx2). Emx1 and Emx2, as well as Pax6 are both required for the formation of the neocortex and subdivision of the dorsal telencephalon (Hebert & Fishell 2008, Muzio et al 2002). Downstream proneural genes like Ngn1, which is induced upon Wnt/β-catenin signaling (Hirabayashi et al 2004), and Ngn2, which is a direct target of Pax6 activation (Scardigli et al 2003) direct neurogenesis in the dorsal telencephalon. The collaborative action of TFs Foxg1, Lhx2, Pax6 and Emx2 imposes cortical lineage determination on progenitor cells in the dorsal telencephalon and enables generation of glutamatergic projection neurons (Molyneaux et al 2007). See Figure 3.

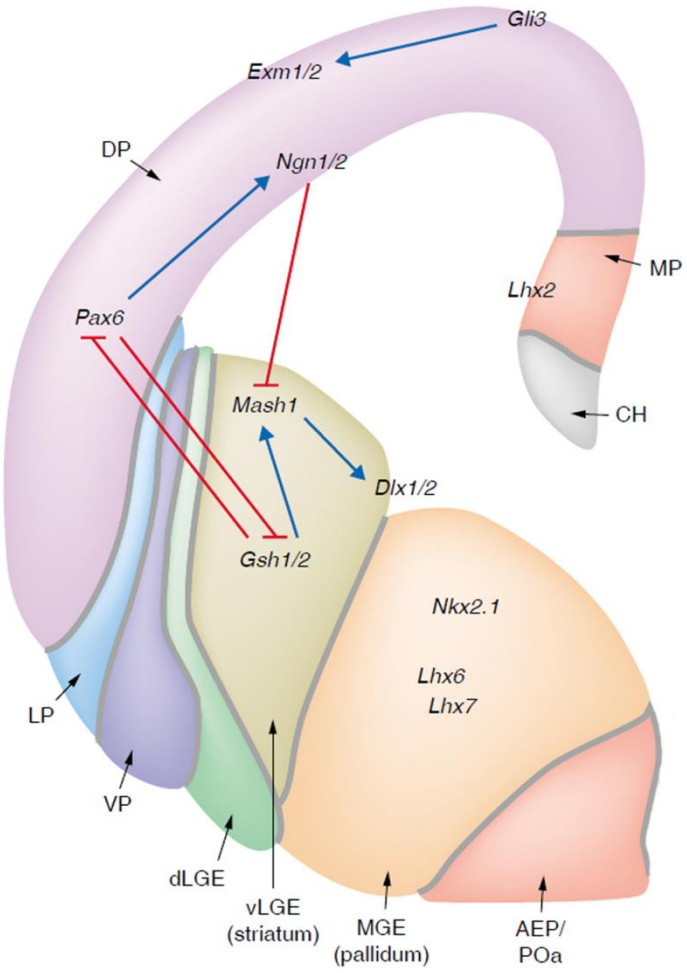

Figure 3 Genetic interactions underlying the regionalization of the mammalian telencephalon. Schematic coronal section through the telencephalic vesicles at E12.5 showing dorsal and ventral subdomains, as defined by their unique patterns of gene expression. Dorsal telencephalic progenitors express high levels of the bHLH transcription factors Ngn1 and Ngn2, and the homeodomain proteins Emx1, Emx2, Lhx2 andPax6, whereas ventral progenitors express the bHLH protein Mash1 and the homeodomain transcription factors Gsh1, Gsh2, Dlx1, Dlx2, Dlx5 and Dlx6. The LGE can be subdivided into dLGE and vLGE compartments on the basis of higher levels of *Pax6*, *Gsh2*, *Dlx2* and *Mash1* in dLGE progenitors, and expression of *Gsh1* only in the vLGE. Progenitor populations in the MGE can be further distinguished from those in the LGE on the basis of expression of *Lhx6*, *Lhx7* and *Nkx2.1*, which also encode homeodomain transcription factors. Important cross-regulatory interactions between *Ngn1/2* and *Mash1* and *Pax6* and *Gsh2* participate in the maintenance of telencephalic progenitor identity. Arrows denote positive interations; T-bars denote inhibitory control. The genetic interactions underlying the ability of *Pax6* to repress MGE fate, *Nkx2.1* to induce MGE and repress LGE fate, and *Lhx2* to induce CH (cortical hem) identity at the expense of pallium, remain unknown. Taken from Schuurmans & Guillemot 2002

1.2.3 Changes in the Pax6 deficient cortex – a ventralized dorsal telencephalon

As described above, Pax6 and Gsx2 are the two key transcription factors to establish dorsal (pallial) and ventral (subpallial) progenitor identity in the telencephalon. The expression of these TFs is overlapping at a special region where the ventral part of the cortex (ventral pallium) and the dorsal aspect of the LGE (dLGE) meet, the pallial-subpallial boundary (PSB). The cross repressive function of both Pax6 and Gsx2 is necessary for proper establishment of the PSB (Toresson et al 2000, Yun et al 2001). Two migratory streams of neurons arise from the PSB: the rostral migratory stream (RMS) of OB interneurons (Waclaw et al 2006) and the lateral cortical stream (LCS) towards the basal telencephalic limbic system, the piriform cortex, the olfactory cortex and the amygdala (Hirata et al 2002, Carney et al 2006, Bai et al 2008). Mouse models mutant for the transcription factor Pax6 (*smalleye* Sey; Hill et al 1991) exhibit changes in dorso-ventral patterning and an expression of TFs typical for ventral progenitors contributing to the GABAergic neuronal lineage like Gsx2, Ascl1 and Dlx1/2 in the cortex (Stoykova et al 2000, Toresson et al 2000, Quinn et al 2007) as well as an expression of typical MGE TFs Nkx2.1 and Lhx6 in the ventral part of the LGE (Stoykova et al 2000). In consequence this leads to a fate change in dorsal-telencephalic progenitors and to the formation of ectopias by Sp8+, Dlx1/2+ interneurons in the perinatal cortex (Kroll & O'Leary 2005). Coinciding with this change in TF factor expression in Pax6 mutant cortices more cells divide in a non-apical position and express Ascl1 instead of Tbr2 that is normally found in cortical basal progenitors (BPs) (Tamai et al 2007, Quinn et al 2007). This is again reminiscent to the situation in the ventral telencephalon. Conversely, the deficiency for Gsx2 leads to the expression of dorsal TFs like Pax6, Ngn2 and Math2 in the LGE (Corbin et al 2000, Takebayashi et al 2000). As Pax6 and Gsx2 cross-repress each other, Pax6 and Gsx2 double mutants show almost a rescued phenotype compared with the single mutants (Takebayashi et al 2000, Waclaw et al 2004).

Cerebral cortical identity is imposed during telencepahlic development by the master regulator genes Pax6 and Emx2, with the expression of each one being sufficient to preserve cortical identity. In the double knockout for the transcription factors Pax6 and Emx2, the cortex has lost any cortical specification and acquired features of the LGE and

the cortical hem, with the LGE and MGE displaying both MGE characteristics (Muzio et al 2002). In addition to the complete loss of cortical TFs (Emx1/2, Pax6, Ngn1/2, Tbr2) and expression of ventral TFs (Vax1, Gsx2,Ebf1) a large number of Islet1+, Gad65/67+ neurons are born from cortical to ventrally specified "cortical" progenitors (Muzio et al 2002).

Taken together the Pax6 deficient cortex acquires ventral TF expression patterns that correlated with progenitor behaviour and neuronal output are reminiscent of the developing ventral telencephalon, mainly the LGE. Accordingly the comparison of both developing LGE and Pax6 mutant cortex can reveal fundamental aspects of Pax6 cellular function.

1.3 Neural diversity in the ventral telencephalon

The LGE gives rise to a variety of different neuronal subtypes during development. How is this heterogeneity in neurons achieved during development? The progenitor cells that precede the neurons reside in specific progenitor domains that are molecularly distinct from each other. See also Figure 4.

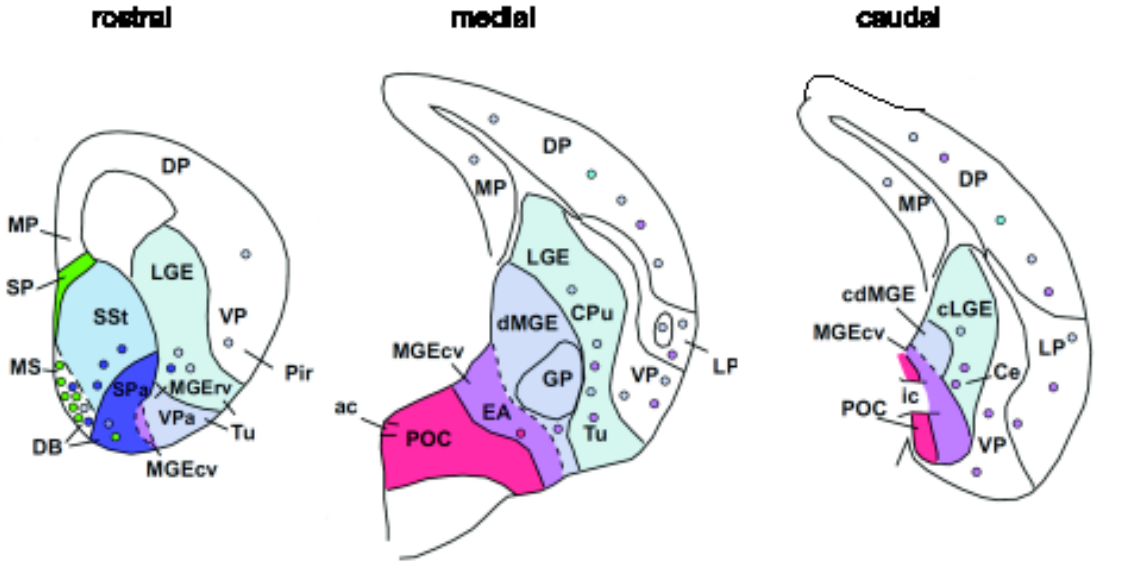

Figure 4 Schemes and telencephalic frontal sections showing the subpallial subdivisions and their derivatives at E12.5–E14.5. In general, LGE produces principal (projection) neurons of striatal structures, such as the caudate-putamen (CPu), nucleus accumbens (Ac), the central amygdalar nucleus (Ce) and the amygdalar intercalated cell masses (ITC). The majority of the interneurons in these striatal structures are immigrants that originate in the pallidal subdivision (MGE; for example, the interneurons containing calcium-binding proteins and/or neuropeptides), or in the preoptic area (PO; for example, the cholinergic

interneurons). In addition to interneurons, the medial part of the central amygdala also appears to receive a specific group of somatostatin-containing cells from the caudoventral subdomain of MGE (MGEcv), which appear to integrate as a subpopulation of projection neurons. dLGE also gives rise to tangentially migrating neurons, some of which migrate to the pallium/cortex to integrate as interneurons, while other cells appear to become part of striatal structures (for example, as cell aggregates or islands in the dorsolateral CPu and the Ac, or the Calleja Islands). MP (medial pallium), SP (pallial septum), MS (medial septal nucleus), DB (diagonal band nuclei) SSt (striatal-like septum), SPa (pallidal septum), DP (dorsal pallium), MGErv (rostroventral part of MGE), VPa (ventral pallidum), MGEcv (caudoventral part of MGE), Tu (olfactory tubercle), VP (ventral pallium), Pir (piriform cortex), ac (anterior commissure), POC (commissural preoptic area), EA (extended amygdala), GP (globus pallidus), LP (lateral pallium), MGEd (dorsal part of MGE), ic (internal capsule), cdMGE (caudo-dorsal part of MGE), cLGE (caudal part of LGE; usually included in CGE), Ce (central amygdala). Taken from Medina & Abellan 2012

One major distinction can be made by dividing the LGE into a dorsal and a ventral aspect (dLGE and vLGE). The dLGE is characterized by expression of the ETS TF Er81 in the SVZ (Stenman et al 2003) and Pax6 in VZ, SVZ and postmitotic neurons (Yun et al 2001, Tole et al 2005). From the progenitor domain of the dLGE several neuron classes arise: interneurons destined for the glomerular layer (GL) of the OB are generated from Dlx5/6+ progenitor cells and can be grouped in 3 major classes that are dependent on different TFs (in brackets): tyrosine hydroxylase (TH) positive interneurons (depend on TFs Er81, Pax6 and Meis2), calbindin positive (CB) interneurons (Meis2, Pax6) and calretinin positive (CR) interneurons (Sp8, Meis2 and Er81) (Anderson et al 1997b, Allen et al 2007). Further a population of interneurons which play a role as intercalated cells (ITCs) in the amydalar fear circuit (Waclaw et al 2010, Kaoru et al 2010) and neurons for the capsular part of the amygdaloid complex (Tole et al 2005) are born in the dLGE. The dLGE is characterized by high Gsx2 expression and analysis on Gsx2 mutants revealed that this part also contributes to the olfactory tubercle (Toresson et al 2000, Yun et al 2003). Further the dLGE also generates some patch neurons of the caudate-putamen (Toresson & Campbell 2001). Fate mapping of Pax6+ progenitors from the dLGE uncovered that this progenitor compartment also gives rise to Npas1+ neurons in the globus pallidus (Nobrega-Pereira et al 2010).

The vLGE which makes up the major part of the LGE is characterized by the presence of Islet1 in postmitotic cells of the SVZ and MZ (Toresson & Campbell 2001, Long et al 2009). From the progenitor domains of the vLGE almost all striatal projection neurons which make up 90% of striatal neurons are generated and populate the caudate-putamen and the nucleus accumbens (Reiner et al 1998, Marin et al 2000, Lobo et al 2008). Two

major types of striatal projection neurons can be distinguished: neurons with the neurotransmitters GABA, substance P and dynorphin that depend on the TF Ebf1 (Lobo et al 2008) and neurons with both GABA and enkephalin which depend on the TF Ikaros. These projection neurons are also different in their projections and functions (Agoston et al 2007, Martin-Ibanez et al 2010, reviewed in Medina & Abellan 2012). In addition progenitors in the vLGE provide neurons for the central part of the amygdala (Waclaw et al 2010) and the nucleus accumbens (Parras et al 2007).

The MGE is the major source of GABAergic interneurons (~60% of all) migrating tangentially into the neocortex and these interneurons are parvalbumin, somatostatin or neuropeptide Y positive (Wichterle et al 2001, Xu et al 2004, Butt et al 2005, reviewed in Wonders & Anderson 2006). Further the globus pallidus, the ventral pallidum, ventral part of the extended amygdala, most of the bed nucleus of the stria terminalis and caudal part of the olfactory tubercle are derivatives of the MGE (all reviewed in Medina & Abellan 2012). Like in the LGE, this enormous variety in cell types and regions is believed to originate from diverse progenitor subdomains in the MGE VZ and SVZ (Flames et al 2007).

The CGE region starts caudally to where LGE and MGE are allied and shares many genes also expressed by the LGE and MGE and therefore can be divided into a dorsal part (dCGE) that shares expression of Gsx2 and Er81 with the LGE and a ventral part (vCGE) that like the MGE expresses Nkx2.1 (reviewed in Wonders & Anderson 2006, Flames et al 2007).

From the CGE both parvalbumin, somatostatin and calretinin interneurons for the cortex and hippocampus as well as neurons for the nucleus accumbens, amygdala, striatum and globus pallidus are generated (Nery et al 2001, Xu et al 2004, Butt et al 2005, Yozu et al 2005). CGE derived interneurons make up 30% of all cortical interneurons, include 9 different subtypes and relocate preferentially to superficial cortical layers (Miyoshi et al 2010). Taken together the ventral telencephalon (LGE, MGE and CGE) is the source of a highly diverse population of neurons (See Figure 5) that either populates ventral structures or migrates long distances to populate the dorsal telencephalon.

The progenitor cell types that have been shown to generate neurons in the dorsal telencephalon, the cerebral neocortex, will be introduced in the following paragraph.

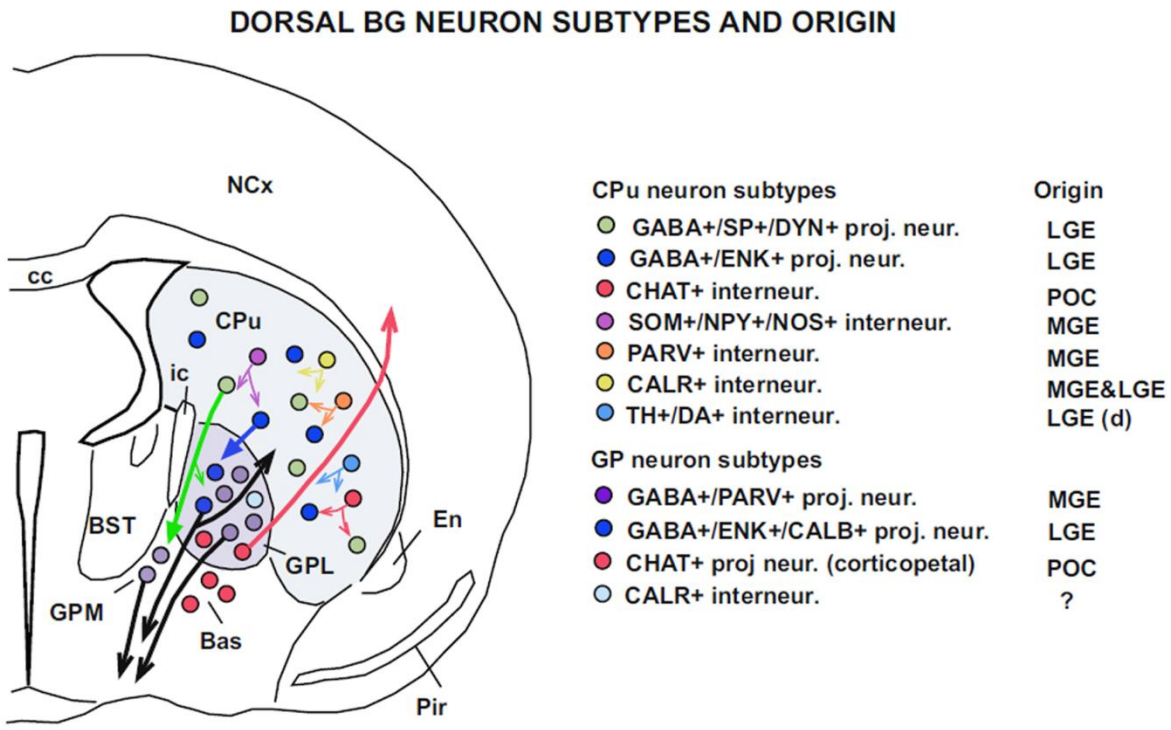

Figure 5 Scheme of a frontal telencephalic section at the level of the caudate-putamen (CPu) and globus pallidus, representing the neuron subpopulations of these nuclei, and their embryonic origin using a color code (explained in a separate list on the right). In the CPu, about 90% of the neurons are GABAergic projection neurons (which typically are medium-sized and with spiny dendrites), and these originate in LGE. About 10% of the remaining neurons include five different subtypes of interneurons, the majority of which originate in the pallidal (MGE) or the preoptic (POC) subdivisions. The globus pallidus contains two major subtypes of principal GABAergic neurons showing descending projections: about two-thirds of them (66%) contain parvalbumin (these cells originate in MGE); and one third of them contain calbindin and enkephalin, and have a descending axon with a collateral projecting back to the striatum (these cells appear to originate in LGE). In addition, the GP contains a subpopulation of cholinergic neurons that belong to the Ch4 corticopetal system (with ascending projections to the cortex/pallium), which appear to originate in the POC. NCx (neocortex), cc (corpus callosum), BST (bed nucleus of the stria terminalis), GPM (globus pallidus, medial segment), Bas (basal nucleus), ic (internal capsule), GPL (globus pallidus, lateral segment), En (endopiriform nucleus), Pir (piriform cortex). Taken from Medina & Abellan 2012

1.4 Progenitor cells during forebrain development

1.4.1 Apical progenitor cells with epithelial characteristics: neuroepithelial cells and radial glia cells

The neuroectoderm closes (in the mouse at E8 Sakai 1989}, in human at E28 O'Rahilly & Muller 1994) to form the neural tube which at this stage is constituted of a single layer of neuroepithelial cells (NE). These radial NE cells are polarized and span from the

ventricular lumen (apical side) towards the basal membrane of the pial surface (basal side). NE cells exhibit true epithelial characteristics, namely apico-basal polarity as they are connected via adherence and tight junctions in their apical plasma membrane to the neighboring cells at the apical surface (Aaku-Saraste et al 1996, Gotz & Huttner 2005) and are anchored via integrins in the basal plasma membrane of their endfeet to the basal lamina (Hirsch et al 1994, Haubst et al 2006). The appearance of the neuroepithelium is pseudostratified as the nucleus of NE cells is translocating to the apical surface for mitosis and towards the basal side during G1- and S-phase of the cells cycle (Taverna & Huttner 2010), a process termed interkinetic nuclear migration (INM). Initially NE expand the pool of neural stem cells by symmetric proliferative divisions resulting in 2 NE cells (Huttner & Kosodo 2005). By this expansion in lateral dimension NE cells constitute the initial pool of neuronal founder stem cells. A minority of NE cells divides in an asymmetric manner, in regard to the fate of the two daughter cells, giving rise either to early Cajal Retzius neurons or a type of basally dividing cells, basal progeniors (BPs), which expand neuronal output beyond the apical surface (Haubensak et al 2004, Kowalczyk et al 2009).

With the start of neurogenesis (E11 in the mouse telencephalon; Gotz & Huttner 2005), NE cells transiently loose some of their epithelial hallmarks like occludin in tight junctions and certain apical plasma membrane proteins (Aaku-Saraste et al 1996, Aaku-Saraste et al 1997) and concomitantly acquire features of astroglial cells like brain lipid binding protein BLBP (Feng et al 1994), vimentin and the glutamate aspartate transporter (Glast) (Shibata et al 1997, Hartfuss et al 2001; for review see Campbell & Gotz 2002 and Kriegstein & Alvarez-Buylla 2009). Another feature that is inherited from NE is the radial morphology and apico-basal polarity. The radial fiber lengthens with increasing radial expansion of the cortex and keeps contact with the basement membrane where retinoic acid signaling from the meninges regulates the switch from symmetric proliferative to asymmetric differentiating divisions (Siegenthaler et al 2009). That these glial cells are actually the primary stem cells of the central nervous system which either directly or indirectly generate the majority of neurons has been discovered a bit more than a decade ago. Since their first description by Wilhelm His in 1889, at that time called “spongioblasts”, they have been rather implicated in being unipotent glial progenitors (Levitt & Rakic 1980) or with their long ascending basal process the frame work neurons migrate along to their final

destination (Rakic 1972, Rakic 1971). The neurogenic function has been attributed to RG after they were shown to be positive for the TF Pax6 and being the major population dividing during telencephalic development (Gotz et al 1998). In order to reveal the true neurogenic lineage potential of RG, cell sorting of RG cells positive for the human glial acidic fiber protein (hGFAP+) and clonal analysis has been performed. These experiments uncovered, that RG are able to generate neuronal cells either in pure neuronal, or in clones together with glial cells apart from pure glial clones (Malatesta et al 2000). Live imaging of single labeled RG in organotypic slice cultures further proofed, that RG are neuronal progenitor cells in the developing forebrain (Miyata et al 2001, Noctor et al 2001, Noctor et al 2004).

Like NE cells RG perform interkinetic nuclear migration and the extent of INM defines the ventricular zone (VZ). RG cells move their nucleus towards the ventricular surface, as the centrosome that serves as basal body of the primary cilium which protrudes into the ventricular lumen, is necessary to organize the spindle apparatus in mitosis (Santos & Reiter 2008, Ishikawa & Marshall 2011). During INM the nucleus is exposed to different external stimuli, one being Notch signaling, that via a cell-cell signaling pathway regulates the balance between progenitor maintenance and differentiation (Gaiano & Fishell 2002, Pierfelice et al 2011). In the developing zebrafish retina it was shown, that Notch acitvity is highest at the apical side where apical progenitors (APs) divide. This exposure to Notch signaling during m-phase keeps APs in a progenitor state (Del Bene et al 2008).

Concurrent with the maturation of NE to RG, the mode of division transits from symmetric proliferative to asymmetric neurogenic, resulting in a RG and a more committed cell, either a neuron (direct neurogenesis) or a basal progenitor (also called intermediate progenitor, IPC; indirect neurogenesis). See Figure 6.

.

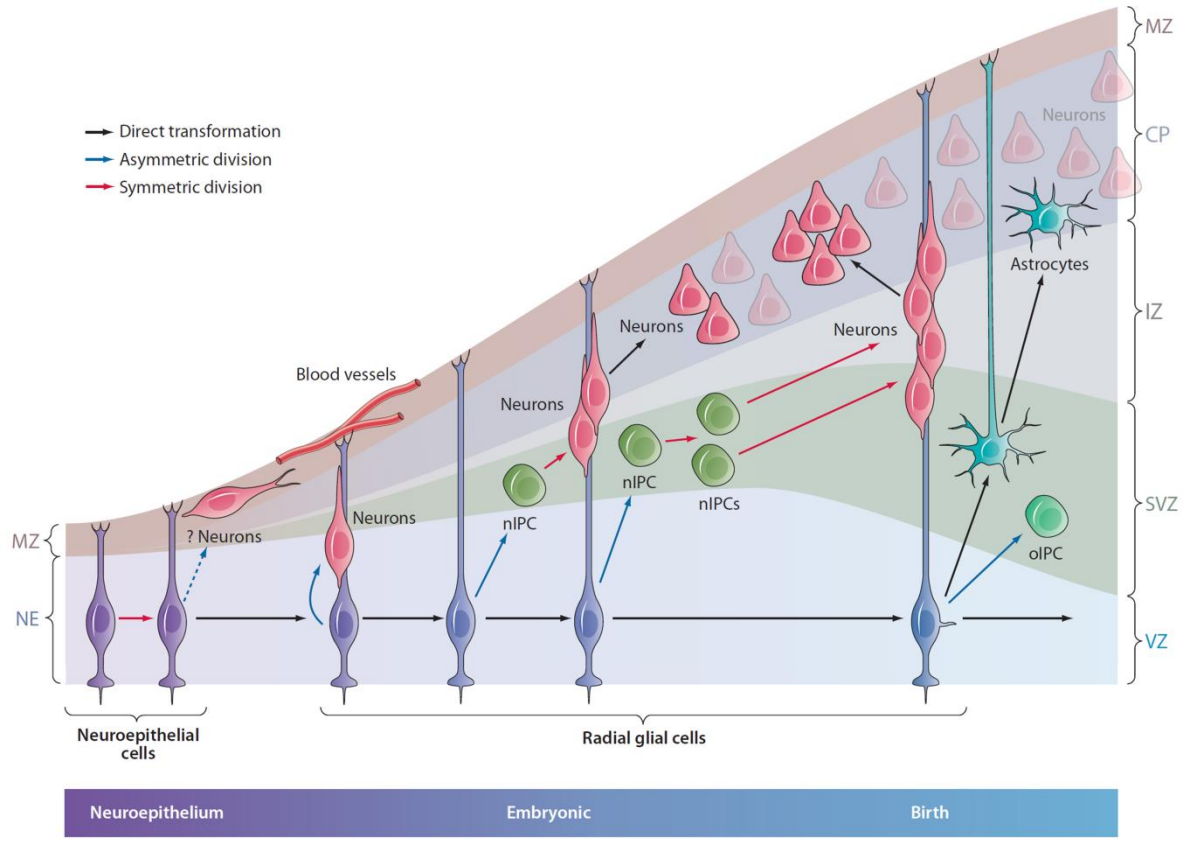

Figure 6 Three modes of neurogenesis during cortical development. RG in cortex generate neurons (*a*) directly through asymmetric division; (*b*) indirectly by generation of nIPCs and one round of amplification; or (*c*) indirectly again through nIPCs, but with two rounds of division and further amplification. This additional amplification stage may be fundamental to increase cortical size during evolution (see text). Subpopulations of nIPCs are likely to divide more than once in subcortical brain regions, but this has not yet been documented. CP, cortical plate; IZ, intermediate zone; MZ, marginal zone; nIPC, neurogenic intermediate progenitor cell; RG, radial glia; SVZ, subventricular zone; VZ, ventricular zone. Taken from Kriegstein & Alvarez-Buylla 2009

1.4.1.1 Determination of radial glia cell fate decisions

Both NE and RG, as well as bRG are capable to perform asymmetric cell divisions regarding daughter cell type and cell fate. This is crucial during forebrain development, as a pool of self-renewing progenitors needs to be maintained while more committed cells (neurons and BPs) are generated. In epithelial cell types (NE, RG, and bRG) cell fate determinants are located either intracellular at the apical ventricular anchoring or the basal side or they are sensed at these sites. In this manner fate determinants will be discriminated and introduced here.

As a component of the apical adherence junction belt and as transcriptional activator, β-catenin serves a dual role during forebrain development. Transcriptional activation via β-catenin prevents RG from early neuronal differentiation and regulates the generation of BPs (Woodhead et al 2006, Mutch et al 2010). Levels of Par3, which is part of the apical protein complex together with Par6 and aPKC, determine the decision of RG daughter cells to remain a self-renewing progenitor or to become more committed and develop to a BP or neuronal fate (Costa et al 2008, Bultje et al 2009). One explanation how Par3 acts might be through tying the Notch inhibitor Numb to the sub-apical cell cortex and thereby enabling strong Notch activity in cells receiving the major part of Par3 (Bultje et al 2009, Peyre & Morin 2012). Apical progenitors reach the ventricular surface for mitosis as the basal body that tethers the primary cilium serves as one centriole of the centrosome in mitosis and the cilium is disassembled just short before mitosis (Taverna & Huttner 2010 and unpublished observation of Sven Falk). During interphase of the next cell cycle centrioles are duplicated in a semiconservative manner resulting in a "younger" and an "older" centriole for the next division (Nigg & Raff 2009, Ishikawa & Marshall 2011). Elegant photoconversion and imaging experiments revealed that the inheritance of the "older" centriole by the apical RG daughter conserves RG fate, due to a re-establishment of the primary cilium from the older centriole (Wang et al 2009). The primary cilium itself serves as an antenna that senses signals from the cerebral spinal fluid it protrudes into (reviewed in Han & Alvarez-Buylla 2010). Indeed many factors, including Shh, IGF-2, BMPs, are contained in the cerebral spinal fluid (CSF) during embryogenesis that act via the primary cilium to influence neural progenitor behavior (Huang et al 2010, Lehtinen et al 2011, Lehtinen & Walsh 2011). The intracellular protein TRIM32 is distributed asymmetrically in APs. The daughter cell that receives TRIM32 will initiate neuronal differentiation, through TRIM32 triggered degradation of c-myc and an activation of micro-RNAs like Let-7a. Conversely a downregulation of TRIM32 or a lower level of TRIM32 after mitosis keeps the cell in a progenitor state (Schwamborn et al 2009).

Intracellular fate determinants in the basal endfoot are less frequently described. The basal endfeet of RG are anchored to the basal plasma membrane and signaling via β3-integrin has been shown to be important for the maintenance of bRG in ferret brain slice

preparations (Fietz et al 2010). On the other hand disrupted contact of RG endfeet to the basement membrane during murine development did not have a strong impact on RG fate (Haubst et al 2006). Further, cyclinD2, which is involved in cell cycle initiation is actively transported into the basal endfoot of RG conveying ability to selfrenew to the daughter cell that inherits the basal process (Glickstein et al 2007, Tsunekawa et al 2012). Signals from the basal side are transmitted via the basal process towards the cell body of APs residing in the VZ. Retinoic acid produced by cells in the meninges plays an important role in RG maturation and BP generation (Siegenthaler et al 2009). Reelin which is secreted from Cajal-Retzius cells in the pre-plate cooperates with Notch signaling to maintain RG via Hes1 and BLBP expression after the onset of neurogenesis (Lakoma et al 2011).

1.4.1.2 Control of spindle and cleavage plane orientation in apical progenitors

The apical membrane that is inherited by some daughter cells of the apically anchored progenitor types was proposed to contain cell fate determinants, that depending on the inheritance after cell division would direct daughter cell fate (Gotz & Huttner 2005). The hypothesis, that the orientation of cleavage plane during mitosis directly impacts daughter cell fate was put forward early (Martin 1967, Langman et al 1966) and was reinforced by a live-imaging study on ferret brain slices, which revealed that cells dividing with a perpendicular (planar) cleavage orientation would acquire equal fates, whereas divisions with horizontal cleavage plane would result in diverging behavior of daughter cells. This difference in cleavage plane orientation was also accompanied by differential inheritance of Notch receptor (Chenn & McConnell 1995; see Figure 7). These observations fitted to the model of dividing neuroblasts in the drosophila embryo, where fate determinants Numb and Prospero are asymmetrically inherited after change in orientation (Hirata et al 1995, Knoblich et al 1995, reviewed in Peyre & Morin 2012). As throughout neurogenesis the majority of APs divides in a perpendicular orientation which cannot account for the neurogenesis taking place at the same time (Smart 1973, Huttner & Brand 1997), it was proposed that a small deviation from the perpendicular cleavage orientation would be sufficient to asymmetrically distribute the very small apical domain together with fate determinants (Kosodo et al 2004). LGN, which is anchored via Gα-GDP subunits to the

lateral cell cortex and forms a complex together with NuMA, orients and maintains the perpendicular cleavage orientation of NE and RG cells and concomitant maintenance of both apical and basal anchoring of these epithelial cells (Konno et al 2008, Peyre et al 2011, Peyre & Morin 2012). Also the homologue of drosophila Inscuteable in mouse (mInsc), acts on spindle orientation in dividing APs, favoring perpendicular divisions at low levels and horizontal divisions when it is overexpressed and leading to an increased generation of BPs (Konno et al 2008, Postiglione et al 2011). Patients with the developmental disorder Human Primary Microcephaly which coincides with mild mental retardation exhibit a reduction in brain size without affecting the overall organization of the brain. The genes linked to this disease (MCPH1, WDR62, CDK5 RAP2, CEP152, ASPM, CENPJ and STIL) are all localized to the mitotic spindle and function either in centrosome assembly or spindle pole organization (Thornton & Woods 2009). The abnormal spindle-like microcephaly-associated protein ASPM is implicated in stabilizing the perpendicular cleavage orientation in NE cells ensuring symmetric progenitor division which leads to a lateral expansion of the founder pool of neural stem cells (NSC; Fish et al 2006). Thus the hypothesis is that upon introducing a disease mutation that mimics the ASPM mutation found in human, mice would resemble this phenotype. However this mouse model shows only a mild microcephaly, but did not alter cleavage orientation or cell fate like in the acute siRNA mediated knockdown (Pulvers et al 2010). In addition, ASPM is positively selected for protein sequence changes during evolution in the primate and human lineage (Zhang 2003). In summary, the orientation of cell division has an impact on fate decisions in telencephalic progenitor cells and therefore forebrain development. Whether the asymmetric distribution of fate determinants or the inheritance of epithelial hallmarks is decisive will be debated in the discussion section.

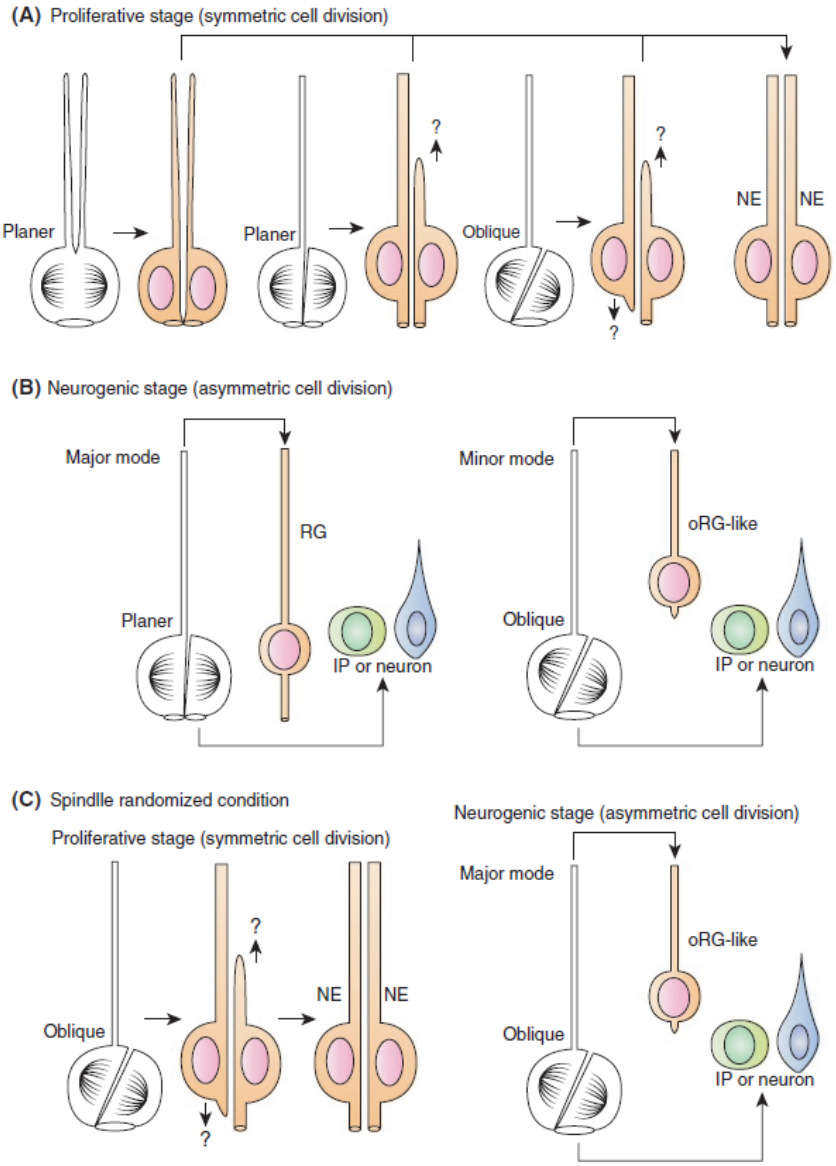

Figure 7 (a) Initial hypotheses both by Chen & McConnell and Huttner postulated that the inheritance of epithelial components would instruct fate decisions depending on the cleavage plane during apical mitosis. In both cases the inheritance of the apical component would dictate progenitor fate in the receiving cell. However, these views have recently been challenged (see text; recent state of the art see b and c). (b) At early stages of development cleavage planes of both planar and oblique orientation result in symmetric proliferative divisions as neuroepithelial cells are potentially believed to be able to regrow their major processes due to the short distance from ventricular to pial surface. (c) At later, neurogenic stages perpendicular cleavage planes, which are the majority throughout corticogenesis, lead to asymmetric fates of RG and BP or neurons. The minor mode of oblique and horizontal divisions results in the generation of bRG cells. Taken from Shitamukai & Matsuzaki 2012

1.4.2 Intermediate progenitor cell types – basal progenitors and short neural precursors

From the beginning of neurogenesis cells that divide at non-apical, in most cases basal positions are present in the developing cortex. These BPs were first considered to be glial progenitors, as retroviral labeling of dividing cells in the postnatal SVZ yielded astrocytes and oligodendrocytes and the embryonic SVZ population was directly related to this lineage (Levison & Goldman 1993, Takahashi et al 1995). Time lapse imaging of progenitors in living organotypic brain slice cultures uncovered that they instead generate neurons at early stages (Haubensak et al 2004, Miyata et al 2004, Noctor et al 2004). BPs are generated by asymmetric cell division of RG, delaminate from the adherence junction belt at the ventricular lining, migrate basally and divide at the basal end of the VZ and in the SVZ. Upon generation from Pax6+ RGs in the cortex, BPs downregulate Pax6 and upregulate the T-domain TF Tbr2 which is then downregulated in Tbr1+ neurons (Englund et al 2005). Interestingly very small numbers of Tbr2+ cells, presumably nascent BPs, were also found to divide in the VZ or at the ventricular surface during neurogenesis (Kowalczyk et al 2009). However the vast majority of BPs divides in the SVZ. There, BPs reside in a vascular niche, with their mitoses taking place in close proximity to the branching point of blood vessels (Javaherian & Kriegstein 2009). In the cortical VZ BPs, identified by Tbr2-GFP, exhibit a bipolar or a multipolar morphology, whereas the multipolar morphology is predominant of BPs in the SVZ. Sometimes BPs in the SVZ still possess apical and basally directed processes that also contact the ventricle (Kowalczyk et al 2009, Nelson et al 2013). In mitosis, BPs retract all their processes, round up and divide. After mitosis both daughter cells reestablish their extensions and behave in a similar way suggesting a similar fate of the daughter cells (Noctor et al 2008, Attardo et al 2008).

Time lapse imaging revealed that BPs in the mouse/rat cerebral cortex mostly divide once, forming first multipolar and then bipolar appearing cells, ultimately giving rise to two neurons. In a minority of cases (10.5%) BPs in the SVZ perform symmetric progenitor divisions, resulting in two BPs and thereby amplifying the neuronal output (Noctor et al 2008). Symmetric proliferative divisions of BPs are regulated by the zinc-finger TF Insm1, which upon overexpression favors the generation of basal mitoses over apical mitoses. These basal mitoses (Tbr2+) are then found to be Tis21-, indicating a proliferative instead

of a symmetric terminal neurogenic division (Farkas et al 2008). Tis21 controls cell cycle progression and is expressed at the transition from G1 to S phase where it inhibits proliferation (Rouault et al 1996, Guardavaccaro et al 2000). In the developing telencephalon, Tis21 is expressed in neurogenic precursor cells but not in postmitotic neurons (Haubensak et al 2004). The effect of Insulinoma-associated 1 (Isnm1) could be mediated by regulation of Robo2, which is downregulated upon Isnm1 KO. Slit/Robo signaling leads to transcription of Hes1 along with self-renewal of APs. Reduced Robo signaling drives APs to generate more BPs that often retain an apical anchoring and divide with a prolonged cell cycle length (Borrell et al 2012). Furthermore FGF signaling plays an important role in controlling the ordered generation of RGs to BPs during cortical development. A triple knockdown of all three FGF-receptors after the onset of neurogenesis (via the hGFAP-Cre) leads to a premature transition of RGs to BPs which in the end results in a thinned cortex (Kang et al 2009). As BPs are present from the onset of neurogenesis they are contributing neurons to all layers of the developing cortex. In contrast to RGs which show less direct neurogenesis, BPs are believed to account for the majority of generated neurons (Kowalczyk et al 2009). In conclusion BPs represent a cell type that amplifies neuronal output from radial glia at basal positions to the ventricular zone (see Figure 6). In the next paragraph a second progenitor type which favors direct neurogenesis will be introduced.

Short neural progenitors (SNPs) were discovered as a cortical progenitor type residing in the VZ, bearing an apical anchoring and being morphologically distinct from RG (Hartfuss et al 2003). This subtype also falls into the category of “apical progenitors”, as they move their nucleus towards the ventricular surface for mitosis. SNPs often exhibit short basal processes of variable length, which are retracted during M-phase (Gal et al 2006), but never possess a full basal process reaching the pial surface like radial glia. This feature clearly distinguishes SNPs from RGs which retain the basal process in mitosis. SNPs are believed to have different cell cycle kinetics than RG, presumably a lengthening in G1 phase of the cell cycle (Stancik et al 2010). In the mouse neocortex SNPs primarily contribute to the generation of layer IV neurons, whereas the direct neuronal progeny of RGs seeds layers VI/V and the progeny of BPs layers IV/III and II of the cortex (Marin &

Muller 2014). This neurogenesis is believed to be carried out mostly directly via one or two divisions at the ventricular surface, with a further step of intermediate progenitors only in the minority of cases. Notably SNPs differ from BPs also by their lack of Tbr2.

Similar to BPs the role of SNPs is to enhance the neuronal output of the VZ. Even though the VZ of the murine neocortex uniformly stains cells for RG specific molecules like nestin, Glast and vimentin (Noctor et al 2002, Malatesta et al 2003, Anthony et al 2004), SNPs differ from RGs by activity of the Notch signaling pathway. Notch signaling via the Notch effector CBF1 is crucial for the maintenance of RG in the VZ, but appears to be active in SNPs in a different CBF independent manner which leads to an earlier differentiation of SNPs and an accelerated neuronal output with very little contribution of SNPs to the astrocytic and oligodendrocytic lineage (Mizutani et al 2007, Stancik et al 2010).

SNPs represent a distinct population to RGs in the VZ, contributing to a different group amongst the projection neurons (mostly layer IV). This difference is also reflected in morphology (long basal process missing), proliferative potential (mostly 1, sometimes 2 cell cycles; Tyler & Haydar 2013) and cell cycle kinetics (longer cell cycle than RG). A recent study confirmed that SNPs can be characterized by activity of the promoter pTα1, but are not active for classical RG promoters like Glast and BLBP (Tyler & Haydar 2013). Interestingly, when fate mapping was carried out using in-utero electroporation of expression plasmids and a Cre plasmid under the control of the promoter pTα1 (half of the SNPs exhibit a short and bipolar morphology and the other half a multipolar morphology reminiscent of BPs (Tyler & Haydar 2013). In line with this, the SNP fate mapping gave rise to a Pax6+ population (presumably SNPs) as well as to a Tbr2+ population (presumably BPs). Using the Glast promoter for 48hrs of fatemapping it was shown that RGs lineally give rise to SNPs. The progenitor subtype of SNPs is also implicated in the neurodevelopmental disease down syndrome (DS). In the Ts65Dn mouse model of DS, the generation of SNPs, and therefore neurogenesis from this progenitor subtype is impaired (Tyler & Haydar 2013).

1.4.3 A radial glia progenitor type in basal positions: basal RG

The role of basal radial glia (bRG) in neurogenesis and the expansion of gyrified cerebral cortices have been discovered initially in both human and ferret brain development (Hansen et al 2010, Fietz et al 2010, Reillo et al 2011). However cells with typical RG morphology, namely long basal process to the pial surface and cell soma located in the SVZ have been described before in monkey and mouse, but were believed to represent translocating RG on their way to become astrocytes (Rakic 1972, Noctor et al 2004). Instead slice imaging in human and retroviral injection in ferret revealed that bRG are divding progenitor cells of the OSVZ that give rise to neurogenic intermediate progenitors (human) and astrocytes (ferret) (Hansen et al 2010, Fietz et al 2010, Reillo et al 2011). These bRG have also been identified as direct neurogenic progenitors being present at very low numbers in the developing mouse cerebral cortex which suggests homology of this cell type between species (Shitamukai et al 2011, Wang et al 2011). Basal RG are generated by apical RG dividing with an oblique and horizontal cleavage plane at the ventricular surface resulting in one daughter cell that inherits the basal fiber and translocates away from the VZ (Shitamukai et al 2011, LaMonica et al 2013). As bRG are directly related to aRG, they share molecular signatures like the expression of GLAST, Nestin, BLBP, the TFs Sox2 and Pax6, and integrin signaling via the basal process but at the same time lack apical molecules like Par3, aPKC, Prominin-1 and ZO-1 (Hansen et al 2010, Fietz et al 2010, Reillo et al 2011, Wang et al 2011). Before mitosis bRG move their cell soma rapidly more basal, following the movement of the centrosome, leading to continuous basally directed movement of bRGs. This process termed mitotic somal translocation is interestingly cell intrinsic, as it is recapitulated by isolated cells in vitro (Hansen et al 2010, Shitamukai et al 2011, Wang et al 2011, LaMonica et al 2013). See Figure 8. How bRG play their role in the expansion of the cortical brain region during evolution will be discussed in the next section.

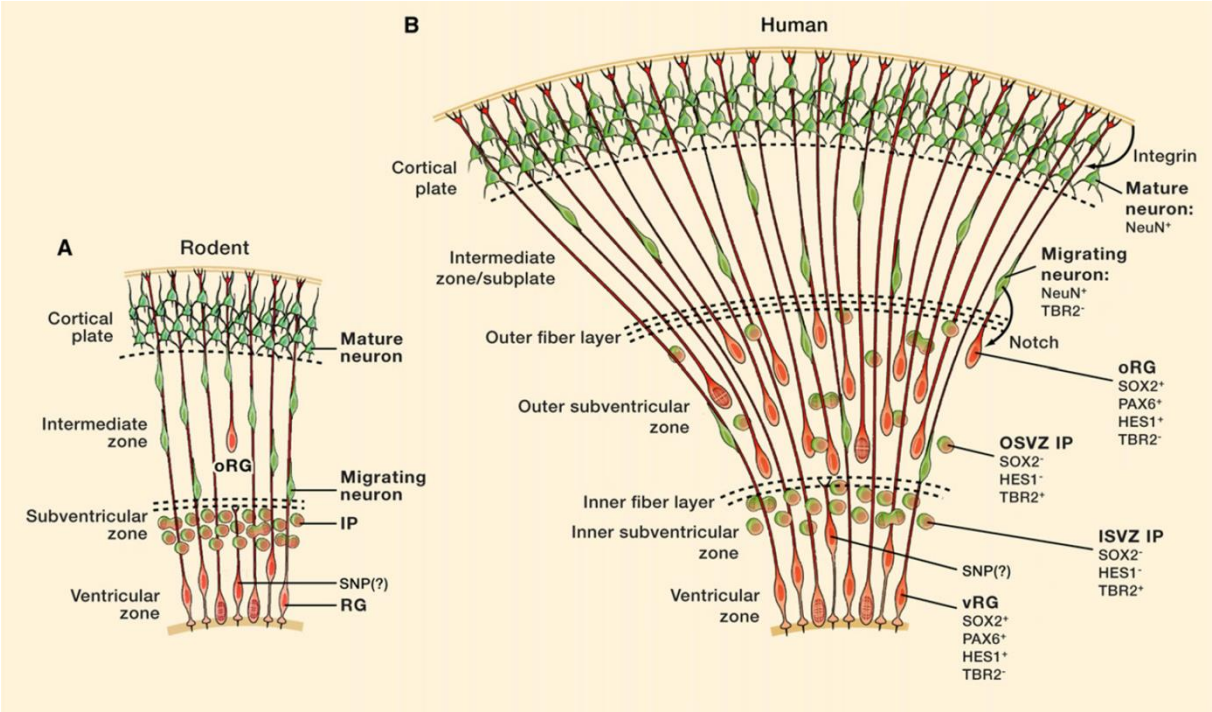

Figure 8 (A) Current view of rodent corticogenesis are illustrated. Radial glial (RG) cells most often generate intermediate progenitor (IP) cells that divide to produce pairs of neurons. These neurons use RG fibers to migrate to the cortical plate. The historical view of neocortical development was that RG and neuronal progenitor cells were lineally distinct and that RG did not have a role in neurogenesis. Our current appreciation of the lineage relationship between RG cells, IP cells, and neurons has revised this view. The recent observation that small numbers of outer subventricular zone radial glia-like (oRG) cells exist in the mouse is also illustrated. (B) We highlight the lineage of oRG cells, IP cells, and migrating neurons (red to green) present in the human outer subventricular zone (OSVZ) and the increased number of radial fibers that neurons can use to migrate to the cortical plate. The number of ontogenetic ‘‘units’’ is significantly increased with the addition of oRG cells over ventricular RG (vRG) cells. Maintenance of oRG cells by Notch and integrin signaling is shown. Short neural precursors (SNP), a transitional cell form between RG and IP cells, are also depicted in (A) and (B). Taken from Lui et al 2011

1.5 Hypothesis to explain brain expansion

Pasko Rakic built his explanation of brain size expansion on the radial unit hypothesis. In this, all neurons that are born by a neural stem cell in the germinal ventricular zone migrate along radial glia fibers, pass each other sequentially as the cortex develops in an inside-out manner, and finally form ontogenetic columns of genetically related and functionally connected neurons (Rakic 1988, Rakic 1995). According to this, an amplification of neural stem cells at early stages by symmetric self-renewing divisions would expand the initial pool for ontogenetic columns, thereby determining the surface of the ventricular zone and in consequence the cortex. With the onset of neurogenesis the rate of asymmetric

neurogenic divisions defines the thickness of the cortical plate, which is only mildly expanded in higher gyrified brains. In this model the convolutions in gyrified brains would result from physical tension exerted by fascicles from cortico-cortico and cortico-thalamic connections (Van Essen 1997, Rakic 2009). In line with the radial unit hypothesis mouse models that expand the pool of neuronal stem cells early in development, like KO mouse models of Caspase3/8 key enzymes in the apoptosis cascade (Kuida et al 1996, Kuida et al 1998) or constitutive active ß-catenin signalling (Chenn & Walsh 2002) should lead to gyrification in lissencephalic mice. However, these mouse models even though showing increased proliferation and foldings of the cortex, do not fulfil all criteria of gyrified brains, namely an increased expansion of the cortical surface from a size restricted ventricular zone.

In contrast to the radial unit hypothesis that linked cortical expansion and convolution to intense proliferation of VZ progenitor cells, Kriegstein and colleagues proposed a model of cortical surface expansion as a result of expanded proliferation of intermediate progenitors in a second proliferative zone basal to the ventricular zone, the SVZ. As these intermediate progenitors amplify neuronal numbers in abventricular position, cortical surface increases while ventricular surface remains small (Kriegstein et al 2006). This hypothesis was based on the discovery of neurogenesis by intermediate progenitors in the SVZ (Noctor et al 2004) and the observation that the size of the SVZ increased with the degree of gyrification in rat, ferret, primate and human (Martinez-Cerdeno et al 2006, Smart et al 2002, Zecevic et al 2005).

The discovery of a new neural progenitor subtype in the expanded SVZ of gyrified species added important functional views on the generation of cortical foldings (Hansen et al 2010, Fietz et al 2010, Reillo et al 2011). This RG type with polar morphology exhibits a long basal fiber, but in contrast to apically dividing RG lacks a ventricular contact. Like BPs this type of RG is dividing in a basal position and is therefore termed bRG to discriminate them from aRG (Hevner & Haydar 2012, Reillo & Borrell 2012). These bRG fulfill two main functions in the process of gyrification: (1) they act as long-term self-renewing progenitor in the I/OSVZ which they seed with further proliferating cells (Hansen et al 2010) and (2) the basal fibers of bRG serve as additional guidance scaffold for neurons generated in the SVZ. The fibers of bRG fill the space between diverging fibers of aRG

ensuring an equally spaced glial fiber scaffold in the expanded outer cortical surface (Reillo & Borrell 2012). However the existence of bRG is per se not sufficient to induce neurogenesis, as this cell type is also present at low numbers in the lissencephalic murine cortex (Shitamukai et al 2011, Wang et al 2011 and also in the lissencephalic primate, the common marmoset (Kelava et al 2012, Garcia-Moreno et al 2012). Rather both numbers of bRG and degree of SVZ proliferation (including BPs) need to be sufficient to lead to a gyrencephalic cortex (Reillo & Borrell 2012)

In summary, the expansion of brain regions, in this case the cerebral cortex, involves different phases during development: the expansion of the founder pool of neural stem cells by symmetric progenitor divisions during early phases, the shift towards neurogenesis from an increased progenitor pool in the I/OSVZ to allow growth of the cortical surface disproportionate to the ventricular surface and an appropriate scaffold of basal RG fibers that allows proper migration of neurons to the cortical plate (Rakic 2009, Reillo & Borrell 2012, Lui et al 2011).

1.5.1 Morphogenesis of the ganglionic eminences

The first visible protrusion from the GE into the lateral ventricle is the medial ganglionic eminence at E11 while the lateral ganglionic eminence is not yet morphologically distinct. By E12 the MGE further increases in size and at E13 both LGE and MGE are prominent bulges protruding into the ventricle. Later at E14 sulci clearly separate LGE both from the dorsal cortex as well as from the MGE. At E16/17 LGE and MGE lateral walls are fused with a loss of the sulcus between the two compartments leading to a uniform flat lateral ventricular wall at E18 (Smart 1976). At the early stage of E11 ventricular mitoses (APs) as well as non-surface mitosis at sub-ependymal position (in or at the basal end of the VZ) or at more basal positions like newborn neurons, are present in the LGE and MGE (Smart 1976, Sheth & Bhide 1997). This is accompanied by an increase in cell cycle length, particularly G1, from E11 to E12 which is also longer than that of cortical progenitors at this stage (Bhide 1996). In both GE divisions the number of non-surface mitoses, both within and basal to the VZ increased during development leading to the formation of a "subependymal proliferative compartment" now considered to be the subventricular zone

(SVZ). At midneurogenesis, E14, mitoses at non surface positions in the MGE already outnumber apical mitoses (57%; Smart 1976). In addition to a rapid increase in the progenitor pool also at non-surface positions already at an early stage (E11) a large fraction of mitoses generates postmitotic daughter cells (30-35%) which are neurons at this stage (Sheth & Bhide 1997). In summary the rapid formation of both ganglionic eminences involves both the early generation and expansion of a non-surface progenitor pool that is also accompanied by an early production of neurons in these compartments. My PhD work aimes to shed light on the cellular processes during development of the murine LGE at stages of midneurogenesis. The LGE has been selected as subject of investigation because its germinal zones give rise to resident neurons of the basal ganglia and less migratory interneurons (like in the MGE and CGE) and due to its direct lineage relationship to major parts of the adult neural stem cell niche, the subependymal zone of the lateral ventricle (Kriegstein & Alvarez-Buylla 2009).

2 Results

2.1 Characterization of progenitor cells in the developing lateral ganglionic eminence

This paragraph includes work published as an article entitled „Amplification of progenitors in the mammalian telencephalon includes a new radial glia cell type" by Gregor-Alexander Pilz, Atsunori Shitamukai, Isabel Reillo, Emilie Pacary, Julia Schwausch, Ronny Stahl, Jovica Ninkovic, Hugo J. Snippert, Hans Clevers, Leanne Godinho, Francois Guillemot, Victor Borrell, Fumio Matsuzaki and Magdalena Götz published in *Nature Communications* 4 (2013) p.2125

Summary: This study aimed to characterize stem and progenitor cells in the developing murine ventral telencephalon, the lateral ganglionic eminence. Quantification of dividing cells throughout neurogenesis revealed a large proportion of non-apically dividing cells including subapically dividing cells (SAPs) in both the LGE and MGE. Direct observation of progenitor cells was carried out by live imaging at E14 after in-utero electroporation of fluorescent protein expression plasmids. This revealed that the population of SAPs which is prominent in the LGE compared to the CTX is heterogeneous in types of their morphology during mitosis and even includes a bipolar subapically dividing RG. This subapical RG divides in the VZ and generates a bRG and a delaminating progenitor. Further, the imaging of RG lineages uncovered an enormous progenitor amplification via different intermediate progenitor steps (SNP and SAP), leading to large clone sizes at midneurogenesis. The SAP population specifically contributes to larger lineages of more than 4 cells. These clonal live imaging data were further confirmed, also in regard to the random localization of clones, by clonal fate mapping using the Glast::Cre^{ERT2} driver mouse line crossed to the multicolor reporter mouse line Confetti. In order to reveal a correlation of bipolar subapical progenitors to the generation of bRG in expanded germinal zones immunohistochemical analysis of progenitor morphology was carried out on embryonic tissue sections of species with gyrified cortices, namely the ferret and the sheep and a lissencephalic primate, the marmoset. This revealed that bipolar RG (bpRG), resembling morphologically subapical RG, are present in elevated numbers in the

expanded germinal zones of ferret and sheep and to a lesser extent in the primate with a smooth cortex. The acute downregulation of the nuclear protein TRNP1 leads to the expansion of the cortical SVZ and subsequently to the formation of gyri and sulci. To test whether also bpRG are involved in this process, the morphology of dividing cells was analyzed after acute TRNP1 knockdown in the cerebral neocortex using the GFP signal. Indeed the knockdown of TRNP1 led to a 25% increase in the number of bpRG. To investigate the regulation of SAPs, Ascl1, a transcription factor expressed in almost all SAPs, was acutely knocked out by electroporating Cre-GFP into the LGE of Ascl1-fl/fl embryos. This resulted in a specific reduction of proliferation amongst SAPs and BPs, but not APs in the LGE.

Author contributions to this publication

Gregor-Alexander Pilz carried out the experiments and analyzed the data unless otherwise stated. Astunori Shitamukai conveyed the long-term embryonic slice imaging method, assisted in performing the initial imaging experiments and analyzed parts of the cell cycle length analysis. Isabel Reillo performed the immunohistochemical studies in ferret, sheep and marmoset and did all related quantifications. The in-utero electroporation into the Ascl1 fl/fl mice and according quantifications were carried out by Emilie Pacary. Ronny Stahl provided the TRNP1 knockdown plasmid, helped with the in-utero electroporation and quantified the data after TRNP1 knockdown. Hans Clevers and Hugo J. Snippert provided the Confetti reporter mouse line and Julia Schwausch and Jovica Ninkovic helped to establish the clonal fate mapping paradigm. Francois Guillemot, Victor Borrell, Leanne Godinho and Fumio Matsuzaki gave conceptual support. Leanne Godinho co-supervised the study and started to establish embryonic brain slice imaging in the lab. Magdalena Götz designed, coordinated and funded the project and wrote the manuscript together with Gregor-Alexander Pilz.

nature COMMUNICATIONS

ARTICLE

Received 12 Nov 2012 | Accepted 7 Jun 2013 | Published 10 Jul 2013

DOI: 10.1038/ncomms3125

OPEN

Amplification of progenitors in the mammalian telencephalon includes a new radial glial cell type

Gregor-Alexander Pilz[1], Atsunori Shitamukai[2], Isabel Reillo[3], Emilie Pacary[4,†], Julia Schwausch[1], Ronny Stahl[5], Jovica Ninkovic[1], Hugo J. Snippert[6], Hans Clevers[6], Leanne Godinho[1,†], Francois Guillemot[4], Victor Borrell[3], Fumio Matsuzaki[2] & Magdalena Götz[1,5,7]

The mechanisms governing the expansion of neuron number in specific brain regions are still poorly understood. Enlarged neuron numbers in different species are often anticipated by increased numbers of progenitors dividing in the subventricular zone. Here we present live imaging analysis of radial glial cells and their progeny in the ventral telencephalon, the region with the largest subventricular zone in the murine brain during neurogenesis. We observe lineage amplification by a new type of progenitor, including bipolar radial glial cells dividing at subapical positions and generating further proliferating progeny. The frequency of this new type of progenitor is increased not only in larger clones of the mouse lateral ganglionic eminence but also in cerebral cortices of gyrated species, and upon inducing gyrification in the murine cerebral cortex. This implies key roles of this new type of radial glia in ontogeny and phylogeny.

[1] Institute of Stem Cell Research, Helmholtz Center Munich, Ingolstädter Landstr. 1, Neuherberg, 85764 Munich, Germany. [2] RIKEN Center for Developmental Biology, Chuo-ku, Kobe 650-0047, Japan. [3] Developmental Neurobiology Unit, Instituto de Neurociencias, Consejo Superior de Investigaciones Científicas—Universidad Miguel Hernández, Sant Joan d'Alacant 03550, Spain. [4] Division of Molecular Neurobiology, MRC National Institute for Medical Research, Mill Hill, London NW7 1AA, UK. [5] Physiological Genomics, University of Munich, Schillerstr. 46, 80336 Munich, Germany. [6] Hubrecht Institute for Developmental Biology and Stem Cell Research and University Medical Center Utrecht, Uppsalalaan 8, Utrecht 3584 CT The Netherlands. [7] Munich Cluster for Systems Neurology (SyNergy), Munich, Germany. †Present addresses: Biomolecular Sensors, Institute of Neuroscience, Technische Universität München, 80802 Munich, Germany (L.G.); Institut National de la Santé et de la Recherche Médicale, Neurocentre Magendie, Physiopathologie de la Plasticité Neuronale, U862, F-33000 Bordeaux, France; Université de Bordeaux, Neurocentre Magendie, Physiopathologie de la Plasticité Neuronale, U862, F-33000 Bordeaux, France (E.P.). Correspondence and requests for materials should be addressed to M.G. (email: Magdalena.goetz@helmholtz-muenchen.de).

Ontogenetic mechanisms in the developing brain are the basis for the increase in neuron numbers in specific brain regions during phylogeny. For example, higher neuron numbers settling in the increased, often gyrated mammalian neocortex arise from increased progenitor numbers during development. These progenitors are accommodated in additional germinal layers, like the inner and outer subventricular zone (i/oSVZ)[1–4] that are located basal to the ventricular zone (VZ), where progenitors are anchored at the ventricular surface (VS). In most regions of the CNS, the vast majority of progenitor cells are within the VZ, where cells possess an epithelial polarity and comprise the stem cells of the developing nervous system, the neuroepithelial cells and later radial glia (RGs)[5]. These undergo interkinetic nuclear migration (INM), with the soma migrating during different phases of the cell cycle towards the apical VS, where M-phase takes place. It has therefore been suggested that the area of the VS may be limiting for the numbers of possible mitoses, and further increase of progenitor numbers is only possible by accommodating these at more basal positions, such as in the SVZ[2,6]. A further possibility that had been postulated is to allow cells maintaining the epithelial hallmarks of stem cells to undergo M-phase at non-apical positions, thereby overcoming the apical space limitations[2]. However, such a progenitor type has been elusive so far and the mechanisms of extended SVZ formation are still ill understood.

Conversely, the cellular composition of the enlarged i/oSVZ has been unravelled in the recent years, and revealed a novel type of RG with long basal process, while lacking an apical anchoring, the basal radial glia (bRGs)[7–9]. These provide additional guiding structures for the higher neuronal numbers expanding the cerebral cortex surface in species with folded cerebral cortices (for reviews, see Borrell and Reillo[3] and Lui *et al.*[4]). However, despite recent progress[10,11], little is known about the cellular mechanisms involved in the generation of the bRGs and the expansion of the SVZ.

In order to gain some insights into these processes, we examined the ventral telencephalon, the region of the murine brain with the largest SVZ. This region forms the ganglionic eminences (GE), two bulges (the lateral GE (LGE) and the medial GE (MGE)) protruding into the ventricle[6]. LGE progenitors generate striatal projection neurons and olfactory bulb interneurons[12,13], that is, a particularly large number of neuronal progeny with the olfactory bulb interneurons continuing to be generated live long. Progenitors in the MGE also generate a large number of neurons, namely, most telencephalic interneurons migrating through the entire telencephalon except to the olfactory bulb, besides giving rise to projection neurons of the globus pallidus[14,15]. These regions are thus well suited to examine the mechanisms of enlarging the number of SVZ progenitors and subsequent neuronal progeny.

By live imaging of brain slices and immunostaining of mitotic cells in the GE, we here discover a novel progenitor type dividing within the VZ but at subapical positions. This includes cells with RG morphology, that is, a bipolar (bp) morphology with a basal and apical process visible during the M-phase, as previously predicted[2]. Such bpRGs are also present in the VZ but are further extended into the i/oSVZ of species with gyrated cerebral cortices. Consistent with their role in amplifying neuron numbers, they are enriched in larger clones generated in the murine ventral telencephalon and the cerebral cortex when gyrification is elicited.

Results

A majority of non-apical progenitors in the developing GE. While most progenitor cells divide at the apical surface (apical progenitors, AP) during brain development, this is strikingly different in the GE, where basally dividing cells (PH3+) gradually outnumber APs, reaching 60–70% in the LGE and MGE, respectively (Fig. 1a,c,d). We also noted non-surface mitoses within the VZ[6] (Fig. 1c), the zone of AP INM covering a distance of 11 cell diameters determined by live imaging (Supplementary Fig. S1a). These subapical progenitors (SAPs) (Fig. 1c) increase from 7% (LGE) and 10% (MGE) at E14 to over 20% of all mitoses at E16 in both these regions (Fig. 1d). Among the mitoses within the VZ, SAPs reached 47% in LGE and 54% in the MGE at E16. Conversely, mitoses at subapical or basal positions remained a minority throughout neurogenesis in the dorsal telencephalon (Fig. 1b,d).

Live imaging of progenitor cells in slices of the LGE. To unravel how these progenitor types dividing at different positions are lineally related, we performed live imaging of cells labelled with GFP-expressing plasmids by *in utero* electroporation (IUE) at E13. In slices of the LGE prepared 24 h later, we observed two types of APs (Fig. 1e) that undergo INM and mitosis at the VS: the classical RGs with a bipolar morphology encompassing a long radial process and an apical process reaching the VS that divide at the apical surface, with only their basal process visible in M-phase (Fig. 1f), and the 'short neural precursor cells' (SNPs)[16–18] that lack a longer basal process but possess an apical process, also undergoing INM and dividing at the VS without any process visible in M-phase (Fig. 2a, Supplementary Fig. S1b). Some cells with only an apical process did not reach the apical surface for mitoses but divided at some distance from the ventricle, at subapical positions (Fig. 1g, yellow arrowhead highlighting the apical process; Supplementary Movie 1). We also detected RGs with both apical and long basal processes during M-phase, dividing at subapical positions (Supplementary Fig. S1c; white arrowhead in scan through z-stack in Supplementary Movie 2). Some cells dividing at subapical positions within the VZ had only short processes and retracted these processes in M-phase, being entirely round and thus morphologically resembling basal progenitors (BPs) (Figs 1h and 2). While cells dividing within the VZ at apical or subapical positions were heterogeneous in their morphology, most cells dividing at further basal positions were multipolar in morphology, lacking any longer apical or basal contact resembling classical BPs (Fig. 1h) as described originally in the neocortex[5]. Thus, the novel population of SAPs is heterogeneous, comprising cells with only an apical process, both apical and basal processes or no longer processing in M-phase (summarized in Fig. 1i).

Given this heterogeneity in progenitor subtypes, we were interested to determine how these progenitor types are connected to each other during lineage progression. We approached this by using sparse clonal labelling[10] by plasmids containing Cre and 2 reporters behind a floxed stop cassette containing cytoplasmic GFP and a membrane-tagged Kasabian orange to visualize all cellular processes (see Supplementary Fig. S1d,e for examples of AP and BP morphology in M-phase). To ensure full process visualization, we imaged in the centre of the slice and started with a RG cell with its long fully-intact basal processes not reaching any of the cut surfaces (Supplementary Movie 3). This revealed a profoundly larger progeny of RGs within 48–56 h compared with the pattern of cell divisions reported for the neocortex at similar developmental stages[19], as almost all daughter cells of RGs continued to divide and no postmitotic cells emerged directly from the apically dividing RGs in the LGE (Fig. 2 and Supplementary Fig. S2a).

Moreover, this extended imaging time revealed a consistent sequence among the diverse progenitor types progressing from APs over SAPs to BPs (Fig. 2). An apically dividing RG always

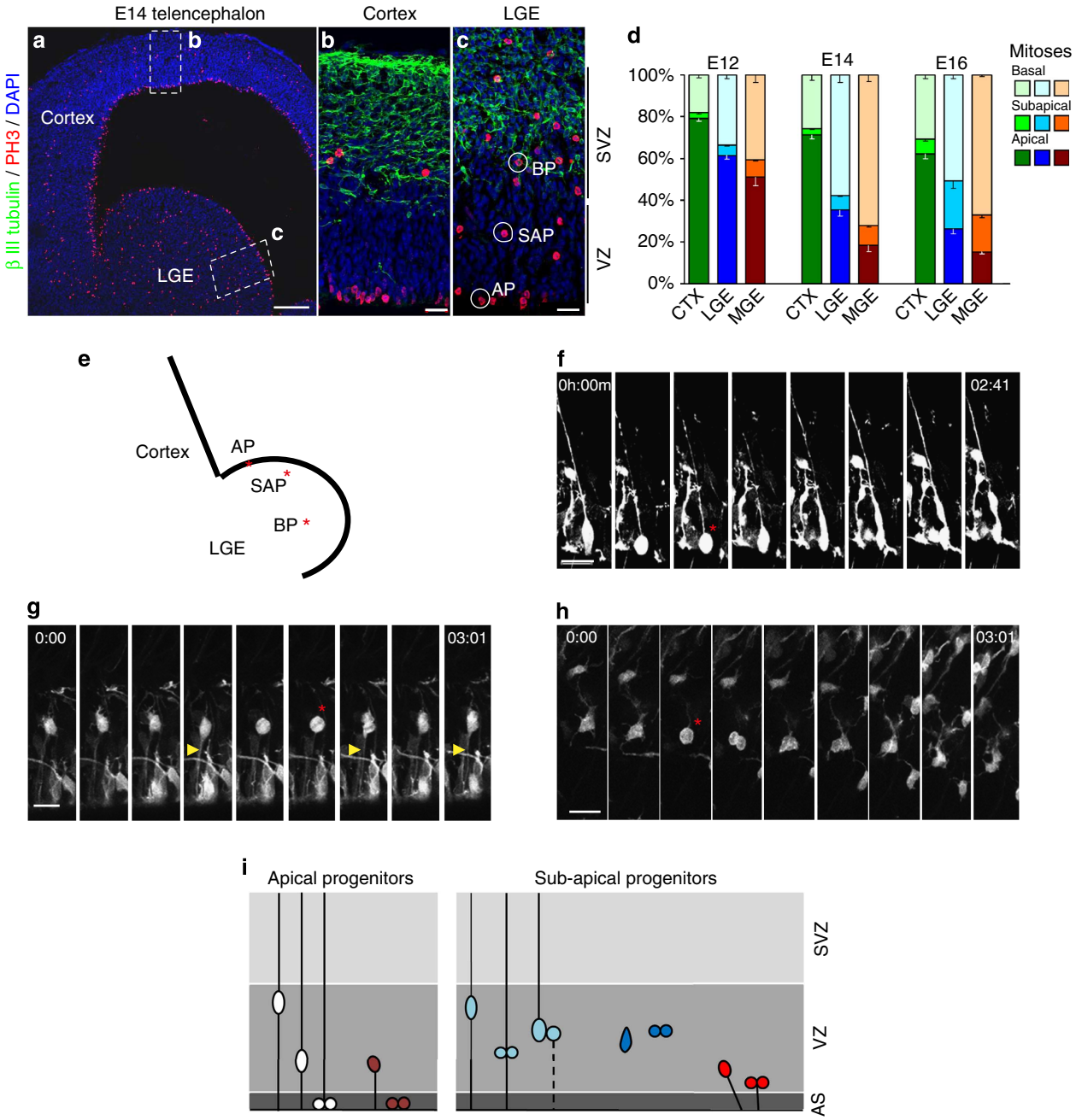

Figure 1 | Distribution of mitotic cells in the ventral telencephalon shows a dominance of non-apical mitoses. (**a**–**c**) Fluorescence micrographs of E14 mouse telencephalon sections immunostained for phosphorylated histone H3 (PH3, cells in mitosis) and βIII-tubulin (neurons) show the predominance of progenitors dividing apically (AP) in the dorsal telencephalon (cortex in **a**,**b**) in contrast to an abundance of non-apical mitoses comprising BP in the SVZ and cells dividing at subapical positions (SAP) within the VZ (**c**) in the lateral ganglionic eminence (LGE in **a**,**c**). (**d**) Histograms depicting the proportion of PH3+ cells dividing at the respective positions (cerebral cortex $n=1{,}201$ cells (E12), 1,498 (E14), 879 (E16); LGE: 594 (E12), 1,569 (E14), 1,069 (E16), three animals at each timepoint; data are mean ± s.e.m.; MGE: 1145 (E12), 1632 (E14), 1632 (E16)). (**e**) Scheme depicting the position of cells observed in mitosis at different positions (**f** apical, **g** subapical, **h** basal, red asterisks) by live imaging, with yellow arrowheads depicting processes (apical in **g**). Time is depicted in hours (h) and minutes (m). (**i**) Scheme illustrating the different VZ progenitor types (APs and SAPs) present in the LGE. Scale bars, 100 μm (**a**), 10 μm (**b**), 20 μm (**f**–**h**).

self-renewed and generated besides itself either an apically dividing SNP or a SAP (Fig. 2a,b,f,g,h and Supplementary Fig. S2a). These SNPs could either generate further SNPs or SAPs and the SAPs could in turn generate SAPs or basally dividing BPs, thereby mediating the lineage progression from apical (RGs and SNPs) through subapical to basal positions (Fig. 2a–h and Supplementary Fig. S2a). Notably, virtually all clones retained an apically dividing radial glia (Fig. 2a,b,f,g), the self-renewing ancestor of the amplifying intermediates.

A series of proliferative amplifying progenitors in the LGE. Importantly, this lineage observed by live imaging revealed various cellular mechanisms of amplifying progenitor numbers. This

included several proliferative, amplifying steps still within the VZ. In most cases, the direct progeny of apically dividing RGs divided again in the VZ (45/52 cells; Fig. 2; Supplementary Movies 4 and 5). These were either APs consisting of RGs or SNPs (SNP; red arrowhead in Fig. 2a t:10:20) or SAPs (Fig. 2a,b t: 35:26). Notably, SNPs also generated daughter cells that further proliferated within the VZ either as SNPs dividing at the apical surface (Fig. 2f,g) or as SAPs dividing at subapical positions (Fig. 2a,b). This is rather different from the cerebral cortex, where SNPs in majority directly generate postmitotic neurons[16–18] and SAPs had not been observed before. Progenitor amplification continued further with SAPs that generated, in most cases (64%, Supplementary Fig. S2b), daughter cells undergoing further divisions (Fig. 2a,b and Supplementary Movie 4). This

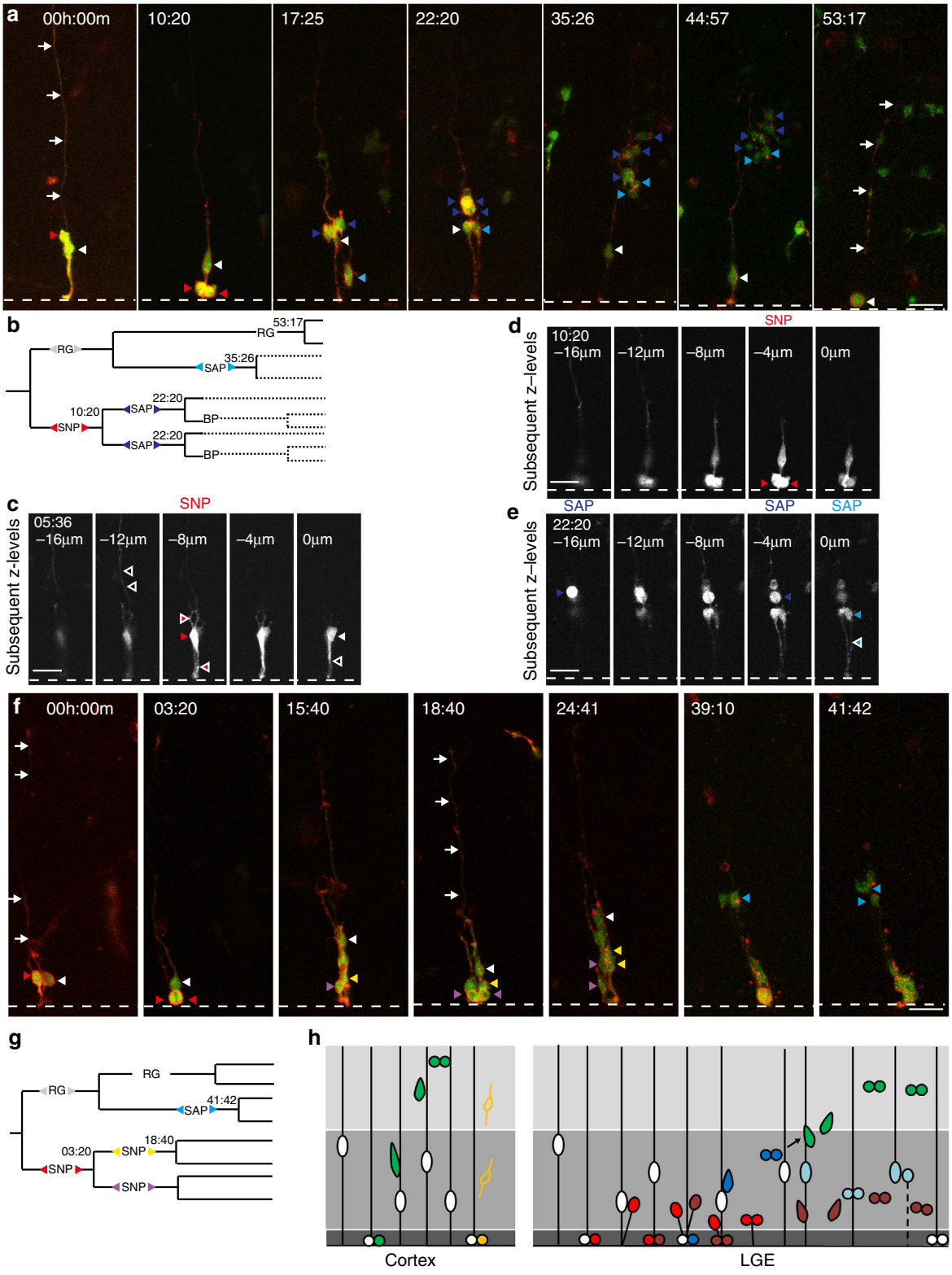

continuous generation of proliferative daughters in the LGE, first in the VZ at apical and subapical positions, and then in the SVZ, could result in as many as 11 daughter cells within 48 h of observation (Supplementary Movie 6 and Fig. 2a; 10 cells within 53 h). Additionally, we also detected proliferative divisions of BPs in the SVZ (Supplementary Fig. S3a and Supplementary Movie 7), rather than undergoing terminal divisions as in the cerebral cortex[19–21]. Thus, live imaging of progenitors in the LGE revealed several rounds of proliferative divisions at various positions, including a novel type of progenitor dividing at subapical locations within the VZ.

Cell cycle shortening in subsequent progenitor divisions. Live imaging further revealed a continuously faster cell cycle with each progenitor generation (Supplementary Fig. S2c). RGs had the longest cell cycle length (25 h mean), whereas their first daughter cells, the apically dividing SNPs or the SAPs, had a mean cell cycle length of 17 h (Supplementary Fig. S2c,d). The second-generation SAPs emerging from either SNPs or SAPs had a significantly shorter cell cycle of about 12 h (Supplementary Fig. S2d). Thus, independent of the progenitor subtype, the cell cycle length shortened with each generation in the LGE (Supplementary Fig. S2c), whereas it increased in cortical BPs imaged under the same conditions (Supplementary Fig. S2e; see also Arai *et al.*[22]). Taken together, besides a series of proliferative divisions the continuously faster cell cycle of the progeny serves to amplify the number of progeny generated in a given time—both hallmarks of the adult neural stem cell lineages[23] emerging from this region.

SAPs are enriched in larger LGE clones. However, not all cells observed by live imaging of the LGE generated a large number of progeny (see Supplementary Movie 8). In a total of 52 lineages observed live, the number of daughter cells ranged from 2 to 11 (Fig. 3a), with clones of either size distributed randomly along the dorsal to ventral axis of the LGE (Fig. 3b), thus lacking a preferential location suggestive of a particular neuronal progeny[13]. While the SAP-containing lineages also showed no specific spatial location, we noted a striking bias of SAPs contributing virtually always to larger clones (clone size ≥ 5, 90%, $n = 21$), whereas smaller size lineages (clone size < 5) contained SAPs only in a minority of cases (29%, $n = 31$). Thus, the presence of SAPs clearly predicts amplification of the progeny typically occurring in the lineage branch comprising the SAPs (Supplementary Fig. S2a). These data suggest that this novel progenitor type serves to amplify the progeny of RGs in the LGE, starting already in the VZ.

Characterization of SAPs in the LGE *in situ*. In order to determine the morphological heterogeneity of SAPs observed by live imaging in slices, also *in situ*, we first examined to what extent immunostaining for the phosphorylated form of vimentin (p-vimentin) reliably labels the major processes of mitotic cells[24]. Immunostaining 31 h after electroporation with a plasmid encoding a membrane-anchored form of GFP (plox-eGFP-farnesylated) showed that p-vimentin labelled in almost all cases the major processes of cells in mitoses (for examples of APs, SAPs and BPs see Supplementary Fig. S4a-c; for 3D reconstructions see Supplementary Movie 9). P-vimentin + cells at subapical positions were relatively frequent in the GE and exhibited a single major process directed either apically (Supplementary Fig. S4d, green arrow, 13%) or basally (Supplementary Fig. S4e, 7%), or were bipolar in M-phase with a major apical and basal process reminiscent of the subapically dividing RGs (Supplementary Fig. S4f, 24%; 3D reconstruction in Supplementary Movie 10). In addition, we also observed 55% of p-vimentin + cells at subapical positions lacking any major process labelling in M-phase (Supplementary Fig. S4d, yellow arrow). Thus, p-vimentin staining revealed a similar morphological heterogeneity of mitotic cells at subapical positions as that observed by live imaging, including a population with RG morphology. Accordingly, some SAPs were also immunopositive for radial glia markers, such as RC2 (Supplementary Fig. S4g), GLAST (Supplementary Fig. S4h) and hGFAP-GFP[25] (Supplementary Fig. S4i). Interestingly, SAPs were rarely positive for BLBP, which was confined to apically dividing radial glia (Supplementary Fig. S4j), but expressed Sox2, Dlx2, Pax6 and Ascl1 (Supplementary Figs S4k, S5a,b and S8a–c), well-known transcription factors in LGE progenitors.

Clonal heterogeneity in the LGE *in situ*. Next we aimed to examine the clone size *in situ* for comparison with the lineage size observed within 40–56 h by live imaging in slices. Towards this aim, we induced genetic recombination in a single RG *in vivo* by low doses of tamoxifen ($5\,\mu g\,g^{-1}$) in GLAST^{CreERT2} mice crossed to the multicolour reporter line Confetti[26]. Analysis of the progeny was performed at a comparable time interval of 2–3 days later. As no cluster contained cells of different colours ($n = 62$), the distinct clusters of cells labelled by the same fluorescent protein are considered as clones (Fig. 3c–q). Comparable to the live imaging data, clones comprised 2–10 cells ($n = 62$) and clones of different sizes were distributed broadly within the LGE (Fig. 3c) as observed by imaging in slices (Fig. 3b). The transcription factor Islet1 begins to be expressed in differentiating striatal projection neurons[13]. Islet1-immunoreactive cells were already observed in about 25% of all clones (10 of 42 clones) 63 h after induction of recombination in RGs. Most of these (80%) comprised

Figure 2 | Live imaging of apical progenitors and their progeny in the LGE. (**a**) Time-lapse series of a clone consisting of a RG (white arrowhead) and a SNP (lacking a basal process, red arrowhead). The SNP divides at the ventricle (dashed white line; two red arrowheads indicate M-phase) (t:10:20), giving rise to two SAPs (dark blue arrowheads) that divide again in the VZ (t:22:20). The RG also divides at the ventricle, giving rise to a RG and a SAP (white and blue arrowhead in t:17:25) that divides in the VZ (two blue arrowheads in t:35:26), whereas the RG undergoes mitosis at the ventricle (t:53:17; white arrowheads: basal process of RG). (**b**) Lineage diagram derived from the time-lapse movie in (**a**); note that BPs continued to proliferate in the SVZ, but could not be individually followed due to their fast movement and decreased GFP signal (dashed lines). Note that the length of the lines in (**b**) and (**g**) are not drawn to scale (time). (**c**–**e**) Single optical sections from z-stacks reveal details of the respective imaging timepoints indicated. Full arrowheads point to the cell body of progenitor cells and white outlined arrowheads point to the respective processes of cells. For example, the short basal and apical process of the SNP in (**a**) are shown in (**c**) at a different timepoint. (**f**) Time-lapse series illustrating the generation of multiple VZ progenitors coming from a single labelled cell. The SNP divides at the ventricle (red arrowheads; t:03:20), giving rise to two SNPs that divide again at the ventricle (red arrowheads at t:18:40). The RG (white arrowhead in t:03:20) gives rise to one RG and one SAP that divides between t:39:10 and t: 41:42 (blue arrowheads). (**g**) Lineage diagram derived from the time-lapse series in (**f**). Note that the two daughter SNPs generated by a SNP (red) divide at a very similar time point at the ventricle. Scale bars, 20 μm (**a**,**d**,**c**,**e**,**f**). (**h**) Scheme illustrating the progenitor lineage detected in the LGE in comparison with the neocortex. For a print-out of this figure please refer to Supplementary Fig. 9 with adjusted gamma value and both channels combined in grayscale to maintain the visibility of fine processes.

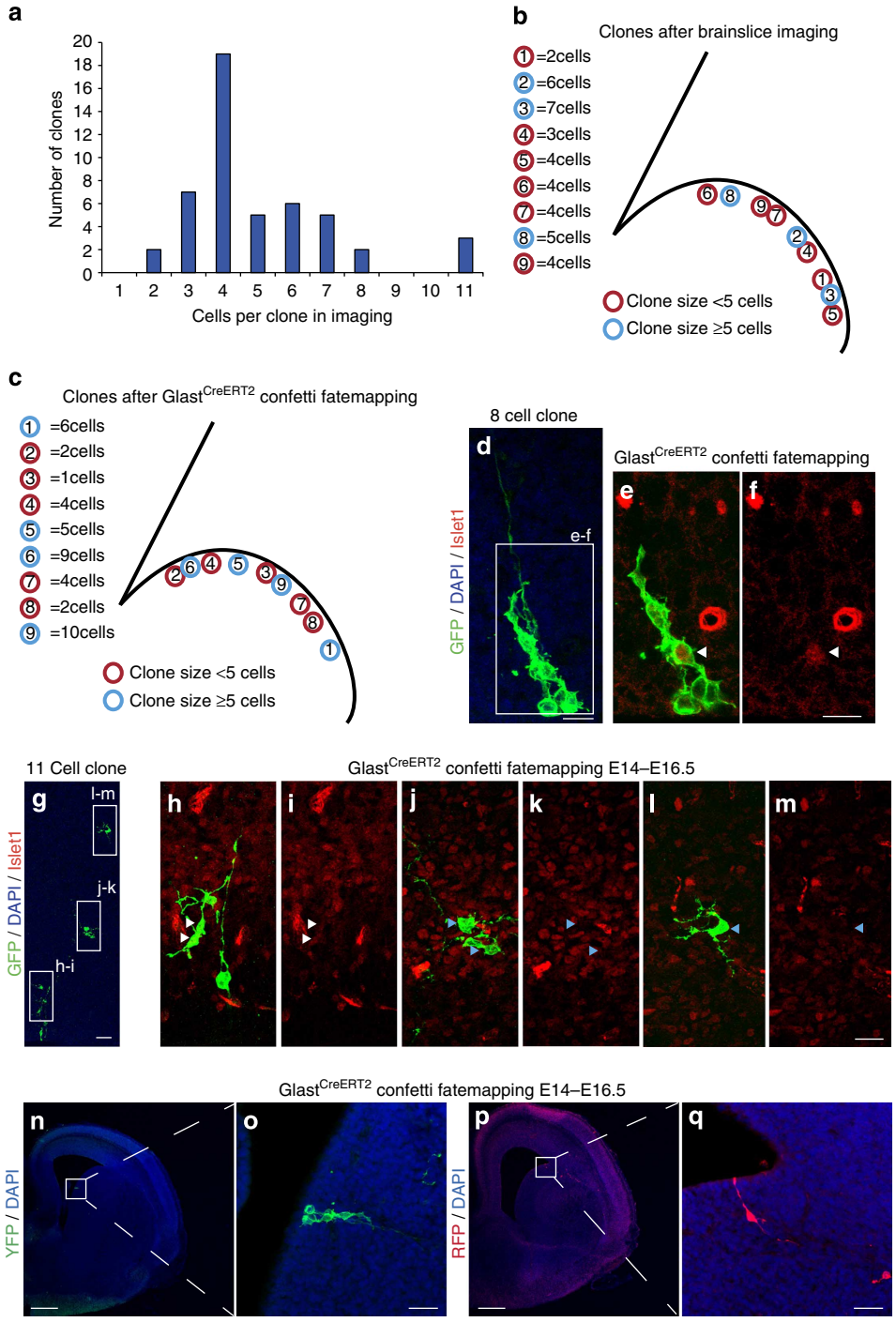

Figure 3 | Progenitors of different proliferative behaviour contribute to the striatal projection neuron lineage in the LGE. (**a**) Summary of clone sizes observed by live imaging (48–62 h) distributed as exemplified in the drawing in (**b**) for one imaging experiment (three slices). (**c**) Distribution of clones observed by genetic fate mapping *in situ* with micrographs of two examples of clones doublestained for Islet1 (red) (white arrowheads: double-positive cells; blue arrowheads: Islet1-negative cells) depicted in (**d**–**m**). (**n**–**q**) Examples of clonally labelled cells induced by TM in Glast^{CreERT2} Confetti reporter mice at E14. Scale bars, 200 μm (**f**,**g**), 50 μm (**e**), 20 μm (**d**,**f**,**m**,**n**–**q**).

more than 5 cells including larger clones with 11, 8 and 15 cells (Fig. 3d–m). Likewise, staining of slices post imaging revealed a daughter cell of a subapically dividing RG beginning to acquire Islet1 (Supplementary Fig. S5c,d). Thus, the heterogeneity of clones, including a contribution to the striatal lineage and the generation of up to 10 daughter cells within 48–56 h, was confirmed *in situ*.

SAPs in the VZ and SVZ of gyrated cortices. As the above analysis implied SAPs in the amplification of daughter cells in several brain regions and lineages, such as striatal neurons in the LGE and the lineage derivatives from the MGE (Fig. 1d), we next asked to what extent SAPs may also be relevant for the expansion of other brain regions, such as gyrated cerebral cortices in other mammalian species[4,27]. Indeed, PH3+ cells at subapical

positions were present in the VZ of the ferret cerebral cortex at postnatal day 2 (P2), accounting for 30% of all VZ divisions by P6 (Fig. 4a,b). Virus-GFP labelling revealed a morphological heterogeneity of cells in the VZ and iSVZ, with some having both basal and apical processes likely resembling the subapically dividing RGs in the murine LGE VZ (Fig. 4d,e). P-vimentin staining of mitotic cells confirmed this heterogeneity, with bipolar cells bearing apical and basal processes in M-phase and others having only one process, either apical or basal (Fig. 4c,g). Strikingly, RG-like p-vimentin+ cells with a basal and apical process extended also into the iSVZ and, to some extent, even to the oSVZ (Fig. 4c,g), that is, far beyond the regions where these cells were observed in the mouse (see also virus-GFP-labelled bipolar cells in Fig. 4f). Thus, bipolar RGs (bpRGs) dividing at non-apical positions can be detected not only in the VZ, but also in the iSVZ/oSVZ of the ferret. As these do not divide at subapical positions within the VZ, we refer to these more globally as bpRGs, thereby discriminating them from bRGs with only a basally oriented process (Fig. 4h,i) and apical RGs dividing at the VS.

To test for a correlation in the frequency of bpRGs and the gyrification index (GI) of the cerebral cortex, we examined the cerebral cortex of a near-lissencephalic primate, the marmoset[28,29], and a mammal with a particularly high GI, the sheep[9,30] (Fig. 4j), at equivalent stages of cortical development[9,28]. Within the VZ, SAPs were very infrequent in both marmoset (2%) and sheep (1%). However, only about 10% of all mitotic p-vimentin+

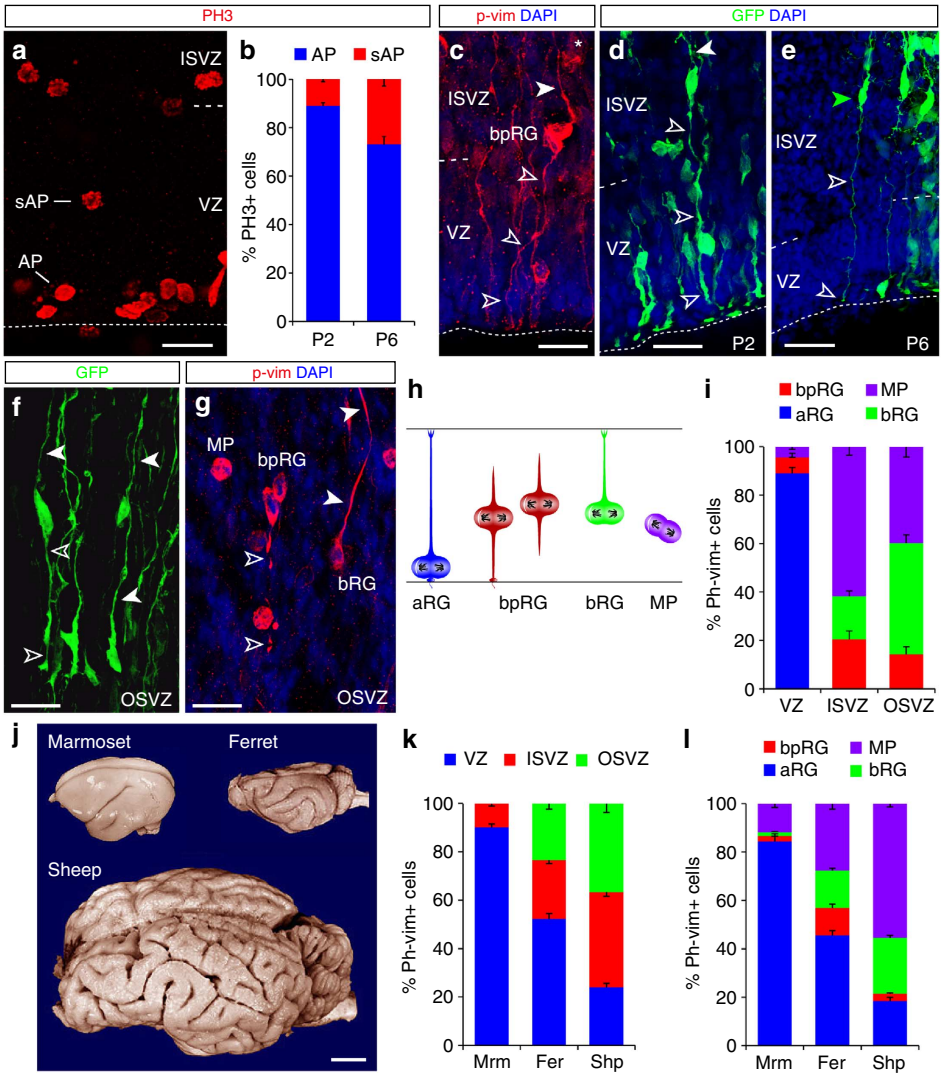

Figure 4 | Distribution of mitotic cells in the neocortex of gyrencephalic species shows a high abundance of bipolar radial glia. (**a**,**c**–**g**) Fluorescence micrographs of ferret neocortex sections (postnatal day 2, P2 (**c**,**d**,**f**,**g**) and P6 (**e**) immunostained as indicated (phosphorylated histone H3 = PH3; phosphorylated-vimentin = p-vim)), showing mitotic apical (AP) and subapical progenitors (SAP) within the VZ and ISVZ (**a**,**c**–**e**) and OSVZ (**f**,**g**). Progenitor cells in ISVZ and OSVZ displaying the typical morphology of bpRGs with a basal process (solid arrowheads) and a long apical process (open arrowheads) were revealed by Rv:*gfp* (**d**,**f**) or Adeno-*gfp* injection (**e**) or p-vim (**c**,**g**). Note also bRGs with only a basal process and multipolar progenitors (MP) without longer processes. Schematic drawings in (**h**) depict the defining characteristics of the different progenitor cell types analysed in the species indicated in (**j**); external view of the adult brains at scale. Histograms in (**b**,**i**,**k**,**l**) depict AP and bpRG, MP and bRG mitoses in the ferret VZ at P2 and P6 (**b**), $n = 982, 250$, respectively (three animals each), proportions of the cell types indicated in (**h**) defined by p-vim in P2 ferret neocortex (**i**), $n = 623$ cells in VZ, 290 ISVZ, 277 OSVZ (three animals), and in all germinative layers (**l**), the contribution of which is shown in (**k**), in the marmoset (Mrm), ferret (Fer) and sheep (Shp) at equivalent stages of cortical development (E85, P2, E65–67, respectively; marmoset, $n = 1{,}743$ cells; ferret, 1,190 cells; sheep, 2,435 cells; three subjects of each species). Data are mean ± s.e.m. Scale bars, 20 μm (**a**,**c**,**d**,**f**,**g**); 40 cm (**e**); 1 cm (**j**).

cells were located in the SVZ of the marmoset, whereas nearly 80% were located there in the sheep embryo (Fig. 4k). Thus, the number of bpRGs was quite large in the developing sheep neocortex even though their proportion is outnumbered by bRGs and BPs (Fig. 4l). Importantly, both bpRGs and bRGs were less than 4% of all cortical progenitors in the marmoset, whereas they comprise nearly 30% of the progenitor pool in the sheep at equivalent stages (Fig. 4l and Supplementary Fig. S6a). Thus, RGs with a bipolar morphology in M-phase dividing at subapical or further basal positions are more abundantly present in the developing cerebral cortex of species with higher gyrification.

Subapically dividing RGs generate bRGs in mouse LGE. Given the above observations, we next examined whether bpRGs dividing non-apically may generate bRGs that have been shown to be a key cell type in gyrification (for reviews, see Borrell and Reillo[3] and Lui *et al.*[4]). Indeed, we readily observed subapical RGs dividing asymmetrically, with a basal daughter cell maintaining the long basal process and an apical daughter cell inheriting the apical process (Supplementary Fig. S7a,b; Supplementary Movie 11; for scan through the z-stack of the mitotic subapical RGs in Supplementary Fig. S7b, see Supplementary Movie 3). These bRG daughter cells then moved further basally and divided within the SVZ (Supplementary Fig. S7a,b), sometimes twice (Supplementary Fig. S7c). Notably, both basal and subapically dividing RGs showed the characteristic pattern of initially apically-directed movements, followed by a fast basal movement and subsequent mitosis (Supplementary Fig. S7b, see also Hansen *et al.*[7], Shitamukai *et al.*[10] and Wang *et al.*[31]). Thus, besides acting as a further amplification step in the progeny amplification in the LGE, SAPs, in particular the subapically dividing RGs, generate bRGs, a key cell type for expansion and folding of the mammalian cerebral cortex.

Subapically dividing RGs increase upon Trnp1 knockdown. This then allowed us to investigate the emergence of subapically dividing RGs in a recent model of gyrification in the murine cerebral cortex[11]. Knockdown of Trnp1 in the mouse cerebral cortex not only results in radial expansion and often folding of the electroporated region[11], but also an expanded SVZ after 24 h (Fig. 5a). Given the expansion of the SVZ including 3x increased bRGs in this experimental model, we used live imaging to assess the abundance of bipolar subapically dividing RGs, the cell type directly generating bRGs in the GE. GFP+ cells were examined 24 h after electroporation with either a control vector or the shTrnp1 vector by immunohistochemistry for their bipolar morphology with longer basal and apical GFP+ processes during mitosis (PH3+) at non-apical positions (Fig. 5b). As expected, virtually no such cells could be detected with the control plasmid, whereas 20% of such cells were detected after knockdown of Trnp1 (Fig. 5c). Excitingly, these subapically dividing RGs could readily be observed in live imaging experiments starting 48 h after IUE in slices prepared 24 h after Trnp1 knockdown in the cerebral cortex (Fig. 5d). Interestingly, they recapitulated the behaviour described above for their counterparts in the LGE, with an initial apically directed movement (first hour in Fig. 5d), but undergoing cell division at subapical positions, that is, prior to reaching the apical surface, generating a basally translocating daughter bRG. Thus, Trnp1 knockdown further links the frequency of subapically dividing RGs to the emergence of bRGs and the extended SVZ even in the murine cerebral cortex.

Ascl1 expression and role in SAPs. To determine the molecular mechanisms regulating the higher numbers of SAPs in the murine LGE, we examined the transcription factor Ascl1, as it regulates progenitor amplification in this region[32]. As all SAPs were Ascl1+ (Supplementary Fig. S8a–c), its functional role was determined by Cre and control plasmid electroporation into the LGE of Ascl1 fl/+ and fl/fl embryos at E12. Interestingly, the proportion of GFP+ APs (PH3+ at the ventricular surface) examined 2 days later was not affected by the loss of Ascl1, whereas SAPs and BPs were significantly reduced in number (Supplementary Fig. S8e,f). Notably, Ascl1 immunoreactivity was also observed in about 30% of bipolar p-vimentin+ cells in the VZ, iSVZ and oSVZ of the ferret cerebral cortex (Supplementary Fig. S6b,c), consistent with Ascl1+ cells in VZ, iSVZ and oSVZ of the developing human cerebral cortex[33], implying Ascl1 in the amplification of non-apical progenitors in various species and brain regions.

Discussion

Taken together, in this study we unravelled several cellular mechanisms contributing to SVZ enlargement in the murine ventral telencephalon and discovered a novel population of progenitors amplifying the progenitor pool in a radial dimension. This involves progenitors that still divide within the VZ but do not return to the apical surface for mitosis, and rather divide at subapical positions. Some of these maintain an apical process and some even possess full RG morphology with both apical and basal processes and undergo mitosis at subapical positions. Intriguingly, such a progenitor cell had been predicted[2] to allow progenitor expansion beyond a limited apical surface[6], and is indeed particularly frequent in developing gyrated cerebral cortices as in ferret and sheep. Interestingly, in these species, RGs with a bipolar morphology in M-phase even extend beyond the VZ into i/oSVZ and thus further amplify in numbers. In summary, we provide four different lines of evidence linking the novel progenitor subset to SVZ and neuronal lineage amplification: (a) they are highly enriched in lineages of the murine LGE generating more than five daughter cells within 40–50 h of observation; (b) they are reduced in number in the murine LGE when SVZ expansion is decreased by deletion of Ascl1; (c) they are potently increased in number in the murine cerebral cortex when the SVZ is expanded by knockdown of Trnp1 and (d) they are increased in number in developing gyrated cerebral cortices of ferrets and sheep. Thus, SAPs are present in various forebrain regions, but their numbers significantly increase when radial expansion occurs and the number of neurons generated per time is increased. Moreover, we showed subapically dividing RGs to generate basal RGs, a cell type thought to be crucial for the expansion of the cerebral cortex in gyrification[3,4], suggesting that the former contribute to expand bRGs beyond the limitations of the ventricular surface, eventually leading to the hugely expanded i/oSVZ in animals with gyrified cortices[2,4,9]. Apically anchored, but subapically dividing cells may thus represent the first steps in overcoming the limitation of the apical surface, allowing further expansion of RG lineages in a non-linear fashion and thereby enabling (radial) expansion of specific brain regions.

Continuous live imaging of LGE progenitor cells further revealed general principles of generating an enlarged SVZ and neuronal output. In contrast to the cerebral cortex, shortening of cell cycle length occurs in subsequent intermediate progenitor cell divisions in the LGE (SNPs, SAPs, BPs), generating a larger number of progeny within a given time period. This differs from most observations in embryonic neurogenesis with subsequent rounds of division typically decreasing cell cycle speed. A second principle of lineage amplification emerging from live imaging in the LGE is repetitive proliferative divisions of all progenitor types. Importantly, both of these amplifying mechanisms are reminiscent of transient

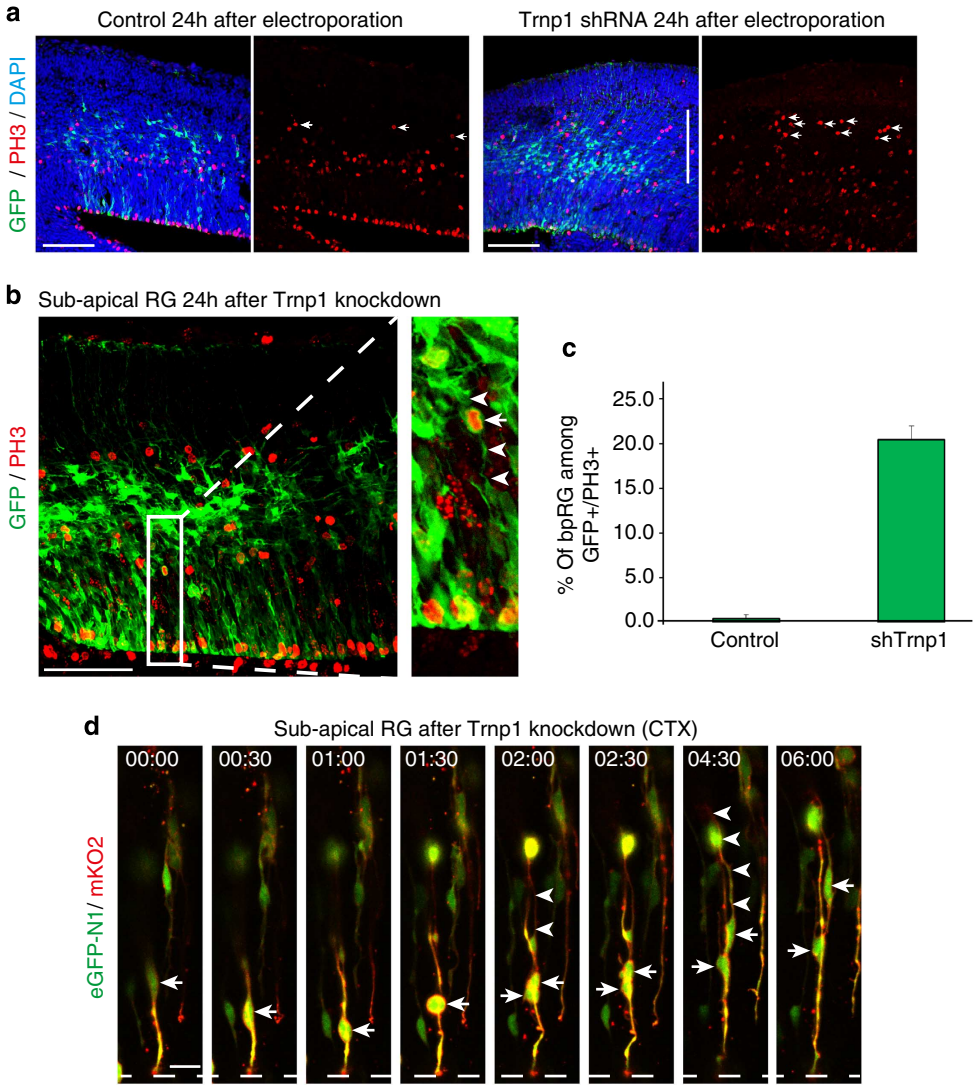

Figure 5 | The number of bipolar subapically dividing RGs is increased in Trnp1-shRNA electroporated cells in the developing mouse cerebral cortex. (**a**) Fluorescent micrograph of a section of embryonic day 14 cerebral cortex 24 h after *in utero* electroporation with either control plasmid (left) or Trnp1-shRNA-GFP plasmid (right). Note the expanded DAPI-dense OSVZ-like region (indicated by the white line in the third panel) with many proliferating (PH3+) cells (indicated by white arrows). (**b**) Subapical RGs after Trnp1 knockdown identified by PH3 (red) and bipolar morphology in M-phase (white arrows pointing to green, GFP-labelled processes). (**c**) Quantification of bipolar-GFP+/PH3+ RGs dividing at non-apical positions among all GFP+/PH3+ cells after Trnp1 knockdown in comparison with the control (control $n=159$ cells; Trnp1-shRNA $n=203$ cells, three animals in each condition; error bars are s.e.m.). (**d**) Still frames of a movie of a subapically dividing RG imaged 48 h after Trnp1-shRNA electroporation. Note the characteristic apically directed movement before dividing at subapical position (arrows point to cell somata, arrowheads towards the long basal process). Scale bars 100 μm (**a**,**b**), 20 μm (**d**).

amplifying progenitors observed with a faster cell cycle in the adult neural stem cell lineages[23], and may predispose this region to contribute to such a lineage in the adult brain.

In this regard, the clear hierarchy among the different progenitor cell types is also important. Radial glia always divided asymmetrically, with distinct daughter cell fates generating one branch amplifying the lineage and the other branch self-renewing themselves (see examples in Supplementary Fig. S2a). Thus, in the mouse LGE, the only self-renewing stem cells are apically dividing RGs, the founder cells of a clear hierarchy of further amplifying progenitors. The first progenitors generated from apical RGs are often SNPs, which we could observe to originate from RGs. Moreover, SNPs give rise to further amplifying progenitors in the LGE, rather than generating postmitotic neurons as suggested for murine cortical SNPs[17,18], thereby also contributing to lineage amplification. However, their presence is not restricted to the larger clones (≥ 5 cells), but SNPs also occur frequently in smaller lineages observed in the LGE (see Supplementary Fig. S2a).

Importantly, this is not the case for SAPs that were largely confined to lineages with larger progeny (≥ 5 cells). SAPs arise either from SNPs as a second intermediate progenitor type, or directly from apical RGs. SAPs proliferate further and generate an enlarged number of BPs and bRGs, the cell types forming the SVZ. BPs in the LGE often undergo proliferative divisions, thereby expanding the pool of SVZ progenitors, contrasting the situation in the mouse cerebral cortex[20,21,34,35]. This difference is also reflected by the proportion of BPs expressing Tis21-GFP, an indicator of terminal neurogenic divisions[34]. While the vast majority of BPs in the cerebral cortex is Tis21-GFP+ [34,36], it is rather a minority in the LGE (Supplementary Fig. S3b,c), further supporting the concept that only a minority undergoes terminal neurogenic divisions at mid-neurogenesis. An intriguing concept

emerging from the possibility of proliferative divisions at all progenitor levels in the LGE is that the number of progeny may be adjusted at each of these stages in the lineage, that is, apically by regulating SNP–SNP divisions, subapically by regulating SAP–SAP divisions and at basal positions by regulation of BP–BP divisions. This may be a mechanism adapting neuronal output by varying signals from several sources at different developmental stages.

RGs are only a subset of SAPs in the murine LGE, but they are special as only they generate bRGs, a key cell type required for gyrification, providing additional sources of neurons and RG guides to expand the cortical plate surface disproportional to the apical, ventricular surface[3,4,11]. Interestingly, this subset of bipolar RGs is particularly expanded in the cerebral cortex of species with a high GI and in the murine cerebral cortex upon Trnp1 knockdown. The latter results in more than 3 × increase in bRGs, the formation of an additional progenitor layer basal to the SVZ, reminiscent of the OSVZ, and even gyrus formation in the murine cerebral cortex[11]. Therefore these data support the concept that the bipolar RG subset serves in expanding SVZ progeny by generating bRGs in the gyrification process. Taken together, this novel progenitor cell has an important role in ontogeny and phylogeny.

Methods

Animals. C57BL/6J and Glast^{CreERT2} (ref. 37) crossed to Confetti reporter mice[26] were kept on a 12-h light–dark cycle. The day of the vaginal plug was considered as embryonic day (E) 0. Tamoxifen (5 μg g^{-1} bodyweight) was injected intraperitoneally. Animal experiments were performed according to the institutional and legal guidelines and were approved by the government of Upper Bavaria, the RIKEN Center for Developmental Biology, the Japanese government and by the local ethical review process (http://www.nimr.mrc.ac.uk/animals-in-research/ethical-review-process/).

IUE and plasmids. IUEs were carried out on anaesthetized time-pregnant mice with the uterine horn constantly rinsed with Ringer solution (Braun) as described previously[36]. For short-term imaging, the plasmids pCIG2 (cytoplasmic GFP; gift from Dr C. Schuurmans) and pCAGGs-GAP43-GFP (ref. 38) were injected at a final concentration of 1 μg μl^{-1} each, together with Fast Green (2.5 μg μl^{-1}; Sigma) into the lateral ventricles of the embryos, and electroporated with 5 pulses applied at ~40 mV for 50 ms each at intervals of 100 ms by an ElectroSquireportator T830 (Harvard Apparatus). For long-term imaging, the plasmids pCAG-Floxp-EGFP-N1 and pCAG-Floxp-mKO2-F (both 0.5–0.8 μg μl^{-1}) together with a low concentration of pCAGCre (0.05–0.3 ng μl^{-1}) were electroporated with the same settings as above. The low concentration of Cre plasmid allowed sparse labelling of progenitor cells due to a recombination of a floxed stop cassette by the Cre recombinase in single cells, as also described in Shitamukai *et al.*[10] For labelling of cellular processes the plasmid pCAG-Floxp-EGFP-farnesylated (0.5–0.8 μg μl^{-1}) was co-electroporated together with a low concentration of pCAGCre (8 ng μl^{-1}).

Slice culture imaging. Slices of the embryonic telencephalon were cut at a thickness of 300 μm on a vibratome (Leica VT1200S or DSK) in ice-cold DMEM (Sigma) gased with oxygen (95%), immersed in a collagen-based matrix (Nitta Gelatin), covered with neurobasal medium with supplements and imaged in a gas (5% carbondioxide) floated wet chamber for short-term imaging (Fig. 1; as also described in Asami *et al.*[36]). For longer-term imaging (Fig. 2; as also described in Shitamukai *et al.*[10]) slices were embedded in the collagen matrix on a filter membrane (Millipore) and the medium consisted of DMEM-F12 (Sigma), 5% fetal calf serum, 5% horse serum, N2 supplement (1:100; Invitrogen), B27 supplement (1:50; Invitrogen), GlutaMax (1:100; Invitrogen), PenStrep (100 U ml^{-1}). Imaging was performed on a confocal laser scanning microscope (FV1000, Olympus) using a 40 × long working distance objective (LUMPlanFl NA0.8, Olympus) and immersion oil for water dipping lenses (Immersol W; Zeiss). During imaging, slices were incubated in a stage-top incubator (Tokai Hit) at 37 °C in a 40% oxygen/5% carbondioxide atmosphere. The time interval between each time point was 20 min. In order to avoid the imaging of cellular artefacts, the first 20 μm of each slice were not recorded. In addition, brightfield images were taken at the same time to monitor the integrity of the slice.

Immunohistochemistry. Whole heads (E12) or mouse embryonic brains from the respective strains (E14–E16) were fixed in paraformaldehyde (PFA; 4% in PBS) for 1 (E12), 2 (E14) or 4 (E16) h. Brains were then either cryoprotected in 30% sucrose in PBS overnight and embedded in Tissue-Tek (Sakura) for sectioning at the cryostat (20–30-μm-thick), or embedded in 3% agarose (Biozym) in PBS for sectioning at the vibratome (70–100-μm-thick). Immunostaining on cryosections was performed by incubating the primary antibody overnight at 4 °C (in TBS with 0.5% Triton-X and 10% normal goat serum), while the vibratome sections were incubated longer (for 2 days, due to the larger thickness of the sections), with the primary antibodies used at the following concentrations: anti-Ascl1 (Developmental Hybridoma Bank, IgG1, 1:200), anti-βIII-tubulin (Sigma, mouse IgG2b, 1:200), anti-GFP (Sigma, chicken, 1:1,000), anti-Glast (Chemicon, Guinea pig, 1:400), anti-Islet1 (Hybridoma Bank, IgG2, 1:50), anti-Pax6 (Chemicon, rabbit, 1:400), anti-pericentrin (Covance, rabbit, 1:1,000), anti-phosphorylated histone H3 (Biomol, rabbit, 1:400), anti-Dlx2 (Millipore, rabbit, 1:200), anti-p-vimentin (MBL, mouse IgG2b, 1:500) RC2 (mouse, IgM, 1:500, kind gift of P. Leprince) and the Sox2 antibody (Millipore, rabbit, 1:500). After washing three times with PBS, sections were incubated with the respective fluorochrome-labelled secondary antibodies overnight, washed again, incubated in DAPI (1/1000; Sigma) and embedded after further washes in Aqua Polymount (Polyscience). Images were taken and analysed using a FV1000 confocal laser scanning microscope (FV1000; Olympus).

Pigmented ferrets (*Mustela putorius furo*) were obtained from Marshall Farms (North Rose, NY) and kept on a 12:12-h light:dark cycle at the Animal Facilities of the Universidad Miguel Hernández, where animals were treated according to the Spanish and EU regulations, and experimental protocols were approved by the Universidad Miguel Hernández IACUC. Viral injections were performed 24 h after the ferrets were born, on individuals of both sexes. Live sheep embryos of both sexes were obtained from the slaughter house MURGACA (Cartagena, Spain) with permission, and under the supervision of the veterinary in chief. The age of the collected embryos was determined *a posteriori* based on the crown-rump length as described[39]. Measurements on sheep embryos were carried out before perfusion. Fixed embryonic brains of common marmoset (*Callithrix jacchus;* no sex preference) were obtained from the Wisconsin National Primate Center in Madison, WI, USA. The stage of pregnancy was determined on the basis of breeding time and embryo size.

Single and double immunostains were performed on 50-μm-thick free-floating sections. Sections were blocked and incubated in the following primary antibodies overnight at 4 °C: anti-phosphohistone 3 (1:1,000, Upstate), anti-phosphovimentin (1:1,000, Abcam), chicken anti-GFP (1:1,000, Aves) and anti-Ascl1 (1:500, Abcam). Sections were then incubated with appropriate fluorescently conjugated secondary antibodies (Chemicon and Jackson) and counterstained with DAPI (SIGMA). Confocal images were acquired using a confocal spectral microscope Leica SP2 AOBS, taken as 0.8-μm (× 40) single optical sections, which were then compressed using their maximum projection. Conventional fluorescence microscopy images were obtained using a Leica CTR5000 microscope.

Cortical layers were determined as described in Reillo *et al.*[9] and Kelava *et al.*[28] Shortly, the VZ was defined as the pseudostratified epithelial layer with constant thickness. The ISVZ lies basally to the VZ, also has a high cell density but no columnar organization. The OSVZ is defined as the columnar cell-sparse layer basal to the ISVZ-containing proliferating cells. The intermediate zone (IZ) is a layer of very low density with virtually no mitotic cells, including the subplate (SP). The cortical plate (CP) was defined as the high-dense layer located between IZ and mantle zone (MZ), including the already formed layers 5 and 6. PH3 + and Ph-Vim + cells were counted from rectangular sectors of the cortex spanning its entire thickness, using Neurolucida and Neurolucida Explorer software (Microbrightfield).

G*fp*-encoding Retrovirus (Rv:*gfp*) and Adenovirus (Adeno:*gfp*) stocks were injected in the outer SVZ and cortical plate, respectively, of the postnatal ferret kits, as described previously[9]. Shortly, the ferret kits were deeply anaesthetized with isoflurane 1.5%. Two microlitres of Rv:*gfp* was injected into the OSVZ. The Adeno:*gfp* was injected into the CP at the age of P4 in several locations to amplify the labelling. All these injection sites were defined by stereotaxic coordinates and the operations were approved by the Universidad Miguel Hernández IACUC All kits were overdosed with pentobarbital and perfused with 4% PFA, and brains were postfixed overnight. Free-floating sections (50 μm thickness) were obtained by cryotome sectioning.

References

1. Dehay, C. & Kennedy, H. Cell-cycle control and cortical development. *Nat. Rev. Neurosci.* **8,** 438–450 (2007).
2. Fish, J. L., Dehay, C., Kennedy, H. & Huttner, W. B. Making bigger brains-the evolution of neural-progenitor-cell division. *J. Cell. Sci.* **121,** 2783–2793 (2008).
3. Borrell, V. & Reillo, I. Emerging roles of neural stem cells in cerebral cortex development and evolution. *Dev. Neurobiol.* **72,** 955–971 (2012).
4. Lui, J. H., Hansen, D. V. & Kriegstein, A. R. Development and evolution of the human neocortex. *Cell* **146,** 18–36 (2011).
5. Götz, M. & Huttner, W. B. The cell biology of neurogenesis. *Nat. Rev. Mol. Cell. Biol.* **6,** 777–788 (2005).
6. Smart, I. H. A pilot study of cell production by the ganglionic eminences of the developing mouse brain. *J. Anat.* **121,** 71–84 (1976).
7. Hansen, D. V., Lui, J. H., Parker, P. R. & Kriegstein, A. R. Neurogenic radial glia in the outer subventricular zone of human neocortex. *Nature* **464,** 554–561 (2010).

8. Fietz, S. A. *et al.* OSVZ progenitors of human and ferret neocortex are epithelial-like and expand by integrin signaling. *Nat. Neurosci.* **13,** 690–699 (2010).
9. Reillo, I., de Juan Romero, C., Garcia-Cabezas, M. A. & Borrell, V. A role for intermediate radial glia in the tangential expansion of the mammalian cerebral cortex. *Cereb. Cortex.* **21,** 1674–1694 (2011).
10. Shitamukai, A., Konno, D. & Matsuzaki, F. Oblique radial glial divisions in the developing mouse neocortex induce self-renewing progenitors outside the germinal zone that resemble primate outer subventricular zone progenitors. *J. Neurosci.* **31,** 3683–3695 (2011).
11. Stahl, R. *et al.* Trnp1 regulates expansion and folding of the mammalian cerebral cortex by control of radial glial fate. *Cell* **153,** 535–549 (2013).
12. Olsson, M., Bjorklund, A. & Campbell, K. Early specification of striatal projection neurons and interneuronal subtypes in the lateral and medial ganglionic eminence. *Neuroscience* **84,** 867–876 (1998).
13. Stenman, J., Toresson, H. & Campbell, K. Identification of two distinct progenitor populations in the lateral ganglionic eminence: implications for striatal and olfactory bulb neurogenesis. *J. Neurosci.* **23,** 167–174 (2003).
14. Flandin, P., Kimura, S. & Rubenstein, J. L. The progenitor zone of the ventral medial ganglionic eminence requires Nkx2-1 to generate most of the globus pallidus but few neocortical interneurons. *J. Neurosci.* **30,** 2812–2823 (2010).
15. Nobrega-Pereira, S. *et al.* Origin and molecular specification of globus pallidus neurons. *J. Neurosci.* **30,** 2824–2834 (2010).
16. Gal, J. S. *et al.* Molecular and morphological heterogeneity of neural precursors in the mouse neocortical proliferative zones. *J. Neurosci.* **26,** 1045–1056 (2006).
17. Stancik, E. K., Navarro-Quiroga, I., Sellke, R. & Haydar, T. F. Heterogeneity in ventricular zone neural precursors contributes to neuronal fate diversity in the postnatal neocortex. *J. Neurosci.* **30,** 7028–7036 (2010).
18. Tyler, W. A. & Haydar, T. F. Multiplex genetic fate mapping reveals a novel route of neocortical neurogenesis, which is altered in the Ts65Dn mouse model of Down syndrome. *J. Neurosci.* **33,** 5106–5119 (2013).
19. Kriegstein, A. & Alvarez-Buylla, A. The glial nature of embryonic and adult neural stem cells. *Annu. Rev. Neurosci.* **32,** 149–184 (2009).
20. Noctor, S. C., Martinez-Cerdeno, V., Ivic, L. & Kriegstein, A. R. Cortical neurons arise in symmetric and asymmetric division zones and migrate through specific phases. *Nat. Neurosci.* **7,** 136–144 (2004).
21. Miyata, T. *et al.* Asymmetric production of surface-dividing and non-surface-dividing cortical progenitor cells. *Development* **131,** 3133–3145 (2004).
22. Arai, Y. *et al.* Neural stem and progenitor cells shorten S-phase on commitment to neuron production. *Nat. Commun.* **2,** 154 (2011).
23. Costa, M. R. *et al.* Continuous live imaging of adult neural stem cell division and lineage progression in vitro. *Development* **138,** 1057–1068 (2011).
24. Kamei, Y. *et al.* Visualization of mitotic radial glial lineage cells in the developing rat brain by Cdc2 kinase-phosphorylated vimentin. *Glia* **23,** 191–199 (1998).
25. Malatesta, P. *et al.* Neuronal or glial progeny: regional differences in radial glia fate. *Neuron* **37,** 751–764 (2003).
26. Snippert, H. J. *et al.* Intestinal crypt homeostasis results from neutral competition between symmetrically dividing Lgr5 stem cells. *Cell* **143,** 134–144 (2010).
27. Reillo, I. & Borrell, V. Germinal zones in the developing cerebral cortex of ferret: ontogeny, cell cycle kinetics, and diversity of progenitors. *Cereb. Cortex.* **22,** 2039–2054 (2012).
28. Kelava, I. *et al.* Abundant occurrence of basal radial glia in the subventricular zone of embryonic neocortex of a lissencephalic primate, the common marmoset Callithrix jacchus. *Cereb. Cortex.* **22,** 469–481 (2012).
29. Garcia-Moreno, F., Vasistha, N. A., Trevia, N., Bourne, J. A. & Molnar, Z. Compartmentalization of cerebral cortical germinal zones in a lissencephalic primate and gyrencephalic rodent. *Cereb. Cortex.* **22,** 482–492 (2012).
30. Pillay, P. Manger PR. Order-specific quantitative patterns of cortical gyrification. *Eur. J. Neurosci.* **25,** 2705–2712 (2007).
31. Wang, X., Tsai, J. W., LaMonica, B. & Kriegstein, A. R. A new subtype of progenitor cell in the mouse embryonic neocortex. *Nat. Neurosci.* **14,** 555–561 (2011).
32. Castro, D. S. *et al.* A novel function of the proneural factor Ascl1 in progenitor proliferation identified by genome-wide characterization of its targets. *Genes Dev.* **25,** 930–945 (2011).
33. Jakovcevski, I., Mayer, N. & Zecevic, N. Multiple origins of human neocortical interneurons are supported by distinct expression of transcription factors. *Cereb. Cortex.* **21,** 1771–1782 (2011).
34. Haubensak, W., Attardo, A., Denk, W. & Huttner, W. B. Neurons arise in the basal neuroepithelium of the early mammalian telencephalon: a major site of neurogenesis. *Proc. Natl Acad. Sci. USA* **101,** 3196–3201 (2004).
35. Wu, S. X. *et al.* Pyramidal neurons of upper cortical layers generated by NEX-positive progenitor cells in the subventricular zone. *Proc. Natl Acad. Sci. USA* **102,** 17172–17177 (2005).
36. Asami, M. *et al.* The role of Pax6 in regulating the orientation and mode of cell division of progenitors in the mouse cerebral cortex. *Development* **138,** 5067–5078 (2011).
37. Mori, T. *et al.* Inducible gene deletion in astroglia and radial glia—a valuable tool for functional and lineage analysis. *Glia* **54,** 21–34 (2006).
38. Attardo, A., Calegari, F., Haubensak, W., Wilsch-Brauninger, M. & Huttner, W. B. Live imaging at the onset of cortical neurogenesis reveals differential appearance of the neuronal phenotype in apical versus basal progenitor progeny. *PLoS One* **3,** e2388 (2008).
39. Noden, D. M. & deLahunta, A. The embryology of domestic animals. *Developmental Mechanisms and Malformations* (Williams and Wilkins, Baltimore, 1985).
40. Alexandre, P., Reugels, A. M., Barker, D., Blanc, E. & Clarke, J. D. Neurons derive from the more apical daughter in asymmetric divisions in the zebrafish neural tube. *Nat. Neurosci.* **13,** 673–679 (2010).

Acknowledgements

We thank A. Steiner-Mezzadri, A. Waiser, E. Baumgart and T. Ötztürk for their excellent technical assistance and members of the Götz lab for their helpful discussion on the manuscript and the German research foundation (DFG) for its funding.

Author contributions

G.A.P., A.S., I.R., E.P. and R.S. performed the experiments and analysed the data. H.J.S. and H.C. provided Confetti reporter mice, and J.S. and J.N. established Confetti fate mapping analysis in the lab. F.G., L.G., V.B. and F.M. cosupervised parts of the project. M.G. designed and supervised the study. M.G. and G.A.P. wrote the manuscript.

Additional information

Supplementary Information accompanies this paper at http://www.nature.com/naturecommunications

Competing financial interests: The authors declare no competing financial interests.

Reprints and permission information is available online at http://npg.nature.com/reprintsandpermissions/

How to cite this article: Pilz, G.-A. *et al.* Amplification of progenitors in the mammalian telencephalon includes a new radial glial cell type. *Nat. Commun.* 4:2125 doi: 10.1038/ncomms3125 (2013).

Supplementary figure S1

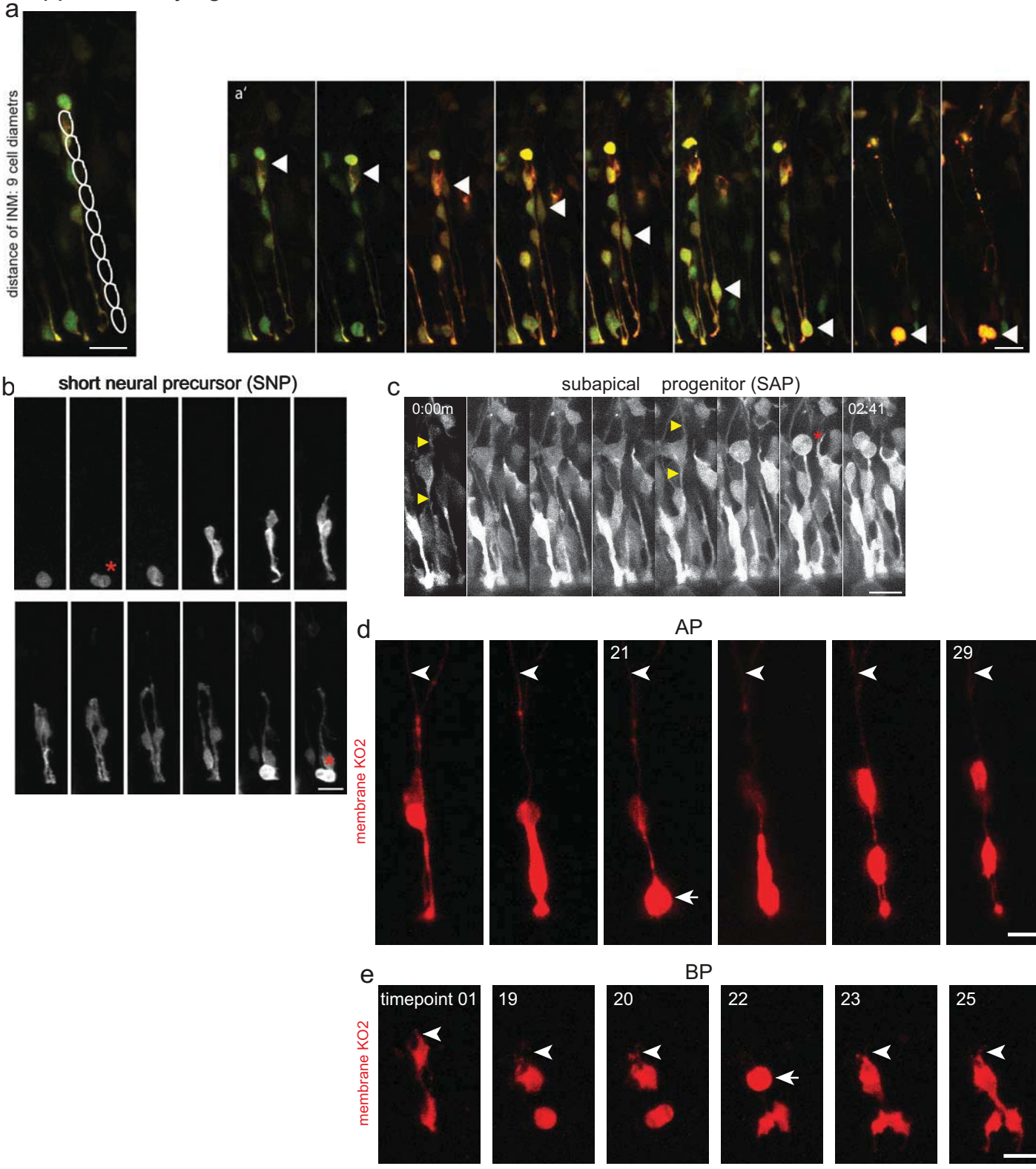

The extent of interkinetic nuclear migration in the LGE defining VZ and SNP/SAP progenitor subtypes extracted from imaging
(a) Example of soma positions (white circles) of a radial glia cell undergoing interkinetic nuclear migration towards the ventricle. White circles in a illustrate the distance travelled as a measure of cell diameters. INM was observed during live imaging in slices. (Single time-lapse pictures of a are depicted in (a'), time-frame is 20min. Note that interkinetic nuclear migration comprises between 8-11 cell diameters, which was used as definition for the ventricular zone thickness. (b) Single timeframes taken from a slice imaging experiment depicting a short neural precursor dividing two times (red asterix). Notably, after the first division, 2 SNP daughter cells are generated (time frame 20min; different timepoints selected, time difference not equal). (c) Images of a bipolar, RG like SAP, that divides in sub-apical position (yellow arrowheads point to apical and basal processes; red asterix marks the cells in m-phase). (d,e) Examples of an AP and BP labeled with a membrane bound form of Kasabian orange (arrows point at cells in M-phase, arrowheads to labeled processes of the cells). Scale bars (a-e): 20µm.

Supplementary figure S2

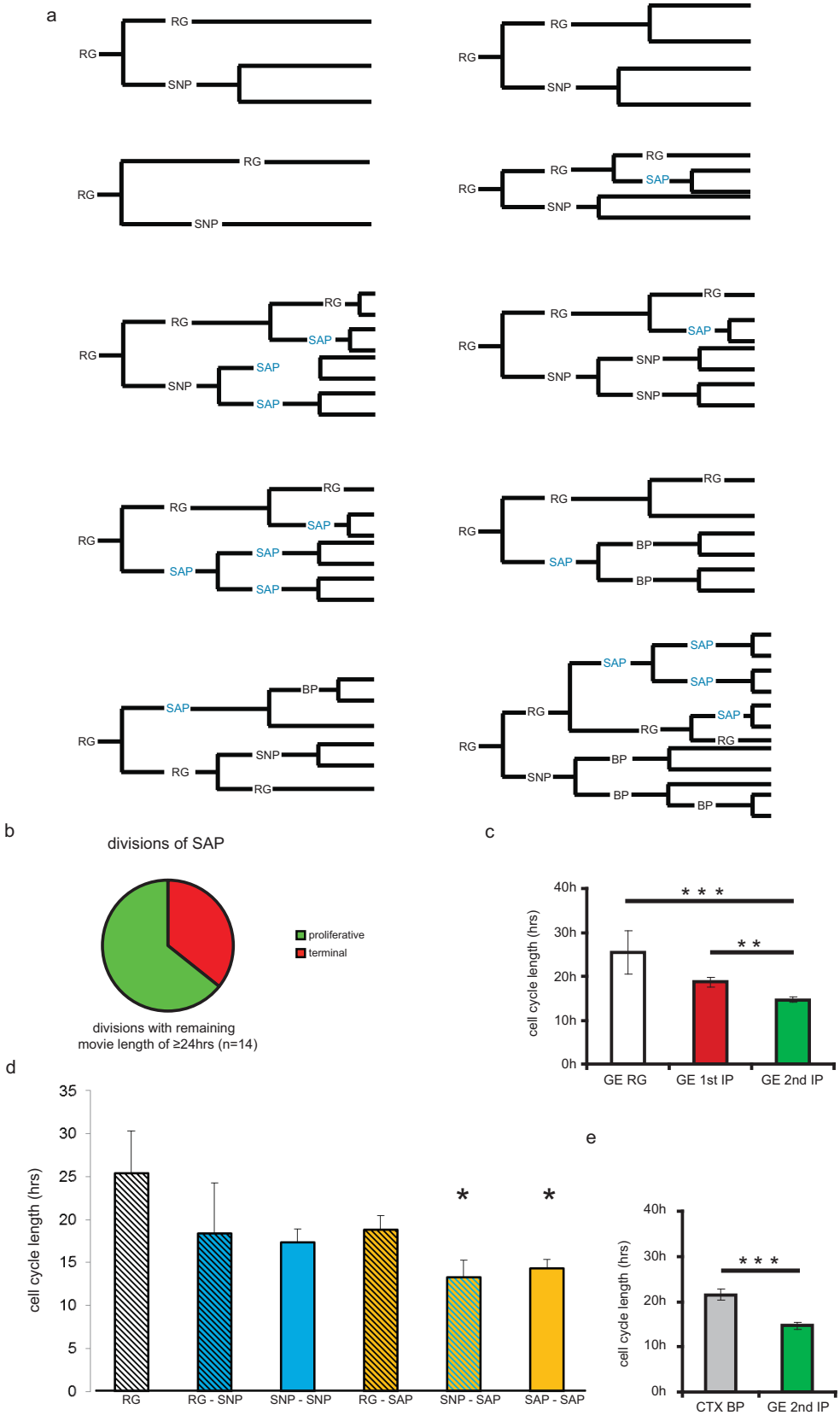

Lineage trees obtained from live imaging show abundance of SAPs in larger clones and cell cycle analysis of divisions in the LGE and cerebral cortex

(a) Exemplary lineage trees obtained from 3 different experiments with the duration of imaging ranging from 47-49hrs. SAPs are highlighted in blue. Note that SAPs are particularly abundant in larger lineages of >4 cells and can be generated by RGs, SNPs and also SAPs. (b) Percentage of proliferative and terminally differentiating SAPs (analyzed when at least 24hrs of movie remained after last SAP division; n=14). (c) Histogram depicting the cell cycle length in hours of subsequent divisions of LGE progenitors determined from time-lapse movies. Note the gradual shortening during subsequent divisions with 2nd intermediate progenitor (IP) divisions showing a significantly shorter cell cycle than RG (p=0.0015; t-test) and first generation IP (generated from RG; p=0.0039; t-test; n=6, 10, 18, respectively; error bars are s.e.m.). (d) Histogram of cell cycle length in regard to the origin of each progenitor class (mother cell is named first). Stars indicate significant difference to cell cycle length of RGs (p=0,05; t-test; RG n=6; RG-SNP n=3; SNP-SNP n=4; RG-SAP n=7; SNP-SAP n=6; SAP-SAP n=8; error bars are s.e.m.) (e) Histogram of cell cycle length comparing the 2nd intermediate progenitor divisions in the LGE to the cell cycle length of BPs in the cerebral cortex revealing a significantly shorted cell cycle of the former compared to the latter (p=0.0001; t-test; GE 2nd generation IPs n=18; CTX BP n=23; error bars are s.e.m.).

Supplementary figure S3

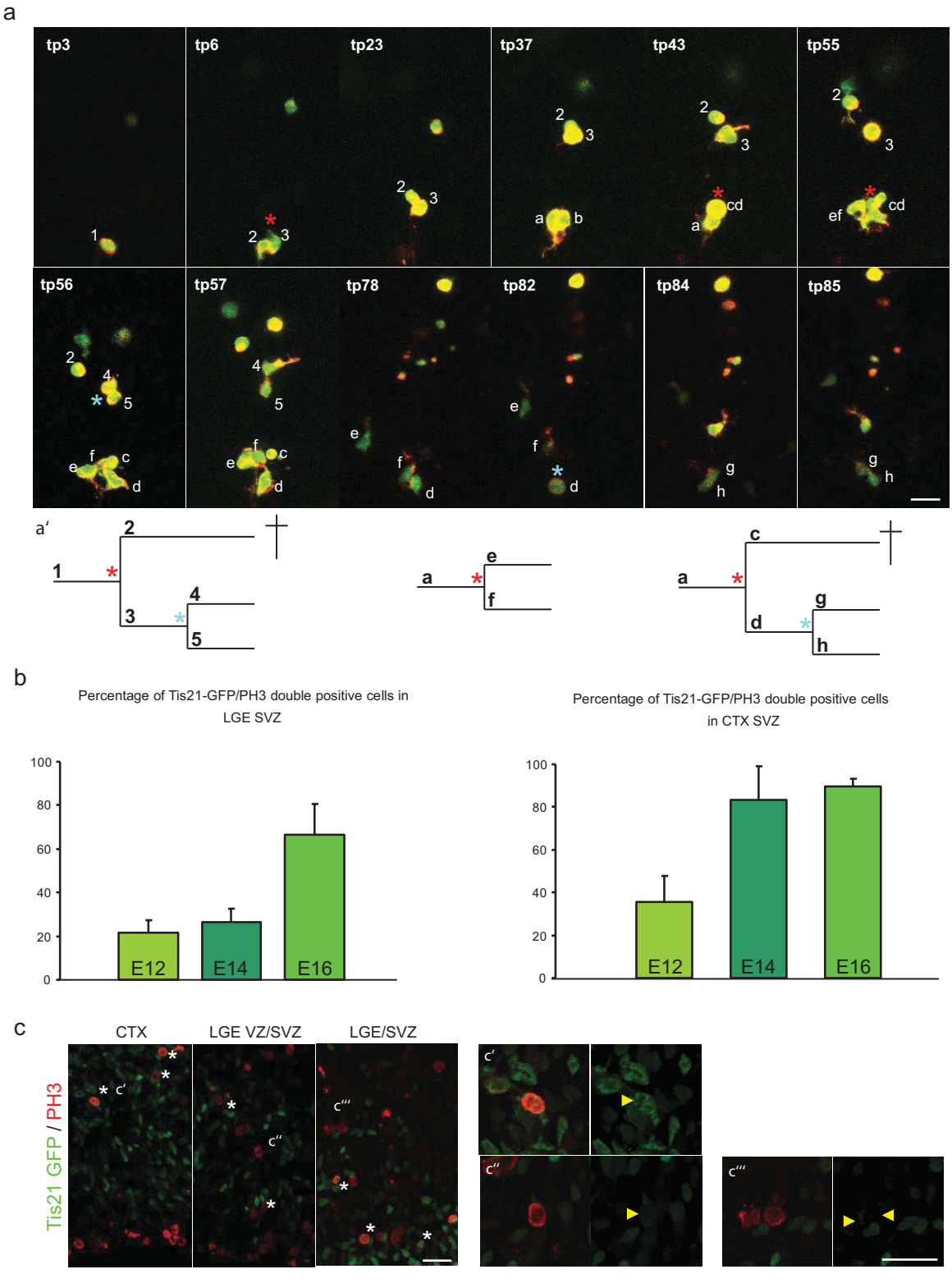

Basal progenitors continue to proliferate in the LGE

(a) Time-lapse series of a basal progenitor (labeled 1) located deep in the SVZ of the LGE that divides at time point 6 (tp6; red star) giving rise to daughter cells 2 and 3 with daughter 3 dividing again (tp56; blue star) to generate cells 4 and 5. Cell b also divides (tp43; red star) generating daughter cells c and d of which cell d divides one more time (tp82; blue star) giving rise to daughter cells g and h. One time frame is 20 minutes. (a') Schemes illustrating the cells tracked in (a) stars indicate divisions of BPs (red=1st, blue= 2nd). Note that the drawing is not to scale. Scale bar (all pictures in a): 20µm. (b) Quantification of Tis21::GFP positive non-apically dividing progenitors in LGE and cerebral cortex from E12 to E16 (error bars are s.d.) (c) Fluorescence micrographs of PH3 staining (red) in Tis21::GFP (green) mice show examples of double-positive progenitors in the cerebral cortex (white asterisks). Inserts c' c'' depict double positive cells and in (c''') Tis21-GFP negative cells indicated by yellow arrowheads. Scale bar (all pictures in c, c'-c''' 30µm).

Supplementary figure S4

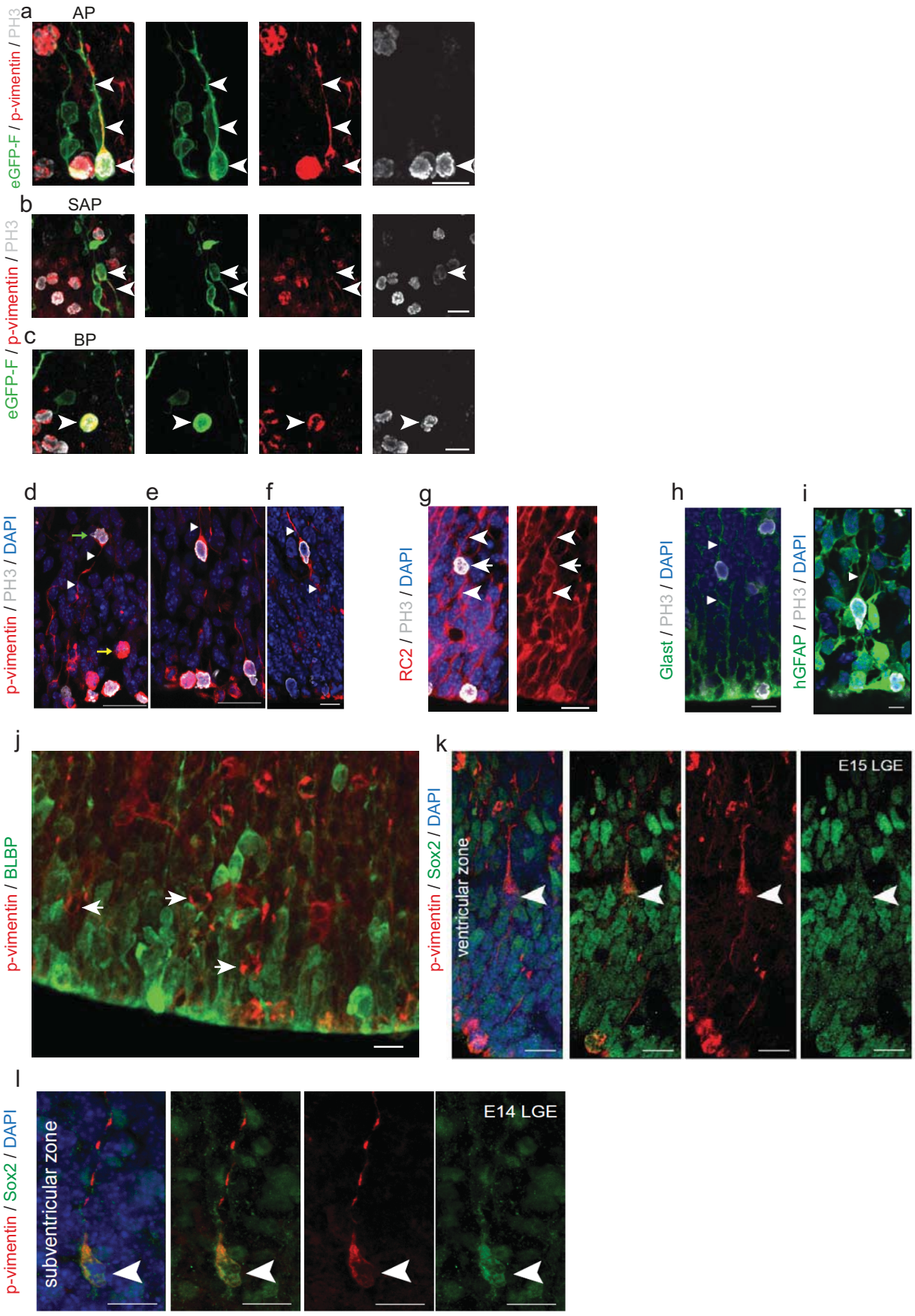

Phospho-vimentin reliably labels cellular processes in M-phase and a part of the heterogeneous population of SAPs shows bipolar morphology and expresses RG specific molecules

(a-c) Examples of an AP, SAP and BP showing co-labeling of membrane bound GFP (eGFP-F; green) and p-vimenin (red; arrows point to cell body in M-phase; arrowheads to cellular processes in a,b) see also 3D reconstructions in Supplementary movie S8; (d-f) Fluorescence micrographs of E14 mouse telencephalon sections immunostained for mitotic cells by phosphorylated histone H3 (PH3) and phosphorylated vimentin (p-vimentin). White arrowheads point at apical (d,f) or basal (e,f) processes of mitotic cells. Note SNP like (green arrow in d) and multipolar cells (yellow arrow in d) dividing in the LGE VZ. (g-i) SAPs express radial glia markers Nestin/RC2 (g) Glast (h) and hGFAP (i). Sub-apical RGs in the VZ and bRG in the SVZ of the LGE also stain positive for Sox2 (white arrowhead in j and k). Scale bars: 20µm (a-g, h,j), 10µm (i).

Supplementary Figure S5

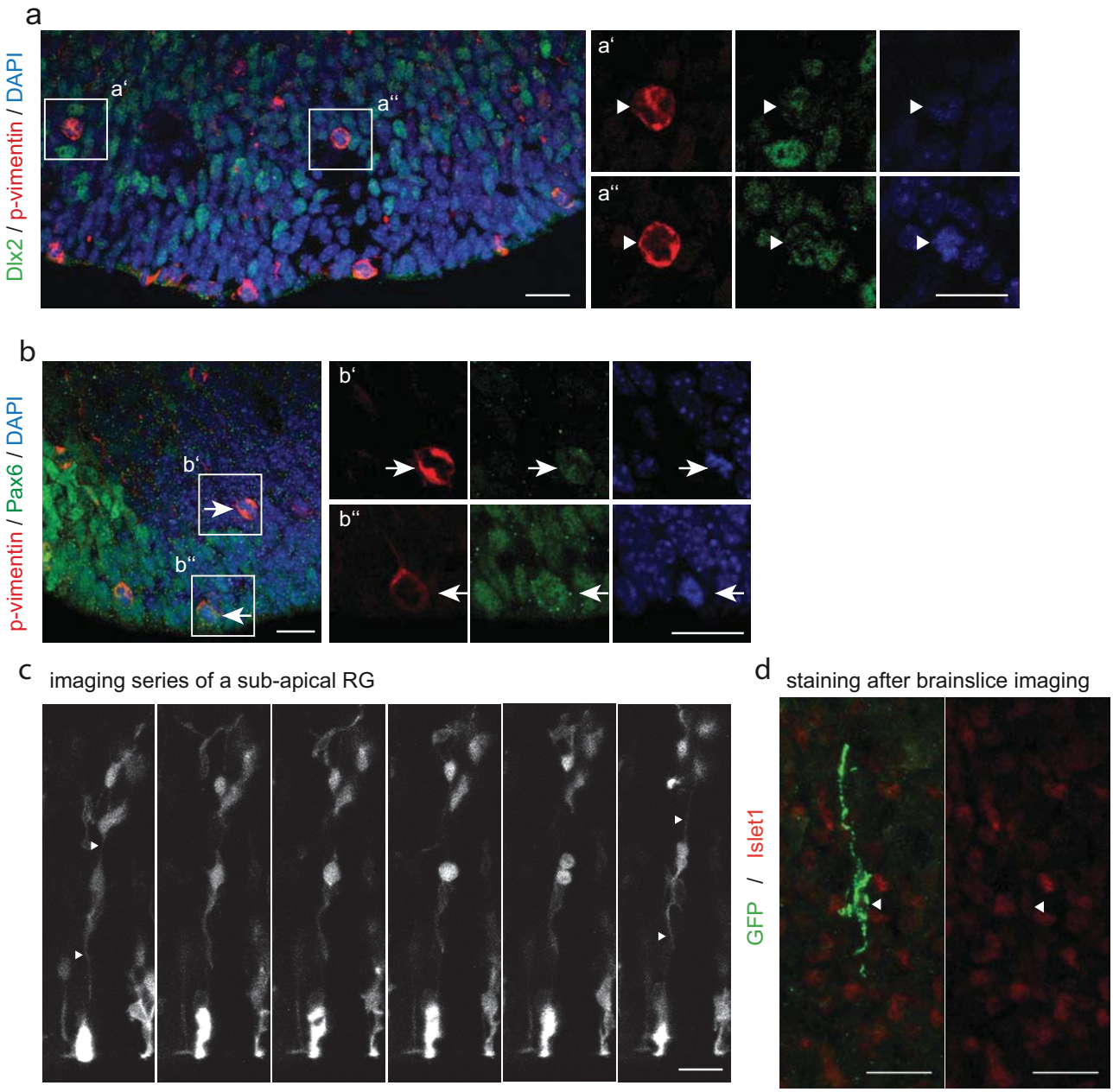

SAPs express Dlx2 and Pax6 transcription factors – sub-apical RG give rise to bRG and Islet1+ neurons
(a,b) Fluorescence micrographs of E14 mouse telencephalon showing the expression of Dlx2 and Pax6 in SAPs and APs of the LGE (boxed panels in a',a'',b' and b'' show a single optical section; arrowhead pointing at mitotic cell). (c) Time-lapse series of a sub-apically dividing RG. White arrowheads point at apical and basal processes. The two daughter cells relocated in the fixed and stained (GFP/green, Islet1/red) slice after 48hrs of imaging. (d) Fluorescence micrograph shows weak expression of Islet1 (white arrowhead) in the more apical located daughter cell. Also in other species the more apical daughter cell is destined to differentiate into a neuron (refrence 40). Scale bars (a-d): 20µm.

Supplementary figure S6

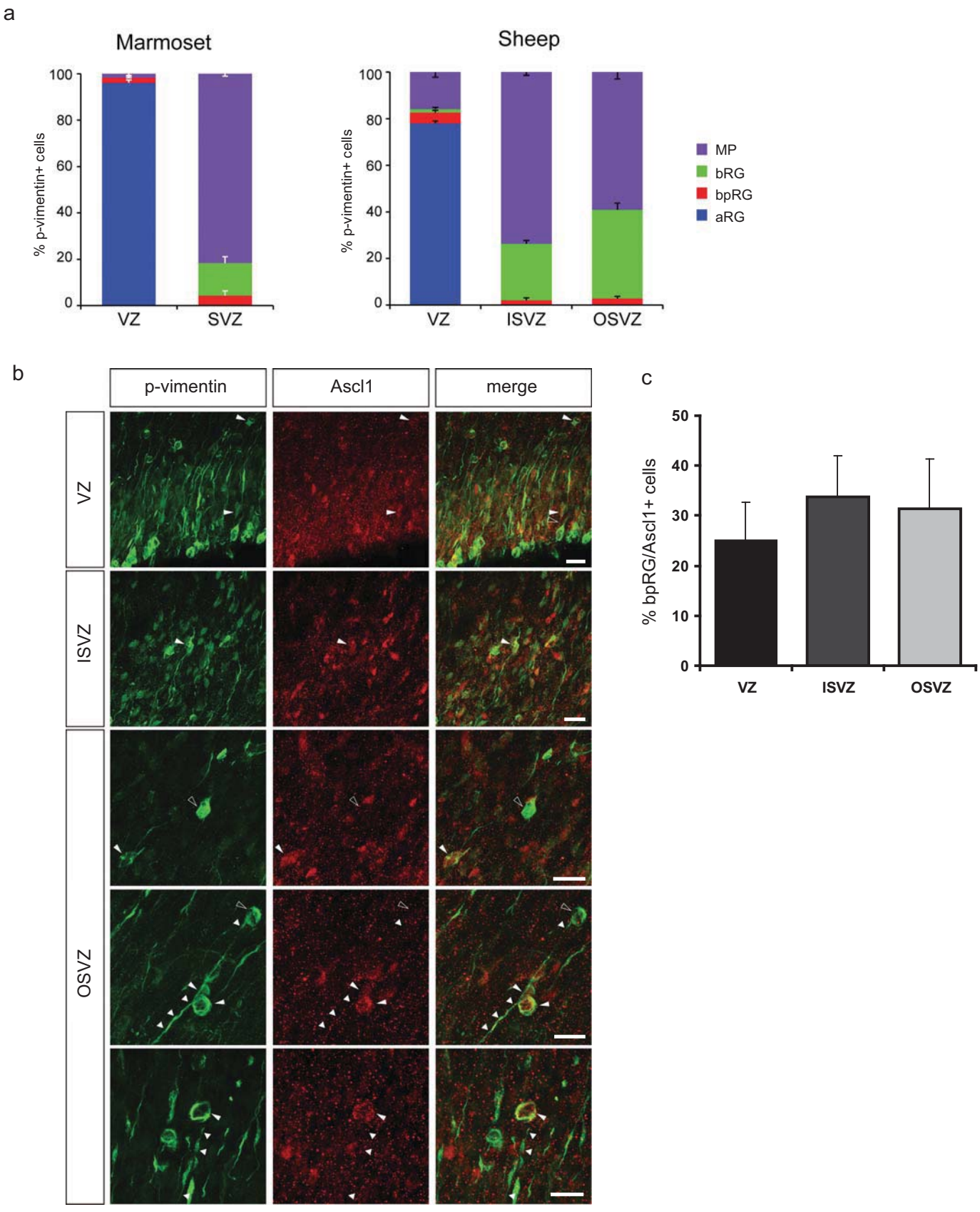

Progenitor subtypes determined by phosphorylated vimentin immunostaining in the developing neocortex of marmoset and sheep embryos
(a) Histograms depict proportions of aRG, bpRG, bRG and MPs within the VZ, SVZ, ISVZ or OSVZ of the neocortex of marmoset (E85) and sheep (E65-67) embryos, as defined by p-vimentin stain (marmoset, n = 1581 cells in VZ, 162 cells in ISVZ; sheep, n = 563 cells in VZ, 932 cells in ISVZ, 940 cells in OSVZ; 3 embryos each). Data are mean +/- S.E.M. (b) Fluorescence micrographs showing the co-labeling of dividing bpRG (p-vimentin; green) with Ascl1 (red) in the VZ, ISVZ and OSVZ of the ferret (P2). Long white arrowheads indicate Ascl1+ cells, empty arrowheads Ascl1- cells, and small white arrowheads point to processes of dividing cells. All scale bars in b: 20μm (c) Quantification of bipolar p-vimentin/Ascl1+ double positive cells in the VZ (n=114), ISVZ (n=90) and OSVZ (n=95) of the ferret cortex (P2) (Error bars are s.e.m).

Supplementary figure S7

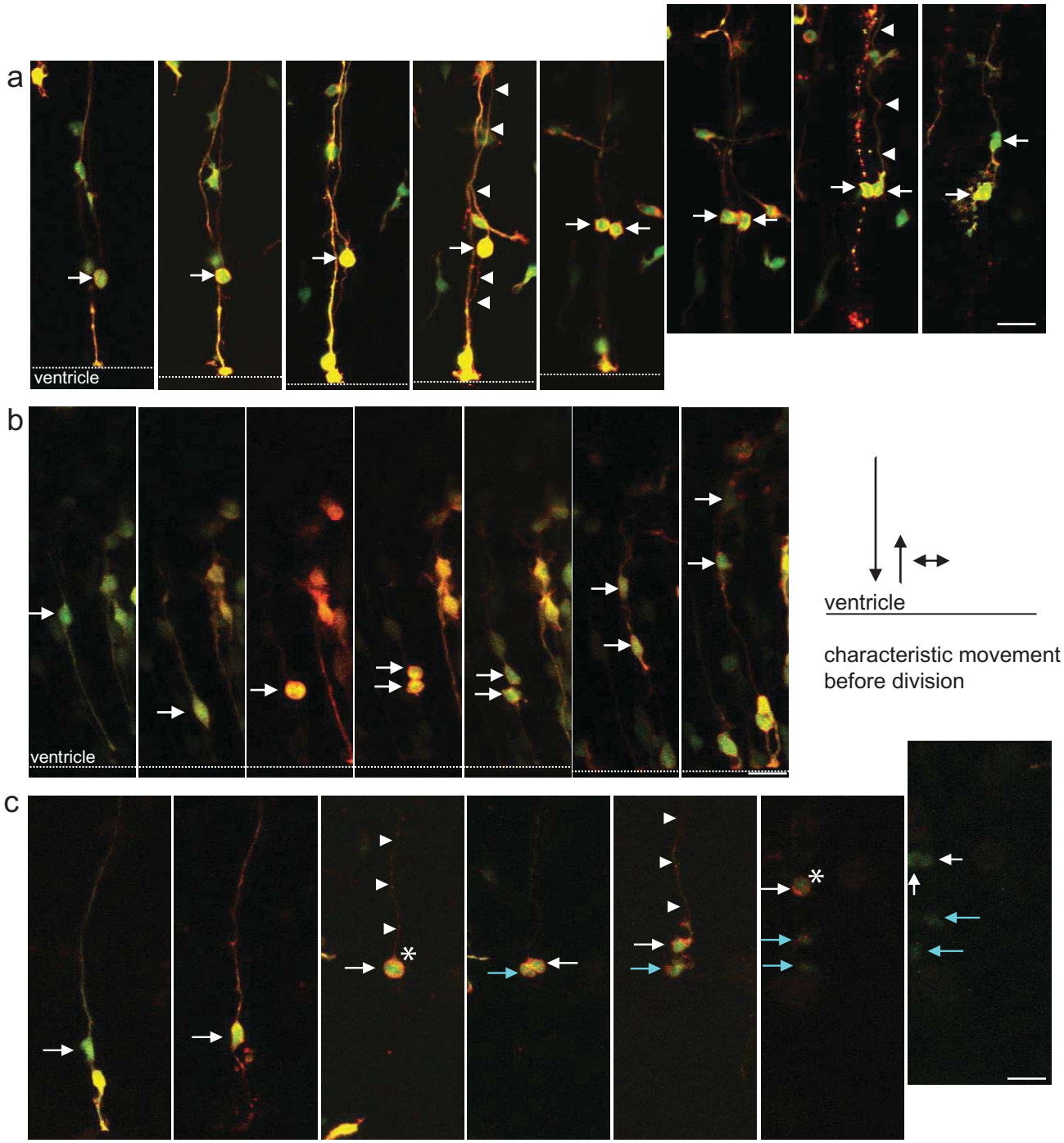

Interkinetic nuclear migration of sub-apical progenitors and basal radial glia
(a) Example of an SAP (white arrow) dividing in the VZ retaining apical and basal processes (white arrowheads). One daughter cell inherits the basal process (white arrowheads) and starts to trans-locate basally, maintaining the basal process reminiscent of basal radial glia (bRG). (b) Characteristic movement of a RG-like SAP soma before division at sub-apical position. The soma moves apically, but before reaching the apical surface returns basally to divide at a sub-apical position (white arrows). The two daughter cells with bipolar morphology move basally. (c) Time lapse series of a bRG (white arrow) originating apically moving basally and dividing twice (white stars). The daughter cell after the first division (blue arrow) divides once more with a shorter cell cycle than the bRG mother cell. Scale bars (a-c): 20µm.

Supplementary figure S8

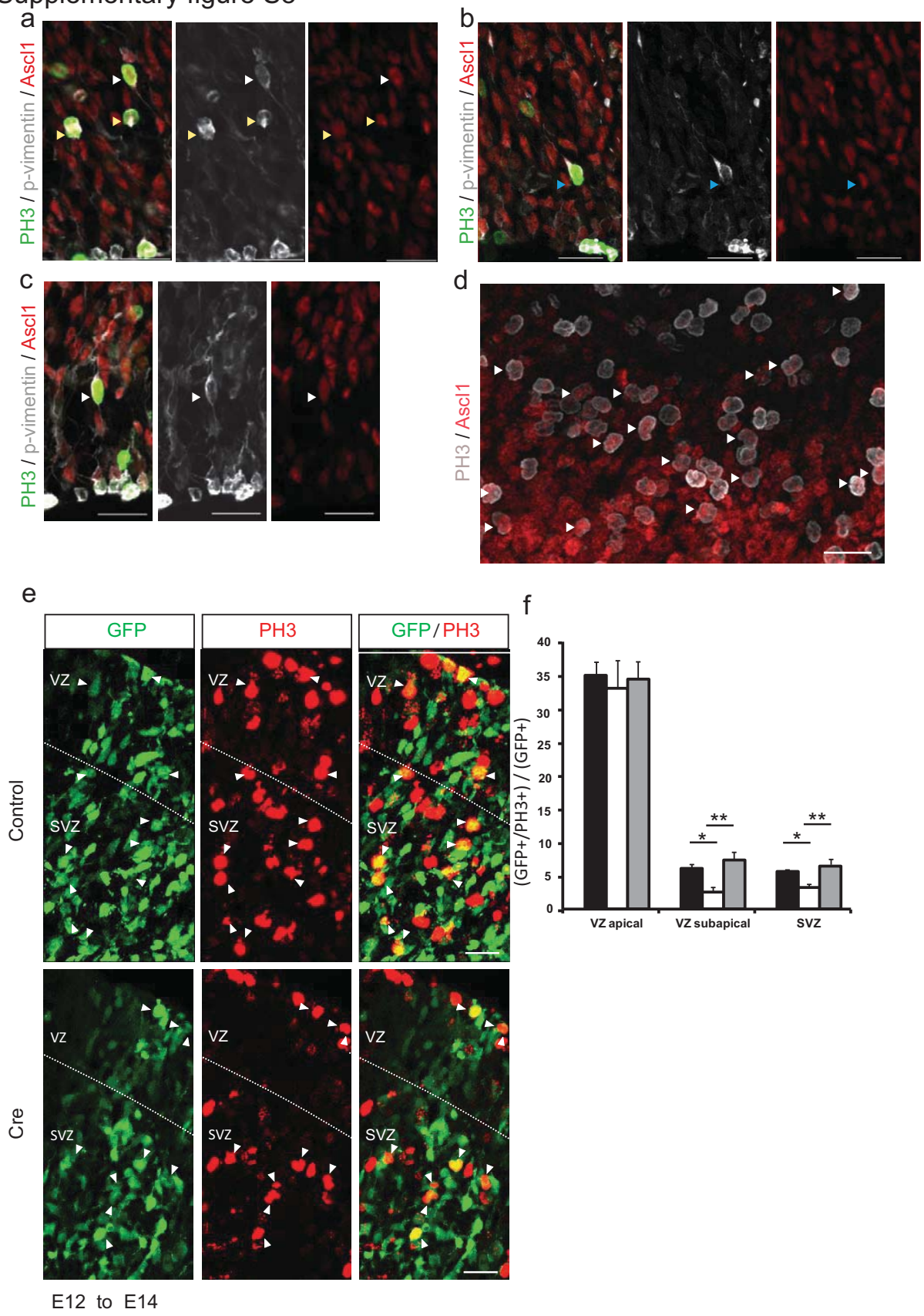

Deletion of the transcription factor Ascl1 reduces the number of SAP and BP in E14 LGE

(a-c) Fluorescence micrographs depicting SNP-like (white arrow in a; only apically directed process), multipolar (yellow arrows in (a)), bRG (green arrow in (b); only basally directed process) and RG-like (white arrow in (c); apical and basal process) SAPs positive for Ascl1. (PH3, green; p-vimentin grey; Ascl1, red). (d) Dividing BPs (PH3; grey) in the SVZ of E14 LGE; BPs positive for Ascl1 (red) are highlighted by white arrowheads; Scale bar: 20µm (e) Fluorescence micrographs of LGE at E14 after electroporation of Cre-GFP together with GFP-control or GFP-control plasmid only into Ascl1flox/flox mice (e) or electroporation of Cre-GFP into Ascl1flox/+ mice (data not shown) at E12. The number of dividing cells in both VZ and SVZ is reduced after electroporation of Cre (note white arrowheads indicating Cre-GFP/PH3 double positive cells; the border between VZ and SVZ is marked by a dashed white line). (f) Quantification of GFP/PH3 double positive cells in apical, VZ/sub-apical and SVZ position after electroporation of GFP-control plasmid or Cre-GFP into the LGE of Ascl1 flox/flox or Ascl1 flox/+ control animals (n=6 animals; VZ sub-apical: * $p<0.05$; SVZ: ** $p<0.01$; student's t-test; error bars are s.e.m.). After knockout of Ascl1 the numbers of cells dividing in VZ/sub-apical or SVZ are reduced, whereas the numbers of apically dividing cells are unchanged. Scale bar (a-c): 20µm.

Supplementary figure S9

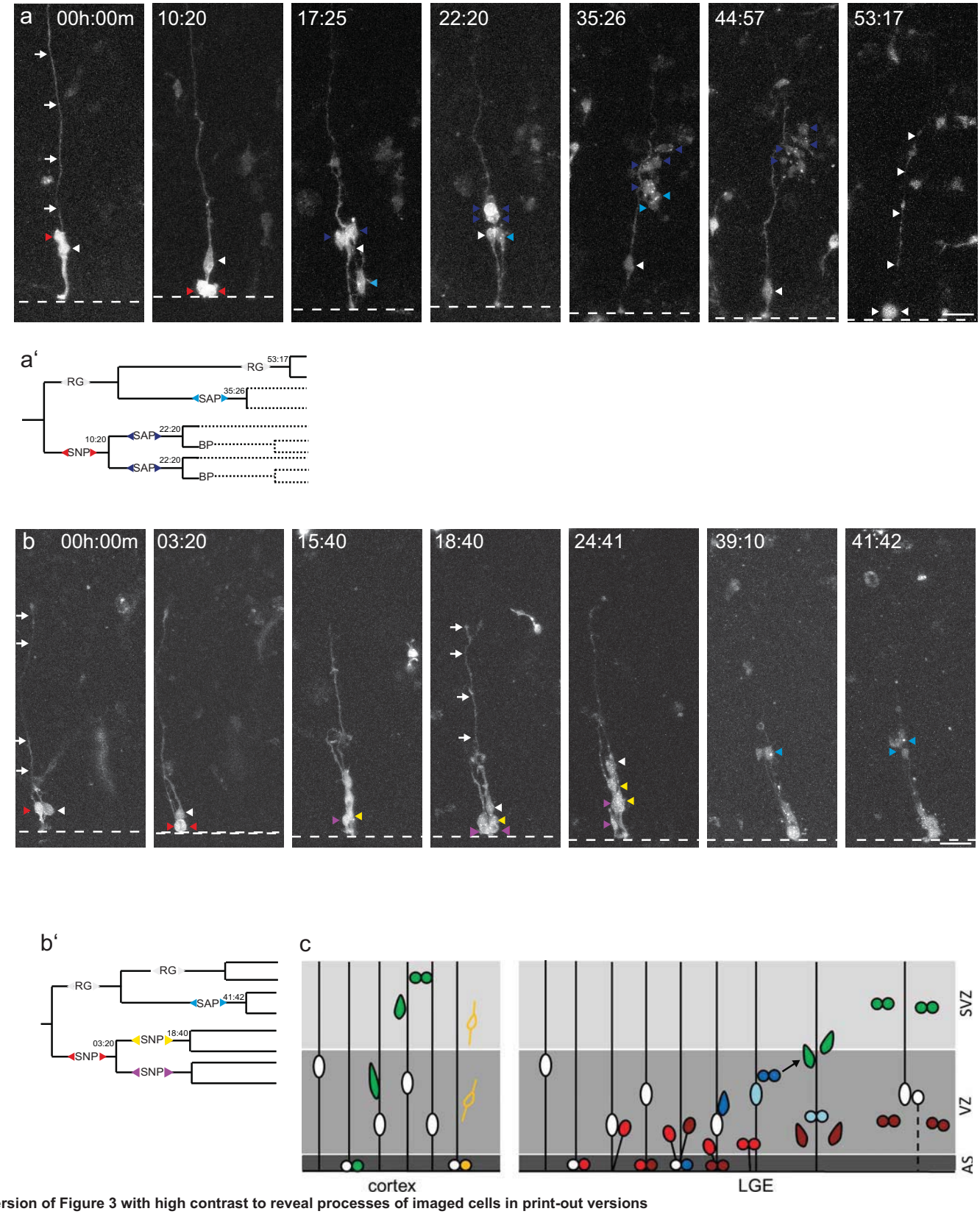

Version of Figure 3 with high contrast to reveal processes of imaged cells in print-out versions

(a) Time-lapse series of a clone consisting of a RG (white arrowhead) and a short neural progenitor (SNP, lacking a basal process, red arrowhead). The SNP divides at the ventricle (dashed white line) (t: 10:20) giving rise to two SAPs (dark blue arrowheads) that divide again in the VZ (t:22:20). The radial glia cell also divides at the ventricle giving rise to a RG and a sub-apically dividing progenitor (SAP, white and blue arrowhead in t:17:25). The SAP divides in the VZ (two blue arrowheads in t:35:26), whereas the RG undergoes mitosis at the ventricle (t:53:17). White arrowheads point at the RGs basal process (t:00:00 and t:53:17). (a') Lineage diagram derived from the time-lapse movie in (a), note that BPs continued to proliferate in the SVZ, but could not be individually followed due to their fast movement and decreased GFP-signal (dashed lines). Note that the length of the lines in (a') and (b') are not drawn to scale (time). Scale bars 20µm (b) Time-lapse series illustrating the generation of multiple VZ progenitors coming from a single labeled cell. The SNP divides at the ventricle (red arrowheads; t:03:20), giving rise to two SNPs that divide again at the ventricle (red arrowheads at t:18:40). The RG (white arrowhead in t:03:20) gives rise to one RG and one SAP that is dividing between t:39:10 and t: 41:42 (blue arrowheads). (b') Lineage diagram derived from the time-lapse series in (b). Note that the two daughter SNPs generated by a SNP (red) divide at a very similar time point at the ventricle. Scale bar: 20µm. (c) Scheme illustrating the progenitor lineage detected in the LGE in comparison to the neocortex. In the developing cortex at midneurogenesis RG divide mostly asymmetrically to give rise to either neurons (yellow) or BPs (green) that migrate to divide in the SVZ. In the LGE RG cells generate progenitor cells that continue to proliferate in the VZ either as SNPs (red) or SAPs (blue). SNPs and SAPs can perform self-renewing divisions in the VZ thereby amplifying the progenitor pool. Sub-apically dividing radial glia also divide in the VZ and sometimes generate a daughter cell with bRG morphology.

2.2 The nuclear protein TRNP1 regulates lateral and radial expansion of cerebral cortical size by influencing radial glia divisions including the generation of subapical bipolar radial glia

This paragraph contains data which was issued in an article in *Cell* 2013 Apr 25; 153(3):535-49 entitled “Trnp1 regulates expansion and folding of the mammalian cerebral cortex by control of radial glial fate” by Ronny Stahl, Tessa Walcher, Camino de Juan Romero, Gregor-Alexander Pilz, Silvia Cappello, Martin Irmler, Jose Miguel Sanz-Aquela, Johannes Beckers, Robert Blum, Victor Borrell and Magdalena Götz.

Summary: In a screen comparing transcriptome data of subsets of RG, the nuclear protein TRNP1 was highly upregulated in RG which do not produce intermediate progenitors. An antibody raised against TRNP1 showed that it is expressed in a subset of RG in the VZ and neurons in the cortical plate, and it is decreasing in its expression with the course of telencephalic development. To study the function of TRNP1 by overexpression in in-vitro cultured embryo- derived NSCs. Clonal analysis and in-vitro timelapse studies showed that TRNP1 overexpression increases clone size by promoting symmetric proliferative divisions and favors mixed clone compositions over pure neuronal clones. In order to investigate the effect of TRNP1 in vivo in the developing embryo, in utero electroporations with constructs overexpressing TRNP1 or knocking it down via shRNA were targeted into the cortical ventricular walls at E13 and analyzed at E16. Overexpression led to an increase in proliferation of apical progenitors and therefore a tangential expansion of cells residing in majority in the VZ. Conversely, the knockdown of TRNP1 led to a decrease in Pax6+ apical progenitors in the ventricular zone and to an increase of Tbr2+ progenitors in the SVZ. Remarkably, the knockdown also led to a dramatic expansion of the cortical thickness overlying the electroporated area. Closer analysis of this expanded region uncovered, that the number of Pax6+ bRG localized in the SVZ and IZ was enormously elevated. Live imaging further revealed, that these bRG are actively dividing therefore actively seeding an enlarged germinal zone. In addition the live imaging in slices showed a massive migration of cells with very fast speed towards the basal side. This migration

occurred along a “fanned array” ultimately leading to the formation of a gyrus structure. Gyri and sulci were also clearly visible from an outside look on postnatal brains. To test if this role in tangential or radial expansion could also be responsible for the formation gyri and sulci during human brain development in situ hybridization were performed on GW 18 and GW 21 sections of human embryonic tissue. Indeed TRNP1 signal was low, where gyrus formation occurs and high where sulci are forming, confirming its potential role in regulating brain cortical expansion and folding.

Author contributions to this publication

Ronny Stahl performed all experiments and analyzed data unless otherwise stated. Tessa Walcher performed in-utero electroporation for the early analyzed timepoints (E13-E16) and Silvia Cappello performed in-utero electroporation for the longer timepoints (until postnatal stages). Gregor-Alexander Pilz performed in-utero electroporations, embryonic slice culture and embryonic slice culture imaging after TRNP1 knockdown. Further Gregor-Alexander Pilz analysed and interpreted the imaging data. Camino de Juan Romero carried out the in-situ hybridisations on human tissue sections and Jose Miguel Sanz-Aquela provided the human specimen. Victor Borrell conducted the work on the human tissue and gave conceptual support. Martin Irmler and Johannes Beckers carried out the microarray and help to analyze the resulting data. Robert Blum helped to design the antibody against TRNP1 and gave initial conceptual support. Magdalena Götz designed and supervised the study and wrote the manuscript together with Ronny Stahl.

Cell

Trnp1 Regulates Expansion and Folding of the Mammalian Cerebral Cortex by Control of Radial Glial Fate

Ronny Stahl,[1,2,3] Tessa Walcher,[3] Camino De Juan Romero,[5] Gregor Alexander Pilz,[3] Silvia Cappello,[3] Martin Irmler,[4] José Miguel Sanz-Aquela,[6] Johannes Beckers,[4,7] Robert Blum,[1,9] Víctor Borrell,[5] and Magdalena Götz[1,2,3,8,*]

[1]Physiological Genomics, Institute of Physiology, Ludwig-Maximilian University Munich, Schillerstrasse 46, 80336 Munich, Germany
[2]Munich Center for Integrated Protein Science CIPSM, Butenandtstrasse 5-13, 81377 Munich, Germany
[3]Institute of Stem Cell Research, German Research Center for Environmental Health
[4]Institute of Experimental Genetics
Helmholtz Center Munich, Ingolstädter Landstrasse 1, 85764 Neuherberg, Germany
[5]Instituto de Neurociencias, Consejo Superior de Investigaciones Cientificas-Universidad Miguel Hernandez, 03550 Sant Joan d'Alacant, Spain
[6]Service of Pathology, Hospital Universitario "Principe de Asturias," 28805 Alcalá de Henares, Spain
[7]Technical University Munich, Chair of Experimental Genetics, 85350 Freising-Weihenstephan, Germany
[8]Munich Cluster for Systems Neurology (SyNergy), 80336 Munich, Germany
[9]Present address: Institute for Clinical Neurobiology, University of Würzburg, 97078 Würzburg, Germany
*Correspondence: magdalena.goetz@helmholtz-muenchen.de
http://dx.doi.org/10.1016/j.cell.2013.03.027

SUMMARY

Evolution of the mammalian brain encompassed a remarkable increase in size of the cerebral cortex, which includes tangential and radial expansion. However, the mechanisms underlying these key features are still largely unknown. Here, we identified the DNA-associated protein Trnp1 as a regulator of cerebral cortex expansion in both of these dimensions. Gain- and loss-of-function experiments in the mouse cerebral cortex in vivo demonstrate that high Trnp1 levels promote neural stem cell self-renewal and tangential expansion. In contrast, lower levels promote radial expansion, with a potent increase of the number of intermediate progenitors and basal radial glial cells leading to folding of the otherwise smooth murine cerebral cortex. Remarkably, *TRNP1* expression levels exhibit regional differences in the cerebral cortex of human fetuses, anticipating radial or tangential expansion. Thus, the dynamic regulation of *Trnp1* is critical to control tangential and radial expansion of the cerebral cortex in mammals.

INTRODUCTION

During mammalian evolution, brain regions were dynamically adapted by selective growth and expansion with a high degree of specificity. An impressive example is the expansion of the mammalian neocortex resulting in profound gyrification to accommodate an enormous increase in neuronal cell numbers (Lui et al., 2011). Notably, distinct brain regions can be expanded selectively in specific species, such as for example the auditory cortex in bats (Krubitzer, 2007; Martínez-Cerdeño et al., 2012). However, the mechanisms regulating evolutionary changes in size of specific brain regions still remain poorly understood.

Regulation of specific stem and progenitor cells during development is closely linked to control of the size of brain regions (Krubitzer, 2007; Fish et al., 2008; Borrell and Reillo, 2012). In particular, expansion of regions within the cerebral cortex occurs in two dimensions: tangential and radial growth (Rakic, 1995). Tangential growth is mediated by expanding neural stem cell (NSC) populations, such as neuroepithelial and radial glial cells (RGs), anchored at the apical surface in the ventricular zone (VZ) (Götz and Huttner, 2005). To increase the number of neurons per area, radial growth is achieved by either a prolonged phase of neurogenesis or through addition of germinal layers beyond the VZ (Rakic, 1995), such as the subventricular zone (SVZ) that is further expanded to an inner and outer SVZ (iSVZ and oSVZ, respectively) in the cerebral cortex of mammals with a larger neocortex, including primates (Smart et al., 2002; Lui et al., 2011; Borrell and Reillo, 2012). In the murine cerebral cortex, the SVZ largely comprises basal progenitors (BPs), which increase the number of neurons generated per time and area (Götz and Huttner, 2005). Besides increased numbers of BPs, additional RGs that have lost their apical anchor and are only connected to the basement membrane (BM) are incorporated in the SVZ (Smart et al., 2002; Fietz and Huttner, 2011; Lui et al., 2011; Reillo et al., 2011; Borrell and Reillo, 2012). Intriguingly, high numbers of such basal radial glia (bRG) correlate with a high gyrification index of the cerebral cortex (Fietz et al., 2010; Hansen et al., 2010; Lui et al., 2011; Reillo et al., 2011; Reillo and Borrell, 2012). In contrast, only few bRG are present in the SVZ of lissencephalic cerebral cortices with a smooth surface (Reillo et al., 2011; Shitamukai et al., 2011; Wang et al., 2011). Notably, the ventricular surface of gyrated brains is smooth, whereas the basal surface is folded due to an increase in gray

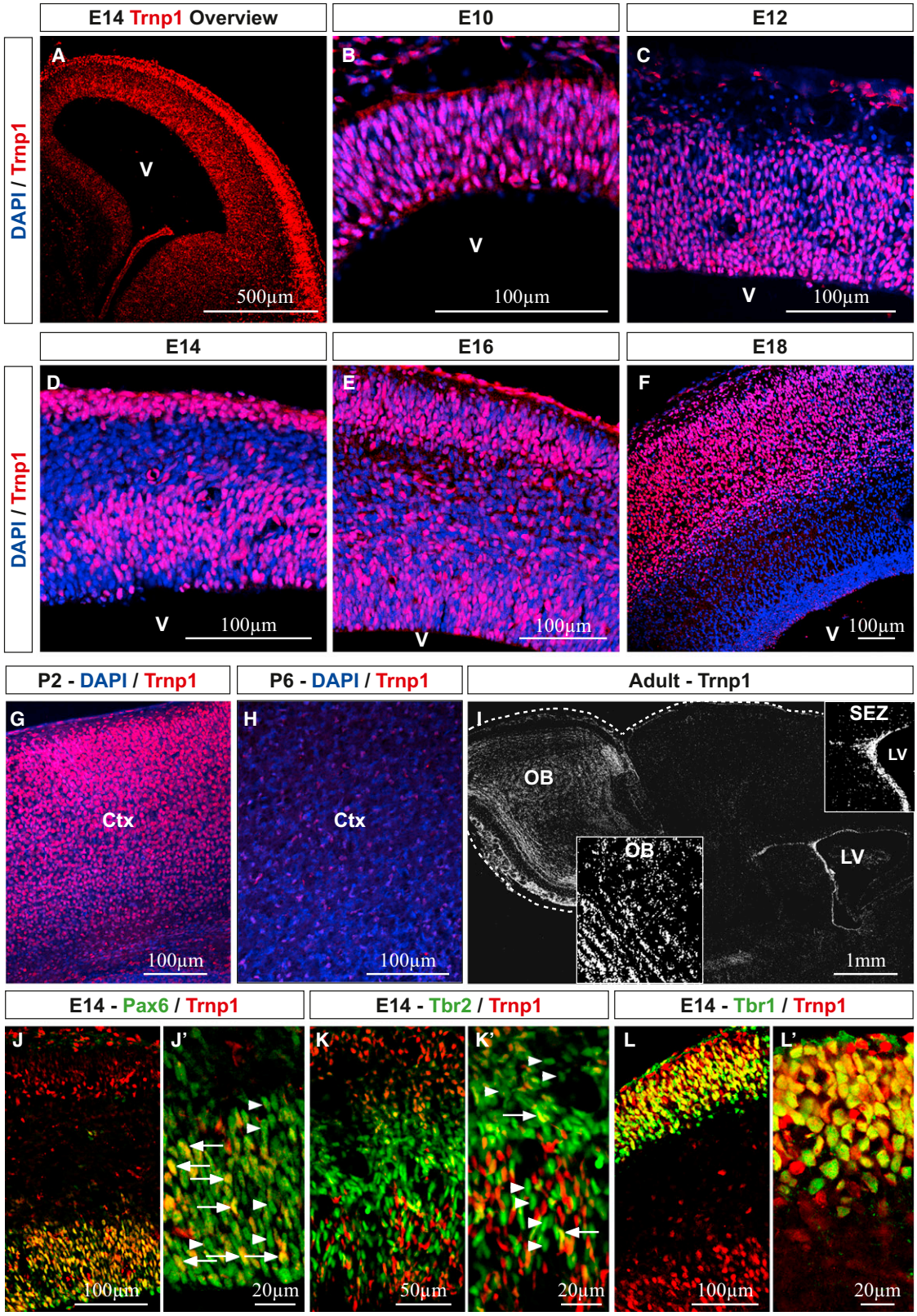

(legend on next page)

and white matter comprising neurons and glia (Borrell and Reillo, 2012). Therefore, gyrification reflects coordination of radial expansion and lateral dispersion of neurons in the cortical plate (CP), which is in profound contrast to a mere overproliferation resulting in an overall folded epithelium (Chenn and Walsh, 2002). This highlights how tangential, radial, and lateral expansion modes must be coordinated during cerebral cortex development and gyrification. Thus, a fascinating question in brain development and evolution is how such complex processes are regulated at the molecular and cellular level.

We set out to search for regulators of radial glia (RG) fate in an unbiased manner by genome-wide expression analysis of RG subpopulations that differ in the generation of BPs (Pinto et al., 2008). The screen was confirmed by the transcription factor AP2γ (identified at higher levels in RG generating BPs) that promotes the generation of BPs (Pinto et al., 2009). In order to identify regulators promoting the maintenance of RG rather than the generation of BPs, we selected a gene with higher expression in the subset of RG generating few BPs for further analysis: *Trnp1* (formerly known as 2300002D11Rik; Pinto et al., 2008). TMF-regulated nuclear protein Trnp1 has so far only been described as a nuclear protein in immortalized cell lines (Volpe et al., 2006); however, its in vivo function remained unknown. Intriguingly, *Trnp1* sequence is very different in nonmammalian vertebrates, whereas it shows clear sequence conservation among mammals (86% in human-mouse orthologs). Because its protein sequence does not carry any known motif or domain (Volpe et al., 2006) and Trnp1 has, to our knowledge never been studied during development or in any in vivo context, we examined first its expression and then its function in the developing cerebral cortex.

RESULTS

Trnp1 Is Specifically Expressed in a Subset of RG and in Newborn Neurons during Cerebral Cortex Development

We generated a specific antibody against Trnp1 (Figures S1A–S1D available online) and examined its localization in the developing forebrain from embryonic day 10 to 18 (E10–E18). Trnp1 was exclusively localized to the nucleus in apical progenitors (APs) in the VZ and newborn neurons in the CP (Figure 1A). Interestingly, Trnp1 immunoreactivity decreased significantly during development with virtually all cells in the VZ being Trnp1+ at E10 to no detectable immunoreactivity at E18, the end of neurogenesis (Figures 1B–1F). We noted some degree of cellular heterogeneity in Trnp1 immunoreactivity that remained higher in a subset of Pax6+ RG in the VZ, whereas virtually no Tbr2+ BPs in the SVZ expressed Trnp1 (Figures 1J–1K′). This is consistent with our previous results identifying lower levels of *Trnp1*-mRNA expression in RG generating BPs (Pinto et al., 2008). Thus, Trnp1 is expressed in an ever-decreasing subset of Pax6+ cells in the VZ, suggestive of an expression in self-renewing NSCs whose number declines during development.

Notably, also the expression of Trnp1 in neurons (as confirmed by double staining with the neuronal marker Tbr1) was transient and vanished within the first postnatal week (Figures 1G, 1H, 1L, and 1L′). At later postnatal stages and in the adult brain, virtually no Trnp1 immunoreactivity was detectable except for one region of adult neurogenesis: the subependymal zone (SEZ) of the lateral ventricle from where newborn neurons migrate via the rostral migratory stream (RMS) to the olfactory bulb (OB; Figures 1I and S1E–S1G). However, cells in the other neurogenic niche, the dentate gyrus, did not express Trnp1 (Figure S1H). Taken together, Trnp1 protein expression is highly restricted to the phase of neurogenesis and Trnp1 remains expressed in the adult neurogenic region with the highest amplification and neuronal output.

Trnp1 Increases Proliferation of Neural Stem Cells In Vitro

Because the aforementioned expression pattern suggested a potential role of Trnp1 in neural stem or progenitor cells, we aimed at determining its function by gain- and loss-of-function approaches. Toward this aim, we cloned *Trnp1* cDNA into a bicistronic retroviral vector with the chicken β-actin (CAG) promoter driving the expression of Trnp1 and GFP linked by an internal ribosomal entry site (IRES) (see Heinrich et al., 2011; Figure S2A). After confirmation of reliable coexpression of GFP and Trnp1 by immunostaining (Figures S2B and S2C), we utilized this virus to overexpress Trnp1 in progenitor cells from dissociated cultures of the E14 cerebral cortex. By use of less than 25 viral particles per well, we ensured clear separation of clones representing the progeny of initially a single infected cell (note that retroviral vectors only integrate into dividing cells; Haubst et al., 2004; Costa et al., 2008). Interestingly, clones transduced with Trnp1 virus contained more than double the number of cells as compared to clones infected with the control virus 7 days posttransduction (Figures 2A–2C), suggesting a profound increase in proliferation.

To determine the composition of these enlarged clones, we stained for the neuron-specific protein βIII-tubulin, and progenitor and glia markers Nestin and GFAP (Figures 2A, 2B, S2D, and S2E). This allowed distinguishing (1) NSC clones (clones with "mixed" identity comprising βIII-tubulin+ neurons and βIII-tubulin− glia or progenitor cells); (2) neuronal clones (all cells βIII-tubulin+); and (3) nonneuronal clones (comprising glial and progenitor cells, but no βIII-tubulin+ cells) (Figures 2A, 2B, and 2D). Trnp1 overexpression significantly increased the percentage of mixed, stem cell clones at the expense of pure neuronal clones (Figure 2D). Interestingly, the proportion of nonneuronal clones was not increased, suggesting that high levels of Trnp1

Figure 1. Endogenous Trnp1 Expression in the Developing and Adult Brain

(A–I) Images of coronal (A–H) or sagittal (I) sections of the developing (A–H, E10–P6) and adult (I; composite of single confocal images created by a Zeiss Tile scan) cerebral cortex (Ctx) labeled for Trnp1 and DAPI. Note that Trnp1 expression is restricted to neurogenic regions. LV, lateral ventricle; V, ventricle.

(J–L′) Trnp1 is expressed in a subpopulation of Pax6+ RG (J and J′) and Tbr1+ neurons (L and L′), whereas it is largely absent in Tbr2+ BPs (K and K′) in E14 cerebral cortex. Arrows indicate examples of double-positive cells; arrowheads point to Pax6+ or Tbr2+ cells that do not express Trnp1.

See also Figure S1.

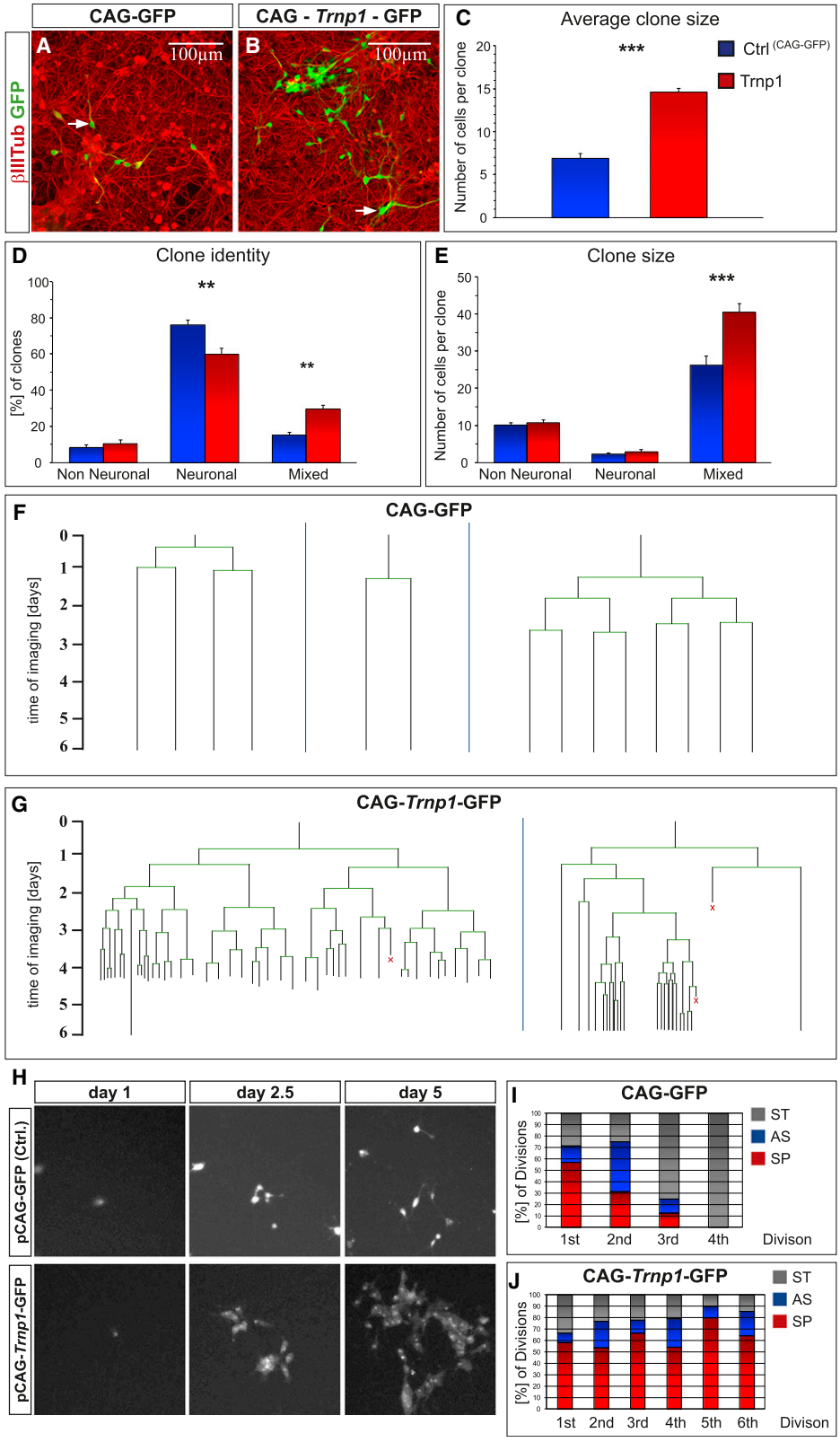

(legend on next page)

do not suppress the generation of neurons per se but, rather, increase self-renewal of NSCs still allowing neurogenesis to occur. Consistent with this, clone size selectively increased in mixed clones, whereas purely neuronal or purely nonneuronal clones were not affected by Trnp1 overexpression (Figure 2E). In order to gain further insights into the mechanism by which the mixed clones increase in size, we used continuous live-cell imaging as described before by Costa et al. (2008) and Asami et al. (2011). Although most cells infected with the control virus generated largely postmitotic daughter cells after two or three rounds of division (Figures 2F, 2H, and 2I), Trnp1-transduced cells still gave rise to proliferating progeny after six rounds of cell division (Figures 2G, 2H, and 2J). Thus, clone size increased due to an increased rate of cell-cycle reentry and symmetric proliferative divisions, whereas the average cell-cycle length was not affected (18.9 hr in control and 18.4 hr upon Trnp1 overexpression). Taken together, these results suggest a role of Trnp1 in cell fate regulation, with high levels of the protein promoting NSC fate maintaining their proliferative potential and inhibiting symmetric terminal divisions that give rise to neuron-only clones (see Costa et al., 2008; Asami et al., 2011).

Trnp1 Increases Proliferation of APs and Inhibits the Generation of BPs In Vivo

Our in vitro data raised the question to what extent forced Trnp1 expression may also promote proliferation of NSCs in vivo. To analyze this question, we electroporated pCAG-*Trnp1*-IRES-GFP or the control vector pCAG-IRES-GFP into E13 cerebral cortices and examined the brains 3 days later at E16. Upon Trnp1 overexpression, we observed a consistent overall increase in the number of GFP immunoreactive cells and a tangential expansion of the electroporated area (compare Figures 3B and 3B′ to 3A and 3A′) with many cells still residing in progenitor areas (Figures 3A–3D′). Quantification confirmed that the majority of Trnp1-electroporated cells (56%) still resided in the VZ and SVZ (Figures 3D, 3D′, and 3G) even 3 days after electroporation, whereas most control-electroporated cells had left the VZ (Figure 3C, bottom). Because many cells in the VZ were weakly GFP+ upon Trnp1 overexpression (suggestive of a high proliferation rate and dilution of the electroporated plasmid and protein; Figure 3D, bottom), we examined the proportion of cells in S phase based on their incorporation of the pyrimidine analog bromodeoxyuridine (BrdU) 1 hr before sacrifice. Remarkably, Trnp1 overexpression led to a significant 3× increase in proliferating (BrdU+) cells compared to the control (Figures 3E, 3F, 3H, and S2F). Consistent with the endogenous expression of Trnp1 in a subset of Pax6+ cells, Trnp1 overexpression significantly increased the proportion of Pax6+ APs at the expense of BPs and neurons in the intermediate zone (IZ) and CP (Figures 3E′, 3F′, 3G, 3I, and 3J). Thus, Trnp1 promotes tangential expansion (Figures 3A–3B′) by increasing Pax6+ apical NSCs and reducing the generation of Tbr2+ BPs in vivo. This finding is consistent with the endogenously higher expression levels of Trnp1 in RG that do not generate BPs (Pinto et al., 2008) and with our in vitro findings of Trnp1 promoting self-renewal of NSCs (Figures 2D and 2E).

Knockdown of Trnp1 Increases the Number of BPs and Leads to Radial Expansion of the Developing Cerebral Cortex In Vivo

To determine if Trnp1 is also necessary for RG self-renewal in vivo, we cloned three different small hairpin RNAs (shRNAs) targeting the 3′ UTR of *Trnp1* mRNA into pSUPER.GFP (expressing both the shRNA and GFP; Figure S3A). Western blotting and immunostaining identified shRNA #1 and shRNA #5 as most effective in reducing Trnp1 protein levels (Figures S3B and S3C), which were then used for in utero electroporations. In pronounced contrast to overexpression, knockdown of Trnp1 at E13 resulted in a significant increase in the proportion of cells located in the CP 3 days after electroporation (Figures 4A–4B′ and 4F). Interestingly, in 13 of 14 electroporated embryos (Table S1), we observed a clear radial expansion of the developing cerebral cortex in the electroporated region as compared to the nonelectroporated hemisphere and to controls (compare Figure 4A′ with 4B′; see Figures S3D–S3F′ for additional examples). As predicted, the number of Pax6+ APs was reduced 3 days after electroporation of either shRNA (Figures 4H and S4D), whereas the proportion of Tbr2+ BPs was significantly increased with both shRNA #1 and shRNA #5 (Figures 4C–4E, 4I, and S4E). This also explains why the overall number of proliferating cells is unchanged (Figure 4G). Notably, the increased number of BPs correlated with a thicker SVZ (compare Figure 4A′ with 4B′; and see Figures S3D–S3F′). To our surprise, Tbr2 immunoreactivity revealed a wide scattering of some Tbr2+ cells toward very basal regions (Figure 4E) reminiscent of the expanded, diffuse Tbr2+ band described in the oSVZ of ferrets, macaques, and humans (Reillo and Borrell, 2012; Martínez-Cerdeño et al., 2012; Bayatti et al., 2008).

As further control for the specificity of the observed effects, we aimed at rescuing the increased generation of Tbr2+ BPs upon RNAi by coexpressing an shRNA-resistant form of *Trnp1* (lacking the targeted 3′ UTR of *Trnp1*, which we tested for shRNA resistance before; see Figure S3B′). Electroporation of shRNA against endogenous *Trnp1* with simultaneous expression of

Figure 2. Effects of Trnp1 Overexpression In Vitro

(A and B) Representative images of GFP+ cells in dissociated cultures from the cerebral cortex isolated at E14 infected with a low titer of either CAG-IRES-GFP control (A) or CAG-*Trnp1*-IRES-GFP virus (B) immunostained for GFP and βIII-tubulin 7 days postinfection. Arrows indicate examples of double-positive cells. (C–E) Histograms depicting quantitative changes in size (C and E) and identity (D and E) of the progeny of single infected cells (clones) after Trnp1 transduction revealing increased number and size of mixed clones containing βIII-tubulin+ and βIII-tubulin− cells. Data are shown as mean ± SEM from four independent experiments. Statistical analysis was performed with the Student's t test in (C) and ANOVA with Tukey's posthoc test in (D) and (E): $^{**}p < 0.01$ and $^{***}p < 0.001$. Blue bars indicate control (Ctrl) virus; red bars show Trnp1 virus.

(F–J) Time-lapse analysis of cells described above showing representative lineage trees obtained by single-cell tracking (F and G; X indicates cell death), representative fluorescence micrographs of GFP+ cells in live imaging (H), and the histograms depicting the frequency of symmetric terminal (ST), asymmetric (AS), and symmetric proliferative (SP) divisions at each round of division (I and J; 14 clones each from two independent experiments).

See also Figure S2.

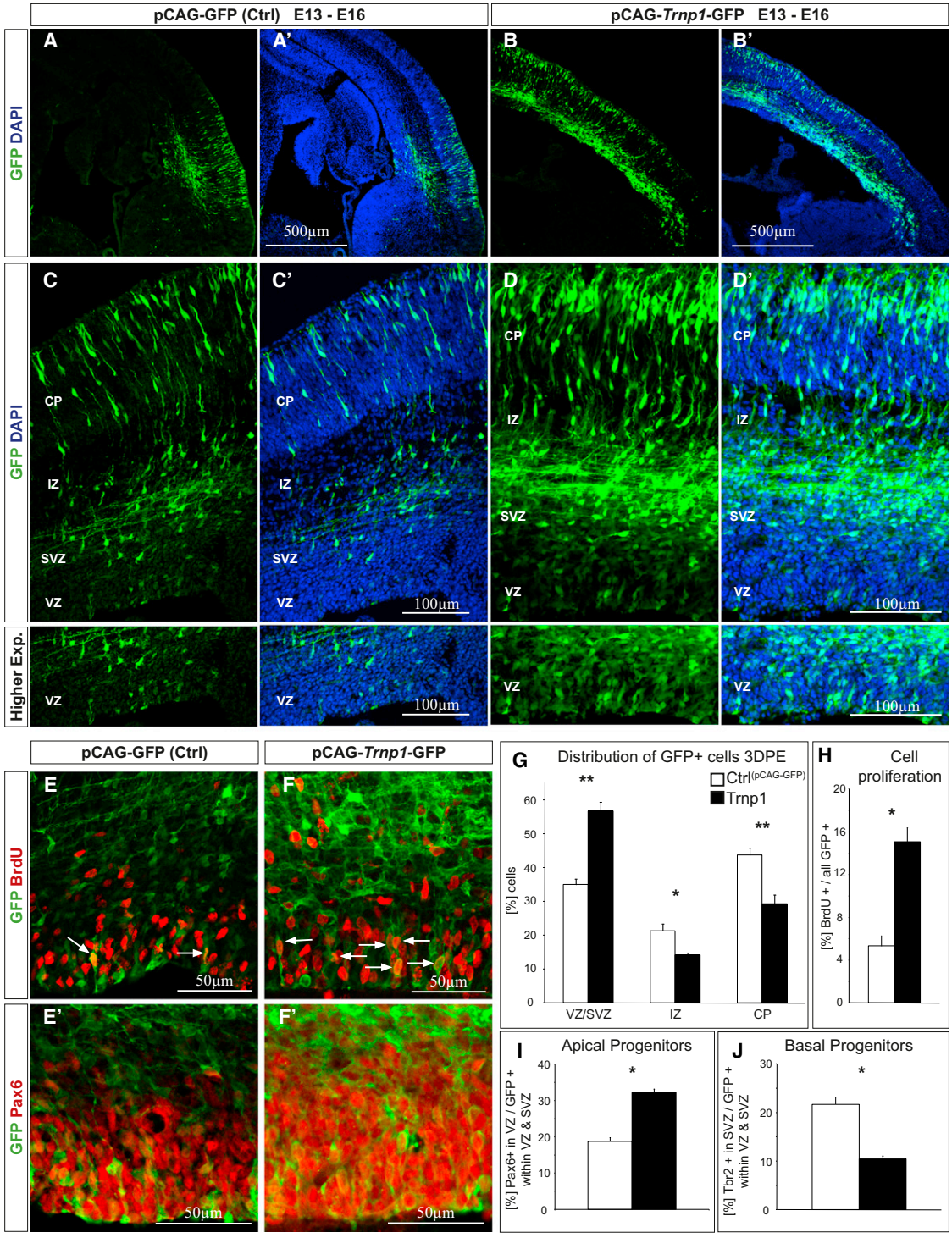

Figure 3. Overexpression of Trnp1 In Vivo Increases AP Numbers and Tangential Expansion

(A–F) Micrographs depicting sections of the cerebral cortex 3 days after electroporation at E13 with either pCAG-IRES-GFP control or pCAG-*Trnp1*-IRES-GFP plasmid with overviews in (A)–(B′), zooms of the electroporated area in (C)–(D′), with higher exposure of the VZ in the bottom panels of (C)–(D′), and double labeling for BrdU (E) and (F) and Pax6 in (E′) and (F′).

(G–J) Note the tangential expansion of the electroporated area (A–B′) due to increased numbers of APs (C–F′) as revealed by quantifications shown in the histograms upon Trnp1 overexpression.

Data are shown as mean ± SEM from five embryos for cellular localization analysis (G), three for cell proliferation, and four for AP and BP analysis (H–J): *$p < 0.05$ and **$p < 0.01$, Mann-Whitney U test. See also Figure S2.

shRNA-resistant *Trnp1* was able to rescue the increase of Tbr2+ BPs to a level comparable to the control situation (Figures 4I–4J′). Importantly, radial expansion of the cortex was also prevented in five out of five rescue-electroporated embryos, thereby clearly demonstrating the specificity of the effects observed upon Trnp1 knockdown. These results strongly support the previously described role of BPs in radial expansion of the neocortex (Haubensak et al., 2004; Farkas et al., 2008; Fietz and Huttner, 2011; Borrell and Reillo, 2012) and identify Trnp1 as a nuclear regulator of this process.

Trnp1 Knockdown Leads to Increased Production of bRG and Subsequent Gyrification of the Cerebral Cortex

Given the radial expansion and increased number of Tbr2+ cells after Trnp1 knockdown, we asked to what extent also bRG may be increased under these conditions. bRG are characterized by their expression of Pax6, the location of their nucleus in the outer (basal) area of the SVZ, together with the lack of an apical process (Fietz et al., 2010; Hansen et al., 2010; Reillo et al., 2011; Shitamukai et al., 2011; Wang et al., 2011). Remarkably, after Trnp1 knockdown, many Pax6+ cells were found to be located in basal SVZ areas beyond the dense band of Tbr2+ cells (Figures 5A–5B). These cells were clearly separated from the VZ where the vast majority of Pax6+ cells are normally located in the murine brain. Consistent with a bRG identity, these cells possessed a long basal but no apical process (Figures 5C and 5C′) and were clearly different from VZ RG and also from SVZ BPs, which are multipolar. These cells are RG and undergo proliferation as indicated by the phosphorylation of vimentin in M phase (Figure 5D). Quantification and comparison with the non-electroporated (control) hemisphere of the same brain section further confirmed the significant (more than three times) increase of basal Pax6+ cells located beyond the dense Tbr2+ band (Figure 5E). Their bRG identity was further corroborated because most (two out of three) were Tbr2−/Pax6+ upon Trnp1 knockdown, whereas in control, only a minority of the few Pax6+ cells at these basal positions are Tbr2− (Figure 5F). To follow these bRG by live imaging, we sliced cerebral cortices electroporated with shRNA against Trnp1 together with constructs to clonally label the cytoplasm with EGFP and the membrane with mKO2-F (Shitamukai et al., 2011). Brains were sliced 24 hr after electroporation, and live imaging was performed to visualize the processes of dividing cells as previously described by Shitamukai et al. (2011). Interestingly, already 24 hr after electroporation of shRNA targeting Trnp1, many labeled cells had delaminated and lost their apical but still retained a basal process. When following these cells more closely, we could clearly observe bRG undergoing cell division in the typical mode with the basal daughter cell inheriting the basal process (Figure 5G).

Because the increased number of bRG provides additional guides for radially migrating neurons, this typically results in a fanning out of such processes in gyrated cerebral cortices (Lui et al., 2011; Reillo et al., 2011; Borrell and Reillo, 2012). Indeed, RC2 immunostaining revealed the general trajectory of RG processes in the Trnp1shRNA-electroporated cerebral cortex demonstrating that radial fibers fanned out when entering the CP (Figures 5H and 5H′). Most strikingly, we even observed folding of the neocortex within the electroporated area in about 63% of the cortices electroporated with shRNA against Trnp1 at E13 (Figures 5I–5L′; Table S1; n = 24). These folds were notably different from neuronal ectopias such as observed in cobblestone lissencephaly (also known as lissencephaly type II) because the BM was fully intact in case of Trnp1 knockdown (Figures S4F–S4F″), and both sulci and gyri could be followed from rostral to caudal levels (see Figures 5I–5I″). Figures 5I–5I″ show a brain 3 days postelectroporation with small sulci at more rostral levels (Figure 5I) developing into a more extended fold at further caudal regions (Figures 5I′ and 5I″). Most importantly, analysis of long-term survival of shRNA-electroporated brains showed increasing gyrification with several macroscopic folds apparent at postnatal stages (Figures 5K–5L′), demonstrating that these are not transient structures but further enlarge during development. Remarkably, we observed a higher frequency of folding in cerebral cortices left to develop into postnatal stages after electroporation with Trnp1 knockdown (Table S1). This suggests that the brains without visible folds at E16 either did not yet have sufficient time to develop bigger folds, or they were missed and interpreted as "only" expansion due to sectioning limitations such as the angle of cutting. However, even without considering such cases, the overall efficiency of emerging folds upon knockdown of Trnp1 still comprised two-thirds of all brains (Table S1), representing an amazing frequency given the normally lissencephalic nature of the murine cerebral cortex.

Given the high frequency of such folds developing in the cerebral cortex upon Trnp1 knockdown, we set out to observe this also by live imaging. The brains were sliced 24 hr after electroporation with shRNA (plus pCAG-GFP for better visualization of the cells) or pCAG-GFP alone as a control, and low-magnification imaging was performed 48 hr later. Following the overall development of the tissue and cells upon Trnp1 knockdown (Movie S1) allowed visualization of a strikingly fast and robust radial and lateral movement of many GFP-labeled cells that followed the paths of additional bRG fibers (compare Movies S1 and S2; see postimaging 3D reconstruction in Movie S3 and Nestin staining in Figures S4G–S4G″; both showing the slice shown in Movie S1). Additionally, these movies confirmed the increase in delamination from the apical surface and increased proliferation at more basal positions (Movie S4) and also revealed a rather fast migration of newborn neurons upon Trnp1 knockdown (Movie S1 compared to Movie S2). Thus, live imaging revealed several coordinated cell biological events contributing to an apparent gyrification in the murine cerebral cortex.

Because delamination of cells occurred almost too fast to visualize this by live imaging, we returned to still analysis in sections and examined the cleavage plane of APs, as increased oblique or horizontal cell divisions had been previously shown to result in increased bRG production (Shitamukai et al., 2011). Consistent with this, 24 hr after shRNA electroporation, we observed a clear shift toward horizontally oriented cleavage angles, thus generating daughter cells lacking an apical contact prone to delaminate from the ventricular surface (Figures S5A and S5B). Taken together, downregulation of Trnp1 leads to cortical expansion and folding in a dual mode. First, reduced Trnp1 levels lead to delamination and increased generation of both BPs and bRGs. This results second in increased production

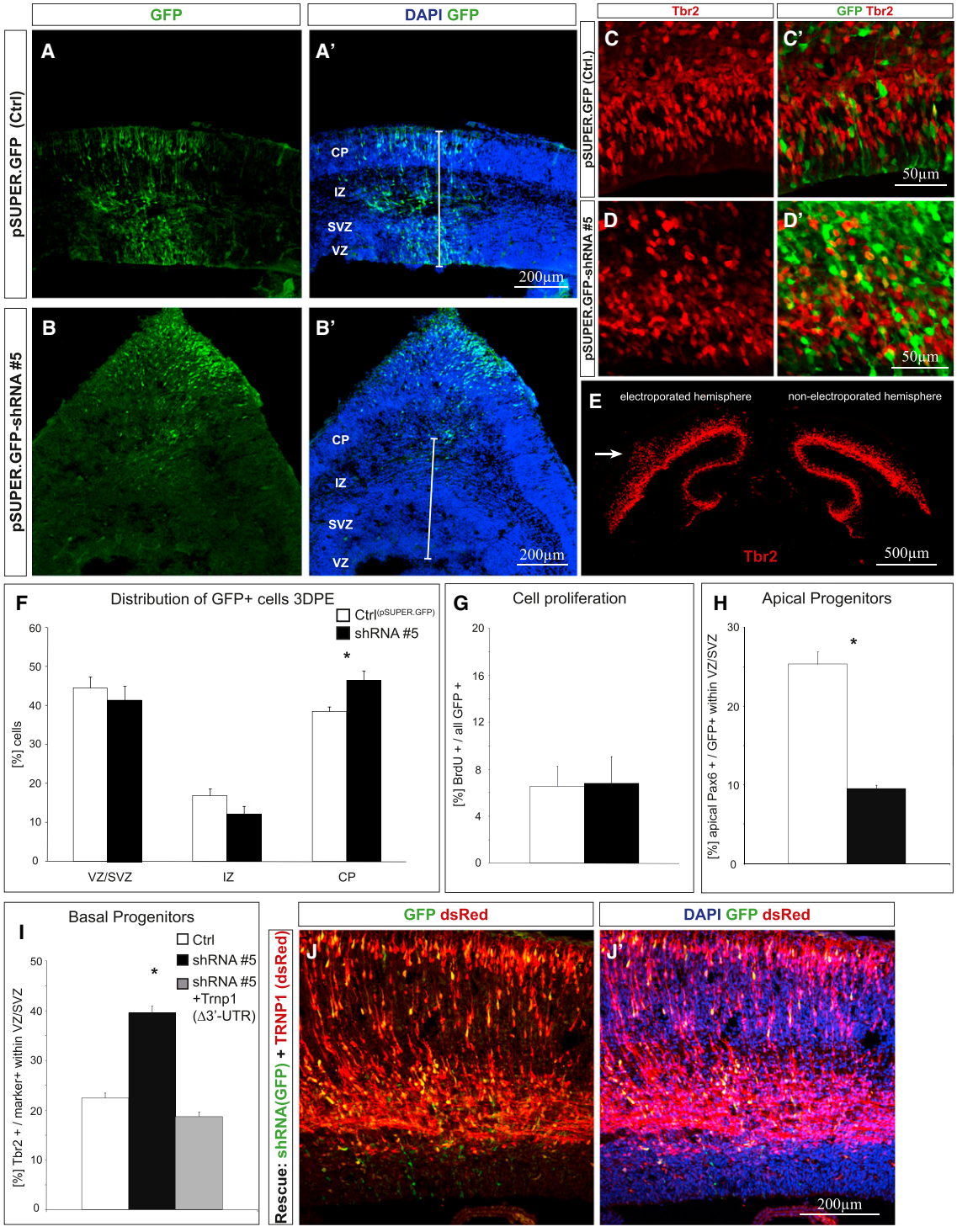

Figure 4. Knockdown of Trnp1 In Vivo Increases the Number of BPs

(A–E) Micrographs of sections of the cerebral cortex analyzed at E16 3 days postelectroporation (DPE) with either pSUPER.GFP control or pSUPER.GFP-shRNA plasmid to knock down Trnp1. Note the strong radial expansion of shRNA-electroporated cortices as visible by the white bar in (A′) and (B′) indicating the radial length of the control-electroporated cortex and the increase of Tbr2+ cells (C–D′), which spread further basally (white arrow in E; reconstruction of one coronal section of an shRNA-electroporated cerebral cortex), absent on the control side (right in E) or after control vector electroporation.

(F–I) Histograms depict the quantification of GFP+ cells (F), their proliferation (G), and progenitor identity (H and I) in these experiments (black bars indicate shRNA; white bars show control).

(legend continued on next page)

of neuron numbers as well as increased bRG fibers that serve as guiding structures. Altogether, such processes cause a lateral dispersion of higher neuron numbers within the CP and ultimately lead to folding of the otherwise lissencephalic murine cerebral cortex.

Trnp1 Is Tightly Associated with DNA and Is Involved in Transcriptional Activation

Given the exciting cell biological functions of Trnp1, we examined its localization within the nucleus more closely to gain insights into its molecular function. Endogenous Trnp1 is homogeneously distributed in euchromatin regions but not detectable in heterochromatin (Figures S5C and S5D). However, in contrast to most transcription factors that dissociate from chromatin in M phase, Trnp1 remained tightly associated with condensed chromosomes during mitosis in vivo and in vitro (Figures S5E, S5F, and S5I–S5I″).

In standard SDS-PAGE analysis, recombinant Trnp1 appears in different bands with a relative molecular weight ranging from 23 to 30 kDa (Figure S1C). This pattern is also observed when endogenous Trnp1 is isolated from brain tissue (Figures S5G and S5H). To test the stringency of Trnp1-DNA interaction, we used an acidic lysis protocol generally used to release basic proteins such as histones from DNA. Strikingly, acidic lysis was not stringent enough to release Trnp1 protein from the nuclear fraction of the developing cerebral cortex at E14. Despite successful release of histones, Trnp1 still remained in the insoluble fraction (Figure S5G). Interestingly, a GFP-fusion construct of Trnp1 no longer showed the strong DNA association of Trnp1 (Figures S5J–S5J″), possibly due to structural alterations of the protein. This fusion protein was also no longer functional because electroporation of the Trnp1-GFP fusion construct was not able to reproduce the overexpression phenotype (Figures S5K and S5L). We thus conclude that the tight DNA association is essential for the molecular function of Trnp1.

Given the role of Trnp1-DNA interaction, we next examined to what extent changes of Trnp1 levels directly affect the transcriptome. We collected RNA from GFP+ cells (isolated by fluorescence-activated cell sorting [FACS]; see Figures S6A–S6B‴) 22–24 hr after electroporation at E13. A gene expression analysis on Affymetrix Gene ST 1.0 arrays revealed a total of 152 differentially expressed probe sets (44 upregulated, 108 downregulated) upon Trnp1 downregulation as compared to control-electorporated samples ($p < 0.01$, fold changes of >1.5, and average expression >50 in at least one group; Figure 6B). Notably, *Trnp1* mRNA was significantly downregulated with a linear ratio of knockdown versus control of 0.76 ($p < 0.01$) (Figure 6A), and random samples of the differentially expressed genes were confirmed by qPCR (Figure S6C). Trnp1 knockdown predominantly resulted in reduced gene expression levels. Gene Ontology term analysis showed a significant ($p < 0.01$) enrichment of terms related to transcriptional regulation (e.g., DNA binding, transcriptional repression or activation, RNA metabolic processes, regulation of gene expression). Specifically, downregulation of Trnp1 resulted in an early response of (1) bHLH transcription factors that play a role in neural differentiation such as NeuroD1/NeuroD2/NeuroD6 and Rnd2; (2) chromatin-remodeling factors such as Chd7, Bmi1, Nuak1, and Smarca5; and (3) histone variants (Hist3h2a, Hist4h4, Hist1h4f, Hist1h4c), which (except for Chd7) were all downregulated. Importantly, no cell-type-specific genes were altered, showing that the time point of analysis (22–24 hr after shRNA electroporation) was sufficiently early to exclude secondary effects based on altered cellular compositions (e.g., apical [Pax6+] or basal [Tbr2+] progenitors). Thus, the observed changes reflect early alterations in gene expression upon Trnp1 knockdown revealing the role of this nuclear protein in activating transcription either directly or indirectly in tight association to euchromatin.

TRNP1 Is Expressed in the Human Developing Brain with Local Differences Correlating with Gyrification

Given the profound effect of Trnp1 on gene expression and the aforementioned phenotype with high levels provoking tangential and low levels resulting in radial expansion, we asked whether Trnp1 may also be expressed in the same layers in the developing human cerebral cortex. In situ hybridization of cerebral cortex sections obtained from specimen at gestational weeks (gws) 12, 18, and 21 (times of early to very late cortical neurogenesis, respectively; Rakic, 1995) revealed a highly specific signal of *TRNP1* mRNA in the developing human brain (no signal was detectable using sense riboprobes; data not shown). Reminiscent of its expression pattern in the murine cerebral cortex, we observed high expression levels in the VZ and in neurons in the CP with rather low expression in the SVZ, where BPs and bRGs are located (Figures 6C–6G). Interestingly, we noted regional differences of *TRNP1* expression in the VZ, which were more pronounced at gws 18 and 21 (see Figures 6D and 6E for an overview). Lower levels of *TRNP1* were found in germinal layers of cortical areas that are known to undergo greater expansion and folding later during development, such as the occipital (Figures 6D and 6D′) and temporal lobes (Figures 6E, 6E′, and 6F), whereas higher levels of *TRNP1* were observed in cortical regions that will undergo little radial expansion and folding, such as the precentral (Figures 6D and 6D″) and parahippocampal gyri (Figures 6E, 6E″, and 6G). These data suggest that TRNP1 plays a central role in mammalian brain development, and differential regulation of its expression levels may be crucial to define the patterns of cortical folding observed in gyrated brains.

DISCUSSION

In this study, we identified Trnp1 as a regulator of mammalian brain development and as a key factor controlling neocortical expansion. Trnp1 levels have striking effects on tangential, radial, and lateral expansion of the cerebral cortex (summarized

(J and J′) Micrographs of the rescue experiments with coelectroporation of the shRNA against *Trnp1* together with the shRNA-resistant form of *Trnp1* and the quantification of resulting BPs in (I) (gray bar shows rescue of the increase in BPs elicited by Trnp1 knockdown). Data are shown as mean ± SEM from five embryos for cellular localization (F), four for APs and BPs (H and I), and three for cell proliferation analysis (G): *$p < 0.05$, Mann-Whitney U test.
See also Figure S3 and Table S1.

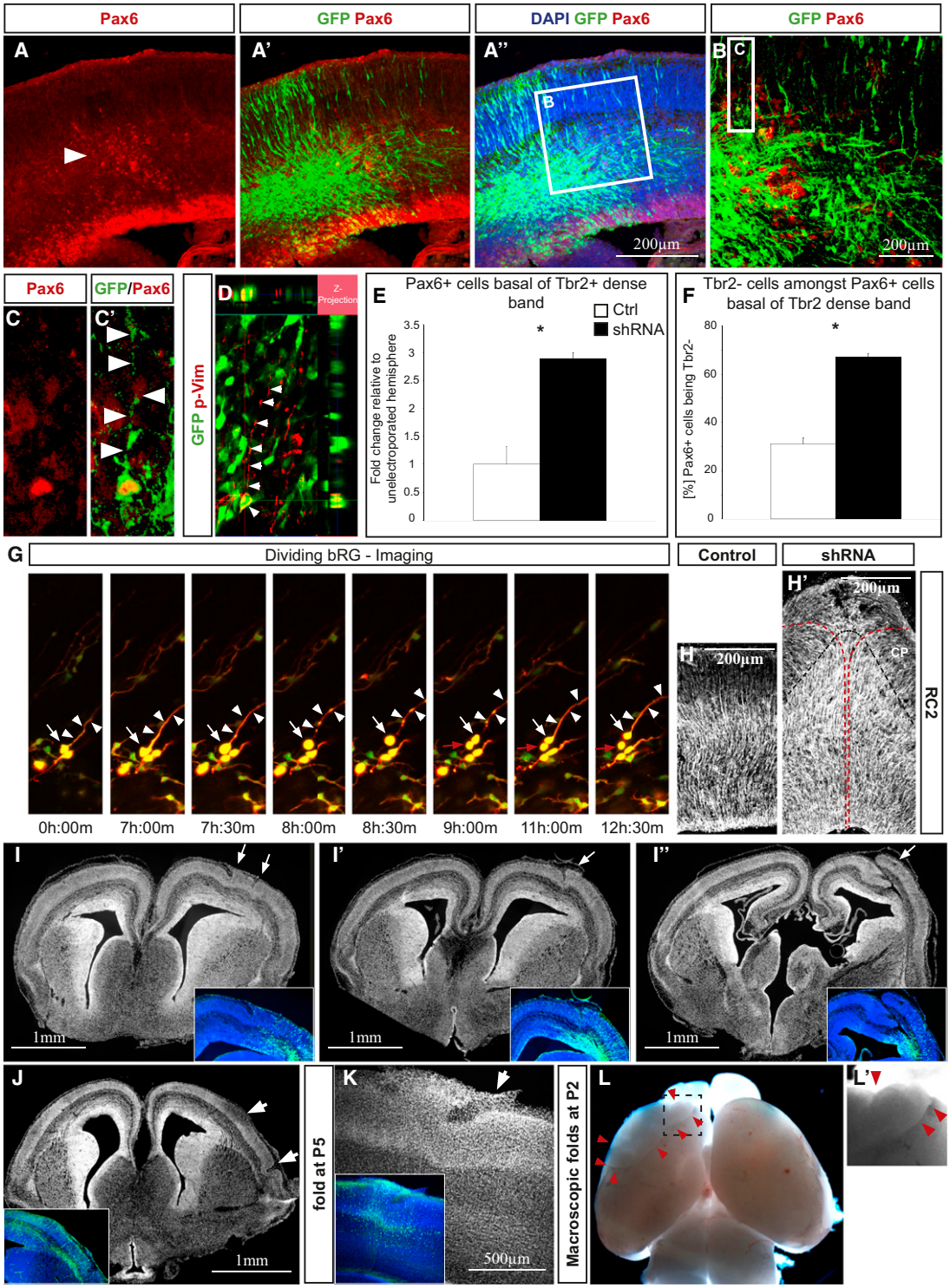

Figure 5. Knockdown of Trnp1 Increases the Number of bRGs and Induces Folding

(A–D) Micrographs of coronal sections from E16 cerebral cortex electroporated at E13 with shRNA against Trnp1 showing more Pax6+ bRG (arrowhead in A) residing far outside the normally Pax6+ VZ (bottom in A–A″) and higher magnifications (B–C′) of the areas indicated in (A″) and (B), respectively. A Z-maximum projection identifying the basal process is shown in (C) and (C′). (D) bRG observed upon knockdown of Trnp1 are p-Vim positive.

(E and F) Histograms of the number of Pax6+ cells at the site of electroporation residing basal of the Tbr2+ dense band (E) (more than 200 µm away from the ventricle) and (F) the percentage of Tbr2− cells among Pax6+ cells counted in (E). Note the significantly increased number of Pax6+ cells in regions basal to the SVZ after Trnp1 knockdown. Data are shown as mean ± SEM from three embryos: *p < 0.05, Mann-Whitney U test.

(legend continued on next page)

in a model in Figure 7). Raising the levels of Trnp1 by overexpression promotes self-renewing RG cell fate, thereby increasing the pool of apically anchored stem cells and causing a tangential expansion of the electroporated region within the murine cerebral cortex (Figures 7A and 7A′). Conversely, lowering the levels of Trnp1 increases the generation of both BPs and bRGs, thereby causing a considerable radial expansion including the formation of gyrus/sulcus-like structures with lateral dispersion of neurons in the CP (Figures 7B and 7B′). Thus, Trnp1 is shown to regulate the generation of apical RG (aRG) versus bRG and BPs at the same time. Therefore, Trnp1 qualifies as a master regulator of RG fate. Furthermore, its manipulation provides a mouse model for gyrification, allowing studying such processes also at the cellular and molecular level.

Mechanisms of Trnp1 Function

Overexpression and knockdown experiments suggest that the levels of Trnp1 expression are crucial for the regulation of tangential versus radial expansion and the choice between apical or basal RG. Importantly, endogenous levels of Trnp1 differ between different subsets of RG: RG generating (Tbr2+) BPs express lower levels of Trnp1, which was the basis for its previous identification by Pinto et al. (2008). Conversely, self-renewing apical RG have higher Trnp1 levels, and their decreasing number during development is reflected by reduced numbers of Trnp1+ cells in the VZ. A role for high levels of Trnp1 in promoting self-renewal of RG was further evident by overexpression in vitro with self-renewing NSCs expanding by cell-cycle reentry and symmetric proliferative divisions and in vivo with increasing Pax6+ and BrdU-incorporating cells in the VZ. Trnp1 overexpression also enhanced proliferation in a breast cancer cell line by promoting G1/S transition (Volpe et al., 2006), suggesting that Trnp1 may act at various levels in regulating proliferation. Indeed, we showed here that it also affects the orientation of cell divisions in the developing cerebral cortex.

However, Trnp1 is also expressed in postmitotic young neurons, and despite its relevance in regulating proliferation, it is important to note that Trnp1 is not generally expressed in all proliferative cells. It is absent in highly proliferative cell lines such as HEK, NRK, or ES cell-derived neural progenitors (data not shown), in BPs and in glial progenitors in vivo and in vitro (data not shown). Thus, Trnp1 is a key regulator of cell fate controlling specific aspects in stem or progenitor cells rather than serving as a common regulator of proliferation.

Trnp1 appears to require extraordinarily strong DNA interaction for its intriguing functions. Although endogenous Trnp1 remained associated with condensed chromosomes during mitosis (contrary to most transcription factors), a Trnp1-GFP fusion protein dissociated from the chromatids during mitosis. The fusion construct could not promote the increase in Pax6+ NSCs but rather exhibited a partial loss-of-function phenotype in vivo, suggesting that this fusion protein may also interfere with the function of the endogenous protein. This effect may be mediated by the formation of helix bundles with the endogenous Trnp1. The central part of the protein contains either one long or multiple short helices (whereas the N- and C-terminal ends are rather unstructured as revealed by in silico analysis) and a strikingly high number of arginines (10%) resulting in its highly basic nature (PI around 12). A similarly high proportion of arginines is found in the protein sequence of UTF1 (van den Boom et al., 2007), which has the capacity to affect chromatin compaction (Kooistra et al., 2010). Intriguingly, genome-wide expression analysis after knockdown of Trnp1 revealed that many of the differentially regulated genes are involved in chromatin regulation, for example chromatin remodeling factors such as Smarca5, Bmi1, Chd7, ccdc101, and several histone variants (Table S2). In addition, mRNA levels of some transcription factors of the NeuroD or zinc finger families were altered (Table S2). Importantly, none of the classical hallmarks for cell or progenitor types was altered in expression in this analysis, demonstrating that we do not monitor the outcome of cell fate changes but rather the very first targets of Trnp1 regulated by its tight association with DNA and chromatin.

Gyrification in the Mouse Cerebral Cortex

Beyond its molecular functions, manipulating Trnp1 levels in vivo resulted in dramatic alterations in mouse cerebral cortex development, culminating in gyrus formation in the brain of this naturally lissencephalic animal. The development of gyrification involves generating a very large number of neurons per ventricular surface area (i.e., per apical RG; radial expansion) and providing these cells with the adequate scaffold to translate their radial migratory movement into lateral dispersion in the CP. In gyrated mammals, this radial expansion and lateral dispersion of neurons is achieved by a dramatic increase in neurogenic progenitor cells and the massive formation of bRG in the oSVZ, which are critical to lead radially migrating neurons into lateral dispersion (Dehay and Kennedy, 2007; Borrell and Reillo, 2012). Remarkably, knockdown of Trnp1 alone was sufficient to induce a rapid progression from apical RG into both BPs and bRG in vivo in the mouse cerebral cortex. In contrast to the normally rather inefficient generation of bRG in the murine cerebral cortex (Shitamukai et al., 2011; Wang et al., 2011), the generation of unusually large numbers of BPs and bRGs after Trnp1 knockdown leads to the formation of a thickened SVZ resembling the

(G) Sequences of a time-lapse movie following a dividing bRG in a cerebral cortex slice prepared at E14 24 hr after electroporation with Trnp1 shRNA and plasmids for Cre, FloxP-EGFP, and mKO2-F for sparse cytoplasmic and membrane labeling (Shitamukai et al., 2011). White arrows and arrowheads indicate the bRG before and after cell division; red arrow indicates the multipolar daughter cell lacking a basal or apical process.

(H and H′) Staining of RG fibers (RC2) in an shRNA-electroporated, radially expanded cerebral cortex (H′) revealing the increase and divergence of radial fibers at basal sides upon loss of Trnp1 (radial processes indicated by red dashed lines; reconstruction from two individual confocal images is shown in H′) compared to the nonelectroporated hemisphere (H).

(I)–(L′) Examples of folds observed in the regions electroporated with Trnp1 shRNA at E13 analyzed at E16 (I–J; with I–I″ showing rostro-caudal series from the same brain with two independent folds rostrally in I, fusing into a big expanded fold more caudally in I″) or postnatal stages (K–L′). Note the macroscopic folds at postnatal stages. Folds are indicated by arrows in (I)–(K) and area with several folds outlined by red arrowheads in (L) and (L′).

See also Figures S4 and S5, Table S1, and Movies S1, S2, S3, and S4.

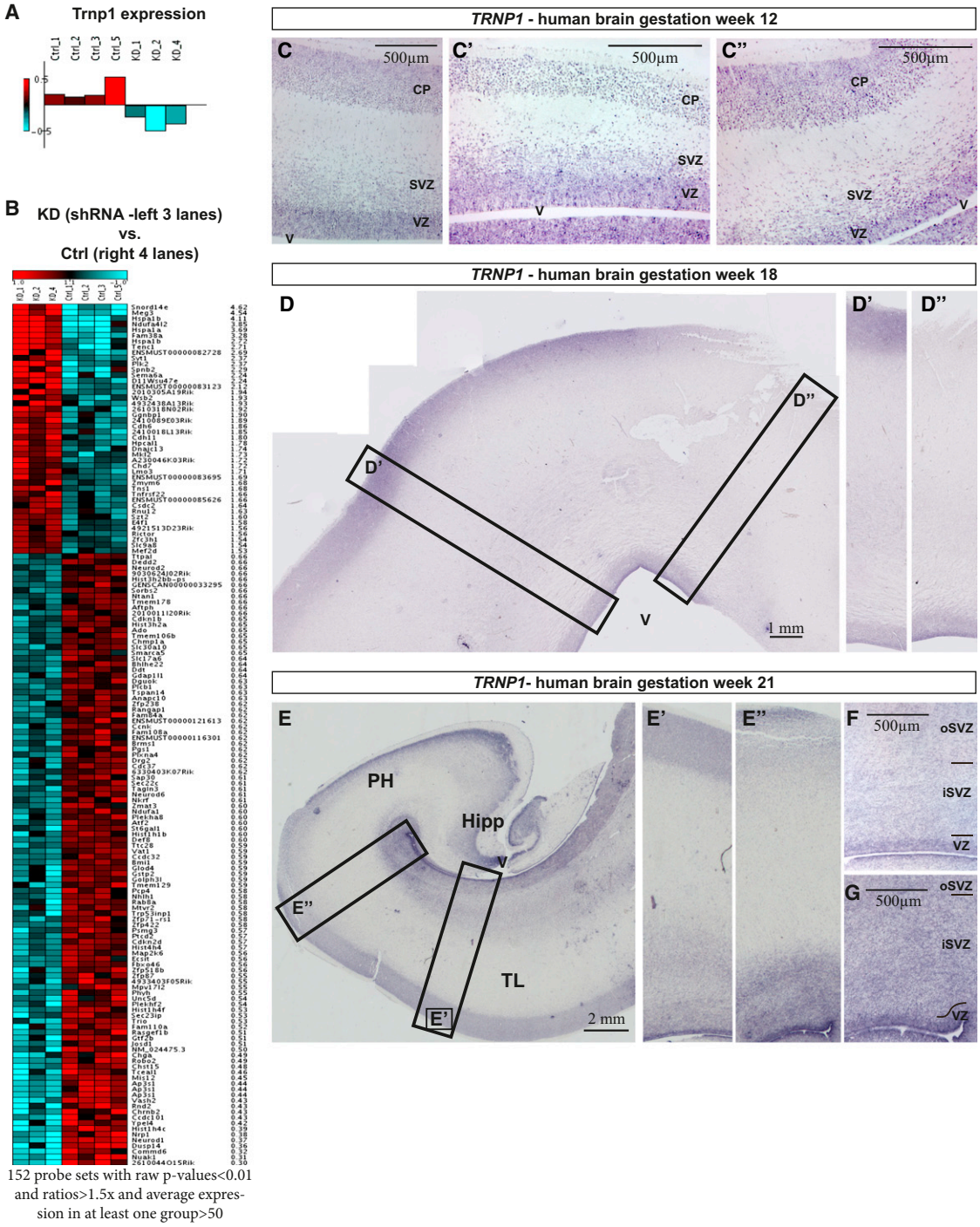

Figure 6. Genome-wide Expression Changes upon Trnp1 Knockdown in Mouse and *TRNP1* Expression in Human Cerebral Cortex

(A and B) Heatmap for Trnp1 probe sets (A) and 152 differentially regulated genes (B; average expression >50 in at least one group, p value <0.01, and linear fold change of >1.5-fold) in samples of GFP+ cells sorted by FACS 24 hr after electroporation of E13 cerebral cortex with Trnp1 shRNA (knockdown, KD) or control (Ctrl) constructs.

(C–G) In situ hybridization with *TRNP1* antisense probe of telencephalon sections from human embryos of gws 12 (C–C″), 18 (D–D″'), and 21 (E–G). Note the differential expression of *TRNP1* in the VZ of different areas (D′, D″, E′, and E″). (F–G) Zoom of the germinal zones of (E′) in (F) and (E″) in (G). Hipp, hippocampus; PH, parahippocampal gyrus; TL, temporal lobe.

See also Figures S5 and S6 and Table S2.

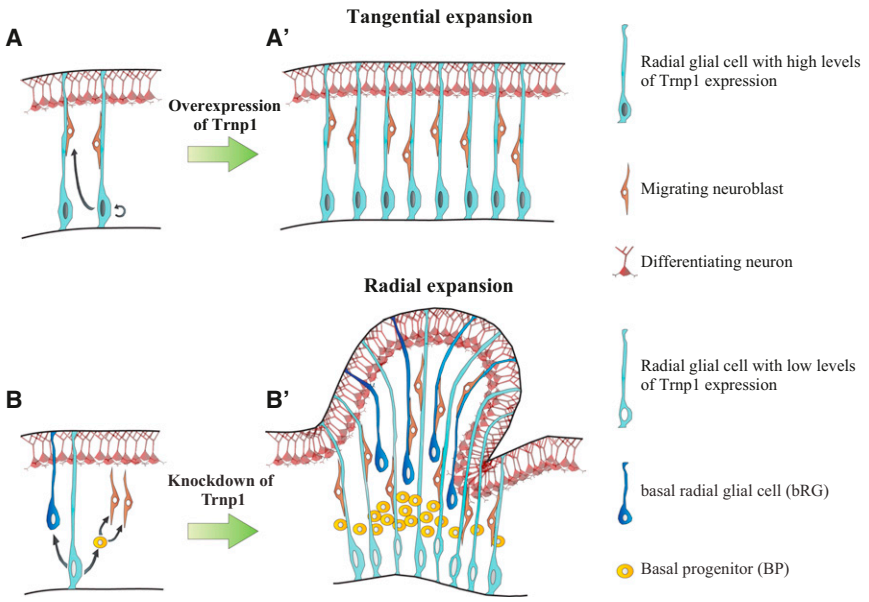

Figure 7. Model of Trnp1 Action in Cerebral Cortex Development

Illustration of the function of Trnp1 in NSCs of the developing cerebral cortex.

(A and A′) RGs with higher levels of Trnp1 expression (dark-blue nucleus) proliferate and self-renew through either symmetric divisions (generating two RGs) or asymmetric divisions (allowing direct neurogenesis at the same time) (A). Trnp1 overexpression enlarges the pool of apical RGs that self-renew, thereby leading to tangential expansion (A′).

(B and B′) Apical RGs with lower levels of Trnp1 (empty nucleus) are engaged in the generation of BPs or bRGs (B). Trnp1 knockdown results in a considerable expansion of both BPs and bRG located even beyond the normal SVZ in the mouse cerebral cortex, thereby forming a kind of oSVZ (B′). These concerted changes lead to a radial expansion of the cerebral cortex and ultimately to folding as naturally occurring in species with gyrated cerebral cortices.

oSVZ in species with enlarged cerebral cortex size (Fietz et al., 2010; Hansen et al., 2010; Reillo and Borrell, 2012). This results in considerable radial expansion and simultaneously generates additional radial fibers for lateral dispersion resembling the diverging radial fibers described for gyrencephalic brains by Smart et al. (2002) and Reillo et al. (2011). This provides additional guiding structures for the higher numbers of neurons generated upon Trnp1 knockdown, and we could indeed observe their diverging lateral dispersion during fold formation by live imaging (see Movies S1, S3, and S4). Thus, acute downregulation of Trnp1 is sufficient to regulate the appearance of these hallmarks in a concerted manner, providing an entry point into the cellular and molecular dynamics regulating such complex processes.

Live imaging and genome-wide expression changes upon Trnp1 knockdown allowed us to gain insights into the events leading to these remarkable phenotypes. Trnp1 knockdown had changed the cleavage angles such that more daughter cells lacking an apical anchor were produced, and live imaging confirmed that many more progenitors had delaminated from the apical surface already 24 hr after electroporation of shRNA against Trnp1 compared to controls. Consistent with these cell biological changes, we observed differential expression of molecules involved in apical anchoring of RGs (Table S2), such as Nrp1, Robo2, Cdh6, and Cdh11 (Borrell et al., 2012), and with GTPase activity, such as Trio, a RhoGEF involved in regulating apical constriction (Plageman et al., 2011).

Besides delaminating, cells subject to Trnp1 knockdown actively proliferated at further basal positions of the expanded SVZ, as frequently observed by live imaging for cells with BP or bRG morphology. Again, microarray data revealed a molecular correlate to this behavior because genes promoting the maturation of BPs toward the postmitotic multipolar stage, such as Unc5d, NeuroD1, and NeuroD6 (Miyoshi and Fishell, 2012), were downregulated (Table S2), thereby delaying the progression from the early to the late multipolar stage (LoTurco and Bai, 2006) and maintaining BPs in the proliferative mode for a longer time. Interestingly, these genes are also regulated by FoxG1 (Miyoshi and Fishell, 2012), whose expression resembles Trnp1 in as much as it is also high in VZ progenitors, then expression is reduced in SVZ progenitors but increased in postmitotic neurons.

Finally, live imaging also revealed an indication of a possible role of Trnp1 in postmitotic neurons because their migration was much faster when Trnp1 levels were reduced (Movie S1 as compared to Movie S2) in correlation with downregulation of proteins involved in regulating neuronal migration (Table S2). Consistent with its endogenous expression, Trnp1 knockdown affected gene expression at various stages in the lineage progression from VZ to SVZ progenitors and differentiating neurons (Table S2). Hence, Trnp1 affects all of these steps in a concerted manner thereby coordinating cellular behaviors that ultimately result in considerable radial expansion and gyrus formation in the cerebral cortex.

Phylogenetic Consideration

This striking phenotype raised the question of to what extent Trnp1 is relevant to regulating gyrification during phylogeny. The degree of cortical gyrification across phylogeny has been shown to correlate positively with the abundance of bRG. Because almost all mammalian superorders comprise species with smooth lissencephalic brains and also folded gyrencephalic brains, regulatory mechanisms may presumably be present in all mammals (Borrell and Reillo, 2012; Kelava et al., 2012; García-Moreno et al., 2012). Rather than the invention of a "new" gene in gyrencephalic mammals, such preexisting genes may have been co-opted via their differential regulation (True and Carroll, 2002). Our findings showing that Trnp1 levels regulate the proportion of BPs and bRGs simultaneously support this hypothesis and provide a mechanistic basis for the finding that

the proportion of bRGs and the extent of gyrification have changed several times during mammalian evolution (Borrell and Reillo, 2012; Kelava et al., 2012). Such mechanisms may also explain the selective expansion of some areas of the cerebral cortex. As a first step toward elucidating these fascinating questions, we show here that *TRNP1* is also expressed in the VZ and neuronal layers of the developing human cerebral cortex, and quantitative differences in *TRNP1* expression seemingly correlate with some of the regions undergoing more or less folding.

Our findings thus unraveled Trnp1 as a molecular factor involved in the regulation of both tangential and radial expansion of the cerebral cortex. This shows that the dynamic regulation of the expression of a single gene is sufficient to orchestrate the events required for gyrus formation even in a naturally lissencephalic cerebral cortex. Manipulations of Trnp1 levels further support a model by which dynamic regulation of one factor can contribute to differential expansion of distinct cortical regions controlling first tangential and then radial expansion of a given neocortical region. This scenario therefore provides a blueprint to study the cellular and molecular mechanisms of cerebral cortex expansion and folding.

EXPERIMENTAL PROCEDURES

Immunostaining, in utero electroporation, dissociated cell cultures, in situ hybridization, and retrovirus production were performed as described previously (Cappello et al., 2012; Flames et al., 2007) and are also available in detail in the Extended Experimental Procedures. All experimental procedures were performed in accordance with the regulations of the Helmholtz Center Munich, and animal experiments were approved by the government of upper Bavaria.

Plasmid Constructs

The coding sequence of *Trnp1* was subcloned from pCMV-Sport6-*Trnp1* (RZPD clone) into pCAG-GFP and pCAG-dsRed (pCAG destination vectors were a kind gift of Paolo Malatesta). To downregulate Trnp1 expression, three different shRNAs were cloned into pSUPER.GFP/Neo: shRNA #1, 5′-ACTCTGCATTGCTTCCCATACACTG-3′; shRNA #4, 5′-GCAGAAAGG CAAGCCACTTCT-3′; and shRNA #5, 5′-GATGGACGGCGTCATCTAC-3′, each targeting different regions of the 3′ UTR of *Trnp1-mRNA*. The target region is not contained in the pCAG-*Trnp1*-GFP/dsRed vector which was therefore usable for rescue of the knockdown effect. Empty pCAG-GFP, pCAG-dsRed, and pSUPER-GFP.Neo vectors were used as controls. For detailed cloning strategy, see the Extended Experimental Procedures.

Human Tissue

Brain sections of human fetuses from spontaneous abortions were obtained from the Service of Pathology, Hospital Universitario Principe de Asturias, Alcalá de Henares, Spain. Brains were removed in routine necropsies in accordance with the Spanish law on clinical autopsies (Boletín Oficial del Estado [BOE] June 27, 1980, and BOE September 11, 1982). After removal, brains were fixed by immersion in buffered 4% paraformaldehyde (PFA) at room temperature during 2 weeks. Then coronal blocks across the entire brain were obtained; these blocks were embedded in toto in paraffin and finally sectioned and stained. For additional methods, please see the Extended Experimental Procedures.

ACCESSION NUMBERS

Array data have been submitted to GEO (record GSE40582), and the following link allows review while it remains in private status: http://www.ncbi.nlm.nih.gov/geo/query/acc.cgi?token=tzcrzsuwmecogbu&acc=GSE40582.

SUPPLEMENTAL INFORMATION

Supplemental Information includes Extended Experimental Procedures, six figures, two tables, and four movies and can be found with this article online at http://dx.doi.org/10.1016/j.cell.2013.03.027.

ACKNOWLEDGMENTS

We are particularly grateful to Gabriele Jäger, Andrea Steiner-Mezzadri, and Emily Violette Baumgart for excellent technical support and to Alexandra Lepier and Simone Bauer for support in regard to viral vector production. We thank Judith Fischer-Sternjak for help with flow cytometry. Particular thanks to Atsunori Shitamukai and Fumio Matsuzaki for the constructs used for electroporation to visualize the morphology of basal radial glial cells by live imaging. We also thank Paolo Malatesta for the pCAG destination vectors. Special thanks to Olga Díez Jambrina (Service of Pathology, Hospital Universitario Principe de Asturias, Alcalá de Henares, Spain) for invaluable help in processing the tissue from human fetal brains and to Wolfgang Enard for great discussions and very helpful comments on the manuscript. This work was funded by MICINN with a "Juan de la Cierva" contract to C.D.J.R. and grants SAF2009-07367 and CONSOLIDER CSD2007-00023 to V.B., and by the DFG via the Gottfried-Wilhelm Leibniz Award, the German Excellence Program (LMU Excellent, CIPS), and the SFB 870 to M.G.

Received: October 8, 2012
Revised: January 31, 2013
Accepted: March 13, 2013
Published: April 25, 2013

REFERENCES

Asami, M., Pilz, G.A., Ninkovic, J., Godinho, L., Schroeder, T., Huttner, W.B., and Götz, M. (2011). The role of Pax6 in regulating the orientation and mode of cell division of progenitors in the mouse cerebral cortex. Development *138*, 5067–5078.

Bayatti, N., Moss, J.A., Sun, L., Ambrose, P., Ward, J.F.H., Lindsay, S., and Clowry, G.J. (2008). A molecular neuroanatomical study of the developing human neocortex from 8 to 17 postconceptional weeks revealing the early differentiation of the subplate and subventricular zone. Cereb. Cortex *18*, 1536–1548.

Borrell, V., and Reillo, I. (2012). Emerging roles of neural stem cells in cerebral cortex development and evolution. Dev. Neurobiol. *72*, 955–971.

Borrell, V., Cárdenas, A., Ciceri, G., Galcerán, J., Flames, N., Pla, R., Nóbrega-Pereira, S., García-Frigola, C., Peregrín, S., Zhao, Z., et al. (2012). Slit/Robo signaling modulates the proliferation of central nervous system progenitors. Neuron *76*, 338–352.

Cappello, S., Böhringer, C.R.J., Bergami, M., Conzelmann, K.-K., Ghanem, A., Tomassy, G.S., Arlotta, P., Mainardi, M., Allegra, M., Caleo, M., et al. (2012). A radial glia-specific role of RhoA in double cortex formation. Neuron *73*, 911–924.

Chenn, A., and Walsh, C.A. (2002). Regulation of cerebral cortical size by control of cell cycle exit in neural precursors. Science *297*, 365–369.

Costa, M.R., Wen, G., Lepier, A., Schroeder, T., and Götz, M. (2008). Par-complex proteins promote proliferative progenitor divisions in the developing mouse cerebral cortex. Development *135*, 11–22.

Dehay, C., and Kennedy, H. (2007). Cell-cycle control and cortical development. Nat. Rev. Neurosci. *8*, 438–450.

Farkas, L.M., Haffner, C., Giger, T., Khaitovich, P., Nowick, K., Birchmeier, C., Pääbo, S., and Huttner, W.B. (2008). Insulinoma-associated 1 has a panneurogenic role and promotes the generation and expansion of basal progenitors in the developing mouse neocortex. Neuron *60*, 40–55.

Fietz, S.A., and Huttner, W.B. (2011). Cortical progenitor expansion, self-renewal and neurogenesis—a polarized perspective. Curr. Opin. Neurobiol. *21*, 23–35.

Fietz, S.A., Kelava, I., Vogt, J., Wilsch-Bräuninger, M., Stenzel, D., Fish, J.L., Corbeil, D., Riehn, A., Distler, W., Nitsch, R., and Huttner, W.B. (2010). OSVZ progenitors of human and ferret neocortex are epithelial-like and expand by integrin signaling. Nat. Neurosci. *13*, 690–699.

Fish, J.L., Dehay, C., Kennedy, H., and Huttner, W.B. (2008). Making bigger brains-the evolution of neural-progenitor-cell division. J. Cell Sci. *121*, 2783–2793.

Flames, N., Pla, R., Gelman, D.M., Rubenstein, J.L., Puelles, L., and Marín, O. (2007). Delineation of multiple subpallial progenitor domains by the combinatorial expression of transcriptional codes. J. Neurosci. *27*, 9682–9695.

García-Moreno, F., Vasistha, N.A., Trevia, N., Bourne, J.A., and Molnár, Z. (2012). Compartmentalization of cerebral cortical germinal zones in a lissencephalic primate and gyrencephalic rodent. Cereb. Cortex *22*, 482–492.

Götz, M., and Huttner, W.B. (2005). The cell biology of neurogenesis. Nat. Rev. Mol. Cell Biol. *6*, 777–788.

Hansen, D.V., Lui, J.H., Parker, P.R.L., and Kriegstein, A.R. (2010). Neurogenic radial glia in the outer subventricular zone of human neocortex. Nature *464*, 554–561.

Haubensak, W., Attardo, A., Denk, W., and Huttner, W.B. (2004). Neurons arise in the basal neuroepithelium of the early mammalian telencephalon: a major site of neurogenesis. Proc. Natl. Acad. Sci. USA *101*, 3196–3201.

Haubst, N., Berger, J., Radjendirane, V., Graw, J., Favor, J., Saunders, G.F., Stoykova, A., and Götz, M. (2004). Molecular dissection of Pax6 function: the specific roles of the paired domain and homeodomain in brain development. Development *131*, 6131–6140.

Heinrich, C., Gascón, S., Masserdotti, G., Lepier, A., Sanchez, R., Simon-Ebert, T., Schroeder, T., Götz, M., and Berninger, B. (2011). Generation of subtype-specific neurons from postnatal astroglia of the mouse cerebral cortex. Nat. Protoc. *6*, 214–228.

Kelava, I., Reillo, I., Murayama, A.Y., Kalinka, A.T., Stenzel, D., Tomancak, P., Matsuzaki, F., Lebrand, C., Sasaki, E., Schwamborn, J.C., et al. (2012). Abundant occurrence of basal radial glia in the subventricular zone of embryonic neocortex of a lissencephalic primate, the common marmoset *Callithrix jacchus*. Cereb. Cortex *22*, 469–481.

Kooistra, S.M., van den Boom, V., Thummer, R.P., Johannes, F., Wardenaar, R., Tesson, B.M., Veenhoff, L.M., Fusetti, F., O'Neill, L.P., Turner, B.M., et al. (2010). Undifferentiated embryonic cell transcription factor 1 regulates ESC chromatin organization and gene expression. Stem Cells *28*, 1703–1714.

Krubitzer, L. (2007). The magnificent compromise: cortical field evolution in mammals. Neuron *56*, 201–208.

LoTurco, J.J., and Bai, J. (2006). The multipolar stage and disruptions in neuronal migration. Trends Neurosci. *29*, 407–413.

Lui, J.H., Hansen, D.V., and Kriegstein, A.R. (2011). Development and evolution of the human neocortex. Cell *146*, 18–36.

Martínez-Cerdeño, V., Cunningham, C.L., Camacho, J., Antczak, J.L., Prakash, A.N., Cziep, M.E., Walker, A.I., and Noctor, S.C. (2012). Comparative analysis of the subventricular zone in rat, ferret and macaque: evidence for an outer subventricular zone in rodents. PLoS One *7*, e30178.

Miyoshi, G., and Fishell, G. (2012). Dynamic FoxG1 expression coordinates the integration of multipolar pyramidal neuron precursors into the cortical plate. Neuron *74*, 1045–1058.

Pinto, L., Mader, M.T., Irmler, M., Gentilini, M., Santoni, F., Drechsel, D., Blum, R., Stahl, R., Bulfone, A., Malatesta, P., et al. (2008). Prospective isolation of functionally distinct radial glial subtypes—lineage and transcriptome analysis. Mol. Cell. Neurosci. *38*, 15–42.

Pinto, L., Drechsel, D., Schmid, M.T., Ninkovic, J., Irmler, M., Brill, M.S., Restani, L., Gianfranceschi, L., Cerri, C., Weber, S.N., et al. (2009). AP2γ regulates basal progenitor fate in a region- and layer-specific manner in the developing cortex. Nat. Neurosci. *12*, 1229–1237.

Plageman, T.F., Jr., Chauhan, B.K., Yang, C., Jaudon, F., Shang, X., Zheng, Y., Lou, M., Debant, A., Hildebrand, J.D., and Lang, R.A. (2011). A Trio-RhoA-Shroom3 pathway is required for apical constriction and epithelial invagination. Development *138*, 5177–5188.

Rakic, P. (1995). A small step for the cell, a giant leap for mankind: a hypothesis of neocortical expansion during evolution. Trends Neurosci. *18*, 383–388.

Reillo, I., and Borrell, V. (2012). Germinal zones in the developing cerebral cortex of ferret: ontogeny, cell cycle kinetics, and diversity of progenitors. Cereb. Cortex *22*, 2039–2054.

Reillo, I., de Juan Romero, C., García-Cabezas, M.A., and Borrell, V. (2011). A role for intermediate radial glia in the tangential expansion of the mammalian cerebral cortex. Cereb. Cortex *21*, 1674–1694.

Shitamukai, A., Konno, D., and Matsuzaki, F. (2011). Oblique radial glial divisions in the developing mouse neocortex induce self-renewing progenitors outside the germinal zone that resemble primate outer subventricular zone progenitors. J. Neurosci. *31*, 3683–3695.

Smart, I.H.M., Dehay, C., Giroud, P., Berland, M., and Kennedy, H. (2002). Unique morphological features of the proliferative zones and postmitotic compartments of the neural epithelium giving rise to striate and extrastriate cortex in the monkey. Cereb. Cortex *12*, 37–53.

True, J.R., and Carroll, S.B. (2002). Gene co-option in physiological and morphological evolution. Annu. Rev. Cell Dev. Biol. *18*, 53–80.

van den Boom, V., Kooistra, S.M., Boesjes, M., Geverts, B., Houtsmuller, A.B., Monzen, K., Komuro, I., Essers, J., Drenth-Diephuis, L.J., and Eggen, B.J.L. (2007). UTF1 is a chromatin-associated protein involved in ES cell differentiation. J. Cell Biol. *178*, 913–924.

Volpe, M., Shpungin, S., Barbi, C., Abrham, G., Malovani, H., Wides, R., and Nir, U. (2006). trnp: a conserved mammalian gene encoding a nuclear protein that accelerates cell-cycle progression. DNA Cell Biol. *25*, 331–339.

Wang, X., Tsai, J.W., LaMonica, B., and Kriegstein, A.R. (2011). A new subtype of progenitor cell in the mouse embryonic neocortex. Nat. Neurosci. *14*, 555–561.

Note Added in Proof

A recent paper by Nonaka-Kinoshita et al. in EMBO J describes effects on gyrification in the ferret cerebral cortex by altering cell-cycle properties, although this is not sufficient to achieve gyrification in mouse cerebral cortex. Nonaka-Kinoshita, M., Reillo, I., Artegiani, B., Martínez-Martínez, M.A., Nelson, M., Borrell, V., and Calegari, F. (2013). Regulation of cerebral cortex size and folding by expansion of basal progenitors. Published online April 26, 2013. http://dx.doi.org/10.1038/emboj.2013.96.

2.3 The loss of the transcription factor Pax6 leads to changes in cleavage angle and mode of division in cerebral cortical progenitors and to more "ventralized" cellular phenotypes

The following section includes work that was published entitled "The role of Pax6 in regulating the orientation and mode of cell division of progenitors in the mouse cerebral cortex" by Maki Asami, Gregor-Alexander Pilz, Jovica Ninkovic, Leanne Godinho, Timm Schröder, Wieland B. Huttner and Magdalena Götz in *Development* 2011 Dec. 138 (23); 5067-78.

Summary: This study aims to unravel the function of Pax6 on a cellular and molecular level during development of the neocortex. For this, either the Pax6 mutant *Sey* mouse line or an acute Pax6 knockdown by Cre electroporation into Pax6 fl/fl mice were utilized. In order to investigate a potential role in mode of division, the cleavage angle of apical progenitors in the *Sey* cortex were analyzed. This revealed that in contrast to the WT cortex more APs divide in an oblique and horizontal cleavage plane, indicative of likely asymmetric daughter cell fates. En face view imaging after in-utero electroporation of the plasmids EGFP-ZO1 and Pact-mKO1 uncovered that in agreement with the altered cleavage angles, also the apical membrane domain was asymmetrically partitioned in the *Sey* cortex. The immunohistochemical analysis of adherence junction proteins uncovered in addition a decreased expression of molecules like N-cadherin, ß-catenin, aPKC, Par3 after loss of Pax6 in the *Sey* adherence junction belt. These changes in cleavage plane and apical anchoring in the adherence junction belt let to the delamination of progenitor cells and the appearance of progenitors with RG specific marker expression (Glast+) dividing at basal positions. Acute deletion of Pax6 by Cre-GFP electroporation into Pax6 fl/fl mice led to an increase of basally dividing cells, with a reduction in Pax6 and Ngn2 positive cells, but an increase in Ascl1 positive characteristic of the loss of Pax6 in the cortex. In order to investigate the effect of Pax6 on proliferation in a cell autonomous manner, single cell tracking of dissociated, in vitro cultured cells from WT and Pax6 *Sey* cortex was carried

out over several days. This revealed an increase in asymmetric and symmetric terminal division modes in comparison to cells from the WT cortex. A search through chromatin immunoprecipitation (ChIP) data led to the identification of Spag5 as a causal downstream target of Pax6, which was confirmed by both luciferase and ChIP assays. To see if the knockdown of Spag5 would phenocopy the situation in the Pax6 *Sey* cortex, Spag5 was acutely downregulated by in-utero electroporation which led to comparable alterations in cleavage planes. This confirmed a role of Spag5 as a downstream target of Pax6 in spindle orientation.

Author contributions to this publication

Maki Asami performed all the experiments and analyzed the data until otherwise stated. Gregor-Alexander Pilz assisted with in-utero electroporation and live brain slice imaging and performed the in-utero electroporations for the Spag5 knockdown including tissue processing and microscopy. Jovica Ninkovic carried out the ChIP – qPCR assay. Leanne Godinho helped to initially establish the slice imaging technique. Timm Schröder provided support and software for in vitro timelapse experiments and tracking. Wieland B Huttner provided the Tis21-GFP and provided conceptual support. Magdalena Götz designed and supervised the study and wrote the manuscript together with Maki Asami.

Development 138, 5067-5078 (2011) doi:10.1242/dev.074591

The role of Pax6 in regulating the orientation and mode of cell division of progenitors in the mouse cerebral cortex

Maki Asami[1], Gregor A. Pilz[1], Jovica Ninkovic[1,4], Leanne Godinho[2], Timm Schroeder[1], Wieland B. Huttner[3] and Magdalena Götz[1,4,*]

SUMMARY

Successful brain development requires tight regulation of sequential symmetric and asymmetric cell division. Although Pax6 is known to exert multiple roles in the developing nervous system, its role in the regulation of cell division is unknown. Here, we demonstrate profound alterations in the orientation and mode of cell division in the cerebral cortex of mice deficient in Pax6 function ($Pax6^{Sey/Sey}$) or after acute induced deletion of Pax6. Live imaging revealed an increase in non-vertical cellular cleavage planes, resulting in an increased number of progenitors with unequal inheritance of the apical membrane domain and adherens junctions in the absence of Pax6 function. This phenotype appears to be mediated by the direct Pax6 target Spag5, a microtubule-associated protein, reduced levels of which result in the replication of the Pax6 phenotype of altered cell division orientation. In addition, lack of Pax6 also results in premature delamination of progenitor cells from the apical surface due to an overall decrease in proteins mediating anchoring at the ventricular surface. Moreover, continuous long-term imaging in vitro revealed that Pax6-deficient progenitors generate daughter cells with asymmetric fates at higher frequencies. These data demonstrate a cell-autonomous role for Pax6 in regulating the mode of cell division independently of apicobasal polarity and cell-cell interactions. Taken together, our work reveals several direct effects that the transcription factor Pax6 has on the machinery that mediates the orientation and mode of cell division.

KEY WORDS: Radial glia, Asymmetric cell division, Neurogenesis, Spag5

INTRODUCTION

The mammalian neocortex develops from a pseudostratified neuroepithelium by progressive cell divisions of neuroepithelial cells and radial glia (Götz and Huttner, 2005). Before the onset of neurogenesis, neuroepithelial cells divide mostly in a symmetric manner to yield exponential progenitor production and tangential growth of the cortex. During neurogenesis, asymmetric cell divisions take over, producing either one neuron or a neurogenic basal progenitor in addition to self-renewal (for a review, see Götz and Huttner, 2005; Kriegstein et al., 2006; Miyata, 2007). Thus, asymmetric cell divisions lead to radial growth of the cerebral cortex, whereas symmetric cell divisions regulate the tangential size of the cerebral cortex (Rakic, 2009; Farkas and Huttner, 2008). Despite the importance of these parameters in mammalian evolution (Molnar et al., 2006; Fish et al., 2008), little is known about the molecular machinery regulating the mode of cell division in the developing cerebral cortex in mammals.

By contrast, in *Drosophila*, the mechanisms of asymmetric cell division are known at high resolution, with a clear link between cleavage plane orientation and asymmetric inheritance of proteins (for reviews, see Matsuzaki, 2000; Doe, 2008; Knoblich, 2008). However, in vertebrate neurogenesis, the link between orientation of cell division and fate of the daughter cells is not as close. For example, in chick and mice, mis-orientation of spindles does not automatically influence cell fate as demonstrated by experimental manipulation of Leu-Gly-Asn repeat-enriched protein (LGN) (Morin et al., 2007; Konno et al., 2008). Moreover, basal localization of the fate determinant Trim32 is independent of spindle orientation (Schwamborn et al., 2009; Godin et al., 2010) and the inheritance of adherens junction or apical membrane components depends on the cleavage furrow (Huttner and Kosodo, 2005; Marthiens and ffrench-Constant, 2009). Finally, daughter cells with asymmetric fates can arise from vertical cell divisions and daughters inheriting the apical domain can become either progenitors or neurons (Wilcock et al., 2007; Alexandre et al., 2010).

To gain new insights into the regulation of the mode of cell division in vertebrate neural development, we took a different approach by examining the role of the transcription factor Pax6, a known regulator of neurogenesis and proliferation (Götz et al., 1998; Warren et al., 1999; Osumi, 2001; Heins et al., 2002; Stoykova et al., 2003; Haubst et al., 2004; Berger et al., 2007; Quinn et al., 2007; Osumi et al., 2008; Sansom et al., 2009). Intriguingly, previous analysis of the cerebral cortex of mice lacking functional Pax6, such as *small eye* (*Sey*) homozygous mutants ($Pax6^{Sey/Sey}$) (Hill et al., 1991) reported a decreased tangential expansion of the $Pax6^{Sey/Sey}$ cerebral cortex (Schmahl et al., 1993), which might be linked to the alterations in the orientation of cell divisions reported previously (Estivill-Torrus et al., 2002). We therefore set out to determine this as yet relatively unexplored role of Pax6.

MATERIALS AND METHODS

Animals

Small eye (*Sey*, designated $Pax6^{Sey}$) mutant mice (Hill et al., 1991) were maintained on a C57BL/6J × DBA/2J (B6D2F1) background, with a 12 hour light-dark cycle and were also crossed with Tis21::GFP (Haubensak

[1]Institute for Stem Cell Research, Helmholtz Zentrum München German Research Center for Environmental Health, Ingolstädter Landstr. 1, 85764 Neuherberg/Munich, Germany. [2]Biomolecular Sensors, Institute of Neuroscience, Technical University Munich, Biedersteinerstr. 29, 80802 Munich, Germany. [3]Max-Planck Institute of Molecular Cell Biology and Genetics, Pfotenhauerstr. 108, 01307 Dresden, Germany. [4]Physiological Genomics, Ludwig-Maximilians University of Munich, Schillerstr. 46, 80639 Munich, Germany.

*Author for correspondence (magdalena.goetz@helmholtz-muenchen.de)

Accepted 21 September 2011

et al., 2004) or YVI mice (George et al., 2007). The day of the vaginal plug was considered as embryonic day (E) 0. For conditional deletion of *Pax6* we used $Pax6^{flox/flox}$ mice (Ashery-Padan et al., 2000).

Immunocytochemistry and immunohistochemistry

Brains isolated from E12-16 embryos were fixed in 4% (w/v) paraformaldehyde (PFA) in phosphate buffered saline (PBS), cryoprotected in 30% (w/v) sucrose in PBS, embedded in Tissue-Tek and cryosectioned (20-40 μm). Cultured cells were fixed and stained as described previously (Haubst et al., 2004) with the following primary antibodies: anti-ASPM (rabbit, 1:1000) (Fish et al., 2006); anti-βIII-tubulin (mouse IgG2b, Sigma, 1:200); anti-MAP2 (mouse IgG1, Sigma, 1:200); anti-GFP (chicken, Sigma, 1:1000); anti-Pax6 [rabbit, Chemicon, 1:400; mouse, Developmental Studies Hybridoma Bank (DSHB), 1:70]; anti-Pard3 (rabbit, Upstate, 1:500); anti-aPKC (mouse, BD Transduction, 1:200); anti-N cadherin (mouse, BD Transduction, 1:1000); anti-β catenin (mouse, BD Transduction, 1:1000; rabbit, Sigma, 1:2000); anti-phosphohistone H3 (PH3, rabbit, Biomol, 1:400); anti-Ngn2 (mouse, provided by D. Anderson, California Institute of Technology, Pasadena, CA, USA, 1:10); anti-Mash1 (mouse, DSHB, 1:150) and anti-Spag5 (rabbit, AB BioTech, 1:200). After staining with fluorescently labelled secondary antibodies, nuclei were labelled by incubation in PBS containing 0.1 μg/ml DAPI (4′,6-diamidino-2-phenylindole, Sigma), and samples were mounted in Aqua Polymount (Polyscience) and analyzed using Olympus FV1000 confocal laser scanning microscopes. Fluorescence-activated-cell-sorting (FACS) based on anti-prominin 1 staining (PE-conjugated, e-Bioscience, 1:400; supplementary material Fig. S4) was performed as previously described (Pinto et al., 2008).

In utero electroporation and en face and sliced cortices live imaging

Pregnant mice were operated as approved by the Government of Upper Bavaria under licence number 55.2-1-54-2531-144/07 and were anaesthetized by intraperitoneal (i.p.) injection of saline solution containing fentanyl (0.05 mg/kg), midazolam (5 mg/kg) and medetomidine (0.5 mg/kg) and E12-13 embryos were electroporated as described by Saito (Saito, 2006). Plasmids pCAG-ZO1-EGFP, pCAG-PACT-mKO1 [gifts from Dr F. Matsuzaki; mKO1 (Medical and Biological Laboratories)] (Konno et al., 2008), pCIG2-CAG (cytoplasmic GFP; gift from Dr C. Schuurmans) (Hand et al., 2005) and pCAGGs-GAP43-GFP (Attardo et al., 2008) were dissolved in saline to give a final concentration of 1 μg/μl and co-introduced with Fast Green (2.5 μg/μl, Sigma). Electric pulses were generated by ElectroSquireportator T830 (Harvard Apparatus) and applied five times at ~40 mV for 50 msec each at intervals of 100 msec. Anaesthesia was terminated by i.p. injection of saline solution containing buprenorphine (0.1 mg/kg), atipamezol (2.5 mg/kg) and flumazenil (0.5 mg/kg). Animals recovered well after the operation and no signs of distress could be observed one day later. The tissues for en face imaging were prepared as described previously (Konno et al., 2008). Slices of the embryonic brains were cut 1 day later at a thickness of 300 μm using a vibratome (Leica VT1200S), embedded into collagen matrix (Nitta Gelatin, Cell Matrix type A) and subsequently covered with neurobasal medium (Gibco) with supplements (Polleux and Ghosh, 2002). Images were captured every 8 minutes for en face imaging using a confocal microscope (Olympus Fluoview 1000) or every 20 minutes for slice imaging using an Olympus microscope Fluoview 1000 equipped with a Ti:sapphire Laser tuned to 880 nm to excite GFP fluorescent protein and analyzed using Olympus FV10-ASW1.7 Viewer software and ImageJ (http://rsbweb.nih.gov/ij).

Continuous live imaging of cortical progenitors in vitro

The cerebral cortex was dissected from E13 or E14 embryos, dissociated and cultured as described previously (Costa et al., 2008). Using cell observer (Zeiss), images were acquired every 4 minutes for phase contrast and every 3 hours for fluorescence for 4-7 days using Axiovision Rel. 4.5 software. Data was analyzed using TTT tracking software as previously described (Costa et al., 2008; Rieger et al., 2009).

Ratiometric semi-quantitative PCR (qPCR)

Total RNA was extracted from E12 or E15 cerebral cortices using RNAeasy mini kit (QIAGEN) followed by reverse transcription to cDNA using SuperScript II Kit (Invitrogen). Real-time PCR was performed by using the DNA Engine Opticon (Bio-Rad Laboratories) and SYBR Green qPCR kit (Bio-Rad) in triplicate at 95°C for 15 minutes, followed by 40 cycles consisting of 94°C for 15 seconds, primer annealing at the optimal temperature for 30 seconds and primer extension at 72°C for 30 seconds. A melting curve analysis was performed from 70°C to 95°C in 0.3°C intervals to demonstrate the specificity of each amplicon and to identify the formation of primer dimers. Gapdh was used to normalize for differences in RNA input. Relative expression of each mRNA was calculated using the ΔCt between the gene of interest and Gapdh ($E=2^{-\Delta\Delta Ct}$). Primers are shown in supplementary material Table S1.

Luciferase assay

Expression plasmids for luciferase reporter assays were constructed using full-length cDNA of mouse *Pax6* (Ninkovic et al., 2010) sub-cloned into the pCAG vector. The empty vector was used as control. The *Spag5* promoter (601 bases) was cloned into the pGL3 vector (Promega). The *Spag5* promoter was PCR amplified from genomic DNA using the following primers: 5′-GCGAAGGCGACAAACCGAGA-3′ and 5′-AGTGGTGGTGTGGGACACGCTGTT-3′. HEK293 cells were transfected with 1 μg expression plasmid, 1.5 μg of the construct containing the *Spag5* promoter driving firefly (*Photinus pyralis*) luciferase and 0.1 μg of the pRL-TK plasmid encoding *Renilla* (sea pansy, *Renilla reniformis*) luciferase (Promega). After 24 hours, medium was changed and cell extracts were prepared the following day for luciferase activity measured with a luminometer (Berthold Centro LB 960) and relative light units were normalized to *Renilla* luciferase activity and then to the control transduced cells.

Chromatin immunoprecipitation (ChIP)-qPCR assay

The qChIP experiments were performed as described elsewhere (Lee et al., 2006) with minor modifications. Chromatin was extracted from E14 mouse cortices and crosslinked, then the Pax6-binding chromatin fragments were immunoprecipitated using polyclonal Pax6 antibodies (rabbit, Chemicon), with pre-immune serum as control (each 5 μg antibody per immunoprecipitation). The immunoprecipitated fragments were purified and amplified for promoter-specific analysis of Spag5 using real-time PCR. Data were normalized using the percent input method (Carey et al., 2009).

shRNA-mediated Spag5 knockdown

The pSuper.gfp/neo-Spag5 construct was generated by digesting the pSuper.gfp/neo vector (Oligoengine) with *Bgl*II and *Hin*dIII and ligating the annealed oligonucleotides (modified from TRCN0000120646:Sigma; top strand, 5′-GATCCCCCCTAACAGAAATTGTTGCTATTCAAGAGA-TAGCAACAATTTCTGTTAGGTTTTTA-3′; bottom strand, 5′-AGCT-TAAAAACCTAACAGAAATTGTTGCTATCTCTTGAATAGCAACA-ATTTCTGTTAGGGGG-3′) that contain a 20-nucleotide *Spag5* target sequence (in cap) using the strategy according to the manufacturer's instructions. The pSuper.gfp/neo-Spag5 (Spag5-shRNA) and blank vector pSuper.gfp/neo as a control were in utero electroporated into E12 wild-type (WT) cerebral cortices and the effect on the cleavage angles of progenitors was analyzed at E14.

Data analysis

Quantitative data are depicted as mean with standard error of the mean (s.e.m.) obtained from least three culture batches or embryos tested for significance by the unpaired Student's *t*-test or one-way ANOVA.

RESULTS

Alterations in the orientation of apical progenitor cell division in the $Pax6^{Sey/Sey}$ cerebral cortex

To gain a better understanding of the characteristics of cell division in $Pax6^{Sey/Sey}$ mutants, we first examined the cleavage angles of progenitor cells dividing at the apical surface in wild-type (WT) and $Pax6^{Sey/Sey}$ cerebral cortices at an embryonic stage

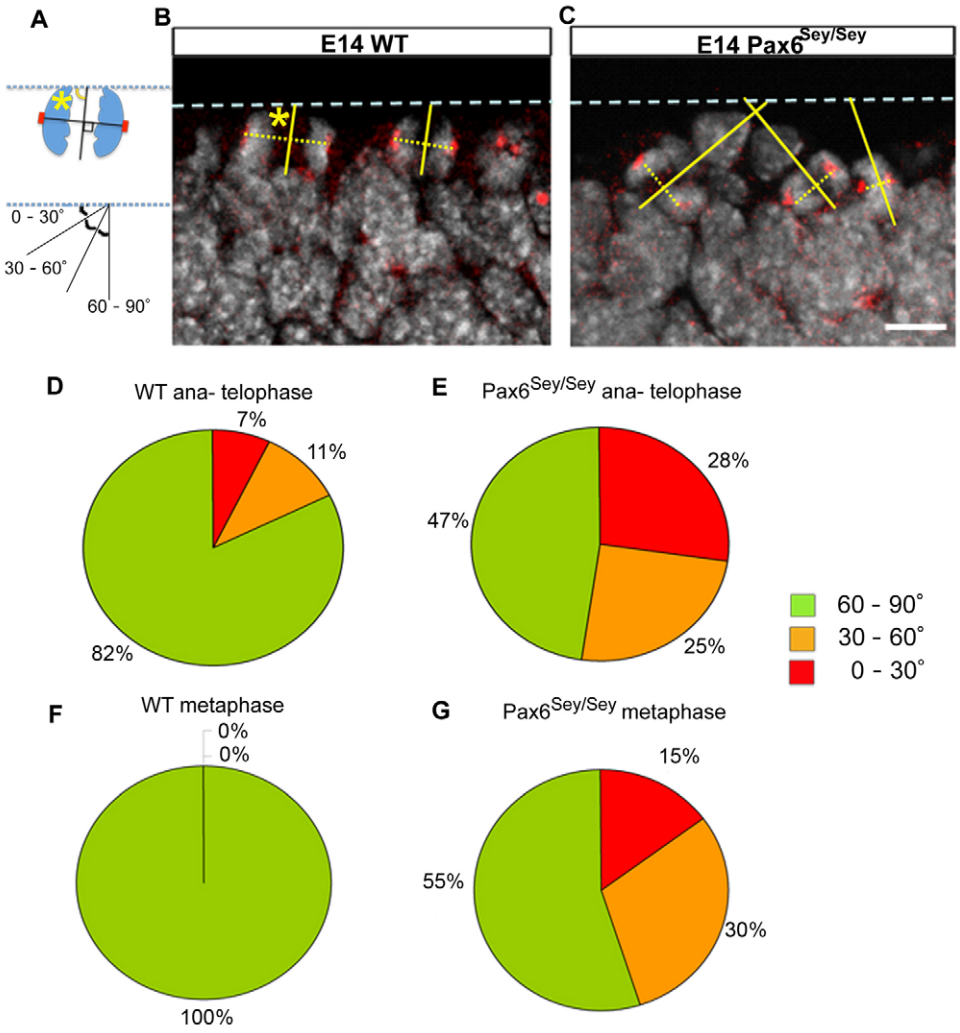

Fig. 1. Apical progenitors often divide non-vertically in mouse Pax6$^{Sey/Sey}$ cerebral cortex at mid-neurogenesis. (**A**) The cleavage angles (yellow asterisk) were measured as shown schematically and grouped into vertical (60-90°), oblique (30-60°) and horizontal (0-30°). (**B**,**C**) Cells labelled for ASPM (red) and DAPI+ nuclei (grey) at the apical surface (dashed line) of coronal sections of E14 WT (B) or Pax6$^{Sey/Sey}$ (C) cerebral cortices. (**D-G**) Pie charts showing the percentage of cells with the colour coded cleavage angle for ana- and telophase (D,E) and for metaphase (F,G) of WT (D,F; 81 cells from three animals) or Pax6$^{Sey/Sey}$ (E,G; 129 cells from three animals). Scale bar: 10 μm.

corresponding to mid-neurogenesis in the mouse (E14). In WT cortices immunostained for the mitotic spindle pole protein Aspm (abnormal spindle-like microcephaly associated), we noted that the spindles of most apically dividing cells (neuroepithelial or radial glia cells) at anaphase were oriented along a horizontal plane (Fig. 1A,B, dashed yellow line) in accordance with previous observations (Chenn and McConnell, 1995; Estivill-Torrus et al., 2002; Kosodo et al., 2004; Stricker et al., 2006; Fish et al., 2006; Konno et al., 2008). In these divisions, the spindle axis is almost parallel to the ventricular, apical surface and the cleavage plane is, accordingly, vertical to the ventricular lining (Fig. 1A). The observed angles of cell divisions were grouped into three classes, with a cleavage plane angle of 60-90° (relative to the apical surface of the cortex) scored as vertical, 30-60° as oblique and 0-30° as horizontal (Fig. 1A).

Orientations were first examined in anaphase and telophase when the final cleavage plane has been established (Adams, 1996; Haydar et al., 2003; Sanada and Tsai, 2005). Most (82%) of the apically located cells divided vertically in WT cortices, 11% divided obliquely and 7% divided horizontally (Fig. 1B,D). By contrast, only 47% of cells in the cerebral cortex of Pax6$^{Sey/Sey}$ mutant mice divided with vertical cleavage planes, whereas oblique and horizontal angles were significantly increased reaching 25% and 28% of the cells, respectively (Fig. 1C,E) (see also Estivill-Torrus et al., 2002). We noticed that this difference in spindle orientation was already evident in metaphase cells (Fig. 1F,G), implying that the spindle orientation is altered prior to chromosome segregation in the Pax6$^{Sey/Sey}$ cerebral cortex. Notably, this difference in cleavage angles was not yet present at E12 when a similar proportion of mitotic cells divided with a non-vertical cleavage plane (25% WT, n=16 cells; 16% Pax6$^{Sey/Sey}$, n=19 cells). However, the profound increase in non-vertical divisions in Pax6$^{Sey/Sey}$ cerebral cortex persisted from E14 to E16 (non-vertical divisions: 30% WT, n=20 cells; 56% Pax6$^{Sey/Sey}$, n=41 cells). Taken together, these results show that Pax6 disruption alters the spindle orientation and cleavage plane in apical progenitors of the cerebral cortex starting at mid-neurogenesis.

Unequal inheritance of adherens junction and apical membrane components is increased in the Pax6$^{Sey/Sey}$ cerebral cortex

To clarify whether these alterations in the cleavage plane result in alterations of the apical membrane partitioning, we examined cell division via en face confocal live imaging (see schematic in Fig. 2A). This permits unambiguous assignment of apical membrane domain inheritance by direct observation from the apical side in a whole-mount preparation. To do this, we electroporated pCAG-PACT-mKO1 and pCAG-ZO-1-GFP plasmids to monitor simultaneously the centrosome (PACT-mKO1, red fluorescence) and junctional component (ZO1-GFP, green fluorescence) as

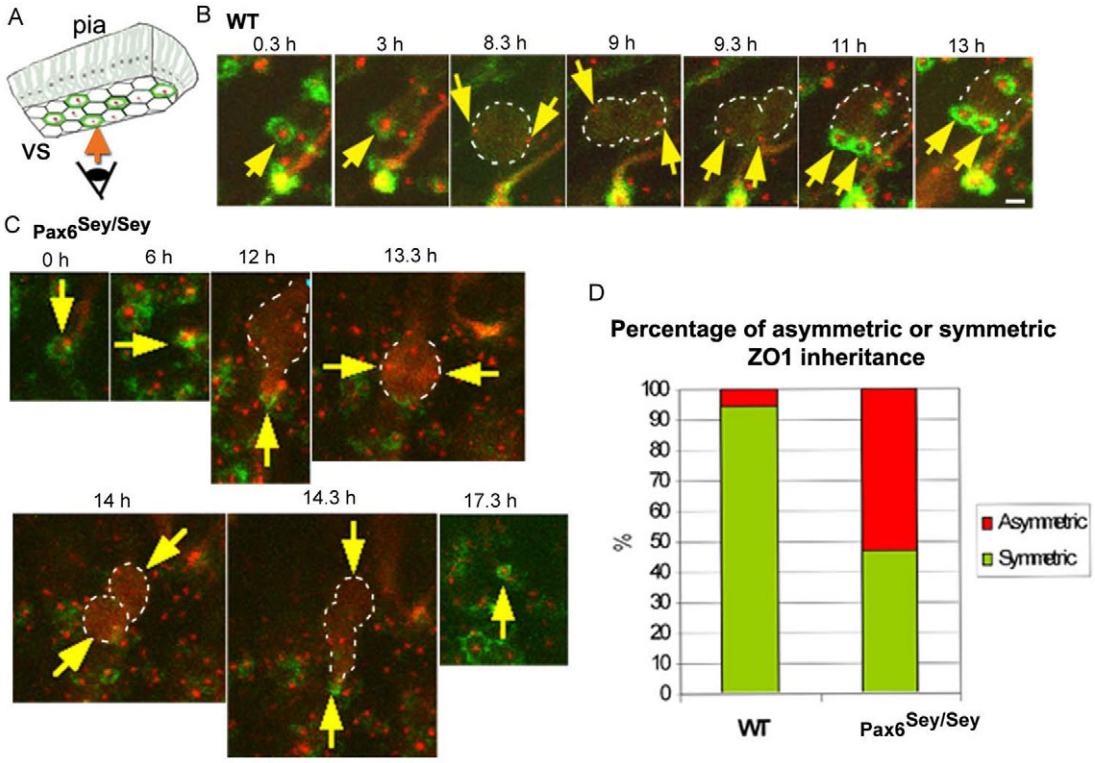

Fig. 2. Increased cell divisions with asymmetric partitioning of the apical membrane in mouse Pax6$^{Sey/Sey}$ cerebral cortex. (**A**) Schematic of en face imaging indicating the green EGFP-ZO1-marked cell boundaries and the red PACT-mKO1-labelled centrosomes at the ventricular surface (vs). (**B**,**C**) Yellow arrows depict red fluorescent centrosomes in micrographs from WT (B) and Pax6$^{Sey/Sey}$ mutant (C) cerebral cortex with low levels of cytoplasmic PACT-mKO1 delineating the cell body (white dashed line) at the times indicated at the top of each panel. B shows an example of symmetric division at the apical surface in WT cerebral cortex with the green ZO1 signal forming two rings after mitosis each containing a red centrosome (at 11 and 13 hours; for details, see supplementary material Movie 1), whereas C shows an example of asymmetric inheritance of the apical domain from Pax6$^{Sey/Sey}$ cerebral cortex with one daughter cell located relatively far from the apical surface (at 14 hours) without reforming a ZO1 ring at the apical surface. This division therefore resulted in a single ring of ZO1 enclosing a centrosome (at 17.3 hours), demonstrating that the apical membrane domain surrounded by the ZO1 ring was unequally inherited by the apical daughter cell. For details, see supplementary material Movie 2. (**D**) The mode of division shown in C occurred infrequently in WT but frequently in the Pax6$^{Sey/Sey}$ mutant as depicted in the histogram [18 (WT) and 16 (Pax6$^{Sey/Sey}$) divisions in more than two movies per genotype].

described previously (Konno et al., 2008). In these experiments, cell bodies located below the apical surface appear weakly red (see also Konno et al., 2008). In E14 WT cerebral cortex, labelled cell bodies occupied different positions according to their cell cycle stage, moving towards the apical surface during G2, consistent with the normal interkinetic nuclear migration of radial glial cells (supplementary material Movie 1). Amongst the observed apical mitoses, >90% generated daughters with near-identical ZO-1-GFP rings (Fig. 2B,D). In E14 Pax6$^{Sey/Sey}$ cerebral cortex, we observed a profound reduction in apical divisions with equal partitioning of the apical membrane to <50% (Fig. 2C,D; supplementary material Movie 2). Rather, the predominant apical division pattern in Pax6$^{Sey/Sey}$ mutant cells generated one daughter cell that did not inherit ZO1-GFP (Fig. 2C). Thus, live imaging not only confirmed the altered cell division angle in Pax6$^{Sey/Sey}$ cerebral cortex but revealed unambiguously that this results in a markedly unequal inheritance of the ZO1-labelled adherens junction components and the apical membrane domain enclosed by these.

In order to monitor the behaviour of the non-apical daughter cell, we also imaged slice preparations from E14 cerebral cortex after DiI labelling or electroporation of two GFP plasmids with cytoplasmic and membrane localization (supplementary material Movies 3-5). As illustrated in supplementary material Fig. S1, we observed many cell divisions in which one daughter cell lost its apical contact and moved basally, and the other daughter cell remained at the apical surface in slices of Pax6$^{Sey/Sey}$ cerebral cortex (e.g. cell indicated by red arrow in supplementary material Fig. S1A; see also supplementary material Movie 4). We also observed that the sub-apical daughter cell often did not migrate as far in the basal direction as those in WT and divided once again at the sub-apical position (11/17 randomly selected divisions; supplementary material Fig. S1B,C and Movie 5). Taken together, these data show that non-vertical cleavage angles in Pax6$^{Sey/Sey}$ cortex give rise to one, often still proliferative, daughter cell moving to a sub-apical position, thereby contributing to the increase in non-apical cell divisions.

β-catenin and Par complex protein and mRNA levels are reduced in the Pax6$^{Sey/Sey}$ cerebral cortex

We asked next whether a decrease in Par proteins or other components of the adherens junctions (AJs) occurs in the absence of Pax6 function, possibly contributing to the alterations described above. aPKC (Fig. 3A) and Par3 (Fig. 3B-B″) immunostaining was very weak or undetectable at the apical surface of the Pax6$^{Sey/Sey}$ ventricular zone (VZ). A moderate decrease of N-cadherin

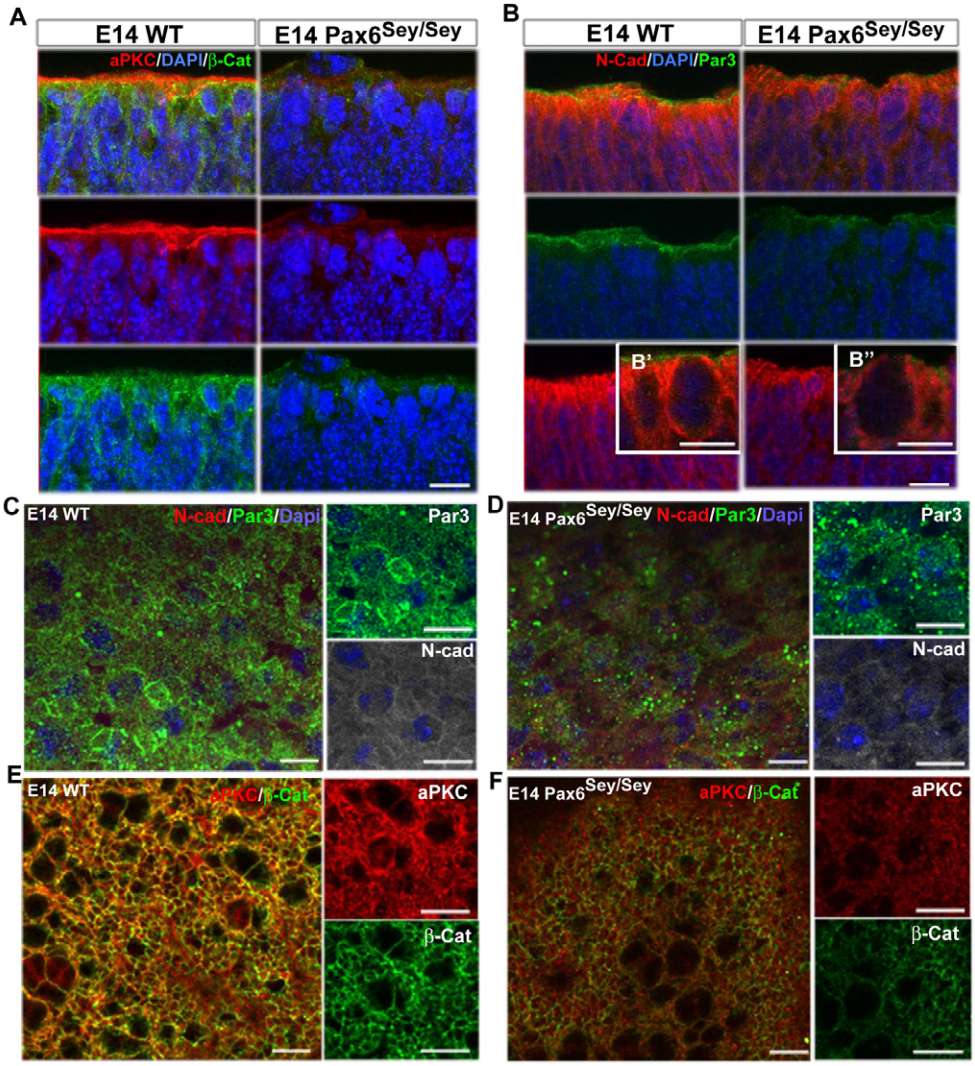

Fig. 3. Decreased expression of adherens junction proteins in mouse Pax6$^{Sey/Sey}$ mutant cerebral cortices. Fluorescence micrographs of coronal sections (**A**,**B**) or whole-mounts (**C-F**) viewed from the apical surface of WT and Pax6$^{Sey/Sey}$ cerebral cortices immunostained as indicated. B′ and B″ depict higher power views. A,B show *z*-stacked images and C-F show single confocal images. Scale bars: 10 μm in A,B; 5 μm in B′,B″; 10 μm in C-F.

immunostaining was observed in Pax6$^{Sey/Sey}$ versus WT cerebral cortex. This observation was confirmed in whole-mount preparations, indicating a profound reduction of Par3 (Fig. 3C,D), aPKC and β-catenin (AJ protein) (Fig. 3E,F) in Pax6$^{Sey/Sey}$ versus WT cerebral cortex. We also noted that the honeycomb structure of Par3 and aPKC immunopositive domains became indistinct, although β-catenin immunopositive domains were weaker but extant (Fig. 3C-F). Western blot analysis of cerebral cortex (supplementary material Fig. S2A) indicated that only the cytoplasmic pool of β-catenin was reduced in E14 Pax6$^{Sey/Sey}$ compared with WT, whereas no changes were visible between the nuclear fractions. Interestingly, qPCR analysis demonstrated a significant reduction of both β-*catenin* and *Pard3* (Par3) mRNA levels in E14 Pax6$^{Sey/Sey}$ to less than half of the levels in the WT cerebral cortex (supplementary material Fig. S2B). This reduction was also observed in apical progenitors isolated by FACS using prominin1 live immunostaining (data not shown). Given that Pax6 binding sites are present in the promoter regions of β-*catenin* and *Pard3* genes (supplementary material Fig. S2C), these data suggest that the decreased transcription levels are due to the lack of Pax6 function, thus contributing to the reduced protein levels. Thus, Pax6 might regulate several components of AJ coupling in order to maintain progenitors at the apical side.

Non-apically dividing cells maintain the features of radial glia in the Pax6$^{Sey/Sey}$ cerebral cortex

Reduced levels of AJ coupling might result in premature delamination of apical progenitor cells, in which case one may expect that the delaminated progenitors retain hallmarks of the radial glial cells rather than maturing into basal progenitors (BPs). BPs are characterized by expression of the anti-proliferative neurogenic gene *Tis21* (*Btg2* – Mouse Genome Informatics), which is expressed in most BPs but only in a minor subpopulation of apical radial glial cells (Haubensak et al., 2004). BPs upregulate *Tis21* but downregulate radial glial hallmarks, such as BLBP (Fabp7 – Mouse Genome Informatics) or GLAST (Slc1a3 – Mouse Genome Informatics) (Pinto et al., 2009). Consistent with previous data (Haubensak et al., 2004), >80% of the basal mitoses immunostained for PH3 were GFP-positive in WT/*Tis21::GFP* cerebral cortices, whereas only 60% were GFP-positive in Pax6$^{Sey/Sey}$/*Tis21::GFP* littermates (Fig. 4A-D). The difference was even more pronounced with regard to GLAST, which was present in <5% of WT BPs, but was expressed in 65% of Pax6$^{Sey/Sey}$ basal mitotic cells (Fig. 4E). These data indicate that most of the basally dividing cells in the Pax6$^{Sey/Sey}$ cerebral cortex retain radial glia hallmarks consistent with their premature delamination.

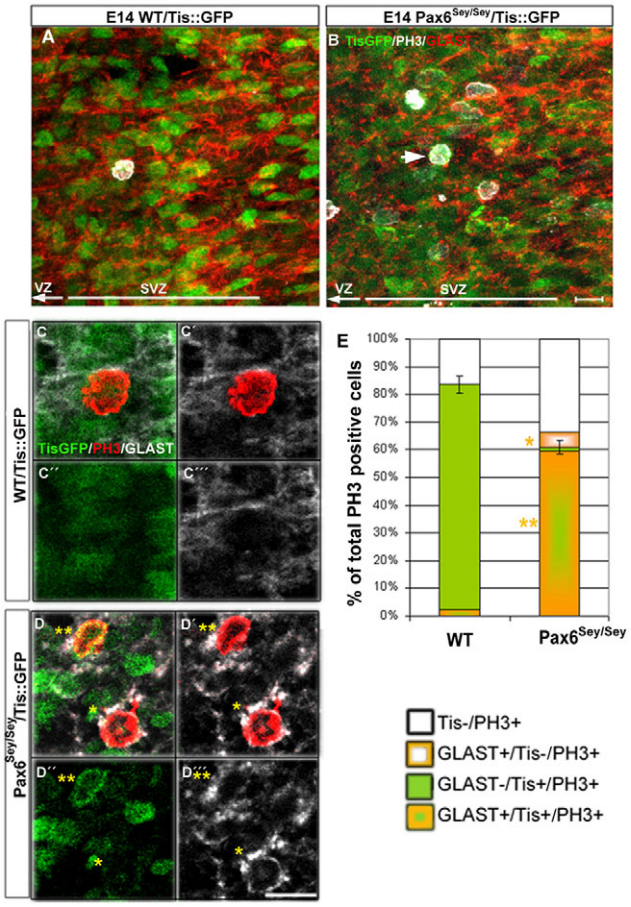

Fig. 4. Basally dividing progenitors in mouse Pax6$^{Sey/Sey}$ cerebral cortex retain radial glia hallmarks. (**A-D‴**) Fluorescence micrographs of the subventricular zone (SVZ) in coronal sections of the cerebral cortex from E14 WT/Tis21::GFP (A,C) and Pax6$^{Sey/Sey}$/Tis21::GFP mice (B,D) labelled as indicated. C-C‴,D-D‴ show single confocal sections. Single asterisk indicates a PH3+/GLAST+ cell and double asterisks a Tis+/PH3+/GLAST+ triple positive cell in D-D‴. (**E**) The proportion of PH3-positive basally dividing cells labelled for these markers as indicated by the colours (15 cells WT; 38 cells Pax6$^{Sey/Sey}$). Scale bars: 10 μm. Error bars represent s.e.m. *P<0.05, **P<0.005.

De novo deletion of Pax6 alters the orientation of cell division and increases sub-apically dividing cells

As the experiments described above were performed in a mouse mutant with constitutive defects in Pax6-mediated transcription, the changes described above might have been indirectly elicited, e.g. as a result of the alterations in patterning (Stoykova et al., 1996; Stoykova et al., 2000; Toresson et al., 2000; Yun et al., 2001). To assess direct effects of Pax6, we acutely deleted it by electroporation of a plasmid containing Cre recombinase and GFP (Cre-PCIG) into the lateral ventricles of a conditional Pax6 mouse line in which exons 4-6 are flanked by *loxP* sites (Ashery-Padan et al., 2000). When GFP-positive cells were examined in the VZ 2 days after electroporation into WT or *Pax6$^{flox/flox}$* E12 embryos, i.e. at E14, Pax6 had been successfully deleted as Pax6-immunoreactive cells were reduced by >80% in *Pax6$^{flox/flox}$* compared with WT (Fig. 5A-C). We also observed downstream effects, including a decrease in the Pax6 target Ngn2 (Neurog2 – Mouse Genome Informatics), but not Tbr2 (Eomes – Mouse Genome Informatics), and a converse increase in Mash1 (Ascl1 – Mouse Genome Informatics) and Gsx2 (Fig. 5D,E; data not shown). Most importantly, within this short time window after elimination of Pax6 protein, the number of PH3-positive cells dividing sub-apically was already increased relative to electroporated cells in WT cortices (Fig. 5F,G). In addition, the orientation of apically dividing cells shifted towards non-vertical orientations upon Pax6 deletion (19% horizontal, 27% oblique, 54% vertical; n=41 cells), whereas most (95%) Cre-electroporated cells in control embryos divided with a vertical angle (n=19 cells; Fig. 5H,I). We also detected a moderate decrease in the gene expression levels of β-*catenin* and *Pard3* two days after Pax6 deletion (supplementary material Fig. S3A), which had not yet translated into decreased protein levels (supplementary material Fig. S3B).

Lineage tracking of dissociated cells in vitro reveals effects of Pax6 on the mode of cell division

The experiments described above showed a rapid effect of Pax6 deletion on the orientation of cell division and increased generation of basally dividing progenitors, but could not determine to what extent these effects were due to alterations in cell polarity. We therefore asked whether alterations in the mode of cell division of Pax6$^{Sey/Sey}$ cerebral cortex cells were also present in a culture system independent of AJ coupling and apicobasal polarity. To this end, cells from cerebral cortices were dissociated and plated at densities at which most lacked cell-cell contacts during the first days of culture (Fig. 6A,B). Single-cell tracking by continuous live imaging (Costa et al., 2008) was then used to determine the mode of cell division by assessing the fate of the daughter cells. If both daughter cells proliferated again we referred to these as symmetric proliferative (SP) divisions; if both daughter cells did not divide for several days thereafter these were defined as symmetric terminal (ST) divisions; and an unequal behaviour with only one daughter cell dividing was designated an asymmetric (AS) division. Examples of such lineages are depicted in Fig. 6C. Consistent with our previous work, most (68%) cell divisions were SP and only a minority (12%) divided in an AS manner when cells had been isolated from E14 WT cerebral cortices (Fig. 6D). Conversely, many more cells isolated from Pax6$^{Sey/Sey}$ cortices generated asymmetric daughter cell fates (Fig. 6D). Thus, even under dissociated cell culture conditions, Pax6-mutant cells exhibit alterations in the mode of cell division.

The increased number of proliferating cells seen in the Pax6$^{Sey/Sey}$ cerebral cortex (Fig. 4A,B) (Haubst et al., 2004), is also maintained in this culture system with many more clones derived from Pax6$^{Sey/Sey}$ cerebral cortex cells containing PH3+ cells in mitoses (59%, n=81 clones) compared with those derived from WT cells (6%, n=31 clones) at 2 days in vitro. Thus, the impression that the increase in AS divisions occurs at the expense of SP divisions (Fig. 6D) is misleading, as SP divisions are only reduced in relative, but not in absolute numbers. Conversely, AS divisions are substantially increased among Pax6$^{Sey/Sey}$ cerebral cortex cells. This increase in AS divisions is not due to alterations in cell-cycle length (Fig. 6E) as is also the case in vivo (Quinn et al., 2007), demonstrating that alterations in the mode of cell division of Pax6$^{Sey/Sey}$ cells also occur independently of apicobasal polarity and AJ coupling.

To eliminate the possibility that the alterations observed in vitro, e.g. the increase in AS divisions, are due to an altered composition in progenitors, we isolated apical progenitor cells by FACS for prominin1, which is localized on the apical membrane of cortical

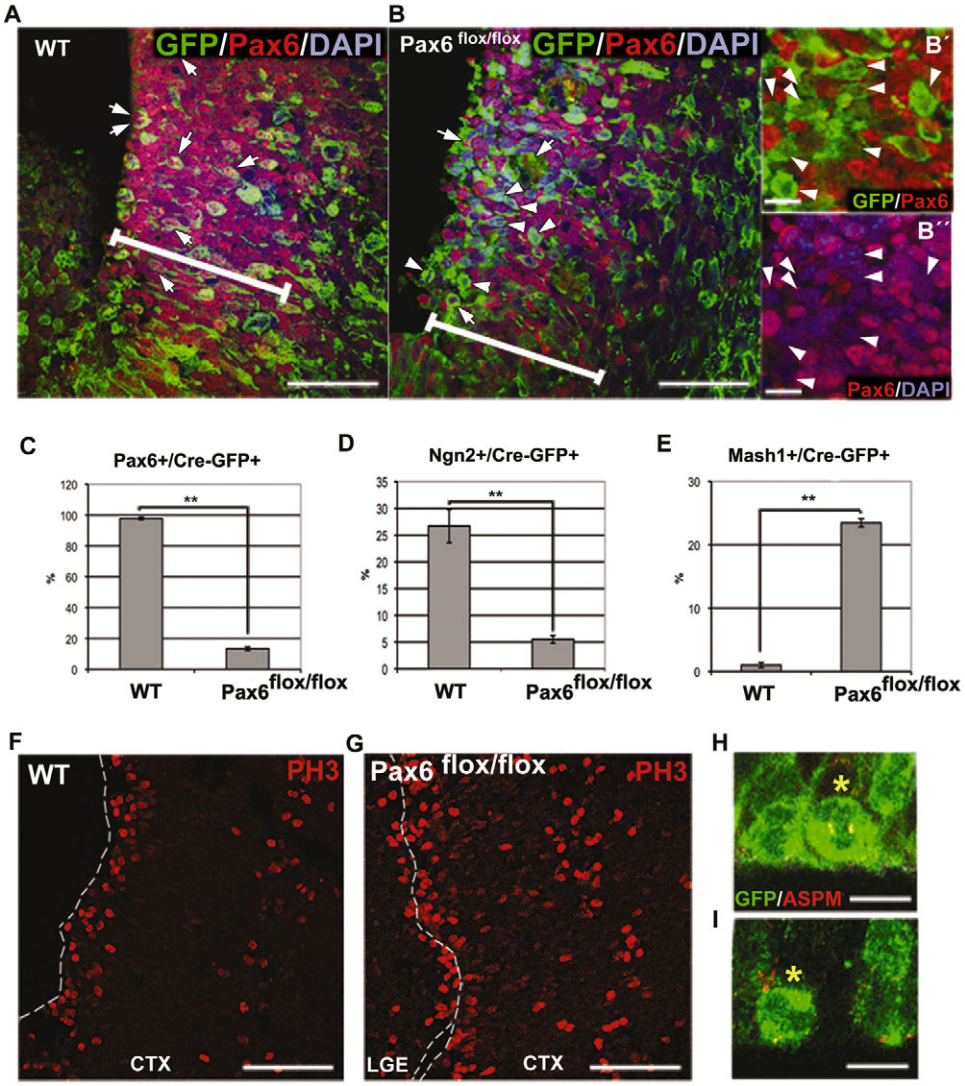

Fig. 5. Increased basal divisions upon acute Pax6 deletion in mouse E14 cerebral cortex. (**A-B″,F-I**) Micrographs depicting coronal sections of E14 WT (A,F,H) and Pax6$^{flox/flox}$ (B,G,I) cerebral cortices 2 days after electroporation with Cre-IRES-GFP plasmids immunolabelled as indicated. Arrows, Cre-GFP+, Pax6+ double-positive cells; arrowheads, Cre-GFP+, Pax6– cells (A,B). B′,B″ show higher magnification of Pax6-negative Cre-GFP+ cells from Pax6$^{flox/flox}$. Cre-GFP positive cell in metaphase is marked by an asterisk showing vertical cleavage angle in WT (H) and non-vertical cleavage angle in Pax6$^{flox/flox}$ (I). Dashed line in F,G indicates the ventricular surface of CTX. (**C-E**) The proportion of immunopositive cells quantified in the region indicated by the white bar in A,B (~100 μm distance from ventricular surface). Numbers of cells analyzed were: in WT brains, 351 (C), 162 (D), 224 (E); in Pax6$^{flox/flox}$ brains, 239 (C), 253 (D), 508 (E). Error bars represent s.e.m. $^{**}P<0.005$. Scale bars: 50 μm in A,B,F,G; 10 μm in B′,B″,H,I.

progenitors (Weigmann et al., 1997; Pinto et al., 2008) (supplementary material Fig. S4A,B). As expected, most of the isolated prominin1-positive cells (96%, *n*=22 trees) continued to proliferate in vitro (supplementary material Movie 6) exhibiting all three types of cell division (data not shown), whereas only 30% of prominin1-negative cells continued to divide (*n*=14 trees), consistent with this fraction comprising many differentiated neurons. Moreover, none of the prominin1-negative cells divided in an SP manner; rather, most (75%) divided in an ST manner, with the two daughters acquiring neuronal morphology (supplementary material Movie 7). This supports the notion that these prominin1-negative progenitors correspond to BPs that predominantly divide with an ST mode also in vivo (Haubensak et al., 2004; Miyata et al., 2004; Noctor et al., 2004; Wu et al., 2005; Attardo et al., 2008).

Cells derived from Pax6$^{Sey/Sey}$ cerebral cortices revealed remarkably different behaviour between prominin1-positive and -negative subpopulations (supplementary material Movies 8, 9): prominin1-positive Pax6$^{Sey/Sey}$ cells contained a higher proportion of non-dividing cells (20%), and amongst those continuing to divide (*n*=16 trees), 31% underwent AS divisions, an almost twofold increase compared with WT cells. The prominin1-negative fraction from Pax6$^{Sey/Sey}$ cortex, comprising the daughter cells losing the apical membrane domain observed in the en face imaging described above, also showed altered behaviour. Consistent with a decreased number of postmitotic neurons in the Pax6$^{Sey/Sey}$ cortex (Heins et al., 2002; Haubst et al., 2004), a larger fraction of prominin1-negative cells proliferated instead of generating two postmitotic neurons (supplementary material Movie 9). Like prominin1-negative cells isolated from WT, none of those from Pax6$^{Sey/Sey}$ cortex divided in an AS manner, further supporting the notion that increased AS division in the bulk cerebral cortex (Fig. 6D) was due to alterations in apical Pax6$^{Sey/Sey}$ mutant progenitors. Most strikingly, however, 40% of all cell divisions of the prominin1-negative fraction from the Pax6$^{Sey/Sey}$ cortex divided in a SP manner, which in WT is restricted to prominin1-positive apical progenitors.

Finally, we asked whether the increase in AS division amongst Pax6$^{Sey/Sey}$ cells is cell-autonomous using co-cultures of E14 WT cells at 100× excess with Pax6$^{Sey/Sey}$ cells crossed with a ubiquitously YFP-expressing mouse line (YVI) (George et al., 2007). Age-matched cells from WT/YVI mice (WT for the *Pax6* allele) served as controls. Also in this case, we observed increased numbers of AS divisions amongst progenitor cells from the Pax6$^{Sey/Sey}$ mutant in the first divisions but not in the second divisions (Fig. 6F; see tree

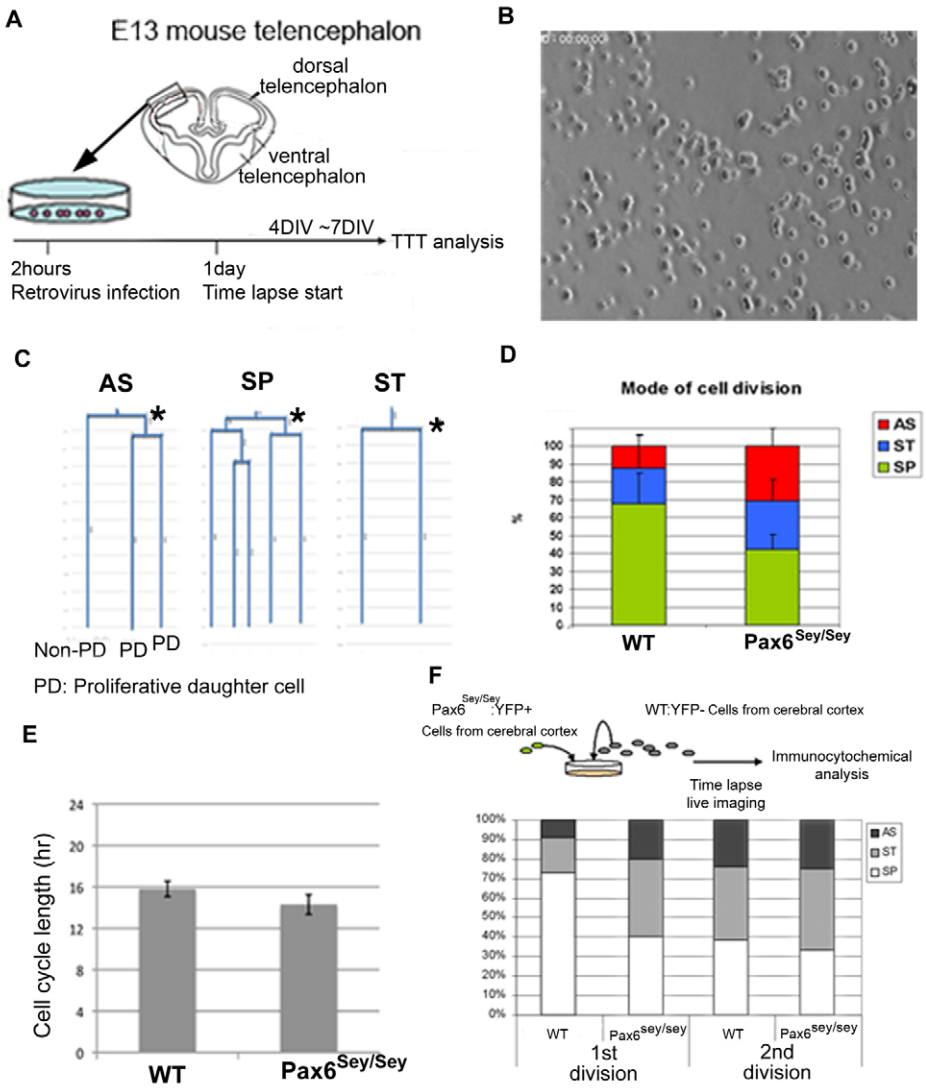

Fig. 6. In vitro time lapse lineage tree analysis reveals increased asymmetric divisions in mouse Pax6$^{Sey/Sey}$ cerebral cortex cells. (**A**) Schematic of the experimental paradigm. TTT, TTT tracking software. (**B**) Phase contrast image of the cell density at the start of the imaging. (**C**,**D**) Examples (indicated by asterisks) of asymmetric cell division (AS), symmetric proliferative division (SP) and symmetric terminal division (ST) in representative lineage trees quantified in D. Numbers of analyzed trees: 62 (WT), 75 (Pax6$^{Sey/Sey}$). (**E**,**F**) Cell cycle length in hours (hr) measured between the first and second division (E) and the proportion of the respective mode of cell division of YFP+ WT or Pax6$^{Sey/Sey}$ cells co-cultured with WT cells (F). Numbers of analyzed trees: 11 (WT), 15 (Pax6$^{Sey/Sey}$). Error bars represent s.e.m. 1st divisions and 2nd divisions correspond to the mode at single asterisk or double asterisks in supplementary material Fig. S4C, respectively.

examples in supplementary material Fig. S4C). This indicates that the increase in AS cell divisions amongst Pax6$^{Sey/Sey}$ progenitors is likely to be caused by cell-intrinsic mechanisms.

Spag5 is a direct target of Pax6 and regulates the orientation of cell division

Given that the cell-autonomous alterations in the cell division mode are independent of apicobasal polarity, we next asked whether Pax6 directly affects the machinery regulating the mode of cell division. We searched the available transcriptome and ChIP data of Pax6 in cerebral cortex and lens (Holm et al., 2007; Sansom et al., 2009; Wolf et al., 2009) to identify possible target genes of Pax6 that might affect cell division. One candidate was the sperm associated antigen 5 (Spag5 or mAstrin), a microtubule-associated protein (Thein et al., 2007; Cheng et al., 2007) localizing to spindle poles and kinetochores in mammalian cells (Mack and Compton, 2001). Consistent with a possible regulation by Pax6, *Spag5* mRNA levels were already reduced in E12 Pax6$^{Sey/Sey}$ cerebral cortex compared with WT littermates (Fig. 7A). Surprisingly, however, mRNA as well as protein levels increased at later stages (Fig. 7A and supplementary material Fig. S5A). In the context of the specific recruitment of Spag5 only to kinetochores of chromosomes in the metaphase plate (Manning et al., 2010), it is of interest that the intensity of Spag5 immunoreactivity in cultured Pax6$^{Sey/Sey}$ cells was affected in prometaphase and metaphase, but not in anaphase, even though Spag5 immunoreactivity was also observed at other locations in the cytoplasm (supplementary material Fig. S5B,C). Given the initial reduction and later increase in *Spag5* mRNA levels in Pax6$^{Sey/Sey}$ mutant, we examined *Spag5* mRNA levels upon de novo elimination of Pax6 by Cre electroporation (supplementary material Fig. S3). Similar to the reduction of *Spag5* mRNA levels in the Pax6$^{Sey/Sey}$ mutant cortex at early developmental time points, acute deletion of Pax6 also caused a reduction in *Spag5* mRNA levels (supplementary material Fig. S3A). As these data were consistent with a direct regulation of *Spag5* by Pax6, we used Genomatix software analysis to assess possible Pax6 binding sites in the *Spag5* promoter region (Fig. 7B) and validated its direct regulation by Pax6 in two independent assays. First, Pax6 transduction positively regulated a luciferase construct containing the *Spag5* promoter region with the Pax6 binding site (Fig. 7C). Second, ChIP with a Pax6 antibody revealed substantial enrichments of *Spag5* promoter regions ~1 kb upstream and downstream of the *Spag5* translational start codon [–1 and +1 (P<0.001) and +2 (P<0.01)] confirming Pax6 binding at these sites (Fig. 7D). Thus, *Spag5* is directly regulated by Pax6 in cortical progenitor cells. In order to determine its role in these progenitor

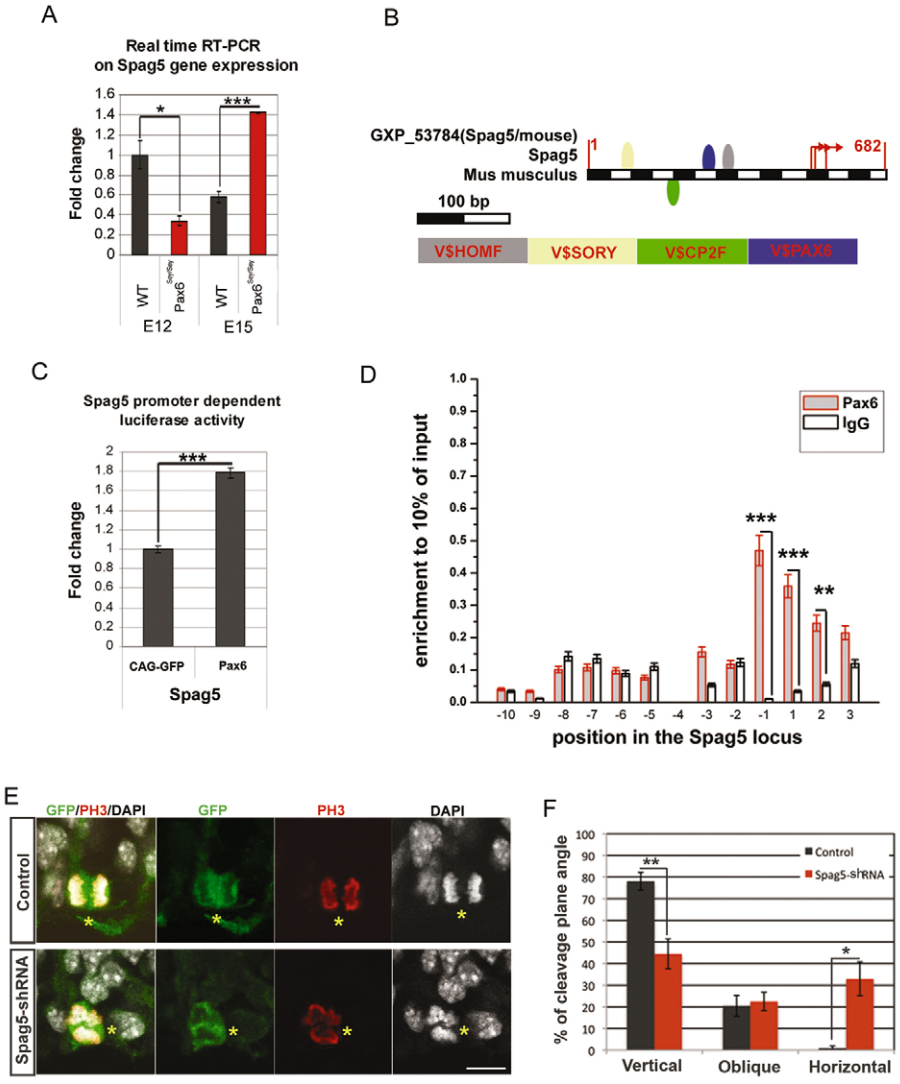

Fig. 7. Direct interaction between Pax6 and *Spag5* promoter region. (**A**) mRNA (triplicates of three different biological replicates per genotype) levels of *Spag5* at E12 and E15. (**B**) Schematic of the mouse *Spag5* gene promoter. Putative Pax6 binding sites are represented by the blue box (Gene2Promoter; Genomatix and FrameWorker). (**C**) The *Spag5*-promoter luciferase construct was co-transduced into HEK293 cells either with Pax6-pCAG or control (pCAG) together with 0.1 μg of the pRL-TK plasmid encoding *Renilla* luciferase. Results are expressed as mean ± s.e.m. of the ratio between *Renilla* luciferase and firefly (control) luciferase activities. (**D**) Pax6 distribution at the mouse *Spag5* gene locus in cerebral cortex chromatin. The numbers on the *x*-axis represent the primer position (~13 kb around ATG) in the *Spag5* locus. The primer position 1 corresponds to ATG of the *Spag5* gene. An anti-IgG immunoprecipitation was performed as a negative control for each primer set. The relative enrichment unit represents 10% of the input. (**E**) E12 cerebral cortices were electroporated with pSuper.gfp/neo-Spag5 or pSuper.gfp/neo and labelled for anti-GFP and anti-PH3 at E14 together with DAPI counter staining. Micrographs depict exemplified pictures of GFP-positive apically dividing cells (indicated by asterisks). Cells with vertical cleavage angle from control (upper panels) or with non-vertical cleavage angle from *Spag5*-shRNA (lower panels) plasmid-electroporated cerebral cortices, respectively, are shown. (**F**) *Spag5*-shRNA-induced alteration of cleavage plane angle amongst apically dividing cells [control: *n*=3 animals (64 cells), *Spag5*-shRNA: *n*=4 animals (78 cells)]. Cleavage plane angle of GFP-positive apically dividing cells was analyzed and classified as described in Fig. 1. Data represent the mean ± s.e.m. **P*<0.05, ***P*<0.01, ****P*<0.001. Scale bar: 10 μm.

cells, we constructed a shRNA vector against *Spag5* and electroporated it into E12 WT cerebral cortices. Notably, this led to a significant increase in non-vertical cleavage planes of apical progenitors compared with cells electroporated with the control vector two days later (E14, Fig. 7E,F), consistent with a role of Spag5 in spindle organization in other cell types (Yuan et al., 2009). Taken together, these data strongly support the concept that Pax6 directly regulates target genes involved in regulating the mode of cell division.

DISCUSSION

Here, we report a novel function for Pax6: namely, its role in regulating the orientation and mode of cell division. We first demonstrated by spindle pole staining that the cleavage plane angle was altered in radial glial cells of $Pax6^{Sey/Sey}$ cerebral cortex starting at mid-neurogenesis. This was confirmed by live imaging in en face preparations, revealing a marked increase in divisions with unequal inheritance of the apical membrane domain in $Pax6^{Sey/Sey}$ cerebral cortex. Acute deletion of Pax6 also lead to

increased non-vertical divisions amongst apical progenitors and an increase in non-apical cell divisions. Finally, we demonstrated an increase in cell divisions with asymmetric daughter cell fates in dissociated cell cultures independent of apicobasal polarity. From these data, we conclude that Pax6 affects cortical progenitor cell division on at least three levels: by weakening the anchoring of apical progenitors, by altering the cleavage plane of apical progenitors and by apicobasal polarity-independent mechanisms.

Pax6 regulates adhesion and apical anchoring of apical progenitors

The increase in non-apically dividing progenitors in the Pax6$^{Sey/Sey}$ cerebral cortex has long been known (Götz et al., 1998), but the different mechanisms contributing to it are only now being elucidated. Impaired interkinetic nuclear migration of radial glial cells, as observed in the rat Pax6$^{Sey/Sey}$ (Tamai et al., 2007) and confirmed in our imaging analysis in the mouse Pax6$^{Sey/Sey}$, causes a subset of cells to undergo cell division prior to reaching the ventricular surface. We demonstrated in this work two additional mechanisms contributing to this phenotype: an increase in delamination of apical progenitors and an increase in apical progenitors dividing with non-vertical orientation to generate one daughter cell devoid of apical membrane and anchoring. Increased apical progenitor cell delamination would be facilitated by the profound decrease in molecules anchoring neuroepithelial and radial glial cells at the ventricular surface in the Pax6$^{Sey/Sey}$ cerebral cortex, such as R-cadherin (Stoykova et al., 1997), β-catenin and members of the Par complex, as shown here. These molecules are all likely to anchor apical progenitors from their function in adherens junction complexes (Cappello et al., 2006; Costa et al., 2008; Bultje et al., 2009; Fumalski et al., 2010; Machon et al., 2003; Woodhead et al., 2006; Zhang et al., 2010); these (supplementary material Fig. S2) and other proteins regulating cell adhesion, such as *Shroom3* and *Olfm3* (optimedin), have been identified as direct Pax6 targets (Plageman et al., 2010; Grinchuk et al., 2005; Sansom et al., 2009). Thus, Pax6 appears to influence AJ coupling and apical anchoring via functionally related target gene regulation.

Pax6 regulates the orientation of cell division via transcriptional regulation of *Spag5*

Alterations in AJ coupling might not only affect anchoring of cells but also spindle orientation, as spindle poles are aligned with junctional complexes in many epithelial cell divisions exhibiting a vertical cleavage angle (Lechler and Fuchs, 2005; Poulson and Lechler, 2010; Zheng et al., 2010). In this regard, the novel Pax6 target gene we describe here, *Spag5*, is of particular interest as its product has been shown to associate with the mitotic spindle and the centrosome, and regulates aurora A (aurora kinase A – Mouse Genome Informatics) localization in mammalian cell division (Chang et al., 2001; Mack and Compton, 2001; Cheng et al., 2007; Du et al., 2008; Yuan et al., 2009). Pax6 regulates the transcription of *Spag5*, as shown here by expression analysis after acute Pax6 deletion, luciferase assays and ChIP, and Spag5 knockdown phenocopies the increase in non-vertical cell divisions as observed in the Pax6-deficient cerebral cortex, both in Pax6$^{Sey/Sey}$ mice or after acute Pax6 depletion by Cre electroporation. Spag5 is associated with the spindle machinery in other cell types and is implicated in regulating kinetochore microtubule dynamics (Manning et al., 2010) and interacts with spindle-associated proteins, such as aurora A (Du et al., 2008) and ninein (Cheng et al., 2007). Ninein is also a Pax6 target regulating centrosomal microtubule nucleation and asymmetric inheritance of the mother centrosome in cerebral cortex progenitor cells (Wang et al., 2009). Indeed, ninein expression levels were also affected in the E15 Pax6$^{Sey/Sey}$ cerebral cortex (supplementary material Fig. S5D), suggesting complex quantitative alterations in proteins associated with centrosome and microtubule function in the absence of Pax6. Taken together, our data suggest the direct regulation of proteins associated with the spindle machinery by Pax6-mediated transcription.

As knockdown of Spag5 increased non-vertical cell division in WT cerebral cortex, these data also demonstrate a role for Pax6 in regulating the orientation of cell division independently of other phenotypes observed in the Pax6$^{Sey/Sey}$ mutant cerebral cortex, such as alterations in patterning (Walther and Gruss, 1991; Stoykova and Gruss, 1994; Stoykova et al., 1996; Torresson et al., 2000; Yun et al., 2001). The extent to which these targets are also responsible for polarity-independent effects of Pax6 on the mode of cell division remains to be determined. Prominin1-expressing VZ progenitor cells from the Pax6$^{Sey/Sey}$ mutant showed an increase in the generation of daughter cells with asymmetric cell fates (postmitotic versus dividing), even in a culture system in which AJ coupling and apicobasal polarity were absent, or upon co-culturing with WT cells. This suggests that Pax6 regulates the mode of cell division independently of apicobasal polarity and AJ coupling. These data, therefore, highlight the importance of examining Pax6 target genes for a better understanding of transcriptional regulation of the mode of cell division.

Phylogenetic relevance

Polarity is important not only for the mode of progenitor cell division, but also to regulate tangential or radial expansion of a given brain region. These mechanisms are of special importance with regard to expansion of the cerebral cortex in primate evolution. Radial glial cells lacking apical contact to the ventricular surface, so-called ‘outer radial glia’ (oRG), have recently been discovered in much larger numbers in ferret and primate cerebral cortex compared with that of mouse (Hansen et al., 2010; Fietz et al., 2010; Reillo et al., 2011). Notably, non-apical progenitor cell increases in Pax6$^{Sey/Sey}$ mutant (mouse) cerebral cortex have some similarities to oRG as they maintain radial glial hallmarks, such as the expression of GLAST, and an SP mode of cell division as observed by single cell tracking of prominin1-negative progenitors in dissociated cultures. This phenotype is also accompanied by reduced tangential expansion of the Pax6$^{Sey/Sey}$ cerebral cortex (supplementary material Fig. S6). It is, therefore, intriguing to speculate that alterations in the orientation of cell division and apical anchoring by AJ coupling might contribute to the generation of sub-apically dividing radial glia, thereby regulating tangential versus radial expansion of the cerebral cortex in ontogeny and phylogeny.

Acknowledgements

We are particularly grateful to Fumio Matsuzaki for providing us with plasmids pCAG-ZO1-EGFP and pCAG-PACT-mKO1 and great advice for establishing the en face imaging. We would like to thank Fumio Matsuzaki, Pia Johansson and Tony Perry for insightful comments on the manuscript as well as Tessa Walcher, Ingo Burtscher and Adam Filipczyk for technical advice in the course of this work. We greatly appreciate the excellent technical assistance of Andrea Steiner, Detlef Franzen, Timucin Öztürk and Angelika Waiser.

Funding

This work was supported by grants of the Bavarian State Ministry of the Sciences, Research and the Arts, Bundesministerium für Bildung und Forschung (BMBF), Deutsche Forschungsgemeinschaft (DFG), European Union (EU) and the Helmholtz Association to M.G. and DFG to T.S.

Competing interests statement
The authors declare no competing financial interests.

Supplementary material
Supplementary material available online at
http://dev.biologists.org/lookup/suppl/doi:10.1242/dev.074591/-/DC1

References

Adams, R. J. (1996). Metaphase spindles rotate in the neuroepithelium of rat cerebral cortex. *J. Neurosci.* **16**, 7610-7618.
Alexandre, P., Reugels, A. M., Barker, D., Blanc, E. and Clarke J. D. (2010). Neurons derive from the more apical daughter in asymmetric divisions in the zebrafish neural tube. *Nat. Neurosci.* **13**, 673-679.
Ashery-Padan, R., Marquardt, T., Zhou, X. and Gruss, P. (2000). Pax6 activity in the lens primordium is required for lens formation and for correct placement of a single retina in the eye. *Genes Dev.* **14**, 2701-2711.
Attardo, A., Calegari, F., Haubensak, W., Wilsch-Brauninger, M. and Huttner, W. B. (2008). Live imaging at the onset of cortical neurogenesis reveals differential appearance of the neuronal phenotype in apical versus basal progenitor progeny. *PLoS ONE* **3**, e2388.
Berger, J., Berger, S., Tuoc, T. C., D'Amelio, M., Cecconi, F., Gorski, J. A., Jones, K. R., Gruss, P. and Stoykova, A. (2007). Conditional activation of Pax6 in the developing cortex of transgenic mice causes progenitor apoptosis. *Development* **134**, 1311-1322.
Bultje, R. S., Castaneda-Castellanos, D. R., Jan, L. Y., Jan, Y. N., Kriegstein, A. R. and Shi, S. H. (2009). Mammalian Par3 regulates progenitor cell asymmetric division via notch signaling in the developing neocortex. *Neuron* **63**, 189-202.
Cappello, S., Attardo, A., Wu, X., Iwasato, T., Itohara, S., Wilsch-Brauninger, M., Eilken, H. M., Rieger, M. A., Schroeder, T. T., Huttner, W. B. et al. (2006). The Rho-GTPase cdc42 regulates neural progenitor fate at the apical surface. *Nat. Neurosci.* **9**, 1099-1107.
Carey, M. F., Peterson, C. L. and Smale, S. T. (2009). Chromatin immunoprecipitation (ChIP). *Cold Spring Harb. Protoc.* **9**, Prot5279.
Chang, M. S., Huang, C. J., Chen, M. L., Chen, S. T., Fan, C. C., Chu, J. M., Lin, W. C. and Yang, Y. C. (2001). Cloning and characterization of hMAP126, a new member of mitotic spindle-associated proteins. *Biochem. Biophys. Res. Commun.* **287**, 116-121.
Cheng, T. S., Hsiao, Y. L., Lin, C. C., Hsu, C. M., Chang, M. S., Lee, C. I., Yu, R. C., Huang, C. Y., Howng, S. L. and Hong, Y. R. (2007). hNinein is required for targeting spindle-associated protein Astrin to the centrosome during the S and G2 phases. *Exp. Cell Res.* **313**, 1710-1721.
Chenn, A. and McConnell, S. K. (1995). Cleavage orientation and the asymmetric inheritance of Notch1 immunoreactivity in mammalian neurogenesis. *Cell* **82**, 631-641.
Costa, M. R., Wen, G., Lepier, A., Schroeder, T. and Gotz, M. (2008). Par-complex proteins promote proliferative progenitor divisions in the developing mouse cerebral cortex. *Development* **135**, 11-22.
Doe, C. Q. (2008). Neural stem cells: balancing self-renewal with differentiation. *Development* **135**, 1575-1587.
Du, J., Jablonski, S., Yen, T. J. and Hannon, G. J. (2008). Astrin regulates Aurora-A localization. *Biochem. Biophys. Res. Commun.* **370**, 213-219.
Estivill-Torrus, G., Pearson, H., van Heyningen, V., Price, D. J. and Rashbass, P. (2002). Pax6 is required to regulate the cell cycle and the rate of progression from symmetrical to asymmetrical division in mammalian cortical progenitors. *Development* **129**, 455-466.
Farkas, L. M. and Huttner, W. B. (2008). The cell biology of neural stem and progenitor cells and its significance for their proliferation versus differentiation during mammalian brain development. *Curr. Opin. Cell Biol.* **20**, 707-715.
Fietz, S. A., Kelava, I., Vogt, J., Wilsch-Brauninger, M., Stenzel, D., Fish, J. L., Corbeil, D., Riehn, A., Distler, W., Nitsch, R. et al. (2010). OSVZ progenitors of human and ferret neocortex are epithelial-like and expand by integrin signaling. *Nat. Neurosci.* **13**, 690-699.
Fish, J. L., Kosodo, Y., Enard, W., Paabo, S. and Huttner, W. B. (2006). Aspm specifically maintains symmetric proliferative divisions of neuroepithelial cells. *Proc. Natl. Acad. Sci. USA* **103**, 10438-10443.
Fish, J. L., Dehay, C., Kennedy, H. and Huttner, W. B. (2008). Making bigger brains-the evolution of neural-progenitor-cell division. *J. Cell Sci.* **121**, 2783-2793.
Fumalski, J. K., Trivedi, N., Howell, D., Yang, Y., Tong, Y., Gilbertson, R. and Solecki, D. J. (2010). Siah regulation of Pard3A controls neuronal cell adhesion during germinal zone exit. *Science* **330**,1834.
George, S. H., Gertsenstein, M., Vintersten, K., Korets-Smith, E., Murphy, J., Stevens, M. E., Haigh, J. J. and Nagy, A. (2007). Developmental and adult phenotyping directly from mutant embryonic stem cells. *Proc. Natl. Acad. Sci. USA* **104**, 4455-4460.
Godin, J. D., Colombo, K., Molina-Calavita, M., Keryer, G., Zala, D., Charrin, B. C., Dietrich, P., Volvert, M. L., Guillemot, F., Dragatsis, I. et al. (2010). Huntingtin is required for mitotic spindle orientation and mammalian neurogenesis. *Neuron* **67**, 392-406.
Götz, M. and Huttner, W. B. (2005). The cell biology of neurogenesis. *Nat. Rev. Mol. Cell. Biol.* **6**, 777-788.
Götz, M., Stoykova, A. and Gruss, P. (1998). Pax6 controls radial glia differentiation in the cerebral cortex. *Neuron* **21**, 1031-1044.
Grinchuk, O., Kozmik, Z., Wu, X. and Tomarev, S. (2005). The Optimedin gene is a downstream target of Pax6. *J. Biol. Chem.* **280**, 35228-35237.
Hand, R., Bortone, D., Mattar, P., Nguyen, L., Heng, J. I., Guerrier, S., Boutt, E., Peters, E., Barnes, A. P., Parras, C. et al. (2005). Phosphorylation of Neurogenin2 specifies the migration properties and the dendritic morphology of pyramidal neurons in the neocortex. *Neuron* **48**, 45-62.
Hansen, D. V., Lui, J. H., Parker, P. R. and Kriegstein, A. R. (2010). Neurogenic radial glia in the outer subventricular zone of human neocortex. *Nature* **464**, 554-561.
Haubensak, W., Attardo, A., Denk, W. and Huttner, W. B. (2004). Neurons arise in the basal neuroepithelium of the early mammalian telencephalon: a major site of neurogenesis. *Proc. Natl. Acad. Sci. USA* **101**, 3196-3201.
Haubst, N., Berger, J., Radjendirane, V., Graw, J., Favor, J., Saunders, G. F., Stoykova, A. and Gotz, M. (2004). Molecular dissection of Pax6 function: the specific roles of the paired domain and homeodomain in brain development. *Development* **131**, 6131-6140.
Haydar, T. F., Ang, E., Jr and Rakic, P. (2003). Mitotic spindle rotation and mode of cell division in the developing telencephalon. *Proc. Natl. Acad. Sci. USA* **100**, 2890-2895.
Heins, N., Malatesta, P., Cecconi, F., Nakafuku, M., Tucker, K. L., Hack, M. A., Chapouton, P., Barde, Y. A. and Götz, M. (2002). Glial cells generate neurons: the role of the transcription factor Pax6. *Nat. Neurosci.* **5**, 308-315.
Hill, R. E., Favor, J., Hogan, B. L., Ton, C. C., Saunders, G. F., Hanson, I. M., Prosser, J., Jordan, T., Hastie, N. D. and van Heyningen, V. (1991). Mouse small eye results from mutations in a paired-like homeobox-containing gene. *Nature* **354**, 522-525.
Holm, P. C., Mader, M. T., Haubst, N., Wizenmann, A., Sigvardsson, M. and Götz, M. (2007). Loss- and gain-of-function analyses reveal targets of Pax6 in the developing mouse telencephalon. *Mol. Cell. Neurosci.* **34**, 99-119.
Huttner, W. B. and Kosodo, Y. (2005). Symmetric versus asymmetric cell division during neurogenesis in the developing vertebrate central nervous system. *Curr. Opin. Cell Biol.* **17**, 648-657.
Knoblich, J. A. (2008). Mechanisms of asymmetric stem cell division. *Cell* **132**, 583-597.
Konno, D., Shioi, G., Shitamukai, A., Mori, A., Kiyonari, H., Miyata, T. and Matsuzaki, F. (2008). Neuroepithelial progenitors undergo LGN-dependent planar divisions to maintain self-renewability during mammalian neurogenesis. *Nat. Cell Biol.* **10**, 93-101.
Kosodo, Y., Roper, K., Haubensak, W., Marzesco, A. M., Corbeil, D. and Huttner, W. B. (2004). Asymmetric distribution of the apical plasma membrane during neurogenic divisions of mammalian neuroepithelial cells. *EMBO J.* **23**, 2314-2324.
Kriegstein, A., Noctor, S. and Martinez-Cerdeno, V. (2006). Patterns of neural stem and progenitor cell division may underlie evolutionary cortical expansion. *Nat. Rev. Neurosci.* **7**, 883-890.
Lechler, T. and Fuchs, E. (2005). Asymmetric cell divisions promote stratification and differentiation of mammalian skin. *Nature* **437**, 275-280.
Lee, T. I., Johnstone, S. E. and Young, R. A. (2006). Chromatin immunoprecipitation and microarray-based analysis of protein location. *Nat. Protoc.* **1**, 729-748.
Machon, O., van den Bout, C. J., Backman, M., Kemler, R. and Krauss, S. (2003). Role of beta-catenin in the developing cortical and hippocampal neuroepithelium. *Neuroscience* **122**, 129-143.
Mack, G. J. and Compton, D. A. (2001). Analysis of mitotic microtubule-associated proteins using mass spectrometry identifies astrin, a spindle-associated protein. *Proc. Natl. Acad. Sci. USA* **98**, 14434-14439.
Manning, A. L., Bakhoum, S. F., Maffini, S., Correia-Melo, C., Maiato, H. and Compton, D. A. (2010). CLASP1, astrin and Kif2b form a molecular switch that regulates kinetochore-microtubule dynamics to promote mitotic progression and fidelity. *EMBO J.* **29**, 3531-3543.
Marthiens, V. and ffrench-Constant, C. (2009). Adherens junction domains are split by asymmetric division of embryonic neural stem cells. *EMBO Rep.* **10**, 515-520.
Matsuzaki, F. (2000). Asymmetric division of *Drosophila* neural stem cells: a basis for neural diversity. *Curr. Opin. Neurobiol.* **10**, 38-44.
Miyata, T. (2007). Asymmetric cell division during brain morphogenesis. *Prog. Mol. Subcell. Biol.* **45**, 121-142.
Miyata, T., Kawaguchi, A., Saito, K., Kawano, M., Muto, T. and Ogawa, M. (2004). Asymmetric production of surface-dividing and non-surface-dividing cortical progenitor cells. *Development* **131**, 3133-3145.
Molnar, Z., Metin, C., Stoykova, A., Tarabykin, V., Price, D. J., Francis, F., Meyer, G., Dehay, C. and Kennedy, H. (2006). Comparative aspects of cerebral cortical development. *Eur. J. Neurosci.* **23**, 921-934.
Morin, X., Jaouen, F. and Durbec, P. (2007). Control of planar divisions by the G-protein regulator LGN maintains progenitors in the chick neuroepithelium. *Nat. Neurosci.* **10**, 1440-1448.

Ninkovic, J., Pinto, L., Petricca, S., Lepier, A., Sun, J., Rieger, M. A., Schroeder, T., Cvekl, A., Favor, J. and Gotz, M. (2010). The transcription factor Pax6 regulates survival of dopaminergic olfactory bulb neurons via crystallin alphaA. *Neuron* **68**, 682-694.
Noctor, S. C., Martinez-Cerdeno, V., Ivic, L. and Kriegstein, A. R. (2004). Cortical neurons arise in symmetric and asymmetric division zones and migrate through specific phases. *Nat. Neurosci.* **7**, 136-144.
Osumi, N. (2001). The role of Pax6 in brain patterning. *Tohoku J. Exp. Med.* **193**, 163-174.
Osumi, N., Shinohara, H., Numayama-Tsuruta, K. and Maekawa, M. (2008). Concise review: Pax6 transcription factor contributes to both embryonic and adult neurogenesis as a multifunctional regulator. *Stem Cells* **26**, 1663-1672.
Pinto, L., Mader, M. T., Irmler, M., Gentilini, M., Santoni, F., Drechsel, D., Blum, R., Stahl, R., Bulfone, A., Malatesta, P. et al. (2008). Prospective isolation of functionally distinct radial glial subtypes-lineage and transcriptome analysis. *Mol. Cell. Neurosci.* **38**, 15-42.
Pinto, L., Drechsel, D., Schmid, M. T., Ninkovic, J., Irmler, M., Brill, M. S., Restani, L., Gianfranceschi, L., Cerri, C., Weber, S. N. et al. (2009). AP2gamma regulates basal progenitor fate in a region- and layer-specific manner in the developing cortex. *Nat. Neurosci.* **12**, 1229-1237.
Plageman, T. F., Jr, Chung, M. I., Lou, M., Smith, A. N., Hildebrand, J. D., Wallingford, J. B. and Lang, R. A. (2010). Pax6-dependent Shroom3 expression regulates apical constriction during lens placode invagination. *Development* **137**, 405-415.
Polleux, F. and Ghosh, A. (2002). The slice overlay assay: a versatile tool to study the influence of extracellular signals on neuronal development. *Sci. STKE* **2002**, pl9.
Poulson, N. D. and Lechler, T. (2010). Robust control of mitotic spindle orientation in the developing epidermis. *J. Cell Biol.* **191**, 915-922.
Quinn, J. C., Molinek, M., Martynoga, B. S., Zaki, P. A., Faedo, A., Bulfone, A., Hevner, R. F., West, J. D. and Price, D. J. (2007). Pax6 controls cerebral cortical cell number by regulating exit from the cell cycle and specifies cortical cell identity by a cell autonomous mechanism. *Dev. Biol.* **302**, 50-65.
Rakic, P. (2009). Evolution of the neocortex: a perspective from developmental biology. *Nat. Rev. Neurosci.* **10**, 724-735.
Reillo, I., de Juan Romero, C., Garcia-Cabezas, M. A. and Borrell, V. (2011). A role for intermediate radial glia in the tangential expansion of the mammalian cerebral cortex. *Cereb. Cortex* **21**, 1674-1694.
Rieger, M. A., Hoppe, P. S., Smejkal, B. M., Eitelhuber, A. C. and Schroeder, T. (2009). Hematopoietic cytokines can instruct lineage choice. *Science* **325**, 217-218.
Saito, T. (2006). In vivo electroporation in the embryonic mouse central nervous system. *Nat. Protoc.* **1**, 1552-1558.
Sanada, K. and Tsai, L. H. (2005). G protein betagamma subunits and AGS3 control spindle orientation and asymmetric cell fate of cerebral cortical progenitors. *Cell* **122**, 119-131.
Sansom, S. N., Griffiths, D. S., Faedo, A., Kleinjan, D. J., Ruan, Y., Smith, J., van Heyningen, V., Rubenstein, J. L. and Livesey, F. J. (2009). The level of the transcription factor Pax6 is essential for controlling the balance between neural stem cell self-renewal and neurogenesis. *PLoS Genet.* **5**, e1000511.
Schmahl, W., Knoedlseder, M., Favor, J. and Davidson, D. (1993). Defects of neuronal migration and the pathogenesis of cortical malformations are associated with Small eye (Sey) in the mouse, a point mutation at the Pax-6-locus. *Acta Neuropathol.* **86**, 126-135.
Schwamborn, J. C., Berezikov, E. and Knoblich, J. A. (2009). The TRIM-NHL protein TRIM32 activates microRNAs and prevents self-renewal in mouse neural progenitors. *Cell* **136**, 913-925.
Stoykova, A. and Gruss, P. (1994). Roles of Pax-genes in developing and adult brain as suggested by expression patterns. *J. Neurosci.* **14**, 1395-1412.
Stoykova, A., Fritsch, R., Walther, C. and Gruss, P. (1996). Forebrain patterning defects in Small eye mutant mice. *Development* **122**, 3453-3465.
Stoykova, A., Götz, M., Gruss, P. and Price, J. (1997). Pax6-dependent regulation of adhesive patterning, R-cadherin expression and boundary formation in developing forebrain. *Development* **124**, 3765-3777.
Stoykova, A., Treichel, D., Hallonet, M. and Gruss, P. (2000). Pax6 modulates the dorsoventral patterning of the mammalian telencephalon. *J. Neurosci.* **20**, 8042-8050.
Stoykova, A., Hatano, O., Gruss, P. and Götz, M. (2003). Increase in reelin-positive cells in the marginal zone of Pax6 mutant mouse cortex. *Cereb. Cortex* **13**, 560-571.
Stricker, S. H., Meiri, K. and Götz, M. (2006). P-GAP-43 is enriched in horizontal cell divisions throughout rat cortical development. *Cereb. Cortex* **16 Suppl. 1**, i121-i131.
Tamai, H., Shinohara, H., Miyata, T., Saito, K., Nishizawa, Y., Nomura, T. and Osumi, N. (2007). Pax6 transcription factor is required for the interkinetic nuclear movement of neuroepithelial cells. *Genes Cells* **12**, 983-996.
Thein, K. H., Kleylein-Sohn, J., Nigg, E. A. and Gruneberg, U. (2007). Astrin is required for the maintenance of sister chromatid cohesion and centrosome integrity. *J. Cell Biol.* **178**, 345-354.
Toresson, H., Potter, S. S. and Campbell, K. (2000). Genetic control of dorsal-ventral identity in the telencephalon: opposing roles for Pax6 and Gsh2. *Development* **127**, 4361-4371.
Walther, C. and Gruss, P. (1991). Pax-6, a murine paired box gene, is expressed in the developing CNS. *Development* **113**, 1435-1449.
Wang, X., Tsai, J. W., Imai, J. H., Lian, W. N., Vallee, R. B. and Shi, S. H. (2009). Asymmetric centrosome inheritance maintains neural progenitors in the neocortex. *Nature* **461**, 947-955.
Warren, N., Caric, D., Pratt, T., Clausen, J. A., Asavaritikrai, P., Mason, J. O., Hill, R. E. and Price, D. J. (1999). The transcription factor, Pax6, is required for cell proliferation and differentiation in the developing cerebral cortex. *Cereb. Cortex* **9**, 627-635.
Weigmann, A., Corbeil, D., Hellwig, A. and Huttner, W. B. (1997). Prominin, a novel microvilli-specific polytopic membrane protein of the apical surface of epithelial cells, is targeted to plasmalemmal protrusions of non-epithelial cells. *Proc. Natl. Acad. Sci. USA* **94**, 12425-12430.
Wilcock, A. C., Swedlow, J. R. and Storey, K. G. (2007). Mitotic spindle orientation distinguishes stem cell and terminal modes of neuron production in the early spinal cord. *Development* **134**, 1943-1954.
Wolf, L. V., Yang, Y., Wang, J., Xie, Q., Braunger, B., Tamm, E. R., Zavadil, J. and Cvekl, A. (2009). Identification of pax6-dependent gene regulatory networks in the mouse lens. *PLoS ONE* **4**, e4159.
Woodhead, G. J., Mutch, C. A., Olson, E. C. and Chenn, A. (2006). Cell-autonomous beta-catenin signaling regulates cortical precursor proliferation. *J. Neurosci.* **29**, 12620-12630.
Wu, S. X., Goebbels, S., Nakamura, K., Nakamura, K., Kometani, K., Minato, N., Kaneko, T., Nave, K. A. and Tamamaki, N. (2005). Pyramidal neurons of upper cortical layers generated by NEX-positive progenitor cells in the subventricular zone. *Proc. Natl. Acad. Sci. USA* **102**, 17172-17177.
Yuan, J., Li, M., Wei, L., Yin, S., Xiong, B., Li, S., Lin, S. L., Schatten, H. and Sun, Q. Y. (2009). Astrin regulates meiotic spindle organization, spindle pole tethering and cell cycle progression in mouse oocyte. *Cell Cycle* **8**, 3384-3395.
Yun, K., Potter, S. and Rubenstein, J. L. (2001). Gsh2 and Pax6 play complementary roles in dorsoventral patterning of the mammalian telencephalon. *Development* **128**, 193-205.
Zhang, J., Woodhead, G. J., Swaminathan, S. K., Noles, S. R., McQuinn, E. R., Pisarek, A. J., Stocker, A. M., Mutch, C. A., Funatsu, N. and Chenn, A. (2010). Cortical neural precursors inhibit their own differentiation via N-cadherin maintenance of beta-catenin signaling. *Dev. Cell* **18**, 472-479.
Zheng, Z., Zhu, H., Wan, Q., Liu, J., Xiao, Z., Siderovski, D. P. and Du, Q. (2010). LGN regulates mitotic spindle orientation during epithelial morphogenesis. *J. Cell Biol.* **189**, 275-288.

3 Discussion

The development of the murine ventral telencephalon is preceding that of the murine cerebral cortex. This is already evident at early stages of neurogenesis, when the distance from ventricular- to pial surface is much larger in the GE compared to the cortex. My PhD work aimed to investigate the dynamics and behaviors of progenitor cells in the developing LGE from stages of midneurogenesis (E14) on. At this stage the majority of cells in the LGE divide in abventricular positions, contrasting the situation in the cortex, where throughout development the majority of progenitor cells divide at the ventricular surface (Pilz et al 2013). Among the abventricularly dividing cells in the LGE are cells that divide in the ventricular zone, the region defined by INM of RGs. These progenitor cells, which were termed sub-apical progenitors (SAP) upon their site of mitosis, are heterogeneous in morphology during mitosis and much less frequent in the cortical VZ. The morphology of SAPs ranges from no-process bearing to cells with an apical process, a basal process or even both, resembling a bipolar RG morphology. In agreement with this bipolar morphology during M-phase, a proportion of SAPs expresses RG specific molecules. Imaging in embryonic slices revealed that these sub-apically dividing RG generate bRG and daughter cells that loose their apical anchoring and both together migrate to more basal positions. In addition, live imaging revealed that RG in the LGE often produce progenitor cells which divide either at the apical surface (SNP) or in the VZ (SAP) before generating BPs. Therefore a cascade of progenitor divisions amplifies the cellular output in the LGE before a terminal neurogenic division. This amplification goes along with a shortening of cell cycle length of second generation (after RG division) progenitors. In summary, a heterogeneous population of progenitor cells in the LGE facilitates the expansion of abventricular progenitor cells which build up the basal ganglia, a large structure in the murine brain.

3.1 Development of the GE in human and monkey

Two studies on the development of the GE in human and monkey, which focused mainly on the developing MGE revealed interesting similarities to murine LGE development but also differences due to the evolutionary rank of these higher mammals (Ma et al 2013, Hansen et al 2013). A striking parallel between the developing human/monkey MGE and the LGE in mice is the early generation and rapid expansion of a basal progenitor pool in the O/SVZ. Whereas at 4.5 gestational week (GW) all mitotic cells line the ventricle, already one week later (5.5 GW), mitotic cells are apparent in a zone 100µm above the ventricular surface in the VZ (Howard et al 2006). These mitotic cells could likely represent SAPs, marking the first steps from the expansion of the AP progenitor pool towards the seeding of basally located I/OSVZ germinal zones. Coinciding with an dramatic increase in O/SVZ size, the size of the VZ decreases constantly in a dramatic fashion, with the O/SVZ being 50x larger than the VZ at postconceptual week14 (PCW14) (Hansen et al 2013). Like in the murine GE development, the SVZ of the human GE appears and expands more rapid than the SVZ of the cortex. Another similarity between murine and human O/SVZ of the GE is its overall cellular architecture. Whereas the cortical OSVZ and SVZ in human and mice is occupied and organized by dense radial fibers of both apical RG and bRG, the SVZ of the murine GE seems less clearly organized and the human MGE OSVZ is densely packed like its VZ (Hansen et al 2013). In the human MGE this is also achieved by self-renewing proliferative divisions which increase the progenitor pool. The molecular signature of these OSVZ progenitors goes from Sox2+/Olig2+/Sox5+ long term self-renewing progenitors towards Ascl1+/Dlx2+ intermediate progenitors with the progenitors in the human MGE being less differentiated compared to LGE (coexpression of Ki67 and Dlx2) supporting the necessity of repeated proliferative divisions of MGE progenitors to yield sufficient cell numbers for generation of interneurons. The morphology of these MGE OSVZ progenitors is in vast majority non-polar, with no prominent process detectable, at least in the p-vimentin staining (Hansen et al 2013). This argues for a more random organization of the GE OSVZ compared to the CTX. The reason for this difference in cytoarchitecture might be that in contrast to the layered structure of the cortex, the organization into patch and matrix does not require a strong guidance by radial fibers. Rather, many tangentially migrating interneurons pass the

corridor of both the MGE as well as the LGE SVZ on their route to the cortex. Interestingly progenitor cells in the monkey LGE and MGE perform extensive tangential migration and proliferate on their route from MGE to LGE or from the LGE to the cerebral cortex (Ma et al 2013). The cytoarchitecture of progenitors in the human MGE is organized around bundles of RG fibers with up to 20µm diameter leading from the ventricle to the OSVZ and Sox2+ progenitors in close association to these bundles and later (PCW14) as streams parallel to the ventricle (Hansen et al 2013). However it is possible, that p-vimentin staining could miss the fine processes, especially as apically directed processes are shorter and thinner (Betizeau et al 2013) and are retracted during mitosis.

The expression of transcription factor codes that are characteristic for the development of the LGE and MGE in mouse are maintained also during human development. The LGE exhibits a strong abundance of the TF Sp8 in the SVZ of its dorsal part and Islet1 weaker in its ventral part but strong in the striatum (Ma et al 2013). In the VZ of the LGE both Gsx2 as well as weak Pax6 (in comparison to the cortex) are expressed. In contrast to the situation in the mouse, where Sp8+ neurons mark the rostral migratory stream towards the OB already during development, the majority of Sp8+ COUP-TFII+ cells migrate into the neocortex and expresses GABA (Ma et al 2013). This shows that the LGE in human contributes more to cortical interneurons than it does in the mouse. As Nkx2.1 is expressed similar in the human like in the mouse, it is believed to be a key TF for development of the MGE and the generation of interneurons (Butt et al 2008, Flandin et al 2010, Hansen et al 2013,Ma et al 2013). Both studies (Hansen et al 2013,Ma et al 2013) suggest, that in human, as well as in monkey development GABA+ interneurons destined for the neocortex are generated in the ganglionic eminences (LGE, and in majority MGE and CGE) and thereby contradict the view of interneurons arising from cortical progenitor zones (Letinic et al 2002, Jakovcevski et al 2011,Yu & Zecevic 2011).

3.2 Progenitor heterogeneity in germinal zones

The developing telencephalon is characterized by an immense heterogeneity in progenitor cells that, according to their position in rostral-caudal and dorsal-ventral dimension and their expression of regional specific transcription factors, facilitate the generation of an

enormous number and diversity of neuronal subtypes and glial cells (Guillemot 2005, Kriegstein & Alvarez-Buylla 2009). Early clonal analysis of single cortical RG by viral transduction or chimeric mice revealed a restriction of most RG to either neuronal or glial lineages with only a minority resembling bi- or even multipotent progenitors (Walsh & Cepko 1990, Qian et al 1997). In vitro timelapse imaging of single isolated cortical progenitor cells then uncovered the sequential generation of neurons and then glial cells at a time course corresponding to their generation in vivo (Qian et al 2000, Shen et al 2006). More recently, fate mapping analysis of neocortical RG under Cux2 and Fezf2 promoters showed that a coexistence between layer and lineage restricted progenitor cells and multipotent, sequentially acting progenitor cells exists (Franco et al 2012, Guo et al 2013). Whether single RG in the developing LGE also exhibit multilineage potential and generate both patch and matrix neurons and later glial cell types sequentially needs to be determined by clonal long-term fate mapping using a suitable LGE specific driver line or a combinatorial Split-Cre approach.

The lineage potential of RG has often been correlated with the expression of molecules that are specifically expressed by RG, like BLBP, Glast and hGFAP (Malatesta et al 2003, Anthony et al 2004, Pinto & Gotz 2007) and just very recently it was shown by Piggy-Bac fate-mapping, that the lineage of Glast+ RG is more prone to generate large astrocytic clones compared to the Nestin+ lineage at later stages of corticogenesis (Siddiqi et al 2014). The heterogeneity in expression of RG specific molecules also exists amongst RG in the LGE (Hartfuss et al 2001). Interestingly virtually all SAPs have been proven to be BLBP negative, whereas a considerable proportion has been shown to be RC2, hGFAP and Glast positive (Pilz et al 2013). This difference in the expression of RG specific molecules may point towards a lineage difference between APs and SAPs and a more limited proliferative and therefore intermediate progenitor character of SAPs in comparison to BLBP positive, longterm self-renewing RGs.

A transcriptome analysis of hGFAP-GFP+ RG with strong and weak GFP expression revealed two subpopulation of RG in the developing cortex: hGFAP-GFP low RGs are prone for direct neurogenesis and hGFAP-GFP high RGs are prone for indirect neurogenesis via BPs (Pinto et al 2008, Pinto & Gotz 2007). As both live imaging as well as clonal analysis revealed different sets of RG: those generating a large progeny via

different sets of intermediate progenitors (SNPs, SAPs, BPs) and those giving rise to clones of smaller cell number, it would be interesting to uncover if like in the CTX, these subpopulations can be distinguished on the basis of differences in their expression profile of molecules like e.g. hGFAP or BLBP. However it has to be noted, that the expression of hGFAP-GFP is magnitudes weaker in the LGE and direct neurogenesis from RG like in the CTX has not been observed by live-imaging. A study on the expression of GFAP in progenitor cells of the pre-natal macaque cortex and GE uncovered also a heterogeneity of GE RGs in GFAP immunoreactivity while all cortical APs and a majority of BPs are positive for GFAP (Cunningham et al 2013). This again points towards heterogeneity of RG cells in the GE and possible lineage differences between CTX and GE RGs. In addition to this diverse molecular identity of progenitor cells they can be distinguished in proliferative capacity, cellular features and morphology. Interestingly, progenitor morphology like epithelial cell shape is associated with proliferative performance. However the view on the morphology especially of intermediate progenitors has changed with cortical BPs (identified by Tbr2-GFP) exhibiting sometimes long and dynamic processes towards the ventricular surface, giving them a (uni-) polar morphology (Nelson et al 2013). This mechanism of feedback signaling from intermediate progenitors via their longer apical processes, e.g. from delaminating SAPs or the more apical daughter of sub-apical RG, for example through the Notch-Delta signaling pathway might also apply for the LGE VZ.

The germinal zones of the developing human brain are characterized by an enlargement in size (I/OSVZ) and an increase in diversity of its progenitor cells. Unipolar RG cells with only an apically directed process were described in the intermediate zone (IZ) and subpial granular layer (SGZ) at midgestation (Howard et al 2006, deAzevedo et al 2003). These "inverted" RG cells were thought to guide migrating interneurons – but rather might represent a RG type, that instead of being anchored at the pial basement membrane or the ventricular surface is attached to e.g. the basement membrane of bloodvessels or extracellular matrix in the germinal zones. In support of this idea, RG with a process directed towards the ventricle that curved and with its end pointing towards the pia, where observed in low numbers (deAzevedo et al 2003). A transcriptome study of VZ, SVZ or I/OSVZ respectively and cortical plate in mouse and human tissue revealed a high

expression of extracellular matrix (ECM) and cell adhesion molecules in the expanded proliferative SVZ in human, pointing at possible additional anchoring and signaling for RG (Fietz et al 2012). To what extent the composition of the ECM in the LGE VZ and SVZ supports repeated progenitor proliferation and how it is composed in comparison to the ECM in expanded I/OSVZ germinal zones, is an interesting question to pursue.

Further imaging of progenitor cells in human slices (GW16/18) revealed that about 20% of bRG possess a short apically directed process and the more apically located daughter cells rapidly grows an apical process, later a basal process, which results in a bipolar morphology (LaMonica et al 2013). The expansion of germinal zones comes along with an increase in progenitor subtypes. An outstanding example for this has been provided by a study on OSVZ progenitor cells in the development of the macaque cortical area 17 which revealed that the heterogeneity of progenitors in the OSVZ both in morphology as well as in lineage potential has been underestimated and likely oversimplified (Betizeau et al 2013, Hansen et al 2010, Fietz & Huttner 2011, Reillo et al 2011). In addition to the unipolar bRGs and their descendants the IPs of shorter multipolar morphology three more cell types have been characterized according to their predominant process inheritance: with long apical process (bRG-apical P), both apical and basal process (bRG-both P) and bRG that change their process morphology frequently (bRG-transient -P). Interestingly, a majority of bRG possess an apical process (60% of all) which is usually thinner and shorter than basal processes are. These apical processes never reach the ventricular surface but extend only for shorter distances into the ISVZ and VZ (Betizeau et al 2013). This points towards a functional role of the apical process rather in cell-cell communication than in sensing of signals in the ventricular fluid or signaling in the apical adherence-junction belt. During imaging of the division of subapical RG in the developing LGE the more apically located daughter, as well as in more rare cases, the basal bRG daughter keeps such an apical process during translocation towards the basal side (Pilz et al 2013, data not shown). The inheritance of such an apical process in subapical RG daughter cells could enable sensing of signaling, e.g. the Notch-Delta pathway (Nelson et al 2013), which may explain higher proliferative capacities.

Excitingly, bRG-both-P, a bRG subtype that exhibits both an apical and a basal process during interphase, is likely the progenitor type being most homologous to subapical RG in

the LGE, exhibiting the highest selfrenewal rates amongst all 5 progenitor types (Betizeau et al 2013), even higher than the one of bRG-basal P which exhibit the lowest self-renewal capability. This suggests, that cellular features associated with a bipolar morphology (present in apical RG and bRG-both-P) are more determining for self-renewal than the inheritance of a basal process and the related ß1-integrin signaling (Fietz & Huttner 2011). The fact, that bRG-both-P in many cases do not reach neither ventricular nor pial surface suggest that rather an interaction with further progenitor cells in I/OSVZ transmits information on these bipolar cells and enables self-renewal. The question to which extent apical and basal processes interact with the vascular system or the extracellular matrix, to which microarray analysis is pointing at (Fietz et al 2012), needs to be determined for both the monkey OSVZ as well as the expanded SVZ of the murine LGE. Further, in the monkey OSVZ, the inheritance of either apical or basal process after division determines if a daughter cell becomes a bRG with a stable process (bRG-basal-P for the upper daughter or bRG-apical-P for the basally located daughter cell) or a bRG-transient-P or an IP respectively. The proper orientation of cell divisions in the OSVZ, which is in 80% of the cases horizontal, is believed to be crucial for a proper lineage progression.

In addition to the highest potential for self-renewal, bRG-both-P also show the highest capability to generate neuronal progeny at E78, the stage when the majority of supragranular neurons in the macaque are generated. At this stage, the percentage of proliferative divisions amongst OSVZ progenitors increases compared to E65, cell cycle exit rates are reduced which goes along with an overall shortening in cell cycle length (Betizeau et al 2013). These phenomena in cell kinetics are equally observed during phases of progenitor expansion in the developing LGE. Also the synchrony in cell cycle time and exact timepoint of division of two related daughter cells is a common phenomenon observed both in the monkey OSVZ and the murine LGE. The shortening of cell cycle length during proliferative divisions is a common feature, which along with repeated divisions of IPs, takes place both in the macaque OSVZ at E78 and the LGE SVZ during midneurogenesis, the phases when the majority of neurons is produced. In fact at this stage IPs in the macaque OSVZ perform only proliferative divisions, possibly increasing the pool of progenitor cells for later stages of gliogenesis. In the mouse LGE, these ongoing divisions of IPs are confined to examples of large lineages. Therefore, the developing

LGE, with its heterogeneity in progenitor cell types regarding proliferative potential and morphology shares similarities with expanded proliferative zone like the monkey OSVZ and is accordingly suited to study enlargement of germinal zones. It further needs to be investigated in depth to which extent molecular and morphological heterogeneity of progenitor cells in the developing LGE reflects also differences in proliferative capacity and multilineage potential.

3.3 Influences of tissue morphogenesis and mechanical forces on progenitor behavior

The early development of the ventral telencephalon precedes that of the neocortex in terms of proliferation and expansion of the germinal zones (Smart 1985). Both rates of apical and basal divisions in the GE lead to the formation of characteristic bulges into the ventricle with a convex surface of the GE ventricular zones in contrast to the concave ventricular zones of the neocortex (Smart 1985). These geometrical differences then exert different mechanic forces on RG in GE and cortex. For example are the basal processes of RG in the GE at midneurogenesis much longer than with their counterparts in the cortex. Recently it was shown that mechanical stress upon congestion of progenitor cells can lead to delamination of cells (Okamoto et al 2013). A similar phenomenon could play a role during GE development, where due to an increasing force on the ventricular zone these progenitor cells leave the VZ and continue proliferation in the SVZ. Until now, no live imaging of RG in the LGE at early stages (E10-E12) or careful quantitative analysis of RG basal processes over time has been carried out, which could resolve this question. Another reason for an increased delamination of RG could be a weaker anchoring of LGE RG in the apical adherence junction belt. In accordance to this a decrease in some adherence junction proteins has been observed in the Pax6 deficient cortex Sey/Sey (Asami et al 2011). As Pax6 is expressed only at lower levels in subsets of APs in the GE it would be worth to investigate how weaker adherence junctions connect APs in the LGE VZ and if the positioning of adherence junctions sculptures the formation of the characteristic GE bulge (Wang et al 2012).

Radial glia that loose their apical anchoring and translocate towards basal positions have been observed in the telencephalic development of various species and were for a long

time implicated in the transition of RG into astrocytes (Schmechel & Rakic 1979). This was supported by slice imaging at later stages of development by Noctor and colleagues that monitored translocating RG after a final division at the ventricular surface which moved towards the pia and divided once more at more basal positions. Electrophysiological recordings revealed non-neuronal currents of all non-RG daughter cells pointing to the generation of astrocytes by translocating RG (Noctor et al 2004, Noctor et al 2008). More recently, these translocating RG have been proven to be a crucial cell type in expanded SVZ of gyrified mammals that aids to amplify neuronal output and serve as additional guidance scaffold (Hansen et al 2010, Fietz & Huttner 2011, Reillo et al 2011, Kelava et al 2012). Interestingly while being mostly neurogenic in the mouse (direct neuron generation; Shitamukai et al 2011, Wang et al 2011) and human (neuron generation via IPCs; Hansen et al 2010), bRG seem indeed to be generating mostly astrocytes in the ferret cortex (Reillo et al 2011).

So far, bRG in the human are thought to arise either by oblique or horizontal divisions of apical RG in the VZ or by self-renewing or amplifying divisions of bRG in the OSVZ (LaMonica et al 2013, Hansen et al 2010). Whether also delamination is relevant for the generation of bRG for expanded OSVZ needs to be investigated. The downregulation of Trnp1 in slices of the developing cortex lead to a delamination of apical RG from the adherence junction belt and an organized OSVZ expansion and gyrus formation (Stahl et al 2013). The inheritance and maintenance of a basal process is crucial for a coordinated layering process, as delaminating progenitors which keep apical RG identity but lost apical and basal processes lead to a disorganized cortex with numerous heterotopias (Okamoto et al 2013).

In contrary to the OSVZ of the developing human cortex, where bRG have been shown to be numerous judged on identification by p-vimentin and live imaging (Hansen et al 2010), the cellular composition of the developing human OSVZ of the ganglionic eminences appears different (Hansen et al 2013). The OSVZ progenitor population of the human MGE expands in the early second trimester and even though these cells remain the molecular characteristics of their VZ precedents (Sox2, Olig2, Sox5), the vast majority shows a round, non-epithelial morphology in m-phase (Hansen et al 2013). Rather OSVZ progenitors bearing a longer process are rare and show a random orientation unlike in the

cortex, which points to a minor role in process guided neuronal migration in the GE compared to the six layered structure of the cortex. It remains to be determined how the OSVZ of the human GE is seeded with non-epithelial progenitor and if repetitive proliferative divisions of SAPs and BPs like in the murine GE SVZ are responsible for this tissue morphogenesis.

3.4 Mechanisms of generating expanded germinal zones

The observation of an expanded SVZ and therefore an increase in cycling progenitors per radial unit can also be explained by an accelerated speed of the cell cycle. It is well accepted, that the length of G1 phase of the cell cycle is directly related to a cell's decision to remain a proliferative progenitor or to become a differentiating postmitotic cell. The cell cycle length of cortical neural progenitors in the VZ increases gradually from the start of neurogenesis (E11; 8hrs) to the end of neurogenesis (E18; 18hrs), consistent with a higher proportion of RG cells undergoing differentiating rather than self-amplifying divisions. This overall increased cell cycle length is caused by an extension of G1 phase with G2-M and S-phase staying rather constant (Caviness & Takahashi 1995). The *cell cycle length hypothesis* put forward by Calegari and Huttner explains that the time during G1 phase a fate determinant is able to act on a cell defines its cell fate (Calegari & Huttner 2003). In the development of the primate cortex the arealization taking place leads to the expansion of certain areas in comparison to neighboring cortical areas as well as in comparison to other species. This is the case for area 17 of the visual cortex in primates (striate cortex) that contains 2.5fold more neurons in the binocular part of area 17 which is also reflected by a higher labeling index of the germinal zone compared to area 18 (Rockel et al 1980, Dehay et al 1993). This higher rate in neurogenesis in area 17 arises from an expanded OSVZ which is characterized by progenitor cells with a shortened cell cycle length (T_C; 10hrs shorter than in area 18) and a higher rate of cell cycle re-entry reflected by strong CyclinE expression (Lukaszewicz et al 2005). Importantly, speeding up the cell cycle without increasing the rate of re-entry into the cell cycle would not allow the expansion of a specific area but both parameters need to be co-regulated (Lukaszewicz et al 2005). The overexpression of cdk4 and cyclin D1 (together: 4D), which promote the G1 transition (Ekholm & Reed 2000), leads to a shortening of G1 phase and a faster cell cycle. This in

turn favors the generation of BPs over neurons and interestingly the overall expansion of BPs by increasing the number of symmetric proliferative divisions (Lange et al 2009). A constitutive overexpression of 4D leads to a progressive increase in BPs, an enlarged SVZ and an increase in cortical surface area, however without the formation of gyri and sulci. This was only observed in the naturally gyrencephalic ferret where it induced a de-novo cortical folding, possibly due to the higher number of bRGs present in the ferret cortex and in the mouse cortex after TRNP1 knockdown (Nonaka-Kinoshita et al 2013, Stahl et al 2013).

Interestingly, the developing LGE in mice fulfills criteria which lead to an increased germinal zone, namely accelerated cell cycle speed of progenitors and continued proliferation of these. The shortening in cell cycle length is most dramatic in the amplifying progenitor lineages observed in the LGE, where second generation intermediate progenitors, the progenitors generated not by the RG but by a descendent SAP, SNP or BP, can exhibit extremely short cell cycles of 10-12hrs. One has to mention that these second generation IPs rarely exist in the developing cortex, where RG generate neurons or terminally dividing IPs (SNPs or BPs) (Noctor et al 2008). In addition BPs in the LGE at midneurogenesis are only in minority terminally neurogenic, indicated by their lack of expression of Tis21-GFP, which means that the progenitor pool in the SVZ is further expanded for later stages by these proliferative divisions. At later stages (E16), this high proliferative potential of SVZ progenitors in the LGE ceases, reaching levels of SVZ progenitor proliferation comparable to all stages of cortical development. This illustrates that whereas in the cerebral cortex the amplification of neuronal output is modest (doubled by symmetric terminal neurogenic divisions of SNP and BP), large progenitor amplification in the LGE occurs during comparable time units by fast cell cycles of continuously dividing progenitor cells.

Which signaling pathways are responsible for the decision where gyri and sulci are formed is largely unknown. Strikingly, the administration of FGF2 into the ventricle at E11.5 led to a robust and reproducible formation of gyri and sulci in the rostrolateral neocortex (Rash et al 2013). Initially this leads to a further ventral expansion of Tbr2+ intermediate progenitors and a reduced volume of the developing LGE at E13.5 with the Dlx2+ ventricular area remaining constant. Remarkably, the ventrally expanded BPs (Tbr2+) also

exhibit the expression of Er81, a TF of the olfactory bulb interneuron lineage (Stenman et al 2003). This "LGE-like identity" is further supported by the progenitor dynamics of first increased self-renewal of RG and then an accelerated production of BPs and basal mitoses followed by a delayed neuron production (Rash et al 2013). As the numbers of bRG were not increased in this model, this model of induced gyrification resembles an initial theory (Martinez-Cerdeno et al 2006) that has been overcome by the more recent discovery of bRG.

Basal progenitors reside in a vascular niche in the developing telencephalon and divide preferentially at branching points of the vascular network. Therefore a support of mitogens and growth factors to BPs either from circulation or by endothelial cells has been suggested (Javaherian & Kriegstein 2009, Stubbs et al 2009). This is supported by the observation that BPs appear after the emergence of a vasculature, which follows a ventral to dorsal gradient, starting in the ventral telencephalon at E9, and reaching the dorsal telencephalon at E10/E11. Interestingly angiogenesis and neurogenesis seem both to rely on TFs crucial for telencephalic patterning like Pax6, Dlx1/2 and Nkx2.1 and loss of these TFs impairs also the generation of blood vessels (Vasudevan et al 2008). An earlier development of a dense vascular network might therefore favor the generation of a SVZ in the ventral telencephalon and support further expansion of the SVZ via a vascular system that covers the entire LGE. As both LGE and MGE contain a prominent population of SAPs the vasculature in the VZ of these compartments might be structured to favor proliferation in this germinal zone. Interestingly confocal analysis of endothelial cells (EC; stained by PECAM; CD31) and dividing progenitor cells (phosphor-histone H3; PH3) in the LGE ventricular zone revealed a close association, like reported, and in addition a dense network of membrane protrusions from ECs towards a majority of cells in M-Phase. This network of filopodia-like cell-cell contacts is more dense in the VZ of the LGE compared to the cortex (observation of Dr. Sven Falk). Whether ECs sense progenitor proliferation via these processes or support progenitors via direct supply with mitogens and growth factors needs to be investigated. One possibility is that these filopodia on tip cells sense VEGF-A secreted by progenitor cells which induces sprouting and later fusion of newly formed blood vessels (Mackenzie & Ruhrberg 2012). An intriguing idea is that the onset of vascularization in the telencephalon coincides and is causally related with the

switch of RG cells from symmetric proliferative divisions to asymmetric divisions. A delay in development of the vascular system could potentially result in a prolonged expansion of the RG progenitor pool and therefore an overall brain expansion. In addition a close association of progenitor cells with the vascular system may be established during development in the LGE and play an important role for adult NSC in the niche of the subependymal zone. A close proximity of aNSC to a blood vessel plexus and the response to secreted factors from the vasculature have been described (Shen et al 2008, Tavazoie et al 2008). Both cell cycle kinetics and support by the vascular network enable a robust expansion of SVZ progenitors during development of the LGE and thereby lead to a rapid expansion of this telencephalic region in the mouse.

3.5 The orientation of cleavage angle during apical progenitor divisions as a mechanism for cellular asymmetry and fate decisions

Apical progenitors return for mitosis to the apical ventricular surface and the cleavage plane orientation during cytokinesis has been implicated in cell fate decisions for the resulting daughter cells. A perpendicular cleavage plane has been associated with symmetric progenitor divisions and is the predominant mode during development of the cortex. Oblique or slightly tilted and horizontal divisions would lead to asymmetric daughter cell fates (Chenn & McConnell 1995, Gotz & Huttner 2005). Throughout corticogenesis the majority of APs divide in a perpendicular cleavage angle even at stages of predominantly asymmetric daughter cell fates which contradicts a simple causal relationship (Noctor et al 2008). It appears that a temporal dependency of cleavage plane orientation exists during cortical development. First, a correct spindle orientation is necessary for survival of NE progenitors, later for the expansion of the NE progenitor pool and then to prevent premature neuronal differentiation (Xie et al 2013). At later stages of midneurogenesis (E14), an induction of oblique and horizontal cleavage planes by overexpression of mInsc leads to both an increase of Pax6+ bRG as well as higher numbers of BPs in more basal positions, therefore an expanded neurogenic zone (Postiglione et al 2011, Konno et al 2008). Interestingly, this reflects to some degree the distribution of cleavage angles in the developing LGE, where throughout development the percentage of

oblique and horizontal apical divisions is higher compared to the cortex (G.-A. Pilz unpublished data). This could indicate that the expanded SVZ of the LGE is seeded to a higher extent with bRG and BPs already from early stages on. In addition, the causal relationship of horizontal cleavage planes observed in human development, where the more basally located daughter inherits all of the basal process and no apical membrane and therefore becomes a bRG (LaMonica et al 2013) needs to be tested for LGE development where horizontal and oblique cleavage angles are numerous, but not as frequent as in human GW16-18. It remains still an open question, which class of apical progenitors, RG and SNPs, are mostly contributing to oblique and horizontal divisions. SNPs, which are according to live imaging data more frequent at midneurogenesis in LGE than in cortex, could be more flexible for rotating and orienting the mitotic spindle, as they are not anchored to the BM via a basal process like RG.

Transcriptome analysis comparing the gene expression levels of APs from CTX and GE at midneurogenesis revealed that the gene ontology (GO) terms “spindle apparatus” and “centrosome” are the most prominently upregulated gene categories in the GE (Luisa Pinto unpublished results). The reason could be, that the orientation of AP divisions in the LGE, due to stronger forces that are exerted along the longer basal processes need more support to mechanistically stabilize and orient the spindle, especially, to yield an oblique or horizontal orientation. Whether the spindle orientation of APs during development of the LGE plays a role for the maintenance of stem cells into the adult SEZ is an interesting path to pursue. Conditional knockout studies of the upregulated genes during development and subsequent analysis of its impact on adult neurogenesis can address this question. Further, any specific manipulation of AP cleavage angles, e.g. by knockout of LGN (Konno et al 2008) or overexpression of mInsc (Postiglione et al 2011) paralleled by clonal live imaging studies will reveal the direct cellular effect on daughter cells after cleavage plane manipulation, e.g. if the delamination of apical RG is promoted under these conditions. The delamination of apical RG, by direct generation of bRG or by division as subapical RG, could indeed be a common scenario at later stages in the developing LGE as apically dividing cells become less frequent, also in comparison to the cortex. Further, the downregulation of Trnp1 in the murine cerebral cortex proved to alter the cleavage plane

of APs and consequently also the delamination of RG leading to an expanded SVZ in the cortex (Stahl et al 2013).

However it has not been fully clarified, if the inheritance of determination factors or cellular morphological features directs daughter cell fate after apical mitoses. Rather, the cleavage orientation of APs seems to influence how long an AP remains attached to the ventricular surface after division and thereby how long also the signaling at this site can influence its fate. It has been observed, that IPs remain a substantial time at the ventricular surface after division and often keep longer processes that contact the ventricle while they are detaching. However live imaging in the zebrafish neural tube revealed that in this system of asymmetric divisions the more apical daughter which remains a longer time at the ventricular surface becomes the differentiating neuron (Alexandre et al 2010).

Despite the observation, that long lasting stemness is not only associated with a basal process in the monkey OSVZ (Betizeau et al 2013), the role of it for apical RG and bRG in the mouse cortex is evident, with inheritance of the basal process being correlated to a/bRG fate and its absence with differentiation (Konno et al 2008, Shitamukai et al 2011, Noctor et al 2008). Therefore, how apical RG divisions are oriented and which daughter cell inherits the basal process accordingly remains a decisive point for the cell fate in the murine VZ.

3.6 The loss of Pax6 function in the neocortex resembles ascpects of progenitor behaviour like in the LGE

The loss of Pax6 protein in the murine embryonic neocortex leads to changes in progenitor cell behavior that resemble more the situation in the developing LGE than in the wildtype neocortex (Tamai et al 2007, Asami et al 2011). Cleavage angles of apical mitoses are not strictly perpendicular but exhibit more often oblique or horizontal cleavage planes and thereby correspond more to the situation in the LGE at midneurogenesis E14 (Asami et al 2011 and G.-A. Pilz unpublished data). These changes are believed to result from weakened apical anchoring of APs and a less robust and precise spindle orientation machinery at work due to lower levels of the protein Spag5 (Asami et al 2011). Even though many genes related to centrosomal proteins and spindle orientation are upregulated

in the LGE compared to the neocortex (Luisa Pinto unpublished data), it would be worthwhile to investigate how strong the genes of these GO terms downstream of Pax6 are expressed in the LGE and thereby, if cleavage orientation of ventral APs results from reduced Pax6 expression levels. Consistent with these data of more oblique and horizontal cleavage planes a more frequent delamination of APs is observed in the Sey mutant and in the developing LGE where subapical RG lead to a reduction in apical RG. As apical RG are returning to the VS for mitosis to recruit the centrosome that acts as basal body of the primary cilium during interphase (Taverna & Huttner 2010), the question arose how the dynamics of cilium disassembly and centrosome motility would behave in subapical RG which do not fully return to the apical side. Elegant imaging of centrosome movements in slices of the embryonic LGE revealed that a movement of the centrosome in the apical process towards the basal side precedes the division of subapical RG (observation of Dr. Sven Falk; unpublished). This movement starts already during G2 phase and the timepoint when centrosome and nucleus meet determines the location of the division. Again, the investigation of centrosome movement prior to division of RG in the WT and *Sey* neocortex would reveal the role of Pax6 in orchestrating centrosome movement and the location of each RG division. In accordance with the observation of RG dividing in subapical positions in both developing LGE (Pilz et al 2013) and in the *Sey* mouse model (Tamai et al 2007,Asami et al 2011) dividing progenitors retain the identity and marker expression of RG (Pilz et al 2013, Asami et al 2011). As such they are prone for repeated proliferation, either as apparent bRG, delaminating RG, or even as APs that have lost a clear bipolar morphology (Okamoto et al 2013). The delamination of shortened APs upon knockdown of Tag-1 leads to the formation of heterotopias and a prolonged neuron production from these progenitors with apparent RG identity (Okamoto et al 2013). In an apparently different way heterotopias with Sp8+ neurons of ventral telencephalic identity (LGE) are formed perinatally in the Pax6 deficient *Sey* neocortex (Kroll & O'Leary 2005). These heterotopias which can lead also to the formation of gyrus- and sulcus-like structures in the postnatal neocortex, are rather supplied by the fate change of progenitors from cortical to ventral forebrain identity leading to paraventricular streams of GABA+ (OB-) interneurons from the cortical VZ which are joined by interneurons from the LGE. It can be concluded that the Pax6 deficient neocortex (*Sey*) exhibits along with its

“ventralization” in progenitor identity many aspects of progenitor behavior and morphogenic dynamics that resemble the situation in the developing LGE. However, as the process of fate change from cortical to ventral progenitor cells in the Sey mouse is gradual and slower during the early stages (Kroll & O'Leary 2005), the overall architecture of the neocortex in these mice is preserved and does not lead to the formation of a second ganglionic eminence –like structure in the pallium.

During evolution of mammalian brains it appears as a common trait, that the expansion of cortical surface coincides and is enabled by an increase in progenitor heterogeneity, both in molecular as well as in morphological means (Hansen et al 2010, Fietz & Huttner 2011, Betizeau et al 2013, Borrell & Gotz 2014). However, many for example cellular features, like bRG are already present in species with a lissencephalic brain (Wang et al 2011, Shitamukai et al 2011, Kelava et al 2012, Borrell & Reillo 2012, Borrell & Gotz 2014). The observed progenitor heterogeneity is paralleled by higher proliferative potential and could be supported by interaction with a more complex ECM in enlarged progenitor zones like the OSVZ (Betizeau et al 2013, Fietz et al 2012). In a way the development of the murine LGE resembles many aspects of expanded progenitor zones in gyrified brains (Pilz et al 2013). The morphological heterogeneity in the LGE is broader than in the murine cortex at these stages, with SAPs bearing processes towards both basal and apical directions, including bpRGs which have also been described in ferret, sheep and primate CTX (Pilz et al 2013,Betizeau et al 2013). Another parallel is the higher proliferative potential of intermediate progenitor cells or as they are also termed transit amplifying progenitors (TAPs; Hansen et al 2010) which are more frequently present in the human OSVZ and also contribute to larger cellular lineages in the LGE. Strikingly the cell cycle length is significantly accelerated in developmental time windows when progenitor numbers are amplified preceding the generation of a large number of neurons : both during midneurogenesis in the LGE (E14) and in the primate during supragranular neuron layer production (E78; Pilz et al 2013, Betizeau et al 2013). A forced shortening in cell cycle length is sufficient to expand cortical thickness in the mouse and to induce additional folds in the ferret (Nonaka-Kinoshita et al 2013). In conclusion the developing LGE suits as a

murine model brain region for brain expansion to study aspects of progenitor signature and behavior.

4 References

Aaku-Saraste E, Hellwig A, Huttner WB. 1996. Loss of occludin and functional tight junctions, but not ZO-1, during neural tube closure--remodeling of the neuroepithelium prior to neurogenesis. *Developmental biology* 180: 664-79

Aaku-Saraste E, Oback B, Hellwig A, Huttner WB. 1997. Neuroepithelial cells downregulate their plasma membrane polarity prior to neural tube closure and neurogenesis. *Mechanisms of development* 69: 71-81

Agoston DV, Szemes M, Dobi A, Palkovits M, Georgopoulos K, et al. 2007. Ikaros is expressed in developing striatal neurons and involved in enkephalinergic differentiation. *Journal of neurochemistry* 102: 1805-16

Alexandre P, Reugels AM, Barker D, Blanc E, Clarke JD. 2010. Neurons derive from the more apical daughter in asymmetric divisions in the zebrafish neural tube. *Nature neuroscience* 13: 673-9

Allen ZJ, 2nd, Waclaw RR, Colbert MC, Campbell K. 2007. Molecular identity of olfactory bulb interneurons: transcriptional codes of periglomerular neuron subtypes. *Journal of molecular histology* 38: 517-25

Anderson S, Mione M, Yun K, Rubenstein JL. 1999. Differential origins of neocortical projection and local circuit neurons: role of Dlx genes in neocortical interneuronogenesis. *Cereb Cortex* 9: 646-54

Anderson SA, Eisenstat DD, Shi L, Rubenstein JL. 1997a. Interneuron migration from basal forebrain to neocortex: dependence on Dlx genes. *Science* 278: 474-6

Anderson SA, Qiu M, Bulfone A, Eisenstat DD, Meneses J, et al. 1997b. Mutations of the homeobox genes Dlx-1 and Dlx-2 disrupt the striatal subventricular zone and differentiation of late born striatal neurons. *Neuron* 19: 27-37

Anthony TE, Klein C, Fishell G, Heintz N. 2004. Radial glia serve as neuronal progenitors in all regions of the central nervous system. *Neuron* 41: 881-90

Aoto K, Nishimura T, Eto K, Motoyama J. 2002. Mouse GLI3 regulates Fgf8 expression and apoptosis in the developing neural tube, face, and limb bud. *Developmental biology* 251: 320-32

Asami M, Pilz GA, Ninkovic J, Godinho L, Schroeder T, et al. 2011. The role of Pax6 in regulating the orientation and mode of cell division of progenitors in the mouse cerebral cortex. *Development* 138: 5067-78

Attardo A, Calegari F, Haubensak W, Wilsch-Brauninger M, Huttner WB. 2008. Live imaging at the onset of cortical neurogenesis reveals differential appearance of the neuronal phenotype in apical versus basal progenitor progeny. *PloS one* 3: e2388

Azevedo FA, Carvalho LR, Grinberg LT, Farfel JM, Ferretti RE, et al. 2009. Equal numbers of neuronal and nonneuronal cells make the human brain an isometrically scaled-up primate brain. *The Journal of comparative neurology* 513: 532-41

Bai J, Ramos RL, Paramasivam M, Siddiqi F, Ackman JB, LoTurco JJ. 2008. The role of DCX and LIS1 in migration through the lateral cortical stream of developing forebrain. *Developmental neuroscience* 30: 144-56

Beck PD, Pospichal MW, Kaas JH. 1996. Topography, architecture, and connections of somatosensory cortex in opossums: evidence for five somatosensory areas. *The Journal of comparative neurology* 366: 109-33

Berninger B, Costa MR, Koch U, Schroeder T, Sutor B, et al. 2007. Functional properties of neurons derived from in vitro reprogrammed postnatal astroglia. *The Journal of neuroscience : the official journal of the Society for Neuroscience* 27: 8654-64

Betizeau M, Cortay V, Patti D, Pfister S, Gautier E, et al. 2013. Precursor diversity and complexity of lineage relationships in the outer subventricular zone of the primate. *Neuron* 80: 442-57

Bhide PG. 1996. Cell cycle kinetics in the embryonic mouse corpus striatum. *The Journal of comparative neurology* 374: 506-22

Borrell V, Cardenas A, Ciceri G, Galceran J, Flames N, et al. 2012. Slit/Robo signaling modulates the proliferation of central nervous system progenitors. *Neuron* 76: 338-52

Borrell V, Gotz M. 2014. Role of radial glial cells in cerebral cortex folding. *Current opinion in neurobiology* 27C: 39-46

Borrell V, Reillo I. 2012. Emerging roles of neural stem cells in cerebral cortex development and evolution. *Developmental neurobiology* 72: 955-71

Bultje RS, Castaneda-Castellanos DR, Jan LY, Jan YN, Kriegstein AR, Shi SH. 2009. Mammalian Par3 regulates progenitor cell asymmetric division via notch signaling in the developing neocortex. *Neuron* 63: 189-202

Butt SJ, Fuccillo M, Nery S, Noctor S, Kriegstein A, et al. 2005. The temporal and spatial origins of cortical interneurons predict their physiological subtype. *Neuron* 48: 591-604

Butt SJ, Sousa VH, Fuccillo MV, Hjerling-Leffler J, Miyoshi G, et al. 2008. The requirement of Nkx2-1 in the temporal specification of cortical interneuron subtypes. *Neuron* 59: 722-32

Calegari F, Huttner WB. 2003. An inhibition of cyclin-dependent kinases that lengthens, but does not arrest, neuroepithelial cell cycle induces premature neurogenesis. *Journal of cell science* 116: 4947-55

Campbell K, Gotz M. 2002. Radial glia: multi-purpose cells for vertebrate brain development. *Trends in neurosciences* 25: 235-8

Carney RS, Alfonso TB, Cohen D, Dai H, Nery S, et al. 2006. Cell migration along the lateral cortical stream to the developing basal telencephalic limbic system. *The Journal of neuroscience : the official journal of the Society for Neuroscience* 26: 11562-74

Casarosa S, Fode C, Guillemot F. 1999. Mash1 regulates neurogenesis in the ventral telencephalon. *Development* 126: 525-34

Castro DS, Martynoga B, Parras C, Ramesh V, Pacary E, et al. 2011. A novel function of the proneural factor Ascl1 in progenitor proliferation identified by genome-wide characterization of its targets. *Genes & development* 25: 930-45

Caviness VS, Jr., Takahashi T. 1995. Proliferative events in the cerebral ventricular zone. *Brain & development* 17: 159-63

Chapman H, Waclaw RR, Pei Z, Nakafuku M, Campbell K. 2013. The homeobox gene Gsx2 controls the timing of oligodendroglial fate specification in mouse lateral ganglionic eminence progenitors. *Development* 140: 2289-98

Chatzi C, Brade T, Duester G. 2011. Retinoic acid functions as a key GABAergic differentiation signal in the basal ganglia. *PLoS biology* 9: e1000609

Chenn A, McConnell SK. 1995. Cleavage orientation and the asymmetric inheritance of Notch1 immunoreactivity in mammalian neurogenesis. *Cell* 82: 631-41

Chenn A, Walsh CA. 2002. Regulation of cerebral cortical size by control of cell cycle exit in neural precursors. *Science* 297: 365-9

Chiang C, Litingtung Y, Lee E, Young KE, Corden JL, et al. 1996. Cyclopia and defective axial patterning in mice lacking Sonic hedgehog gene function. *Nature* 383: 407-13

Corbin JG, Gaiano N, Machold RP, Langston A, Fishell G. 2000. The Gsh2 homeodomain gene controls multiple aspects of telencephalic development. *Development* 127: 5007-20

Corbin JG, Rutlin M, Gaiano N, Fishell G. 2003. Combinatorial function of the homeodomain proteins Nkx2.1 and Gsh2 in ventral telencephalic patterning. *Development* 130: 4895-906

Costa MR, Wen G, Lepier A, Schroeder T, Gotz M. 2008. Par-complex proteins promote proliferative progenitor divisions in the developing mouse cerebral cortex. *Development* 135: 11-22

Cunningham CL, Martinez-Cerdeno V, Noctor SC. 2013. Diversity of neural precursor cell types in the prenatal macaque cerebral cortex exists largely within the astroglial cell lineage. *PloS one* 8: e63848

deAzevedo LC, Fallet C, Moura-Neto V, Daumas-Duport C, Hedin-Pereira C, Lent R. 2003. Cortical radial glial cells in human fetuses: depth-correlated transformation into astrocytes. *Journal of neurobiology* 55: 288-98

Dehay C, Giroud P, Berland M, Smart I, Kennedy H. 1993. Modulation of the cell cycle contributes to the parcellation of the primate visual cortex. *Nature* 366: 464-6

Del Bene F, Wehman AM, Link BA, Baier H. 2008. Regulation of neurogenesis by interkinetic nuclear migration through an apical-basal notch gradient. *Cell* 134: 1055-65

Dou CL, Li S, Lai E. 1999. Dual role of brain factor-1 in regulating growth and patterning of the cerebral hemispheres. *Cereb Cortex* 9: 543-50

Ekholm SV, Reed SI. 2000. Regulation of G(1) cyclin-dependent kinases in the mammalian cell cycle. *Current opinion in cell biology* 12: 676-84

Elston GN, Benavides-Piccione R, Elston A, Zietsch B, Defelipe J, et al. 2006. Specializations of the granular prefrontal cortex of primates: implications for cognitive processing. *The anatomical record. Part A, Discoveries in molecular, cellular, and evolutionary biology* 288: 26-35

Englund C, Fink A, Lau C, Pham D, Daza RA, et al. 2005. Pax6, Tbr2, and Tbr1 are expressed sequentially by radial glia, intermediate progenitor cells, and postmitotic neurons in developing neocortex. *The Journal of neuroscience : the official journal of the Society for Neuroscience* 25: 247-51

Farah MH, Olson JM, Sucic HB, Hume RI, Tapscott SJ, Turner DL. 2000. Generation of neurons by transient expression of neural bHLH proteins in mammalian cells. *Development* 127: 693-702

Farkas LM, Haffner C, Giger T, Khaitovich P, Nowick K, et al. 2008. Insulinoma-associated 1 has a panneurogenic role and promotes the generation and expansion of basal progenitors in the developing mouse neocortex. *Neuron* 60: 40-55

Feng L, Hatten ME, Heintz N. 1994. Brain lipid-binding protein (BLBP): a novel signaling system in the developing mammalian CNS. *Neuron* 12: 895-908

Fietz SA, Huttner WB. 2011. Cortical progenitor expansion, self-renewal and neurogenesis-a polarized perspective. *Current opinion in neurobiology* 21: 23-35

Fietz SA, Kelava I, Vogt J, Wilsch-Brauninger M, Stenzel D, et al. 2010. OSVZ progenitors of human and ferret neocortex are epithelial-like and expand by integrin signaling. *Nature neuroscience* 13: 690-9

Fietz SA, Lachmann R, Brandl H, Kircher M, Samusik N, et al. 2012. Transcriptomes of germinal zones of human and mouse fetal neocortex suggest a role of extracellular matrix in progenitor self-renewal. *Proceedings of the National Academy of Sciences of the United States of America* 109: 11836-41

Fish JL, Kosodo Y, Enard W, Paabo S, Huttner WB. 2006. Aspm specifically maintains symmetric proliferative divisions of neuroepithelial cells. *Proceedings of the National Academy of Sciences of the United States of America* 103: 10438-43

Fishell G, van der Kooy D. 1987. Pattern formation in the striatum: developmental changes in the distribution of striatonigral neurons. *The Journal of neuroscience : the official journal of the Society for Neuroscience* 7: 1969-78

Flames N, Pla R, Gelman DM, Rubenstein JL, Puelles L, Marin O. 2007. Delineation of multiple subpallial progenitor domains by the combinatorial expression of transcriptional codes. *The Journal of neuroscience : the official journal of the Society for Neuroscience* 27: 9682-95

Flandin P, Kimura S, Rubenstein JL. 2010. The progenitor zone of the ventral medial ganglionic eminence requires Nkx2-1 to generate most of the globus pallidus but few neocortical interneurons. *The Journal of neuroscience : the official journal of the Society for Neuroscience* 30: 2812-23

Franco SJ, Gil-Sanz C, Martinez-Garay I, Espinosa A, Harkins-Perry SR, et al. 2012. Fate-restricted neural progenitors in the mammalian cerebral cortex. *Science* 337: 746-9

Fuccillo M, Rallu M, McMahon AP, Fishell G. 2004. Temporal requirement for hedgehog signaling in ventral telencephalic patterning. *Development* 131: 5031-40

Furusho M, Ono K, Takebayashi H, Masahira N, Kagawa T, et al. 2006. Involvement of the Olig2 transcription factor in cholinergic neuron development of the basal forebrain. *Developmental biology* 293: 348-57

Gaiano N, Fishell G. 2002. The role of notch in promoting glial and neural stem cell fates. *Annual review of neuroscience* 25: 471-90

Gal JS, Morozov YM, Ayoub AE, Chatterjee M, Rakic P, Haydar TF. 2006. Molecular and morphological heterogeneity of neural precursors in the mouse neocortical proliferative zones. *The Journal of neuroscience : the official journal of the Society for Neuroscience* 26: 1045-56

Garcia-Moreno F, Vasistha NA, Trevia N, Bourne JA, Molnar Z. 2012. Compartmentalization of cerebral cortical germinal zones in a lissencephalic primate and gyrencephalic rodent. *Cereb Cortex* 22: 482-92

Gerfen CR. 1992. The neostriatal mosaic: multiple levels of compartmental organization in the basal ganglia. *Annual review of neuroscience* 15: 285-320

Glickstein SB, Alexander S, Ross ME. 2007. Differences in cyclin D2 and D1 protein expression distinguish forebrain progenitor subsets. *Cereb Cortex* 17: 632-42

Gotz M, Huttner WB. 2005. The cell biology of neurogenesis. *Nature reviews. Molecular cell biology* 6: 777-88

Gotz M, Stoykova A, Gruss P. 1998. Pax6 controls radial glia differentiation in the cerebral cortex. *Neuron* 21: 1031-44

Guardavaccaro D, Corrente G, Covone F, Micheli L, D'Agnano I, et al. 2000. Arrest of G(1)-S progression by the p53-inducible gene PC3 is Rb dependent and relies on the inhibition of cyclin D1 transcription. *Molecular and cellular biology* 20: 1797-815

Guillemot F. 2005. Cellular and molecular control of neurogenesis in the mammalian telencephalon. *Current opinion in cell biology* 17: 639-47

Guo C, Eckler MJ, McKenna WL, McKinsey GL, Rubenstein JL, Chen B. 2013. Fezf2 expression identifies a multipotent progenitor for neocortical projection neurons, astrocytes, and oligodendrocytes. *Neuron* 80: 1167-74

Gutin G, Fernandes M, Palazzolo L, Paek H, Yu K, et al. 2006. FGF signalling generates ventral telencephalic cells independently of SHH. *Development* 133: 2937-46

Hallonet M, Hollemann T, Wehr R, Jenkins NA, Copeland NG, et al. 1998. Vax1 is a novel homeobox-containing gene expressed in the developing anterior ventral forebrain. *Development* 125: 2599-610

Han YG, Alvarez-Buylla A. 2010. Role of primary cilia in brain development and cancer. *Current opinion in neurobiology* 20: 58-67

Hanashima C, Shen L, Li SC, Lai E. 2002. Brain factor-1 controls the proliferation and differentiation of neocortical progenitor cells through independent mechanisms. *The Journal of neuroscience : the official journal of the Society for Neuroscience* 22: 6526-36

Hansen DV, Lui JH, Flandin P, Yoshikawa K, Rubenstein JL, et al. 2013. Non-epithelial stem cells and cortical interneuron production in the human ganglionic eminences. *Nature neuroscience* 16: 1576-87

Hansen DV, Lui JH, Parker PR, Kriegstein AR. 2010. Neurogenic radial glia in the outer subventricular zone of human neocortex. *Nature* 464: 554-61

Hartfuss E, Forster E, Bock HH, Hack MA, Leprince P, et al. 2003. Reelin signaling directly affects radial glia morphology and biochemical maturation. *Development* 130: 4597-609

Hartfuss E, Galli R, Heins N, Gotz M. 2001. Characterization of CNS precursor subtypes and radial glia. *Developmental biology* 229: 15-30

Haskell GT, LaMantia AS. 2005. Retinoic acid signaling identifies a distinct precursor population in the developing and adult forebrain. *The Journal of neuroscience : the official journal of the Society for Neuroscience* 25: 7636-47

Haubensak W, Attardo A, Denk W, Huttner WB. 2004. Neurons arise in the basal neuroepithelium of the early mammalian telencephalon: a major site of neurogenesis. *Proceedings of the National Academy of Sciences of the United States of America* 101: 3196-201

Haubst N, Georges-Labouesse E, De Arcangelis A, Mayer U, Gotz M. 2006. Basement membrane attachment is dispensable for radial glial cell fate and for proliferation, but affects positioning of neuronal subtypes. *Development* 133: 3245-54

Hebert JM, Fishell G. 2008. The genetics of early telencephalon patterning: some assembly required. *Nature reviews. Neuroscience* 9: 678-85

Hebert JM, McConnell SK. 2000. Targeting of cre to the Foxg1 (BF-1) locus mediates loxP recombination in the telencephalon and other developing head structures. *Developmental biology* 222: 296-306

Heinrich C, Blum R, Gascon S, Masserdotti G, Tripathi P, et al. 2010. Directing astroglia from the cerebral cortex into subtype specific functional neurons. *PLoS biology* 8: e1000373

Herculano-Houzel S, Collins CE, Wong P, Kaas JH. 2007. Cellular scaling rules for primate brains. *Proceedings of the National Academy of Sciences of the United States of America* 104: 3562-7

Herculano-Houzel S, Mota B, Lent R. 2006. Cellular scaling rules for rodent brains. *Proceedings of the National Academy of Sciences of the United States of America* 103: 12138-43

Hevner RF, Haydar TF. 2012. The (not necessarily) convoluted role of basal radial glia in cortical neurogenesis. *Cereb Cortex* 22: 465-8

Hill J, Inder T, Neil J, Dierker D, Harwell J, Van Essen D. 2010. Similar patterns of cortical expansion during human development and evolution. *Proceedings of the National Academy of Sciences of the United States of America* 107: 13135-40

Hill RE, Favor J, Hogan BL, Ton CC, Saunders GF, et al. 1991. Mouse small eye results from mutations in a paired-like homeobox-containing gene. *Nature* 354: 522-5

Hirabayashi Y, Itoh Y, Tabata H, Nakajima K, Akiyama T, et al. 2004. The Wnt/beta-catenin pathway directs neuronal differentiation of cortical neural precursor cells. *Development* 131: 2791-801

Hirata J, Nakagoshi H, Nabeshima Y, Matsuzaki F. 1995. Asymmetric segregation of the homeodomain protein Prospero during Drosophila development. *Nature* 377: 627-30

Hirata T, Nomura T, Takagi Y, Sato Y, Tomioka N, et al. 2002. Mosaic development of the olfactory cortex with Pax6-dependent and -independent components. *Brain research. Developmental brain research* 136: 17-26

Hirsch E, Gullberg D, Balzac F, Altruda F, Silengo L, Tarone G. 1994. Alpha v integrin subunit is predominantly located in nervous tissue and skeletal muscle during mouse development. *Developmental dynamics : an official publication of the American Association of Anatomists* 201: 108-20

Howard B, Chen Y, Zecevic N. 2006. Cortical progenitor cells in the developing human telencephalon. *Glia* 53: 57-66

Huang X, Liu J, Ketova T, Fleming JT, Grover VK, et al. 2010. Transventricular delivery of Sonic hedgehog is essential to cerebellar ventricular zone development. *Proceedings of the National Academy of Sciences of the United States of America* 107: 8422-7

Huttner WB, Brand M. 1997. Asymmetric division and polarity of neuroepithelial cells. *Current opinion in neurobiology* 7: 29-39

Huttner WB, Kosodo Y. 2005. Symmetric versus asymmetric cell division during neurogenesis in the developing vertebrate central nervous system. *Current opinion in cell biology* 17: 648-57

Ishikawa H, Marshall WF. 2011. Ciliogenesis: building the cell's antenna. *Nature reviews. Molecular cell biology* 12: 222-34

Jakovcevski I, Mayer N, Zecevic N. 2011. Multiple origins of human neocortical interneurons are supported by distinct expression of transcription factors. *Cereb Cortex* 21: 1771-82

Javaherian A, Kriegstein A. 2009. A stem cell niche for intermediate progenitor cells of the embryonic cortex. *Cereb Cortex* 19 Suppl 1: i70-7

Kaas JH. 2013. The Evolution of Brains from Early Mammals to Humans. *Wiley interdisciplinary reviews. Cognitive science* 4: 33-45

Kang W, Wong LC, Shi SH, Hebert JM. 2009. The transition from radial glial to intermediate progenitor cell is inhibited by FGF signaling during corticogenesis. *The Journal of neuroscience : the official journal of the Society for Neuroscience* 29: 14571-80

Kaoru T, Liu FC, Ishida M, Oishi T, Hayashi M, et al. 2010. Molecular characterization of the intercalated cell masses of the amygdala: implications for the relationship with the striatum. *Neuroscience* 166: 220-30

Karow M, Sanchez R, Schichor C, Masserdotti G, Ortega F, et al. 2012. Reprogramming of pericyte-derived cells of the adult human brain into induced neuronal cells. *Cell stem cell* 11: 471-6

Karten HJ. 1997. Evolutionary developmental biology meets the brain: the origins of mammalian cortex. *Proceedings of the National Academy of Sciences of the United States of America* 94: 2800-4

Kelava I, Lewitus E, Huttner WB. 2013. The secondary loss of gyrencephaly as an example of evolutionary phenotypical reversal. *Frontiers in neuroanatomy* 7: 16

Kelava I, Reillo I, Murayama AY, Kalinka AT, Stenzel D, et al. 2012. Abundant occurrence of basal radial glia in the subventricular zone of embryonic neocortex of a lissencephalic primate, the common marmoset Callithrix jacchus. *Cereb Cortex* 22: 469-81

Kessaris N, Fogarty M, Iannarelli P, Grist M, Wegner M, Richardson WD. 2006. Competing waves of oligodendrocytes in the forebrain and postnatal elimination of an embryonic lineage. *Nature neuroscience* 9: 173-9

Knoblich JA, Jan LY, Jan YN. 1995. Asymmetric segregation of Numb and Prospero during cell division. *Nature* 377: 624-7

Kohtz JD, Baker DP, Corte G, Fishell G. 1998. Regionalization within the mammalian telencephalon is mediated by changes in responsiveness to Sonic Hedgehog. *Development* 125: 5079-89

Konno D, Shioi G, Shitamukai A, Mori A, Kiyonari H, et al. 2008. Neuroepithelial progenitors undergo LGN-dependent planar divisions to maintain self-renewability during mammalian neurogenesis. *Nature cell biology* 10: 93-101

Kosodo Y, Roper K, Haubensak W, Marzesco AM, Corbeil D, Huttner WB. 2004. Asymmetric distribution of the apical plasma membrane during neurogenic divisions of mammalian neuroepithelial cells. *The EMBO journal* 23: 2314-24

Kowalczyk T, Pontious A, Englund C, Daza RA, Bedogni F, et al. 2009. Intermediate neuronal progenitors (basal progenitors) produce pyramidal-projection neurons for all layers of cerebral cortex. *Cereb Cortex* 19: 2439-50

Kriegstein A, Alvarez-Buylla A. 2009. The glial nature of embryonic and adult neural stem cells. *Annual review of neuroscience* 32: 149-84

Kriegstein A, Noctor S, Martinez-Cerdeno V. 2006. Patterns of neural stem and progenitor cell division may underlie evolutionary cortical expansion. *Nature reviews. Neuroscience* 7: 883-90

Kroll TT, O'Leary DD. 2005. Ventralized dorsal telencephalic progenitors in Pax6 mutant mice generate GABA interneurons of a lateral ganglionic eminence fate. *Proceedings of the National Academy of Sciences of the United States of America* 102: 7374-9

Kuida K, Haydar TF, Kuan CY, Gu Y, Taya C, et al. 1998. Reduced apoptosis and cytochrome c-mediated caspase activation in mice lacking caspase 9. *Cell* 94: 325-37

Kuida K, Zheng TS, Na S, Kuan C, Yang D, et al. 1996. Decreased apoptosis in the brain and premature lethality in CPP32-deficient mice. *Nature* 384: 368-72

Lakoma J, Garcia-Alonso L, Luque JM. 2011. Reelin sets the pace of neocortical neurogenesis. *Development* 138: 5223-34

LaMonica BE, Lui JH, Hansen DV, Kriegstein AR. 2013. Mitotic spindle orientation predicts outer radial glial cell generation in human neocortex. *Nature communications* 4: 1665

Lange C, Huttner WB, Calegari F. 2009. Cdk4/cyclinD1 overexpression in neural stem cells shortens G1, delays neurogenesis, and promotes the generation and expansion of basal progenitors. *Cell stem cell* 5: 320-31

Langman J, Guerrant RL, Freeman BG. 1966. Behavior of neuro-epithelial cells during closure of the neural tube. *The Journal of comparative neurology* 127: 399-411

Lehtinen MK, Walsh CA. 2011. Neurogenesis at the brain-cerebrospinal fluid interface. *Annual review of cell and developmental biology* 27: 653-79

Lehtinen MK, Zappaterra MW, Chen X, Yang YJ, Hill AD, et al. 2011. The cerebrospinal fluid provides a proliferative niche for neural progenitor cells. *Neuron* 69: 893-905

Letinic K, Zoncu R, Rakic P. 2002. Origin of GABAergic neurons in the human neocortex. *Nature* 417: 645-9

Levison SW, Goldman JE. 1993. Both oligodendrocytes and astrocytes develop from progenitors in the subventricular zone of postnatal rat forebrain. *Neuron* 10: 201-12

Levitt P, Rakic P. 1980. Immunoperoxidase localization of glial fibrillary acidic protein in radial glial cells and astrocytes of the developing rhesus monkey brain. *The Journal of comparative neurology* 193: 815-40

Li H, Wagner E, McCaffery P, Smith D, Andreadis A, Drager UC. 2000. A retinoic acid synthesizing enzyme in ventral retina and telencephalon of the embryonic mouse. *Mechanisms of development* 95: 283-9

Liao WL, Tsai HC, Wang HF, Chang J, Lu KM, et al. 2008. Modular patterning of structure and function of the striatum by retinoid receptor signaling. *Proceedings of the National Academy of Sciences of the United States of America* 105: 6765-70

Lobo MK, Yeh C, Yang XW. 2008. Pivotal role of early B-cell factor 1 in development of striatonigral medium spiny neurons in the matrix compartment. *Journal of neuroscience research* 86: 2134-46

Long JE, Garel S, Alvarez-Dolado M, Yoshikawa K, Osumi N, et al. 2007. Dlx-dependent and -independent regulation of olfactory bulb interneuron differentiation. *The Journal of neuroscience : the official journal of the Society for Neuroscience* 27: 3230-43

Long JE, Swan C, Liang WS, Cobos I, Potter GB, Rubenstein JL. 2009. Dlx1&2 and Mash1 transcription factors control striatal patterning and differentiation through parallel and overlapping pathways. *The Journal of comparative neurology* 512: 556-72

Lu QR, Yuk D, Alberta JA, Zhu Z, Pawlitzky I, et al. 2000. Sonic hedgehog--regulated oligodendrocyte lineage genes encoding bHLH proteins in the mammalian central nervous system. *Neuron* 25: 317-29

Lui JH, Hansen DV, Kriegstein AR. 2011. Development and evolution of the human neocortex. *Cell* 146: 18-36

Lukaszewicz A, Savatier P, Cortay V, Giroud P, Huissoud C, et al. 2005. G1 phase regulation, area-specific cell cycle control, and cytoarchitectonics in the primate cortex. *Neuron* 47: 353-64

Ma T, Wang C, Wang L, Zhou X, Tian M, et al. 2013. Subcortical origins of human and monkey neocortical interneurons. *Nature neuroscience* 16: 1588-97

Mackenzie F, Ruhrberg C. 2012. Diverse roles for VEGF-A in the nervous system. *Development* 139: 1371-80

Malatesta P, Hack MA, Hartfuss E, Kettenmann H, Klinkert W, et al. 2003. Neuronal or glial progeny: regional differences in radial glia fate. *Neuron* 37: 751-64

Malatesta P, Hartfuss E, Gotz M. 2000. Isolation of radial glial cells by fluorescent-activated cell sorting reveals a neuronal lineage. *Development* 127: 5253-63

Mangale VS, Hirokawa KE, Satyaki PR, Gokulchandran N, Chikbire S, et al. 2008. Lhx2 selector activity specifies cortical identity and suppresses hippocampal organizer fate. *Science* 319: 304-9

Manuel MN, Martynoga B, Molinek MD, Quinn JC, Kroemmer C, et al. 2011. The transcription factor Foxg1 regulates telencephalic progenitor proliferation cell autonomously, in part by controlling Pax6 expression levels. *Neural development* 6: 9

Marin O, Anderson SA, Rubenstein JL. 2000. Origin and molecular specification of striatal interneurons. *The Journal of neuroscience : the official journal of the Society for Neuroscience* 20: 6063-76

Marin O, Muller U. 2014. Lineage origins of GABAergic versus glutamatergic neurons in the neocortex. *Current opinion in neurobiology* 26C: 132-41

Martin-Ibanez R, Crespo E, Urban N, Sergent-Tanguy S, Herranz C, et al. 2010. Ikaros-1 couples cell cycle arrest of late striatal precursors with neurogenesis of enkephalinergic neurons. *The Journal of comparative neurology* 518: 329-51

Martin AH. 1967. Significance of mitotic spindle fibre orientation in the neural tube. *Nature* 216: 1133-4

Martinez-Cerdeno V, Noctor SC, Kriegstein AR. 2006. The role of intermediate progenitor cells in the evolutionary expansion of the cerebral cortex. *Cereb Cortex* 16 Suppl 1: i152-61

Martynoga B, Morrison H, Price DJ, Mason JO. 2005. Foxg1 is required for specification of ventral telencephalon and region-specific regulation of dorsal telencephalic precursor proliferation and apoptosis. *Developmental biology* 283: 113-27

Mason HA, Rakowiecki SM, Raftopoulou M, Nery S, Huang Y, et al. 2005. Notch signaling coordinates the patterning of striatal compartments. *Development* 132: 4247-58

Medina L, Abellan A. 2012. In *The mouse nervous system*, ed. C Watson

Metin C, Alvarez C, Moudoux D, Vitalis T, Pieau C, Molnar Z. 2007. Conserved pattern of tangential neuronal migration during forebrain development. *Development* 134: 2815-27

Miller EK, Cohen JD. 2001. An integrative theory of prefrontal cortex function. *Annual review of neuroscience* 24: 167-202

Miyata T, Kawaguchi A, Okano H, Ogawa M. 2001. Asymmetric inheritance of radial glial fibers by cortical neurons. *Neuron* 31: 727-41

Miyata T, Kawaguchi A, Saito K, Kawano M, Muto T, Ogawa M. 2004. Asymmetric production of surface-dividing and non-surface-dividing cortical progenitor cells. *Development* 131: 3133-45

Miyoshi G, Butt SJ, Takebayashi H, Fishell G. 2007. Physiologically distinct temporal cohorts of cortical interneurons arise from telencephalic Olig2-expressing precursors. *The Journal of neuroscience : the official journal of the Society for Neuroscience* 27: 7786-98

Miyoshi G, Hjerling-Leffler J, Karayannis T, Sousa VH, Butt SJ, et al. 2010. Genetic fate mapping reveals that the caudal ganglionic eminence produces a large and diverse population of superficial cortical interneurons. *The Journal of neuroscience : the official journal of the Society for Neuroscience* 30: 1582-94

Mizutani K, Yoon K, Dang L, Tokunaga A, Gaiano N. 2007. Differential Notch signalling distinguishes neural stem cells from intermediate progenitors. *Nature* 449: 351-5

Molnar Z. 2011. Evolution of cerebral cortical development. *Brain, behavior and evolution* 78: 94-107

Molnar Z, Metin C, Stoykova A, Tarabykin V, Price DJ, et al. 2006. Comparative aspects of cerebral cortical development. *The European journal of neuroscience* 23: 921-34

Molyneaux BJ, Arlotta P, Menezes JR, Macklis JD. 2007. Neuronal subtype specification in the cerebral cortex. *Nature reviews. Neuroscience* 8: 427-37

Monuki ES, Porter FD, Walsh CA. 2001. Patterning of the dorsal telencephalon and cerebral cortex by a roof plate-Lhx2 pathway. *Neuron* 32: 591-604

Moreno N, Gonzalez A, Retaux S. 2009. Development and evolution of the subpallium. *Seminars in cell & developmental biology* 20: 735-43

Mutch CA, Schulte JD, Olson E, Chenn A. 2010. Beta-catenin signaling negatively regulates intermediate progenitor population numbers in the developing cortex. *PloS one* 5: e12376

Muzio L, Di Benedetto B, Stoykova A, Boncinelli E, Gruss P, Mallamaci A. 2002. Conversion of cerebral cortex into basal ganglia in Emx2(-/-) Pax6(Sey/Sey) double-mutant mice. *Nature neuroscience* 5: 737-45

Nelson BR, Hodge RD, Bedogni F, Hevner RF. 2013. Dynamic interactions between intermediate neurogenic progenitors and radial glia in embryonic mouse neocortex: potential role in Dll1-Notch signaling. *The Journal of neuroscience : the official journal of the Society for Neuroscience* 33: 9122-39

Nery S, Wichterle H, Fishell G. 2001. Sonic hedgehog contributes to oligodendrocyte specification in the mammalian forebrain. *Development* 128: 527-40

Nigg EA, Raff JW. 2009. Centrioles, centrosomes, and cilia in health and disease. *Cell* 139: 663-78

Nobrega-Pereira S, Gelman D, Bartolini G, Pla R, Pierani A, Marin O. 2010. Origin and molecular specification of globus pallidus neurons. *The Journal of neuroscience : the official journal of the Society for Neuroscience* 30: 2824-34

Noctor SC, Flint AC, Weissman TA, Dammerman RS, Kriegstein AR. 2001. Neurons derived from radial glial cells establish radial units in neocortex. *Nature* 409: 714-20

Noctor SC, Flint AC, Weissman TA, Wong WS, Clinton BK, Kriegstein AR. 2002. Dividing precursor cells of the embryonic cortical ventricular zone have morphological and molecular characteristics of radial glia. *The Journal of neuroscience : the official journal of the Society for Neuroscience* 22: 3161-73

Noctor SC, Martinez-Cerdeno V, Ivic L, Kriegstein AR. 2004. Cortical neurons arise in symmetric and asymmetric division zones and migrate through specific phases. *Nature neuroscience* 7: 136-44

Noctor SC, Martinez-Cerdeno V, Kriegstein AR. 2008. Distinct behaviors of neural stem and progenitor cells underlie cortical neurogenesis. *The Journal of comparative neurology* 508: 28-44

Nonaka-Kinoshita M, Reillo I, Artegiani B, Martinez-Martinez MA, Nelson M, et al. 2013. Regulation of cerebral cortex size and folding by expansion of basal progenitors. *The EMBO journal* 32: 1817-28

O'Rahilly R, Muller F. 1994. Neurulation in the normal human embryo. *Ciba Foundation symposium* 181: 70-82; discussion 82-9

Okamoto M, Namba T, Shinoda T, Kondo T, Watanabe T, et al. 2013. TAG-1-assisted progenitor elongation streamlines nuclear migration to optimize subapical crowding. *Nature neuroscience* 16: 1556-66

Ono K, Takebayashi H, Ikeda K, Furusho M, Nishizawa T, et al. 2008. Regional- and temporal-dependent changes in the differentiation of Olig2 progenitors in the forebrain, and the impact on astrocyte development in the dorsal pallium. *Developmental biology* 320: 456-68

Parras CM, Hunt C, Sugimori M, Nakafuku M, Rowitch D, Guillemot F. 2007. The proneural gene Mash1 specifies an early population of telencephalic oligodendrocytes. *The Journal of neuroscience : the official journal of the Society for Neuroscience* 27: 4233-42

Passante L, Gaspard N, Degraeve M, Frisen J, Kullander K, et al. 2008. Temporal regulation of ephrin/Eph signalling is required for the spatial patterning of the mammalian striatum. *Development* 135: 3281-90

Petryniak MA, Potter GB, Rowitch DH, Rubenstein JL. 2007. Dlx1 and Dlx2 control neuronal versus oligodendroglial cell fate acquisition in the developing forebrain. *Neuron* 55: 417-33

Peyre E, Jaouen F, Saadaoui M, Haren L, Merdes A, et al. 2011. A lateral belt of cortical LGN and NuMA guides mitotic spindle movements and planar division in neuroepithelial cells. *The Journal of cell biology* 193: 141-54

Peyre E, Morin X. 2012. An oblique view on the role of spindle orientation in vertebrate neurogenesis. *Development, growth & differentiation* 54: 287-305

Pierfelice T, Alberi L, Gaiano N. 2011. Notch in the vertebrate nervous system: an old dog with new tricks. *Neuron* 69: 840-55

Pilz GA, Shitamukai A, Reillo I, Pacary E, Schwausch J, et al. 2013. Amplification of progenitors in the mammalian telencephalon includes a new radial glial cell type. *Nature communications* 4: 2125

Pinto L, Gotz M. 2007. Radial glial cell heterogeneity--the source of diverse progeny in the CNS. *Progress in neurobiology* 83: 2-23

Pinto L, Mader MT, Irmler M, Gentilini M, Santoni F, et al. 2008. Prospective isolation of functionally distinct radial glial subtypes--lineage and transcriptome analysis. *Molecular and cellular neurosciences* 38: 15-42

Poitras L, Ghanem N, Hatch G, Ekker M. 2007. The proneural determinant MASH1 regulates forebrain Dlx1/2 expression through the I12b intergenic enhancer. *Development* 134: 1755-65

Postiglione MP, Juschke C, Xie Y, Haas GA, Charalambous C, Knoblich JA. 2011. Mouse inscuteable induces apical-basal spindle orientation to facilitate intermediate progenitor generation in the developing neocortex. *Neuron* 72: 269-84

Pulvers JN, Bryk J, Fish JL, Wilsch-Brauninger M, Arai Y, et al. 2010. Mutations in mouse Aspm (abnormal spindle-like microcephaly associated) cause not only microcephaly but also major defects in the germline. *Proceedings of the National Academy of Sciences of the United States of America* 107: 16595-600

Qian X, Davis AA, Goderie SK, Temple S. 1997. FGF2 concentration regulates the generation of neurons and glia from multipotent cortical stem cells. *Neuron* 18: 81-93

Qian X, Shen Q, Goderie SK, He W, Capela A, et al. 2000. Timing of CNS cell generation: a programmed sequence of neuron and glial cell production from isolated murine cortical stem cells. *Neuron* 28: 69-80

Quinn JC, Molinek M, Martynoga BS, Zaki PA, Faedo A, et al. 2007. Pax6 controls cerebral cortical cell number by regulating exit from the cell cycle and specifies cortical cell identity by a cell autonomous mechanism. *Developmental biology* 302: 50-65

Rakic P. 1971. Guidance of neurons migrating to the fetal monkey neocortex. *Brain research* 33: 471-6

Rakic P. 1972. Mode of cell migration to the superficial layers of fetal monkey neocortex. *The Journal of comparative neurology* 145: 61-83

Rakic P. 1988. Specification of cerebral cortical areas. *Science* 241: 170-6

Rakic P. 1995. A small step for the cell, a giant leap for mankind: a hypothesis of neocortical expansion during evolution. *Trends in neurosciences* 18: 383-8

Rakic P. 2009. Evolution of the neocortex: a perspective from developmental biology. *Nature reviews. Neuroscience* 10: 724-35

Rallu M, Corbin JG, Fishell G. 2002a. Parsing the prosencephalon. *Nature reviews. Neuroscience* 3: 943-51

Rallu M, Machold R, Gaiano N, Corbin JG, McMahon AP, Fishell G. 2002b. Dorsoventral patterning is established in the telencephalon of mutants lacking both Gli3 and Hedgehog signaling. *Development* 129: 4963-74

Rash BG, Tomasi S, Lim HD, Suh CY, Vaccarino FM. 2013. Cortical gyrification induced by fibroblast growth factor 2 in the mouse brain. *The Journal of neuroscience : the official journal of the Society for Neuroscience* 33: 10802-14

Reillo I, Borrell V. 2012. Germinal zones in the developing cerebral cortex of ferret: ontogeny, cell cycle kinetics, and diversity of progenitors. *Cereb Cortex* 22: 2039-54

Reillo I, de Juan Romero C, Garcia-Cabezas MA, Borrell V. 2011. A role for intermediate radial glia in the tangential expansion of the mammalian cerebral cortex. *Cereb Cortex* 21: 1674-94

Reiner A, Medina L, Veenman CL. 1998. Structural and functional evolution of the basal ganglia in vertebrates. *Brain research. Brain research reviews* 28: 235-85

Rhinn M, Dolle P. 2012. Retinoic acid signalling during development. *Development* 139: 843-58

Richardson WD, Kessaris N, Pringle N. 2006. Oligodendrocyte wars. *Nature reviews. Neuroscience* 7: 11-8

Ringo JL, Doty RW, Demeter S, Simard PY. 1994. Time is of the essence: a conjecture that hemispheric specialization arises from interhemispheric conduction delay. *Cereb Cortex* 4: 331-43

Rockel AJ, Hiorns RW, Powell TP. 1980. The basic uniformity in structure of the neocortex. *Brain : a journal of neurology* 103: 221-44

Rouault JP, Falette N, Guehenneux F, Guillot C, Rimokh R, et al. 1996. Identification of BTG2, an antiproliferative p53-dependent component of the DNA damage cellular response pathway. *Nature genetics* 14: 482-6

Sakai Y. 1989. Neurulation in the mouse: manner and timing of neural tube closure. *The Anatomical record* 223: 194-203

Santos N, Reiter JF. 2008. Building it up and taking it down: the regulation of vertebrate ciliogenesis. *Developmental dynamics : an official publication of the American Association of Anatomists* 237: 1972-81

Scardigli R, Baumer N, Gruss P, Guillemot F, Le Roux I. 2003. Direct and concentration-dependent regulation of the proneural gene Neurogenin2 by Pax6. *Development* 130: 3269-81

Schmechel DE, Rakic P. 1979. A Golgi study of radial glial cells in developing monkey telencephalon: morphogenesis and transformation into astrocytes. *Anatomy and embryology* 156: 115-52

Schneider RA, Hu D, Rubenstein JL, Maden M, Helms JA. 2001. Local retinoid signaling coordinates forebrain and facial morphogenesis by maintaining FGF8 and SHH. *Development* 128: 2755-67

Schuurmans C, Guillemot F. 2002. Molecular mechanisms underlying cell fate specification in the developing telencephalon. *Current opinion in neurobiology* 12: 26-34

Schwamborn JC, Berezikov E, Knoblich JA. 2009. The TRIM-NHL protein TRIM32 activates microRNAs and prevents self-renewal in mouse neural progenitors. *Cell* 136: 913-25

Shen Q, Wang Y, Dimos JT, Fasano CA, Phoenix TN, et al. 2006. The timing of cortical neurogenesis is encoded within lineages of individual progenitor cells. *Nature neuroscience* 9: 743-51

Shen Q, Wang Y, Kokovay E, Lin G, Chuang SM, et al. 2008. Adult SVZ stem cells lie in a vascular niche: a quantitative analysis of niche cell-cell interactions. *Cell stem cell* 3: 289-300

Sheth AN, Bhide PG. 1997. Concurrent cellular output from two proliferative populations in the early embryonic mouse corpus striatum. *The Journal of comparative neurology* 383: 220-30

Shibata T, Yamada K, Watanabe M, Ikenaka K, Wada K, et al. 1997. Glutamate transporter GLAST is expressed in the radial glia-astrocyte lineage of developing mouse spinal cord. *The Journal of neuroscience : the official journal of the Society for Neuroscience* 17: 9212-9

Shimamura K, Hartigan DJ, Martinez S, Puelles L, Rubenstein JL. 1995. Longitudinal organization of the anterior neural plate and neural tube. *Development* 121: 3923-33

Shimamura K, Rubenstein JL. 1997. Inductive interactions direct early regionalization of the mouse forebrain. *Development* 124: 2709-18

Shitamukai A, Konno D, Matsuzaki F. 2011. Oblique radial glial divisions in the developing mouse neocortex induce self-renewing progenitors outside the germinal zone that resemble primate outer subventricular zone progenitors. *The Journal of neuroscience : the official journal of the Society for Neuroscience* 31: 3683-95

Shitamukai A, Matsuzaki F. 2012. Control of asymmetric cell division of mammalian neural progenitors. *Development, growth & differentiation* 54: 277-86

Siddiqi F, Chen F, Aron AW, Fiondella CG, Patel K, LoTurco JJ. 2014. Fate mapping by piggyBac transposase reveals that neocortical GLAST+ progenitors generate more astrocytes than Nestin+ progenitors in rat neocortex. *Cereb Cortex* 24: 508-20

Siegenthaler JA, Ashique AM, Zarbalis K, Patterson KP, Hecht JH, et al. 2009. Retinoic acid from the meninges regulates cortical neuron generation. *Cell* 139: 597-609

Smart IH. 1973. Proliferative characteristics of the ependymal layer during the early development of the mouse neocortex: a pilot study based on recording the number, location and plane of cleavage of mitotic figures. *Journal of anatomy* 116: 67-91

Smart IH. 1976. A pilot study of cell production by the ganglionic eminences of the developing mouse brain. *Journal of anatomy* 121: 71-84

Smart IH. 1985. Differential growth of the cell production systems in the lateral wall of the developing mouse telencephalon. *Journal of anatomy* 141: 219-29

Smart IH, Dehay C, Giroud P, Berland M, Kennedy H. 2002. Unique morphological features of the proliferative zones and postmitotic compartments of the neural epithelium giving rise to striate and extrastriate cortex in the monkey. *Cereb Cortex* 12: 37-53

Stahl R, Walcher T, De Juan Romero C, Pilz GA, Cappello S, et al. 2013. Trnp1 regulates expansion and folding of the mammalian cerebral cortex by control of radial glial fate. *Cell* 153: 535-49

Stancik EK, Navarro-Quiroga I, Sellke R, Haydar TF. 2010. Heterogeneity in ventricular zone neural precursors contributes to neuronal fate diversity in the postnatal neocortex. *The Journal of neuroscience : the official journal of the Society for Neuroscience* 30: 7028-36

Stenman J, Toresson H, Campbell K. 2003. Identification of two distinct progenitor populations in the lateral ganglionic eminence: implications for striatal and olfactory bulb neurogenesis. *The Journal of neuroscience : the official journal of the Society for Neuroscience* 23: 167-74

Storm EE, Garel S, Borello U, Hebert JM, Martinez S, et al. 2006. Dose-dependent functions of Fgf8 in regulating telencephalic patterning centers. *Development* 133: 1831-44

Stoykova A, Treichel D, Hallonet M, Gruss P. 2000. Pax6 modulates the dorsoventral patterning of the mammalian telencephalon. *The Journal of neuroscience : the official journal of the Society for Neuroscience* 20: 8042-50

Striedter GF. 2005. *Principles Of Brain Evolution*. Sunderland, MA: Sinauer Associates, Incorporated.

Stubbs D, DeProto J, Nie K, Englund C, Mahmud I, et al. 2009. Neurovascular congruence during cerebral cortical development. *Cereb Cortex* 19 Suppl 1: i32-41

Sussel L, Marin O, Kimura S, Rubenstein JL. 1999. Loss of Nkx2.1 homeobox gene function results in a ventral to dorsal molecular respecification within the basal telencephalon: evidence for a transformation of the pallidum into the striatum. *Development* 126: 3359-70

Takahashi T, Nowakowski RS, Caviness VS, Jr. 1995. Early ontogeny of the secondary proliferative population of the embryonic murine cerebral wall. *The Journal of neuroscience : the official journal of the Society for Neuroscience* 15: 6058-68

Takebayashi H, Yoshida S, Sugimori M, Kosako H, Kominami R, et al. 2000. Dynamic expression of basic helix-loop-helix Olig family members: implication of Olig2 in neuron and oligodendrocyte differentiation and identification of a new member, Olig3. *Mechanisms of development* 99: 143-8

Tamai H, Shinohara H, Miyata T, Saito K, Nishizawa Y, et al. 2007. Pax6 transcription factor is required for the interkinetic nuclear movement of neuroepithelial cells. *Genes to cells : devoted to molecular & cellular mechanisms* 12: 983-96

Tanaka DH, Nakajima K. 2012. GABAergic interneuron migration and the evolution of the neocortex. *Development, growth & differentiation* 54: 366-72

Tavazoie M, Van der Veken L, Silva-Vargas V, Louissaint M, Colonna L, et al. 2008. A specialized vascular niche for adult neural stem cells. *Cell stem cell* 3: 279-88

Taverna E, Huttner WB. 2010. Neural progenitor nuclei IN motion. *Neuron* 67: 906-14

Thornton GK, Woods CG. 2009. Primary microcephaly: do all roads lead to Rome? *Trends in genetics : TIG* 25: 501-10

Tole S, Remedios R, Saha B, Stoykova A. 2005. Selective requirement of Pax6, but not Emx2, in the specification and development of several nuclei of the amygdaloid complex. *The Journal of neuroscience : the official journal of the Society for Neuroscience* 25: 2753-60

Tong F. 2003. Primary visual cortex and visual awareness. *Nature reviews. Neuroscience* 4: 219-29

Toresson H, Campbell K. 2001. A role for Gsh1 in the developing striatum and olfactory bulb of Gsh2 mutant mice. *Development* 128: 4769-80

Toresson H, Mata de Urquiza A, Fagerstrom C, Perlmann T, Campbell K. 1999. Retinoids are produced by glia in the lateral ganglionic eminence and regulate striatal neuron differentiation. *Development* 126: 1317-26

Toresson H, Potter SS, Campbell K. 2000. Genetic control of dorsal-ventral identity in the telencephalon: opposing roles for Pax6 and Gsh2. *Development* 127: 4361-71

Tsunekawa Y, Britto JM, Takahashi M, Polleux F, Tan SS, Osumi N. 2012. Cyclin D2 in the basal process of neural progenitors is linked to non-equivalent cell fates. *The EMBO journal* 31: 1879-92

Tyler WA, Haydar TF. 2013. Multiplex genetic fate mapping reveals a novel route of neocortical neurogenesis, which is altered in the Ts65Dn mouse model of Down syndrome. *The Journal of neuroscience : the official journal of the Society for Neuroscience* 33: 5106-19

Urban N, Martin-Ibanez R, Herranz C, Esgleas M, Crespo E, et al. 2010. Nolz1 promotes striatal neurogenesis through the regulation of retinoic acid signaling. *Neural development* 5: 21

Van Essen DC. 1997. A tension-based theory of morphogenesis and compact wiring in the central nervous system. *Nature* 385: 313-8

Vasudevan A, Long JE, Crandall JE, Rubenstein JL, Bhide PG. 2008. Compartment-specific transcription factors orchestrate angiogenesis gradients in the embryonic brain. *Nature neuroscience* 11: 429-39

Waclaw RR, Allen ZJ, 2nd, Bell SM, Erdelyi F, Szabo G, et al. 2006. The zinc finger transcription factor Sp8 regulates the generation and diversity of olfactory bulb interneurons. *Neuron* 49: 503-16

Waclaw RR, Ehrman LA, Pierani A, Campbell K. 2010. Developmental origin of the neuronal subtypes that comprise the amygdalar fear circuit in the mouse. *The Journal of neuroscience : the official journal of the Society for Neuroscience* 30: 6944-53

Waclaw RR, Wang B, Campbell K. 2004. The homeobox gene Gsh2 is required for retinoid production in the embryonic mouse telencephalon. *Development* 131: 4013-20

Waclaw RR, Wang B, Pei Z, Ehrman LA, Campbell K. 2009. Distinct temporal requirements for the homeobox gene Gsx2 in specifying striatal and olfactory bulb neuronal fates. *Neuron* 63: 451-65

Walsh C, Cepko CL. 1990. Cell lineage and cell migration in the developing cerebral cortex. *Experientia* 46: 940-7

Wang B, Long JE, Flandin P, Pla R, Waclaw RR, et al. 2013. Loss of Gsx1 and Gsx2 function rescues distinct phenotypes in Dlx1/2 mutants. *The Journal of comparative neurology* 521: 1561-84

Wang X, Merzenich MM, Sameshima K, Jenkins WM. 1995. Remodelling of hand representation in adult cortex determined by timing of tactile stimulation. *Nature* 378: 71-5

Wang X, Tsai JW, Imai JH, Lian WN, Vallee RB, Shi SH. 2009. Asymmetric centrosome inheritance maintains neural progenitors in the neocortex. *Nature* 461: 947-55

Wang X, Tsai JW, LaMonica B, Kriegstein AR. 2011. A new subtype of progenitor cell in the mouse embryonic neocortex. *Nature neuroscience* 14: 555-61

Wang Y, Brzozowska-Prechtl A, Karten HJ. 2010. Laminar and columnar auditory cortex in avian brain. *Proceedings of the National Academy of Sciences of the United States of America* 107: 12676-81

Wang YC, Khan Z, Kaschube M, Wieschaus EF. 2012. Differential positioning of adherens junctions is associated with initiation of epithelial folding. *Nature* 484: 390-3

Wichterle H, Turnbull DH, Nery S, Fishell G, Alvarez-Buylla A. 2001. In utero fate mapping reveals distinct migratory pathways and fates of neurons born in the mammalian basal forebrain. *Development* 128: 3759-71

Wonders CP, Anderson SA. 2006. The origin and specification of cortical interneurons. *Nature reviews. Neuroscience* 7: 687-96

Woodhead GJ, Mutch CA, Olson EC, Chenn A. 2006. Cell-autonomous beta-catenin signaling regulates cortical precursor proliferation. *The Journal of neuroscience : the official journal of the Society for Neuroscience* 26: 12620-30

Xie Y, Juschke C, Esk C, Hirotsune S, Knoblich JA. 2013. The phosphatase PP4c controls spindle orientation to maintain proliferative symmetric divisions in the developing neocortex. *Neuron* 79: 254-65

Xu Q, Cobos I, De La Cruz E, Rubenstein JL, Anderson SA. 2004. Origins of cortical interneuron subtypes. *The Journal of neuroscience : the official journal of the Society for Neuroscience* 24: 2612-22

Xuan S, Baptista CA, Balas G, Tao W, Soares VC, Lai E. 1995. Winged helix transcription factor BF-1 is essential for the development of the cerebral hemispheres. *Neuron* 14: 1141-52

Yozu M, Tabata H, Nakajima K. 2005. The caudal migratory stream: a novel migratory stream of interneurons derived from the caudal ganglionic eminence in the developing mouse forebrain. *The Journal of neuroscience : the official journal of the Society for Neuroscience* 25: 7268-77

Yu X, Zecevic N. 2011. Dorsal radial glial cells have the potential to generate cortical interneurons in human but not in mouse brain. *The Journal of neuroscience : the official journal of the Society for Neuroscience* 31: 2413-20

Yun K, Fischman S, Johnson J, Hrabe de Angelis M, Weinmaster G, Rubenstein JL. 2002. Modulation of the notch signaling by Mash1 and Dlx1/2 regulates sequential specification and differentiation of progenitor cell types in the subcortical telencephalon. *Development* 129: 5029-40

Yun K, Garel S, Fischman S, Rubenstein JL. 2003. Patterning of the lateral ganglionic eminence by the Gsh1 and Gsh2 homeobox genes regulates striatal and olfactory bulb histogenesis and the growth of axons through the basal ganglia. *The Journal of comparative neurology* 461: 151-65

Yun K, Potter S, Rubenstein JL. 2001. Gsh2 and Pax6 play complementary roles in dorsoventral patterning of the mammalian telencephalon. *Development* 128: 193-205

Zecevic N, Chen Y, Filipovic R. 2005. Contributions of cortical subventricular zone to the development of the human cerebral cortex. *The Journal of comparative neurology* 491: 109-22

Zhang J. 2003. Evolution of the human ASPM gene, a major determinant of brain size. *Genetics* 165: 2063-70

5 Appendix

Abbreviations

ANR	anterior neural ridge
(a)NSC	(adult) neural stem cells
Ascl1	acheate
AP	apical progenitor
aPKC	atypical protein kinase C
ASPM	abnormal spindle-like microcephaly-associated protein
BF1	brain factor-1
BG	basal ganglia
bHLH	basic helix-loop-helix
BLBP	brain lipid binding protein
BMP	bone morphogenic protein
BP	basal progenitor
bRG	basal radial glia
CB	calbindin
CGE	caudal ganglionic eminence
ChIP	chromatin immunoprecipitation
CR	calrethinin
CSF	cerebral spinal fluid
DS	down syndrome
DVR	dorsal ventricular ridge
EC	endothelial cell
ECM	extracellular matrix
Emx2	empty spiracles homoloque2
FGF	fibroblast growth factor
FNP	frontonasal process
GABA(ergic)	gamma-aminobutyric acid
GL	glomerular layer
Glast	glutamate aspartate transporter
hGFAP	human glial acidic fiber protein
GW	gestational week
GO	gene ontology
IGF	insulin-like growth factor
INM	interkinetic nuclear migration
mInsc	mouse Inscutetable
Isnm1	Insulinoma-associated 1
IPC	intermediate progenitor cell
ITC	intercalated cells
IZ	intermediate zone
KO	knock out

LCS	lateral cortical stream
LGE	lateral ganglionic eminence
MGE	medial ganglionic eminence
MZ	mantle zone
NE	neuroepithelial cell
OB	olfactory bulb
OPC	oligodendrocyte progenitor cell
PH3	phospho histone H3
PSB	pallial-subpallial boundary
RA	retinoic acid
RG	radial glia
RMS	rostral migratory stream
Sey	smalleye
SEZ	subependymal zone
SGZ	subpial granular layer
Shh	Sonic hedgehog
(I/O) SVZ	(inner/outer) subventricular zone
TAP	transit amplifying progenitor
TF	transcription factor
TH	tyrosin hydroxylase
VZ	ventricular zone
Wnt	wingless/INT proteins
WT	wildtype

List of figures

Acknowledgements

First and foremost I would like to thank Prof. **Magdalena Götz** for her excellent supervision of this PhD project and her support and mentoring during these steps of my academic career. Magdalenas enthusiasm for science and her creative ideas were a strong motivating force and inspiration to me.

Many thanks also to **Leanne Godinho,** who co-supervised me, initially advised me in slice culture and imaging and always had time for technical and strategic discussions.

Great thanks to Prof. **Fumio Matsuzaki** and **Atsunori Shitamukai** for giving me the chance to learn longterm embryonic slice imaging in their lab at the RIKEN in Kobe, Japan. I enjoyed wonderful hospitality and insight into excellent scientific work in a fascinating cultural setting. Working together with both of them was the ideal experience of scientific collaboration.

I want to acknowledge the great contribution of **Victor Borrell** and **Isabel Reillo** from Alicante, Spain. Their data on ferret, sheep and marmoset provided exciting evolutionary aspect to this study and discussing aspects of progenitor heterogeneity and brain expansion was very fruitful.

I am also grateful for the collaboration with **Francois Guillemot** and **Emilie Pacary** who added insight to the molecular mechanism of SAP proliferation.

Also, I want to say "arigato" to **Maki Asami** who shared the office with me in the beginning and gave me great scientific support during my starting phase and was a very cheerful colleague. The Oktoberfest visits with her are unforgettable.

My office mates **Pia Johannsson**, **Silvia Cappello**, **Vidya Ramesh**, **Tessa Walcher** and **Sven Falk** for a very relaxed atmosphere and interesting open scientific and non-scientific discussions.

I am thankful to all members of the **Embryonic Development Club** and all members of the Götz lab for helpful input and scientific discussions after club- and labmeetings during these years in Munich.

Andrea Steiner, **Timucin Öztürk**, **Angelika Waiser** and **Emily Baumgart** for their excellent technical assistance and their transfer of yearlong practical knowledge.

Joana Santos Barbosa, **Philipp Hoppe** and **Max Endele** exemplary for all the graduate students at the ISF who became great friends with whom I share remarkable memories during this time in Munich.

My loved **Antonia**, who gave me strong support and got interested in my enthusiasm for science.

Above all, I want to thank my parents, **Marlis** and **Claus-Peter** for their livelong support and their seeding of deep fascination for natures wonders. This was and is still driving me. I dedicate this work to you.